

**An Investigation of Wave-Kinetic Theory:
Hierarchy Equations, Phase Measure, and Resonance Singularity**

by

Yi-Kang Shi

A dissertation submitted to The Johns Hopkins University in conformity with the requirements for
the degree of Doctor of Philosophy.

Baltimore, Maryland

May, 2016

© Yi-Kang Shi 2016

All rights reserved

Abstract

Wave-kinetic theory has been developed to describe the statistical dynamics of weakly nonlinear, dispersive waves. In the first part of this dissertation, we derive the wave-kinetic equations formally from a general model of Hamiltonian wave systems, in the standard limit of a continuum of weakly interacting dispersive waves with random phases. In this asymptotic limit we show that the correct dynamical equation for multi-mode amplitude distributions is *not* the well-known Peierls equation but is instead a reduced equation with only a subset of the terms in that equation. The equations that we derive are the direct analogue of the Boltzmann hierarchy obtained from the BBGKY hierarchy in the low-density limit for gases. We show that the asymptotic multi-mode equations possess factorized solutions for factorized initial data, which correspond to preservation in time of the property of “random phases & amplitudes”. The factors satisfy the equations for the 1-mode probability density functions (PDF’s) previously derived by Jakobsen & Newell and Choi et al. Analogous to the Klimontovich density in the kinetic theory of gases, we introduce the concepts of the “empirical spectrum” and the “empirical 1-mode PDF”. We show

ABSTRACT

that the factorization of the hierarchy equations implies that these quantities are self-averaging: they satisfy the wave-kinetic equations of the spectrum and 1-mode PDF for almost any selection of phases and amplitudes from the initial ensemble. We show that both of these equations satisfy an H -theorem for an entropy defined by Boltzmann's prescription $S = k_B \log W$. We also characterize the general solutions of our multi-mode distribution equations, for initial conditions with random phases but with no statistical assumptions on the amplitudes. Analogous to a result of Spohn for the Boltzmann hierarchy, these are “super-statistical solutions” that correspond to ensembles of solutions of the wave-kinetic equations with random initial conditions or random forces. On the basis of our results, we discuss possible kinetic explanations of intermittency and non-Gaussian statistics in wave turbulence. In particular, we advance the explanation of a “super-turbulence” produced by stochastic or turbulent solutions of the wave-kinetic equations themselves.

In the second part of the dissertation, we investigate a key assumption of wave-kinetic theory – dispersivity. We show that systems which are generally dispersive can have resonant sets of wave modes with identical group velocities, leading to a local breakdown of dispersivity. This shows up as a geometric singularity of the resonant manifold and possibly as an infinite phase measure in the collision integral. Such singularities occur widely for classical wave systems, including acoustical waves, Rossby waves, helical waves in rotating fluids, light waves in nonlinear optics and also in quantum transport, e.g. kinetics of electron-hole excitations (matter waves)

ABSTRACT

in graphene. These singularities are the exact analogue of the critical points found by Van Hove in 1953 for phonon dispersion relations in crystals. The importance of these singularities in wave kinetics depends on the dimension of phase space $D = (N - 2)d$ (d physical space dimension, N the number of waves in resonance) and the degree of degeneracy δ of the critical points. Following Van Hove, we show that non-degenerate singularities lead to finite phase measures for $D > 2$ but produce divergences when $D \leq 2$ and possible breakdown of wave kinetics if the collision integral itself becomes too large (or even infinite). Similar divergences and possible breakdown can occur for degenerate singularities, when $D - \delta \leq 2$, as we find for several physical examples, including electron-hole kinetics in graphene. When the standard kinetic equation breaks down, one must develop a new singular wave kinetics. We discuss approaches from pioneering 1971 work of Newell & Aucoin on multi-scale perturbation theory for acoustic waves and field-theoretic methods based on exact Schwinger-Dyson integral equations for the wave dynamics.

Primary Reader: Gregory L. Eyink

Secondary Reader: Oleg Tchernyshyov

Acknowledgments

First and foremost, I would like to thank my advisor, Prof. Gregory L. Eyink, for the boundless support, for tolerating my mistakes and always encouraging me to push forward, and ultimately for making this research possible with his dedication and generosity. The journey to study turbulence and science from him and with him is all the fun a student could ask for. It is also a journey travelled with colleagues and friends, Theodore Drivas, Cristian Lalescu, and Damien Benveniste. Their help is indispensable to me. I can only regret not staying long enough for Turbulence Theory IV and V.

I would also like to extend my deep appreciation for the Applied Mathematics and Statistics Department at the John Hopkins University for the nurturing environment and the financial support. My life is much easier and enjoyable with the help of Kristin Bechtel, Sandy Kirt, and Ann Gibbins. I am grateful for the high quality education provided by the faculty and the warm friendship of other students here. It is impossible for me to mention everyone who have helped me along the way, but special thanks are due to my roommates Hao Jiang, Bo Liu, Heng Wang, and Percy

ACKNOWLEDGMENTS

Li for the great times. I would also like to thank the Institute for Pure and Applied Mathematics at University of California, Los Angeles for the financial support during my one semester there and the Acheson J. Duncan Fund for the travel grant.

My gratitude is also for my family, my parents Jiansun Shi, Qiming Jiang, and my wife Jing Wang. I cannot imagine myself pushing through difficult times without their unconditional support and almost blind trust.

This thesis is benefited by many useful comments from people including Alan Newell, Sergey Nazarenko, Herbert Spohn, Jani Lukkarinen, Gregory Falkovich, and many more. I am especially indebted to those who have served on my exam committees and provided me with constructive criticism and guidance: Profs. James Fill, Hans Lindblad, Oleg Tchernyshyov, Charles Meneveau, and Robert Dalrymple.

Finally I would like to thank Prof. Oleg Tchernyshyov for being the Second Reader of the thesis and Profs. Charles Meneveau, Daniel Naiman, Nicholas Charon for serving on the defense committee. Your time is much appreciated.

Dedication

This thesis is dedicated to my wife, Jing Wang, for always being there for me, no matter how far we are apart. I would not be who I am without her continual love and unconditional support.

Contents

Abstract	ii
Acknowledgments	v
List of Tables	xi
List of Figures	xii
1 Introduction	1
2 Multi-Mode Hierarchy Equations	6
2.1 Summary of the Main Results	6
2.2 Model and Notations	15
2.3 Fields with Random Phases and Amplitudes	18
2.4 Perturbation Expansion and Diagrammatics	25
2.5 Spectral Hierarchy	30
2.5.1 Derivation	30
2.5.2 Properties	35
2.6 PDF Hierarchy	41
2.6.1 Derivation	41
2.6.2 Properties	43

CONTENTS

2.7	Intermittency in Kinetic Wave Turbulence	51
2.7.1	Cascade in Amplitude Space?	51
2.7.2	Super-Turbulence of Wave Kinetics?	55
2.8	Conclusion	60
3	Resonance Van Hove Singularities: Case Studies	62
3.1	Introduction	62
3.2	Triplet Resonances	66
3.2.1	Isotropic Power Law	67
3.2.2	Lattice Regularization of Power Laws	69
3.2.3	Anisotropic Dispersion Relations	75
	Rosby/drift waves	76
	Inertial waves	79
	Internal gravity waves	80
	Summary	82
3.3	Quartet Resonances	82
3.3.1	Surface gravity-capillary waves	84
3.3.2	Wave propagation along an optical fiber	86
3.3.3	Electrons and holes in graphene	89
3.4	Conclusion	93
4	Resonance Van Hove Singularities: Physical Consequences	94
4.1	Introduction	94
4.2	Local Finiteness of the Phase Measure	96
4.3	Singular Wave Kinetics: Electron-Hole Plasma in Graphene	100
4.3.1	Derivation of the Singular Kinetic Equation	101
4.3.2	Properties of the Singular Kinetic Equation	108

CONTENTS

4.4 Conclusion	114
5 Conclusion	117
A Derivation of the Spectral Hierarchy	122
B Derivation of the PDF Hierarchy	133
C Construction of the Phase Measure	136
D Perturbative Derivation of the Quantum Boltzmann Equation	142
E Lattice Wigner Function in Finite Volume	148
F Derivation of the Linear Transport Equation for the Wigner Function	154
Vita	169

List of Tables

4.1 Summary 116

List of Figures

2.1	Zeroth-order terms $a_1^{(0)+}$ and $a_1^{(0)-}$	27
2.2	First-order terms $a_1^{(1)+}$ and $a_1^{(1)-}$	27
2.3	Second-order term $a_1^{(2)+}$	27
2.4	First-order term $\sum_1(\lambda_1 + \frac{\mu_1}{2J_1})a_1^{(1)}a_1^{(0)*}$	29
2.5	Second-order term $\sum_1(\lambda_1 + \lambda_1^2 J_1 - \frac{\mu_1^2}{4J_1}) a_1^{(1)} ^2$	29
2.6	Contributions to \mathcal{J}_1	29
2.7	Leading contribution to \mathcal{J}_2	30
3.1	Three-wave resonant manifold $\mathcal{R}_{\mathbf{k}} = \{\mathbf{p} : \omega(\mathbf{p}) + \omega(\mathbf{k} - \mathbf{p}) - \omega(\mathbf{k}) = 0\}$ for dispersion relation $\omega(\mathbf{k}) = \left[4 \sum_{i=1}^3 \sin^2\left(\frac{k_i}{2}\right)\right]^{\alpha/2}$, $\alpha = \frac{1}{1+\log_2 \cos(1/4)}$, on the 3-torus $[-\pi, \pi]^3$, and for the specific wavevector $\mathbf{k} = (0, 0, 1)$. There is a critical point (black dot) at $\mathbf{p} = \mathbf{k}/2$	65
3.2	Resonant manifold $\mathcal{R}_{\mathbf{k}}^{++} = \{\mathbf{p} : \omega(\mathbf{p}) + \omega(\mathbf{k} - \mathbf{p}) - \omega(\mathbf{k}) = 0\}$ for dispersion relation $\omega(\mathbf{k}) = \left[4 \sum_{i=1}^3 \sin^2\left(\frac{k_i}{2}\right)\right]^{\alpha/2}$, $\alpha = \frac{1}{1+\log_2 \sin(3/4)}$, on the 3-torus $[\frac{1}{2}\pi, \frac{5}{2}\pi] \times [-\frac{3}{2}\pi, \frac{1}{2}\pi] \times [\frac{1}{2}\pi, \frac{5}{2}\pi]$, and for the specific wavevector $\mathbf{k} = (3, 3, 3)$. There is a critical point (black dot) at $\mathbf{p} = \mathbf{k}/2 - \pi$	73
3.3	Resonant manifold $\mathcal{R}_{\mathbf{k}}^{+-}$ for dispersion relation $\omega(\mathbf{k}) = \left[4 \sum_{i=1}^2 \sin^2\left(\frac{k_i}{2}\right)\right]^{\alpha/2}$ with $\alpha = 2.5$, on the 2-torus $[-\pi/2, 3/2\pi] \times [\pi/2, 5/2\pi]$, and for the specific wavevector $\mathbf{k} = (.2, -.2)$ on the top left and $\mathbf{k} = (.18, -.2)$ on the top right. For the specific numerically approximated wavevector $\mathbf{k} = (.1887713, -.2)$ (bottom figure), there is a critical point (black dot) at $\mathbf{p} = (-1.4716, 4.6016)$	74
3.4	Resonant manifold $\mathcal{R}_{\mathbf{k}}^{++}$, $\mathbf{k} = (\cos \theta, \sin \theta)$ for Rossby/drift waves, plotted as gray lines. The black arrow is the vector \mathbf{k} . Here $\theta = \frac{\pi}{2} - 0.05$ for the top left panel, $\theta = \frac{\pi}{2} + 0.05$ for the top right panel, and $\theta = \frac{\pi}{2}$ for the bottom panel.	77
3.5	Resonant manifold $\mathcal{R}_{\mathbf{k}}^{++}$, $\mathbf{k} = (1, 0, 0)$ for inertial waves with rotation about the z-axis. The black arrow is the vector \mathbf{k}	79
3.6	Resonant manifold $\mathcal{R}_{\mathbf{k}}^{++}$, $\mathbf{k} = (1, 0, 0)$ for internal gravity waves with vertical direction along the z-axis. The black arrow is the vector \mathbf{k}	81
3.7	Resonant manifold $\mathcal{R}_k^{(4)}$, $k = 1$ for surface gravity waves in $d = 1$, with the non-trivial part plotted in gray and the trivial part in dashed black. Here ■ indicates pseudo-critical points.	85

LIST OF FIGURES

3.8	The figures show the resonant manifold $\mathcal{R}_k^{(4)}$ for surface gravity waves in $d = 1$ for $g = \sigma$, with the non-trivial part plotted in gray and the trivial part in dashed black. Here $k = 0.3$ for the top left panel; $k = \sqrt{(2 - \sqrt{3})/\sqrt{3}}$ for the bottom panel; $k = 0.5$ for the top right panel. ■ indicates pseudo-critical points; ● indicates non-degenerate critical points; ► indicates degenerate critical points.	86
3.9	Resonant manifold $\mathcal{R}_k^{(4)}$, $k = 1$ of one-dimensional 3rd-order dispersive optical waves for $s = -1$, $\alpha = 3$, so that $k_* = 1$, with the non-trivial part of the manifold plotted in gray and the trivial part in dashed black. The triple intersection is a degenerate critical point, indicated by ►.	88
3.10	The section of the resonant manifold $\mathcal{R}_{\mathbf{k}}^{(++++)}$, $\mathbf{k} = (1, 0)$ for fixed p_y ($p_y < 0$ for the top left panel; $p_y = 0$ for the bottom panel; $p_y > 0$ for the top right panel), with the non-trivial part plotted in gray and the trivial part in dashed black. The 2D critical set in the bottom panel is plotted in dark gray. For $p_y \neq 0$ the horizontal sections of the resonant manifold at fixed p_x -values are ellipses, but for $p_y = 0$ and $p_x \geq 0$ these sections are line-segments.	90
A.1	Terms in \mathcal{J}_1 before phase averaging.	123
A.2	Contributions in \mathcal{J}_1 after phase averaging.	123
A.3	Terms in \mathcal{J}_2 before phase averaging.	124
A.4	Type I diagram in \mathcal{J}_2	124
A.5	Type II diagram in \mathcal{J}_2	125
A.6	Type II diagram in \mathcal{J}_2	125
A.7	Type III diagram in \mathcal{J}_2	126
A.8	Terms in \mathcal{J}_3 before phase averaging.	127
A.9	Type I diagram in \mathcal{J}_3	127
A.10	Type II diagram in \mathcal{J}_3	128
A.11	Terms in \mathcal{J}_4 before phase averaging.	129
A.12	Type I diagram in \mathcal{J}_4	129
A.13	Terms in \mathcal{J}_5 before phase averaging.	131
A.14	Type I diagram for \mathcal{B}_1 in \mathcal{J}_5	131
A.15	Type II diagram for \mathcal{B}_1 in \mathcal{J}_5	132

Chapter 1

Introduction

It is generally very hard to follow in detail the solutions of the nonlinear field equations that describe turbulence (for example, the forced Navier-Stokes equation). Therefore one major theme is to understand the long-time statistical behavior of solutions. A major obstacle is the lack of a closure equation for the statistical moments of the underlying field. On the other hand, there is a situation known as wave turbulence where closure equations seem to be available. Wave turbulence involves the dynamics of dispersive wave trains with weak interaction. The wave-action density (or, the spectrum) $n_{\mathbf{k}} = n(\mathbf{k}, t)$, which is proportional to the Fourier transform of two-point averages, is supposed to satisfy a closed (Boltzmann-like, kinetic) equation. For example, in the 3-wave case the kinetic equation is

$$\partial_{\tau} n(\mathbf{k}, \tau) = \eta_{\mathbf{k}} - \gamma_{\mathbf{k}} n(\mathbf{k}, \tau) \quad (1.1)$$

with the internal (turbulent) driving $\eta_{\mathbf{k}}$ and the damping $\gamma_{\mathbf{k}}$ given by

$$\eta_{\mathbf{k}} = 4\pi \sum_{\underline{\sigma}=(-1, \sigma_2, \sigma_3)} \int d^d k_2 d^d k_3 \delta^d(\underline{\sigma} \cdot \underline{\mathbf{k}}) \delta^d(\underline{\sigma} \cdot \omega(\underline{\mathbf{k}})) |L_{\underline{\mathbf{k}}}^{\underline{\sigma}}|^2 n(\mathbf{k}_2, \tau) n(\mathbf{k}_3, \tau)$$

CHAPTER 1. INTRODUCTION

$$\gamma_{\mathbf{k}} = 4\pi \sum_{\underline{\sigma}=(-1,\sigma_2,\sigma_3)} \int d^d k_2 d^d k_3 \delta^d(\underline{\sigma} \cdot \mathbf{k}) \delta^d(\underline{\sigma} \cdot \omega(\mathbf{k})) |L_{\mathbf{k}}^{\underline{\sigma}}|^2 [\sigma_2 n(\mathbf{k}_3) + \sigma_3 n(\mathbf{k}_2)], \quad (1.2)$$

where $\underline{\mathbf{k}} = (\mathbf{k}, \mathbf{k}_2, \mathbf{k}_3)$. See section 2.2 for the definitions of the quantities in the equation. Here the Dirac delta function enforces resonances condition so that the limiting dynamics only involve interaction between resonant waves. The theory goes back to Peierls (1929), who studied phonons (sound waves) in anharmonic crystals. Peierls (1929) obtained not only the kinetic equation for the spectrum in both classical and quantum systems, but also the evolution equation for the joint PDF (probability density function). Brout and Prigogine (1956) also discussed these evolution equations in the general setting of weakly coupled classical systems. The theory was rediscovered independently in the context of water waves by Hasselmann (1962, 1963a,b), and in the context of plasma waves by Zaslavskii and Sagdeev (1967). Later Benney and Newell (1967, 1969) derived the hierarchy of moment equations as a natural asymptotic closure using the multi-scale perturbation theory. The wave-kinetic equation (1.1) does not only admit entropy-maximizing thermal equilibrium solutions, but Zakharov and Filonenko (1967a,b) discovered that it also admits finite-flux turbulent solutions where conserved densities such as energy and wave-action flow from large scales to small scales (or vice versa).

However, the empirical verification of the wave-kinetic theory is quite difficult. Experimentally, to resolve the Dirac delta function in the wave-kinetic equation requires that the time for a wave packet traveling at the group velocity to cross the box must be longer than the nonlinear interaction time. Newell and Rumpf (2011) have estimated that for surface gravity waves with nonlinearity of order 0.1, to resolve resonances involving waves of 60 m would require a tank of 60 km on a side. Numerically, there is some success in studying 2D systems. For example, Zakharov *et al.* (2005) reported qualitative agreement with the statistical description of the wave kinetic theory. Unfortunately the “mesoscopic” region they probed still does not have enough harmonics to quantitatively verify the prediction of wave-kinetic theory. The situation is even worse for systems in higher dimensions. Mathematically, the only rigorous result so far is Lukkarinen and Spohn (2011).

CHAPTER 1. INTRODUCTION

They have studied the solution $\psi(\mathbf{x}, t)$ of nonlinear Schrödinger equation with lattice regularization for random initial data distributed according to a Gibbs measure. In the limit of volume going to infinity and nonlinearity ϵ going to zero, they prove that the space-time covariance of $\psi(\mathbf{x}, \epsilon^{-2}\tau)$ with fixed τ has a limit that agrees with the thermal equilibrium solution of the kinetic equation. For turbulent solutions, even the complete set of a priori assumptions for validity of wave-kinetic theory still remains controversial. There is a counterexample known as the MMT model (Majda *et al.*, 1997) where it is found numerically that the turbulent regime is not described by the solution of the kinetic equation. It has recently been shown by Rumpf *et al.* (2009) and Newell *et al.* (2012) that the Kolmogorov solutions in this case are unstable to spatially inhomogeneous perturbations. As a result, the long time dynamics is not dominated by weakly interacting wave trains but coherent structures created from the instability.

We do not attempt at a rigorous mathematical proof of the wave kinetic theory; rather, our goal here is the more directly physical one of formulating the limiting equations of wave kinetics and understanding their content. In Chap. 2, we use probabilistic tools from the work of Lanford (1975) on the Boltzmann hierarchy to systematize the derivation of hierarchy equations for higher-order correlation functions, assuming initial randomness in phases and amplitudes. A lot of the properties actually propagate in time, which rely on the preservation of the factorized solutions of these hierarchy equations. This preservation is equivalent to the propagation of chaos by the BBGKY hierarchy in the kinetic limit for gases.

On the other hand, even the finiteness of the collision integral, i.e. the right hand side of equation (1.1), is an open mathematical issue. There is a construction of the phase measure for the collision integral by Lukkarinen and Spohn (2007) who assume that the dispersion relation is a Morse function (C^2 and has only isolated, non-degenerate critical points) in dimension $d = 3$. However, this assumption is too restrictive as it rules out the most physically relevant wave dispersion relations, which often are power-law form $\propto k^\alpha$ at zero wavenumber and not C^2 when $\alpha < 2$. We pursue a different approach which works for a wider class of dispersion relations. Our approach is based on a

CHAPTER 1. INTRODUCTION

direct representation of the singular measure by an integral with respect to the surface measure dS on the resonant manifold $\mathcal{R}_{\mathbf{k}}^{\sigma_2\sigma_3} = \{\mathbf{p} : E_{\sigma_2,\sigma_3}(\mathbf{p}; \mathbf{k}) \equiv \sigma_2\omega(\mathbf{p}) + \sigma_3\omega(\mathbf{q}) - \omega(\mathbf{k}) = 0, \mathbf{k} = \sigma_2\mathbf{p} + \sigma_3\mathbf{q}\}$.

In many interesting cases, we find that the phase measure has the form, for 3-wave resonance,

$$\int d^d p d^d q \delta^d(\underline{\sigma} \cdot \underline{\mathbf{k}}) \delta(\underline{\sigma} \cdot \omega(\underline{\mathbf{k}})) f(\mathbf{p}, \mathbf{q}; \mathbf{k}) = \int_{\mathcal{R}_{\mathbf{k}}^{\sigma_2\sigma_3}} \frac{dS(\mathbf{p})}{|\nabla_{\mathbf{p}} E_{\sigma_2,\sigma_3}(\mathbf{p}; \mathbf{k})|} f(\mathbf{p}, \mathbf{q}; \mathbf{k}). \quad (1.3)$$

This representation also makes more transparent the crucial role of critical points where $\nabla_{\mathbf{p}} E_{\sigma_2,\sigma_3}(\mathbf{p}; \mathbf{k}) = \mathbf{0}$, an issue usually overlooked in the literature. Physically, such points correspond to wavevector triads at which the dispersivity of the wave system breaks down locally and for which two distinct wave packets from the triad propagate together for all times with the same velocity. Geometrically, these points show up as a singularity of the resonant manifold and give rise to possible divergence of the collision integral. In Chap. 3 we show that such singularities occur widely in many examples including acoustic waves, Rossby waves, helical waves in rotating fluids, electron-hole matter waves in graphene, etc. They are the exact analogue of the critical points found by Van Hove (1953) for phonon dispersion relations in crystals. We therefore term them resonance Van Hove singularities. The importance of these singularities in wave kinetics depends on the dimension of phase space $D = (N - 2)d$ (here d is physical space dimension and N is the number of waves in resonance) and the degree of degeneracy of the critical points. See Chap. 4 for more details on the varying consequences of different types of singularities.

We outline the contents of this dissertation here, which can be divided into two parts. In the first part (Chap. 2), we show that the well-known Peierls equation (Peierls, 1929) is not the correct limit equation for wave-kinetic theory. We then systematize the derivation of the multi-mode hierarchy equations (with some details presented in Appendices A and B) and completely classify all the realizable solutions of our multi-mode equations. We exploit these results to discuss the possibilities of explaining intermittency and non-Gaussian statistics of wave turbulence within the kinetic description. In the second part of this dissertation, we investigate the phase measure

CHAPTER 1. INTRODUCTION

and the impact of resonance Van Hove singularities on the validity of wave-kinetic theory. The technical details on the construction of the phase measure are discussed in Appendix C. We study the existence of resonance singularities in many different wave systems in Chap. 3 and their physical consequences in Chap. 4. We discuss both generally and concretely the effects of the singularities on the kinetic theory, which can range from none at all, to moderate, to quite destructive. Finally, when the standard kinetic equation breaks down, we develop a new singular wave kinetics. The important example here is the electron-hole plasma in graphene (with details on the perturbative derivation of the quantum Boltzmann equation given in Appendix D). We discuss approaches from the pioneering work of Newell and Aucoin (1971) on multi-scale perturbation theory for acoustic waves and field-theoretic methods of L'vov *et al.* (1997) based on exact Schwinger-Dyson integral equations for the wave dynamics in section 4.3. In Chap. 5, we conclude the dissertation with a summary of our results and the outlook for future work. In particular, we discuss the generalization of the spectrum and of the kinetic equation to systems with spatially inhomogeneous statistics. Some preliminary results on this problem are discussed in Appendices E and F.

Chapter 2

Multi-Mode Hierarchy Equations

2.1 Summary of the Main Results

Wave-kinetic theory has traditionally focused on the wavevector spectrum, which is expected to satisfy the wave-kinetic equation in the limit of a continuum of weakly interacting, phase-incoherent waves (Zakharov *et al.*, 1992). However, recent very interesting works of Jakobsen and Newell (2004) and Choi *et al.* (2005a,b) have studied higher-order fluctuations of wave amplitudes by deriving equations for probability density functions (PDF's) in this same kinetic limit. These works generalized the results of a pioneering study of Zaslavskii and Sagdeev (1967), who obtained in some special 3-wave systems a set of evolution equations for multi-mode PDF's of wave amplitudes and phases. These are analogues of the equations found even earlier by Peierls (1929) and Brout and Prigogine (1956) for phonons (sound waves) in anharmonic crystals. The recent works cast new light on some outstanding problems of wave turbulence. On the one hand, the papers of Jakobsen and Newell (2004) and Choi *et al.* (2005a,b) have made an important contribution to the foundations of wave-kinetic theory, by showing that the “random phase” and “random phases & amplitudes” properties of initial wave fields are preserved in time by their multi-mode equations. Another important result of Jakobsen and Newell (2004) and Choi *et al.* (2005a,b) is a closed equation for the 1-mode

CHAPTER 2. MULTI-MODE HIERARCHY EQUATIONS

PDF's of the independent wave amplitudes. These equations can have as solutions 1-mode PDF's that are far from Gaussian, especially when the equations are supplemented with boundary conditions and additional terms to represent strongly nonlinear process, such as wave-breaking, that lie outside the validity of weakly-interacting wave kinetics (Choi *et al.*, 2005b; Nazarenko *et al.*, 2010). These results show promise to explain observations of intermittency and anomalous scaling in some recent experiments (Falcon *et al.*, 2007; Nazarenko *et al.*, 2010) and simulations (Yokoyama, 2004) of gravity-capillary wave turbulence, especially for wavevector regimes where such intermittency was not previously expected (Connaughton *et al.*, 2003).

Unfortunately, the Peierls equations for multi-mode PDF's are not correct for wave kinetics. As we shall show in this chapter, these equations have no asymptotic validity in the standard limit of a continuum of weakly interacting, incoherent waves. The works of Jakobsen and Newell (2004) and Choi *et al.* (2005a,b) made errors in estimating the sizes of relevant terms, which we shall discuss in detail in section 2.5. Using the same methods as theirs but with a correct estimation of the terms, we shall obtain a novel set of multi-mode equations distinct from the Peierls equations. On the other hand, we shall show using these new multi-mode equations that the 1-mode PDF equations obtained by Jakobsen and Newell (2004) and Choi *et al.* (2005a,b) *are* correct, under the assumption that initial wave modes have statistically-independent random amplitudes as well as phases. More generally, we shall classify all possible realizable solutions of the new multi-mode equations, for initial conditions with independent (and uniform) random phases but with no assumption on the statistics of initial wave amplitudes. We find that *the most general solutions correspond to “super-ensembles” of solutions of the wave-kinetic equations with random initial conditions for the spectrum or with random forcings*. This represents another possible mechanism for intermittency and non-Gaussian distributions by a “super-turbulence” of chaotic or stochastic solutions of the kinetic equations. As we discuss in detail in section 2.7, existing results on linear stability of Kolmogorov cascade solutions of the wave-kinetic equations do not rule out transition to such “super-turbulence.” In fact, this possibility was anticipated in a review of the stability theory by Zakharov *et al.* (1992, section 4.2.2),

CHAPTER 2. MULTI-MODE HIERARCHY EQUATIONS

who referred to this possibility as “secondary turbulence”. The results of this chapter show that this is the *only* possibility for explaining intermittency and anomalous scaling of wave turbulence strictly within the wave kinetics framework.

The failure of the Peierls equation will be shown below by specific, detailed calculations, but it can be understood on the basis of simple, general considerations. It will be useful to present such arguments here as a preliminary to the concrete calculations. This will also permit us to give an overview of the important new concepts, tools and results of this chapter. We must begin with a brief summary of the main results of Jakobsen and Newell (2004) and Choi *et al.* (2005a) for a general Hamiltonian dynamics with 3-wave interactions:

$$\dot{a}_{\mathbf{k}}^{\sigma} = \epsilon \sum_{\sigma_1, \sigma_2} \sum_{\mathbf{k}_1, \mathbf{k}_2} L_{\mathbf{k}, \mathbf{k}_1, \mathbf{k}_2}^{\sigma, \sigma_1, \sigma_2} a_{\mathbf{k}_1}^{\sigma_1} a_{\mathbf{k}_2}^{\sigma_2} e^{i(\sigma_1 \omega(\mathbf{k}_1) + \sigma_2 \omega(\mathbf{k}_2) - \sigma \omega(\mathbf{k}))t} \delta_{\sigma_1 \mathbf{k}_1 + \sigma_2 \mathbf{k}_2, \sigma \mathbf{k}}$$

where the wave triplet nonlinear interaction $L_{\mathbf{k}_1, \mathbf{k}_2, \mathbf{k}_3}^{\sigma_1, \sigma_2, \sigma_3} = 3i\sigma_1 H_{\mathbf{k}_1, \mathbf{k}_2, \mathbf{k}_3}^{-\sigma_1, \sigma_2, \sigma_3}$ in terms of the coefficient of the cubic term in the Hamiltonian and where the summations range over wavevectors $\mathbf{k} \in \frac{2\pi}{L}\mathbb{Z}^d$ and a degeneracy index $\sigma = \pm 1$, with L the side-length of a periodic box containing the wave system. For a systematic discussion of the notations used in this chapter, see section 2.2. The analysis of Jakobsen and Newell (2004) and Choi *et al.* (2005a) is based on action-angle variables $(J_{\mathbf{k}}, \varphi_{\mathbf{k}})$ for the linear wave dynamics, defined by $a_{\mathbf{k}}^{\sigma} = \sqrt{J_{\mathbf{k}}} e^{i\sigma \varphi_{\mathbf{k}}}$. Note that the standard spectral density is related to the action variables as

$$n(\mathbf{k}) = \lim_{L \rightarrow \infty} \left(\frac{L}{2\pi} \right)^d \langle J_{\mathbf{k}} \rangle$$

in the infinite-volume limit, with total wave action given by $N = \int d^d k n(\mathbf{k})$. Jakobsen and Newell (2004) and Choi *et al.* (2005a) exploit a generating functional for action and angle variables, defined by

$$\mathcal{Z}_L(\lambda, \mu) = \left\langle \exp \left(\sum_{\mathbf{k}} i\lambda_{\mathbf{k}} J_{\mathbf{k}} + i\mu_{\mathbf{k}} \varphi_{\mathbf{k}} \right) \right\rangle. \quad (2.1)$$

CHAPTER 2. MULTI-MODE HIERARCHY EQUATIONS

In the large-box limit ($L \rightarrow \infty$) followed by the weak nonlinearity limit ($\epsilon \rightarrow 0$), for an initial distribution with independent, uniform phases, this generating function is claimed to satisfy the Peierls equation in the form

$$\frac{d\mathcal{Z}}{d\tau} = -6\pi i \delta_{\mu,0} \sum_{\mathbf{k}, \underline{\sigma}} |H_{\mathbf{k}}^{\underline{\sigma}}|^2 \delta^d(\underline{\sigma} \cdot \mathbf{k}) \delta(\underline{\sigma} \cdot \omega(\mathbf{k})) (\underline{\sigma} \cdot \lambda_{\mathbf{k}}) \partial_{\lambda_{\mathbf{k}_1}} \partial_{\lambda_{\mathbf{k}_2}} \partial_{\lambda_{\mathbf{k}_3}} (\underline{\sigma} \cdot \lambda_{\mathbf{k}}) \mathcal{Z} \quad (2.2)$$

with $\underline{\sigma} = (\sigma_1, \sigma_2, \sigma_3)$ and $\mathbf{k} = (\mathbf{k}_1, \mathbf{k}_2, \mathbf{k}_3)$, where $\tau = \epsilon^2 t$ is the nonlinear time. From this equation, Jakobsen and Newell (2004) and Choi *et al.* (2005a) derived results on the higher-order fluctuations and statistical distributions of the wave mode amplitudes.

To see that the results, as stated above, cannot be asymptotically correct, consider the limiting behavior of the generating functional (2.1) when the field $a_{\mathbf{k}}$ is assumed to be “RPA”, i.e. to have amplitudes and phases for distinct Fourier modes given by mutually independent random variables. In that case, the generating functional must factorize for all independent variables, in particular for the amplitudes, as:

$$\mathcal{Z}_L(\lambda, \mu = 0) = \left\langle \exp \left(\sum_{\mathbf{k}} i \lambda_{\mathbf{k}} J_{\mathbf{k}} \right) \right\rangle = \prod_{\mathbf{k}} \left\langle \exp (i \lambda_{\mathbf{k}} J_{\mathbf{k}}) \right\rangle, \quad (2.3)$$

where each factor is a 1-mode generating function $\mathcal{Z}^{(1)}(\lambda_{\mathbf{k}}; \mathbf{k}) = \left\langle \exp (i \lambda_{\mathbf{k}} J_{\mathbf{k}}) \right\rangle$. However, the definition of the spectrum implies that the rescaled variable

$$\tilde{J}_{\mathbf{k}} := (L/2\pi)^d J_{\mathbf{k}} \quad (2.4)$$

must be $O(1)$ in the limit as $L \rightarrow \infty$. For the 1-mode generating function this gives, employing the cumulant expansion, the result:

$$\mathcal{Z}^{(1)}(\lambda_{\mathbf{k}}; \mathbf{k}) = \left\langle \exp \left(i \lambda_{\mathbf{k}} \left(\frac{2\pi}{L} \right)^d \tilde{J}_{\mathbf{k}} \right) \right\rangle = \exp \left(\sum_{p=1}^{\infty} \frac{i^p}{p!} \left(\frac{2\pi}{L} \right)^{pd} \lambda_{\mathbf{k}}^p \langle \tilde{J}_{\mathbf{k}}^p \rangle^c \right), \quad (2.5)$$

CHAPTER 2. MULTI-MODE HIERARCHY EQUATIONS

where $\langle \tilde{J}_{\mathbf{k}}^p \rangle^c$ is the p th-order cumulant. Inserting back into the product (2.3), one obtains

$$\mathcal{Z}_L(\lambda, \mu = 0) = \exp \left(\sum_{p=1}^{\infty} \frac{i^p}{p!} \left(\frac{2\pi}{L} \right)^{pd} \sum_{\mathbf{k}} \lambda_{\mathbf{k}}^p \langle \tilde{J}_{\mathbf{k}}^p \rangle^c \right). \quad (2.6)$$

Now assume that $\lambda_{\mathbf{k}} = \lambda(\mathbf{k})$ for some smooth function $\lambda(\mathbf{k})$. Since for $L \rightarrow \infty$

$$\left(\frac{2\pi}{L} \right)^{pd} \sum_{\mathbf{k}} \lambda^p(\mathbf{k}) \langle \tilde{J}_{\mathbf{k}}^p \rangle^c \sim \left(\frac{2\pi}{L} \right)^{(p-1)d} \int d^d k \lambda^p(\mathbf{k}) \langle \tilde{J}_{\mathbf{k}}^p \rangle^c, \quad (2.7)$$

the contributions of p th-order cumulants are $O(L^{-d(p-1)})$. Only the $p = 1$ contribution $n(\mathbf{k}) = \langle \tilde{J}_{\mathbf{k}} \rangle$ survives for very large L

$$\mathcal{Z}_L(\lambda, \mu = 0) = \exp \left(i \int d^d k \lambda(\mathbf{k}) n(\mathbf{k}) + O(L^{-d}) \right) \xrightarrow{L \rightarrow \infty} \exp \left(i \int d^d k \lambda(\mathbf{k}) n(\mathbf{k}) \right). \quad (2.8)$$

Thus, the generating functional $\mathcal{Z}_L(\lambda, \mu)$ of an RPA field is completely determined by its spectrum $n(\mathbf{k})$ in the limit as $L \rightarrow \infty$ and it then contains no information about higher-order fluctuations. This result, which we have derived here assuming existence of all higher-order cumulants, can be proved under much weaker assumptions (see section 2.3).

There is a simple interpretation of the above limit in terms of the *empirical spectrum*, defined as

$$\hat{n}_L(\mathbf{k}) = \left(\frac{2\pi}{L} \right)^d \sum_{\mathbf{k}_1 \in \Lambda_L^*} \tilde{J}_{\mathbf{k}_1} \delta^d(\mathbf{k} - \mathbf{k}_1).$$

For an RPA field, this quantity is a sum of a large number of independent variables. It is exactly analogous to the “Klimontovich density” or empirical 1-particle density in the kinetic theory of gases (Klimontovich, 1967). Unlike the usual spectrum $n(\mathbf{k})$, the empirical spectrum is a random variable that incorporates the information about amplitude fluctuations. The amplitude generating function

CHAPTER 2. MULTI-MODE HIERARCHY EQUATIONS

$\mathcal{Z}_L(\lambda) = \mathcal{Z}_L(\lambda, \mu = 0)$ is just the characteristic functional of the empirical spectrum:

$$\mathcal{Z}_L(\lambda) = \left\langle \exp \left(i \int d^d k \lambda(\mathbf{k}) \hat{n}_L(\mathbf{k}) \right) \right\rangle. \quad (2.9)$$

The previous limiting result for $\mathcal{Z}_L(\lambda)$ is mathematically equivalent to the statement that the empirical spectrum has a *deterministic* limit for $L \rightarrow \infty$ which is just the usual spectrum:

$$\lim_{L \rightarrow \infty} \hat{n}_L(\mathbf{k}) = n(\mathbf{k}).$$

This limit is a probabilistic law of large numbers for the empirical spectrum. There is a precisely analogous law of large numbers for the empirical 1-particle distribution in the low-density limit for the kinetic theory of gases, as first shown by Lanford (1975, 1976).

The above results should hold not only for RPA fields at initial times, but also for the evolved fields in the kinetic regime of wave turbulence, if the RPA property is propagated in time as expected. For example, Choi *et al.* (2005b, section 5) and Nazarenko (2011, section 11.4) argue that the RPA property will be preserved in a somewhat weaker form. As we shall discuss in detail below (see eq.(2.29)), these weaker forms still suffice to derive the limiting exponential expression (2.8) for the generating functional. However, the Peierls equation does not have such exponential solutions. We shall see that when carried out carefully, with due regard to the scaling of various terms with ϵ and L , the standard analytical methods of wave-kinetic theory yield *not* the Peierls equation in the limit as first $L \rightarrow \infty$ then $\epsilon \rightarrow 0$, but instead the following equation:

$$\begin{aligned} \dot{\mathcal{Z}}[\lambda, \mu] = & -36i\pi\delta_{\mu,0} \sum_{\underline{\sigma}=(-1,\sigma_2,\sigma_3)} \int d^d k_1 d^d k_2 d^d k_3 \delta^d(\underline{\sigma} \cdot \underline{\mathbf{k}}) \delta(\underline{\sigma} \cdot \omega(\underline{\mathbf{k}})) |H_{\underline{\mathbf{k}}}^{\underline{\sigma}}|^2 \\ & \times \lambda(\mathbf{k}_1) \left\{ \frac{\delta^2 \mathcal{Z}}{\delta \lambda(\mathbf{k}_2) \delta \lambda(\mathbf{k}_3)} - \sigma_2 \frac{\delta^2 \mathcal{Z}}{\delta \lambda(\mathbf{k}_1) \delta \lambda(\mathbf{k}_3)} - \sigma_3 \frac{\delta^2 \mathcal{Z}}{\delta \lambda(\mathbf{k}_1) \delta \lambda(\mathbf{k}_2)} \right\}. \end{aligned}$$

This equation will be justified in detail in section 2.5. Here we note only that it indeed differs from the Peierls equation. It contains only a subset of the terms in the Peierls equation, lacking in

CHAPTER 2. MULTI-MODE HIERARCHY EQUATIONS

particular all the terms involving third-order derivatives in λ . The important property of the above corrected equation is that it has solutions of exponential form

$$\mathcal{Z}[\lambda, \mu, \tau] = \exp \left(i \int d^d k \lambda(\mathbf{k}) n(\mathbf{k}, \tau) \right)$$

where $n(\mathbf{k}, \tau)$ solves the classical wave-kinetic equation, *if* the initial conditions $\mathcal{Z}[\lambda, \mu, \tau = 0]$ are also of this exponential form. As we have discussed above, this exponential form indeed holds if the initial conditions are RPA fields. The property of preserving exponential solutions implies a law of large-numbers for the empirical spectrum $\hat{n}_L(\mathbf{k}, \tau)$ at times $\tau > 0$ and is equivalent to the “propagation of chaos” by the BBGKY hierarchy in the kinetic limit for gases.

The analogy of kinetic wave turbulence with the kinetic theory of gases is in fact quite close. As we shall show below, the above equation for \mathcal{Z} is equivalent to a hierarchy of equations for M -point correlation functions of the empirical spectrum, which is exactly analogous to the “Boltzmann hierarchy” obtained from the BBGKY hierarchy for low-density gases (Lanford, 1975, 1976). Just as the Boltzmann hierarchy has factorized solutions for factorized initial conditions, so does the kinetic wave hierarchy for all multi-point spectral correlation functions. The factors in both cases solve the relevant kinetic equation, which satisfies an H -theorem corresponding to positive entropy production. For both hierarchies the general solutions without assuming factorized initial data are “super-statistical solutions” which represent statistical mixtures of factorized solutions. This was first discussed for the Boltzmann hierarchy by Spohn (1984). For wave turbulence these “super-statistical solutions” of the spectral hierarchy correspond to ensembles of solutions $n(\mathbf{k}, \tau)$ of the classical wave-kinetic equation with random initial conditions $n_0(\mathbf{k})$. We shall discuss in this chapter both the mathematical derivation and the physical relevance of the “super-statistical solutions”. These are a possible source of non-Gaussian statistics and intermittency not widely appreciated in the wave turbulence literature.

Previous attempts to calculate intermittency effects within wave-kinetic theory have em-

CHAPTER 2. MULTI-MODE HIERARCHY EQUATIONS

ployed the Peierls equation or its reduced forms for the PDFs of a finite number of modes (Choi *et al.*, 2005a,b, 2009). If the Peierls equation is not asymptotically valid in the usual wave-kinetic limit (first $L \rightarrow \infty$, then $\epsilon \rightarrow 0$), then does this mean that the previously claimed results for the finite-mode PDF's are also incorrect? The answer is yes, but fortunately only partially. The joint PDF of a set of M wavevector modes $\tilde{J}_{\mathbf{k}_1}, \dots, \tilde{J}_{\mathbf{k}_M}$ is characterized by its Fourier transform, the M -mode generating function:

$$\mathcal{Z}^{(M)}(\lambda_1, \dots, \lambda_M, \mu = 0; \mathbf{k}_1, \dots, \mathbf{k}_M) = \left\langle \exp \left(\sum_{m=1}^M i\lambda_m \tilde{J}_{\mathbf{k}_m} \right) \right\rangle.$$

We find that these objects do not individually satisfy closed equations but instead satisfy a hierarchy of equations that link M -mode functions to $(M+1)$ - and $(M+2)$ -mode functions:

$$\begin{aligned} \dot{\mathcal{Z}}^{(M)} = & -36i\pi \sum_{j=1}^M \sum_{\bar{\sigma}_2, \bar{\sigma}_3} \int d^d \bar{k}_2 d^d \bar{k}_3 \delta^d(\underline{\sigma} \cdot \underline{\mathbf{k}}_j) \delta(\underline{\sigma} \cdot \omega(\underline{\mathbf{k}}_j)) |H_{\underline{\mathbf{k}}_j}^{\underline{\sigma}}|^2 \\ & \times \left\{ \left(\lambda_j + \lambda_j^2 \frac{\partial}{\partial \lambda_j} \right) \frac{\partial^2 \mathcal{Z}^{(M+2)}}{\partial \bar{\lambda}_2 \partial \bar{\lambda}_3} \Big|_{\bar{\lambda}_2 = \bar{\lambda}_3 = 0} - \bar{\sigma}_2 \lambda_j \frac{\partial \mathcal{Z}^{(M+1)}}{\partial \bar{\lambda}_3 \partial \lambda_j} \Big|_{\bar{\lambda}_3 = 0} - \bar{\sigma}_3 \lambda_j \frac{\partial \mathcal{Z}^{(M+1)}}{\partial \bar{\lambda}_2 \partial \lambda_j} \Big|_{\bar{\lambda}_2 = 0} \right\}. \end{aligned} \quad (2.10)$$

with the notations $\underline{\sigma} = (-1, \bar{\sigma}_2, \bar{\sigma}_3)$ and $\underline{\mathbf{k}}_j = (\mathbf{k}_j, \bar{\mathbf{k}}_2, \bar{\mathbf{k}}_3)$. The equations in this hierarchy can also be obtained from the Peierls equation, by setting all except M of the λ 's equal to 0 and by retaining only a subset of terms. As in the previous equation for the generating functional, no third-order derivatives in λ 's occur but now there are terms involving $\lambda_j^2 \partial / \partial \lambda_j$ that were absent in that equation. The above hierarchy for the M -mode generating functions is equivalent to a hierarchy for the joint PDF's $\mathcal{P}^{(M)}(s_1, \dots, s_M; \mathbf{k}_1, \dots, \mathbf{k}_M)$ of M Fourier modes $\mathbf{k}_1, \dots, \mathbf{k}_M$:

$$\dot{\mathcal{P}}^{(M)} + \sum_{j=1}^M \frac{\partial}{\partial s_j} \mathcal{F}_j^{(M)} = 0, \quad (2.11)$$

CHAPTER 2. MULTI-MODE HIERARCHY EQUATIONS

where, with the same notations as above,

$$\begin{aligned} \mathcal{F}_j^{(M)} = & -36\pi s_j \sum_{\underline{\sigma}=(-1, \bar{\sigma}_2, \bar{\sigma}_3)} \int d^d \bar{k}_2 d^d \bar{k}_3 \delta^d(\underline{\sigma} \cdot \underline{\mathbf{k}}_j) \delta(\underline{\sigma} \cdot \omega(\underline{\mathbf{k}}_j)) |H_{\underline{\mathbf{k}}_j}^{\underline{\sigma}}|^2 \\ & \left[\int d\bar{s}_2 d\bar{s}_3 \frac{\partial \mathcal{P}^{(M+2)}}{\partial s_j}(s_1, \dots, s_M, \bar{s}_2, \bar{s}_3) \bar{s}_2 \bar{s}_3 \right. \\ & \left. + \bar{\sigma}_2 \int d\bar{s}_2 \mathcal{P}^{(M+1)}(s_1, \dots, s_M, \bar{s}_3) \bar{s}_3 + \bar{\sigma}_3 \int d\bar{s}_2 \mathcal{P}^{(M+1)}(s_1, \dots, s_M, \bar{s}_2) \bar{s}_2 \right]. \end{aligned} \quad (2.12)$$

Previously proposed closed equations for multi-mode equations, e.g. for $M = 2$ in Choi *et al.* (2009), are not asymptotically valid in the usual kinetic limit for wave turbulence.

On the other hand, the one-mode equation that was derived by Jakobsen and Newell (2004) and Choi *et al.* (2005a) for the PDF $P(s, \tau; \mathbf{k}) = \mathcal{P}^{(1)}(s, \tau; \mathbf{k})$ of a single amplitude $\tilde{J}_{\mathbf{k}}$:

$$\frac{\partial}{\partial \tau} P = \frac{\partial}{\partial s} \left[s \left(\eta_{\mathbf{k}} \frac{\partial P}{\partial s} + \gamma_{\mathbf{k}} P \right) \right] \quad (2.13)$$

is obtained from the above hierarchy for factorized solutions of the form:

$$\mathcal{P}^{(M)}(s_1, \dots, s_M, \tau; \mathbf{k}_1, \dots, \mathbf{k}_M) = \prod_{m=1}^M P(s_m, \tau; \mathbf{k}_m). \quad (2.14)$$

The coefficients $\eta_{\mathbf{k}}$, $\gamma_{\mathbf{k}}$ that appear also in the kinetic equation $\dot{n}_{\mathbf{k}} = \eta_{\mathbf{k}} - \gamma_{\mathbf{k}} n_{\mathbf{k}}$ are obtained from the condition $n_{\mathbf{k}} = \int ds s P(s; \mathbf{k})$ and the standard wavevector integrals over products of n . The one-mode equation is thus a nonlinear Fokker-Planck equation in the sense of McKean (1966). Factorized solutions of the form (2.14) are obtained for factorized initial data, corresponding to RPA fields. The hierarchy thus preserves in this sense the statistical independence of amplitudes. Just as for the spectral hierarchy, this factorization property of solutions implies a law of large numbers for *empirical 1-mode PDFs*

$$\hat{P}_L(s, \Delta, t) = \frac{1}{N_L(\Delta)} \sum_{\mathbf{k} \in \frac{2\pi}{L} \mathbb{Z}^d \cap \Delta} \delta(s - \tilde{J}_{\mathbf{k}})$$

with $\Delta \subset \mathbb{R}^d$ a subset of continuous wavevectors and with $N_L(\Delta)$ the number of elements in $\frac{2\pi}{L} \mathbb{Z}^d \cap \Delta$.

CHAPTER 2. MULTI-MODE HIERARCHY EQUATIONS

Also as for the spectral hierarchy, the general solutions of the PDF hierarchy are “super-statistical solutions” that correspond to ensembles of solutions of the 1-mode equation (2.13) with random initial conditions $P_0(s; \mathbf{k})$. As we shall discuss, such ensembles may be physically relevant to explain non-Gaussian statistics in weakly nonlinear wave systems if the solutions of (2.13) themselves become random, either through fluctuating driving forces or internal chaos/turbulence.

2.2 Model and Notations

We summarize here briefly the class of models considered and the notations employed in this chapter. We consider a system consisting of a complex wavefield $u(\mathbf{x}, t)$, for simplicity, in a d -dimensional periodic cube with side L . As in Jakobsen and Newell (2004) and Choi *et al.* (2005a), we assume that there is a maximum wavenumber k_{\max} , to avoid ultraviolet divergences. This can be achieved by a lattice regularization with spacing $a = L/M$, for some large integer M , so that $k_{\max} = \pi/a$. The location variable \mathbf{x} then ranges over the physical space

$$\Lambda_L = a\mathbb{Z}_M^d \quad (2.15)$$

with the usual notation \mathbb{Z}_M for the field of integers modulo M . This space has volume $V = L^d$ whose infinite-volume limit is

$$\Lambda = a\mathbb{Z}^d \quad (2.16)$$

with \mathbb{Z} for the field of integers. The dual space of wavevectors is

$$\Lambda_L^* = \frac{2\pi}{L}\mathbb{Z}_M^d \quad (2.17)$$

CHAPTER 2. MULTI-MODE HIERARCHY EQUATIONS

with $k_{\min} = 2\pi/L$. The total number of modes is $N = M^d$, so that spatial volume $V = Na^d$. The infinite-volume limit of Λ_L^* is the d -torus

$$\Lambda^* = \frac{2\pi}{a} \mathbb{T}^d = \left[-\frac{\pi}{a}, \frac{\pi}{a} \right]^d. \quad (2.18)$$

We use the following index notation

$$u^\sigma(\mathbf{x}) = \begin{cases} u(\mathbf{x}), & \sigma = +1 \\ u^*(\mathbf{x}), & \sigma = -1 \end{cases}$$

for u and its complex-conjugate u^* , following Jakobsen and Newell (2004). Likewise, we adopt their convention for (discrete) Fourier transform

$$A^\sigma(\mathbf{k}) = \frac{1}{N} \sum_{\mathbf{x} \in \Lambda_L} u^\sigma(\mathbf{x}, t) \exp(-i\sigma \mathbf{k} \cdot \mathbf{x})$$

so that $A^+(\mathbf{k})$ and $A^-(\mathbf{k})$ are complex conjugates. Notice that this quantity converges to the continuous Fourier transform $\frac{1}{L^d} \int_{[0,L]^d} d^d x u^\sigma(\mathbf{x}, t) \exp(-i\sigma \mathbf{k} \cdot \mathbf{x})$ in the limit $a \rightarrow 0$. The discrete inverse transform is

$$u^\sigma(\mathbf{x}) = \sum_{\mathbf{k} \in \Lambda_L^*} A^\sigma(\mathbf{k}) \exp(i\sigma \mathbf{k} \cdot \mathbf{x}).$$

We assume the dynamics is canonical Hamiltonian with a cubic Hamiltonian density (energy per volume) describing 3-wave interactions

$$H = H_0 + \delta H = \sum_{\sigma, \mathbf{k}} \omega(\mathbf{k}) A_{\mathbf{k}}^\sigma A_{\mathbf{k}}^{-\sigma} + \epsilon \sum_{\underline{\sigma}, \underline{\mathbf{k}}} H_{\underline{\mathbf{k}}}^\sigma A_{\mathbf{k}_1}^{\sigma_1} A_{\mathbf{k}_2}^{\sigma_2} A_{\mathbf{k}_3}^{\sigma_3} \delta_{\underline{\sigma}, \underline{\mathbf{k}}, \mathbf{0}}. \quad (2.19)$$

In Chaps. 3 and 4, we also consider 4-wave and quantum interactions. As in Jakobsen and Newell (2004), we denote triplets of variables by the notation $\underline{\sigma} = (\sigma_1, \sigma_2, \sigma_3)$, $\underline{\mathbf{k}} = (\mathbf{k}_1, \mathbf{k}_2, \mathbf{k}_3)$ and define the dot product $\underline{\sigma} \cdot \underline{\mathbf{k}} = \sigma_1 \mathbf{k}_1 + \sigma_2 \mathbf{k}_2 + \sigma_3 \mathbf{k}_3$. The Kronecker delta function in the triplet interaction

CHAPTER 2. MULTI-MODE HIERARCHY EQUATIONS

term enforces the symmetry of the dynamics under the group of (discrete) space translations. The interaction coefficients $H_{\underline{\mathbf{k}}}^{\sigma}$ are furthermore assumed to satisfy

$$H_{\underline{\mathbf{k}}}^{\sigma*} = H_{\underline{\mathbf{k}}}^{-\sigma} \quad \text{and} \quad H_{\underline{\mathbf{k}}}^{\sigma} = H_{\pi(\mathbf{k})}^{\pi(\sigma)} \quad (2.20)$$

for any permutation $\pi \in S_3$. The first condition guarantees the reality of the Hamiltonian and the second can always be assumed without loss of generality. The Hamiltonian equations of motion for the Fourier coefficients are

$$\frac{\partial A_{\mathbf{k}}^{\sigma}}{\partial t} = i\sigma \frac{\partial H}{\partial A_{\mathbf{k}}^{-\sigma}} = i\sigma\omega(\mathbf{k})A_{\mathbf{k}}^{\sigma} + \epsilon \sum_{\sigma_1, \sigma_2} \sum_{\mathbf{k}_1, \mathbf{k}_2} L_{\mathbf{k}, \mathbf{k}_1, \mathbf{k}_2}^{\sigma, \sigma_1, \sigma_2} A_{\mathbf{k}_1}^{\sigma_1} A_{\mathbf{k}_2}^{\sigma_2} \delta_{\sigma_1 \mathbf{k}_1 + \sigma_2 \mathbf{k}_2, \sigma \mathbf{k}}. \quad (2.21)$$

where $L_{\mathbf{k}, \mathbf{k}_1, \mathbf{k}_2}^{\sigma, \sigma_1, \sigma_2} = 3i\sigma H_{\mathbf{k}, \mathbf{k}_1, \mathbf{k}_2}^{-\sigma, \sigma_1, \sigma_2}$. It is useful to introduce action-angle variables for the linear dynamics, $J_{\mathbf{k}} = |A_{\mathbf{k}}^{\sigma}|^2$ and $\varphi_{\mathbf{k}} = \sigma \arg(A_{\mathbf{k}}^{\sigma})$, so that $A_{\mathbf{k}}^{\sigma} = \sqrt{J_{\mathbf{k}}} \psi_{\mathbf{k}}^{\sigma}$, where $\psi_{\mathbf{k}} = \exp(i\varphi_{\mathbf{k}})$. In these variables, the Liouville measure μ conserved by the Hamiltonian flow can be written variously as

$$d\mu = \prod_{\mathbf{k}} dq_{\mathbf{k}} dp_{\mathbf{k}} = \prod_{\mathbf{k}} \frac{1}{i} dA_{\mathbf{k}}^{+} dA_{\mathbf{k}}^{-} = \prod_{\mathbf{k}} dJ_{\mathbf{k}} d\varphi_{\mathbf{k}}$$

where the canonical momenta and coordinates are given by real and imaginary parts of $A_{\mathbf{k}}^{\sigma} = \frac{1}{\sqrt{2}}(p_{\mathbf{k}} + i\sigma q_{\mathbf{k}})$.

As usual in wave-kinetic theory, we introduce the “interaction representation”

$$a_{\mathbf{k}}^{\sigma} = A_{\mathbf{k}}^{\sigma} e^{-i\sigma\omega(\mathbf{k})t} \quad (2.22)$$

which removes the rapid wave oscillations. The Liouville measure is invariant under this transformation because of the rotation-invariance of the Haar measure on $\psi \in S^1$. We shall often use the

CHAPTER 2. MULTI-MODE HIERARCHY EQUATIONS

shorthand notation $a_1 = a_{\mathbf{k}_1}^{\sigma_1}$ together with $\sum_1 := \sum_{\sigma_1, \mathbf{k}_1}$ and

$$\begin{aligned}\omega_{23}^1 &:= -\sigma_1\omega(\mathbf{k}_1) + \sigma_2\omega(\mathbf{k}_2) + \sigma_3\omega(\mathbf{k}_3), \\ \delta_{23}^1 &:= \delta_{\sigma_1\mathbf{k}_1, \sigma_2\mathbf{k}_2 + \sigma_3\mathbf{k}_3}.\end{aligned}$$

The dynamical equation of motion can then be written succinctly as

$$\dot{a}_1 = \epsilon \sum_{2,3} L_{123} a_2 a_3 e^{i\omega_{23}^1 t} \delta_{23}^1. \quad (2.23)$$

2.3 Fields with Random Phases and Amplitudes

It is often assumed in derivations of wave-kinetic equations that initial fields have Fourier coefficients with random (and statistically independent) phases and amplitudes. Furthermore, these properties are expected to be preserved in time, in some suitable sense, in the wave-kinetic limit. See the discussions in Jakobsen and Newell (2004) and, particularly, Choi *et al.* (2005a,b). It is therefore important to review here the definitions and properties of such “RPA” fields¹. Our discussion shall be largely complementary to Choi *et al.* (2005a), emphasizing the probabilistic characteristics of such fields.

Consider then N complex-valued random variables $a_{\mathbf{k}}$, $\mathbf{k} \in \Lambda_L^*$ taken to be the Fourier coefficients of a random space field:

$$u(\mathbf{x}) = \sum_{\mathbf{k} \in \Lambda_L^*} a_{\mathbf{k}} \exp(i\mathbf{k} \cdot \mathbf{x}).$$

Here $a_{\mathbf{k}}$ corresponds to $a_{\mathbf{k}}^+ = A_{\mathbf{k}}^+$ in the previous section (no distinction need be made between the

¹More accurate acronyms would be “IUP” for “independent uniform phases” rather than “RP” and “IPA” for “independent phases & amplitudes” rather than “RPA”. However, we shall stick here to the abbreviations already employed in the literature.

CHAPTER 2. MULTI-MODE HIERARCHY EQUATIONS

two at time $t = 0$). It will be very important in what follows to work with normalized variables

$$\tilde{a}_{\mathbf{k}} = \left(\frac{L}{2\pi}\right)^{d/2} a_{\mathbf{k}}$$

which are assumed to remain finite in the large-box limit $L \rightarrow \infty$. As we shall remind the reader below, this normalization is required so that the spectrum of the random field is well defined in that limit. It is convenient to write the complex variables in polar coordinates $a_{\mathbf{k}} = \sqrt{J_{\mathbf{k}}} e^{i\varphi_{\mathbf{k}}}$ (action-angle variables) with the normalized action $\tilde{J}_{\mathbf{k}} = \left(\frac{L}{2\pi}\right)^d J_{\mathbf{k}}$. We use the notations $s_{\mathbf{k}}$ and $\xi_{\mathbf{k}}$ for possible values of the random variables $\tilde{J}_{\mathbf{k}} \in \mathbb{R}^+$ and $\psi_{\mathbf{k}} = e^{i\varphi_{\mathbf{k}}} \in S^1$. The Liouville measure of the previous section becomes

$$d\mu(s, \xi) = \prod_{\mathbf{k} \in \Lambda_L^*} ds_{\mathbf{k}} \frac{|d\xi_{\mathbf{k}}|}{2\pi} \quad (2.24)$$

suitably normalized. We define the N -mode joint probability density function $\mathcal{P}^{(N)}(s, \xi)$ with respect to Liouville measure, such that the average of the random variable $f(\tilde{J}, \psi)$ is given by

$$\langle f(\tilde{J}, \psi) \rangle = \int d\mu(s, \xi) \mathcal{P}^{(N)}(s, \xi) f(s, \xi)$$

where the integral is over (s, ξ) in the product space $(\mathbb{R}^+)^N \times (S^1)^N$.

Following Jakobsen and Newell (2004) and Choi *et al.* (2005a) we define $u(\mathbf{x})$ to be a *random-phase field* (RP) if $\psi_{\mathbf{k}} = e^{i\varphi_{\mathbf{k}}}$ for all $\mathbf{k} \in \Lambda_L^*$ are independent and identically distributed (i.i.d.) random variables, uniformly distributed over the unit circle S^1 in the complex plane. In terms of the joint PDF, this is equivalent to the condition that

$$\mathcal{P}^{(N)}(s, \xi) = \mathcal{P}^{(N)}(s)$$

independent of ξ . It is easy to see that an RP $u(\mathbf{x})$ is a homogeneous random field on Λ_L , statistically invariant under space-translations by the finite group $a\mathbb{Z}_M^d$. This follows from the rotation invariance

CHAPTER 2. MULTI-MODE HIERARCHY EQUATIONS

of the Haar measures $|d\xi_{\mathbf{k}}|/2\pi$ on the phase variables and by the representation of the translations $u(\mathbf{x}) \rightarrow u(\mathbf{x} + \mathbf{r})$ for $\mathbf{r} \in a\mathbb{Z}_M^d$ as phase-rotations: $\psi_{\mathbf{k}} \rightarrow \psi_{\mathbf{k}} e^{i\mathbf{k} \cdot \mathbf{r}}$. In the limit $L \rightarrow \infty$ the field $u_L(\mathbf{x})$ defined with appropriately chosen $\tilde{J}_{\mathbf{k},L}$ will converge to a homogeneous random field $u(\mathbf{x})$ invariant under translations by $a\mathbb{Z}^d$. The standard definition of the spectrum $n(\mathbf{k}) = \lim_{L \rightarrow \infty} (L/2\pi)^d \langle |a_{\mathbf{k},L}|^2 \rangle$ implies that one must choose

$$\lim_{L \rightarrow \infty} \langle \tilde{J}_{\mathbf{k},L} \rangle = n(\mathbf{k}), \quad (2.25)$$

for $\mathbf{k} \in \Lambda^* = [-k_{\max}, +k_{\max}]^d$, where $\mathbf{k}_L = \frac{\mathbf{k}L}{2\pi} \pmod{M} \cdot \frac{2\pi}{L} \in \Lambda_L^*$ converges to \mathbf{k} as $L = aM \rightarrow \infty$ (for fixed a). In this case, $u_L(\mathbf{x})$ converges in distribution as $L \rightarrow \infty$ to a homogeneous field $u(\mathbf{x})$ with spectrum $n(\mathbf{k})$.

Again following Choi *et al.* (2005a,b), we define $u(\mathbf{x})$ to be a *random-phase and amplitude field* (RPA) if $u(\mathbf{x})$ is RP and if also $\tilde{J}_{\mathbf{k}}$'s are mutually independent random variables for all $\mathbf{k} \in \Lambda_L^*$. This is equivalent to the factorization of the N -mode PDF into a product of 1-mode PDF's:

$$\mathcal{P}^{(N)}(s) = \prod_{\mathbf{k} \in \Lambda_L^*} P(s_{\mathbf{k}}; \mathbf{k}).$$

All homogeneous Gaussian random fields are RPA. Conversely, for any sequence of RPA fields satisfying condition (2.25) the field $u_L(\mathbf{x})$ converges in distribution to the homogeneous Gaussian field with mean zero and spectrum $n(\mathbf{k})$ as $L \rightarrow \infty$. See Kurbanmuradov (1995) for related rigorous results. Here we note only that

$$u_L(\mathbf{x}) = \left(\frac{2\pi}{L} \right)^{d/2} \sum_{\mathbf{k} \in \Lambda_L^*} \sqrt{\tilde{J}_{\mathbf{k},L}} \exp(i\mathbf{k} \cdot \mathbf{x} + i\varphi_{\mathbf{k}})$$

is a sum of N independent variables scaled by $1/\sqrt{N}$. It is important to emphasize that the Fourier coefficients $\tilde{a}_{\mathbf{k},L}$ can remain far from Gaussian in this limit. In physical space also there are non-vanishing cumulants for large but finite L . A curious property of RPA fields for finite L is the slow

CHAPTER 2. MULTI-MODE HIERARCHY EQUATIONS

decay of their cumulants in certain directions. For example, it is easy to calculate the 4th-order cumulant as

$$\begin{aligned} & \langle u(\mathbf{x}_1)u(\mathbf{x}_2)u^*(\mathbf{x}_3)u^*(\mathbf{x}_4) \rangle - [\langle u(\mathbf{x}_1)u^*(\mathbf{x}_3) \rangle \langle u(\mathbf{x}_2)u^*(\mathbf{x}_4) \rangle + (1 \leftrightarrow 2)] \\ &= \left(\frac{2\pi}{L}\right)^{2d} \sum_{\mathbf{k} \in \Lambda_L^*} [\langle \tilde{J}_{\mathbf{k}}^2 \rangle - 2\langle \tilde{J}_{\mathbf{k}} \rangle^2] e^{i\mathbf{k} \cdot (\mathbf{x}_1 + \mathbf{x}_2 - \mathbf{x}_3 - \mathbf{x}_4)} \\ &\sim \left(\frac{2\pi}{L}\right)^d \int d^d k [\langle \tilde{J}_{\mathbf{k}}^2 \rangle - 2\langle \tilde{J}_{\mathbf{k}} \rangle^2] e^{i\mathbf{k} \cdot (\mathbf{x}_1 + \mathbf{x}_2 - \mathbf{x}_3 - \mathbf{x}_4)} \end{aligned}$$

asymptotically as $L \rightarrow \infty$. As expected, this goes to zero as $O(L^{-d})$ for $L \rightarrow \infty$, but for finite L the cumulant is constant on the hyperplane $\mathbf{x}_1 + \mathbf{x}_2 = \mathbf{x}_3 + \mathbf{x}_4$, even when the pair of points $\mathbf{x}_1, \mathbf{x}_3$ are separated very far from the pair $\mathbf{x}_2, \mathbf{x}_4$, for example. This is in contrast to some more traditional derivations of wave-kinetic equations directly in infinite volume, which assume rapid spatial decay of higher-order cumulants (Benney and Newell, 1969).

A most important result for RPA fields is that the *empirical spectrum*

$$\hat{n}_L(\mathbf{k}) = \left(\frac{2\pi}{L}\right)^d \sum_{\mathbf{k}_1 \in \Lambda_L^*} \tilde{J}_{\mathbf{k}_1, L} \delta^d(\mathbf{k} - \mathbf{k}_1), \quad \mathbf{k} \in \Lambda^* \quad (2.26)$$

converges under the condition (2.25) to the deterministic spectrum $n(\mathbf{k})$ with probability going to 1 in the limit $L \rightarrow \infty$ (weak law of large numbers). It is worth sketching the simple proof. Note for any continuous function λ on Λ^* that

$$\int_{\Lambda^*} d^d k \lambda(\mathbf{k}) \hat{n}_L(\mathbf{k}) = \left(\frac{2\pi}{L}\right)^d \sum_{\mathbf{k}_1 \in \Lambda_L^*} \lambda(\mathbf{k}_1) \tilde{J}_{\mathbf{k}_1, L}.$$

Crucially,

$$\begin{aligned} & \left\langle \left| \left(\frac{2\pi}{L}\right)^d \sum_{\mathbf{k}_1 \in \Lambda_L^*} \lambda(\mathbf{k}_1) \tilde{J}_{\mathbf{k}_1} - \left(\frac{2\pi}{L}\right)^d \sum_{\mathbf{k}_1 \in \Lambda_L^*} \lambda(\mathbf{k}_1) n(\mathbf{k}_1) \right|^2 \right\rangle \\ &= \left(\frac{2\pi}{L}\right)^{2d} \sum_{\mathbf{k}_1 \in \Lambda_L^*} \lambda^2(\mathbf{k}_1) \langle |\tilde{J}_{\mathbf{k}_1} - n(\mathbf{k}_1)|^2 \rangle \end{aligned}$$

CHAPTER 2. MULTI-MODE HIERARCHY EQUATIONS

$$\sim \left(\frac{2\pi}{L}\right)^d \int d^d k \lambda^2(\mathbf{k}) \langle |\tilde{J}_{\mathbf{k}} - n(\mathbf{k})|^2 \rangle = O(L^{-d})$$

under the modest assumption that $\int d^d k \langle |\tilde{J}_{\mathbf{k}} - n(\mathbf{k})|^2 \rangle < \infty$. Since also $\lim_{L \rightarrow \infty} \left(\frac{2\pi}{L}\right)^d \sum_{\mathbf{k}_1 \in \Lambda_L^*} \lambda(\mathbf{k}_1) n(\mathbf{k}_1) = \int d^d k \lambda(\mathbf{k}) n(\mathbf{k})$, the L^2 -convergence follows

$$\lim_{L \rightarrow \infty} \left\langle \left| \int d^d k \lambda(\mathbf{k}) \hat{n}_L(\mathbf{k}) - \int d^d k \lambda(\mathbf{k}) n(\mathbf{k}) \right|^2 \right\rangle = 0$$

and thus $\int d^d k \lambda(\mathbf{k}) \hat{n}_L(\mathbf{k})$ converges in probability to $\int d^d k \lambda(\mathbf{k}) n(\mathbf{k})$ for every bounded, continuous

λ .² This is sufficient to infer that the amplitude generating function

$$\mathcal{Z}_L(\lambda) = \left\langle \exp \left(\sum_{\mathbf{k} \in \Lambda_L^*} i \lambda_{\mathbf{k}} J_{\mathbf{k}} \right) \right\rangle \quad (2.27)$$

satisfies³

$$\lim_{L \rightarrow \infty} \mathcal{Z}_L(\lambda) = \exp \left(i \int d^d k \lambda(\mathbf{k}) n(\mathbf{k}) \right) \quad (2.28)$$

with $n(\mathbf{k})$ the deterministic spectrum. The law of large numbers (LLN) derived above means that for RPA fields the empirical spectrum $\hat{n}_L(\mathbf{k})$ coincides with $n(\mathbf{k})$ at large L for almost every realization of the random phases and amplitudes, not just after averaging over these variables.

Notice that for the above result one does not actually need the full independence assumption

²Technically, the convergence is in the weak- \star topology for $\hat{n}_L(\mathbf{k}), n(\mathbf{k})$ as bounded, positive measures on Λ^* . More physically, the function $\lambda(\mathbf{k})$ may be taken to be a smooth kernel $G_\delta(\mathbf{k} - \mathbf{k}_0)$ of width δ centered around a particular wavevector \mathbf{k}_0 . The coarse-grained spectrum $\hat{n}_{L,\delta}(\mathbf{k}_0) = \int d^d k G_\delta(\mathbf{k} - \mathbf{k}_0) \hat{n}_L(\mathbf{k})$ can then be interpreted as the result of measuring the spectrum at \mathbf{k}_0 with a finite resolution δ in wavevector. The weak- \star topology implies the convergence of such coarse-grained spectra in the limit $L \rightarrow \infty$, when arbitrarily many wavevectors lie within distance δ of \mathbf{k}_0 .

³This is another standard result in probability theory, but, for completeness, we here recall the proof. Let $X_L = \int_{\Lambda^*} d^d k \lambda(\mathbf{k}) \hat{n}_L(\mathbf{k})$ and $x = \int_{\Lambda^*} d^d k \lambda(\mathbf{k}) n(\mathbf{k})$. For $\epsilon > 0$, write

$$\left| \langle e^{iX_L} - e^{ix} \rangle \right| \leq \left| \langle e^{i(X_L - x)} - 1 \rangle : |X_L - x| < \epsilon \right| + \left| \langle e^{i(X_L - x)} - 1 \rangle : |X_L - x| > \epsilon \right|$$

For any $\delta > 0$, one can choose ϵ so that $|e^{iz} - 1| < \delta$ when $|z| < \epsilon$. The first term is thus bounded by δ . By Chebyshev inequality the second term is bounded as

$$\left| \langle e^{i(X_L - x)} - 1 \rangle : |X_L - x| > \epsilon \right| \leq 2P(|X_L - x| > \epsilon) \leq \frac{2}{\epsilon^2} \langle |X_L - x|^2 \rangle \rightarrow 0$$

for fixed ϵ as $L \rightarrow \infty$. Thus,

$$\limsup_{L \rightarrow \infty} \left| \langle e^{iX_L} - e^{ix} \rangle \right| \leq \delta.$$

Since δ is arbitrary, it follows that $\lim_{L \rightarrow \infty} \langle e^{iX_L} \rangle = e^{ix}$.

CHAPTER 2. MULTI-MODE HIERARCHY EQUATIONS

in RPA, but only uncorrelated amplitudes:

$$\langle \tilde{J}_{\mathbf{k}_1} \tilde{J}_{\mathbf{k}_2} \rangle = \langle \tilde{J}_{\mathbf{k}_1} \rangle \langle \tilde{J}_{\mathbf{k}_2} \rangle, \quad \mathbf{k}_1 \neq \mathbf{k}_2.$$

An even weaker and more general condition can be stated in terms of the *M-mode correlation functions* of the empirical spectrum, defined as:

$$\mathcal{N}_L^{(M)}(\mathbf{k}_1, \dots, \mathbf{k}_M) = \langle \hat{n}_L(\mathbf{k}_1) \cdots \hat{n}_L(\mathbf{k}_M) \rangle.$$

Note that (2.25) implies that $\lim_{L \rightarrow \infty} \mathcal{N}_L^{(1)}(\mathbf{k}) = n(\mathbf{k})$. A careful examination of the previous proof shows that, in order to obtain the LLN for the empirical spectrum, it suffices that

$$\lim_{L \rightarrow \infty} [\mathcal{N}_L^{(2)}(\mathbf{k}_1, \mathbf{k}_2) - \mathcal{N}_L^{(1)}(\mathbf{k}_1) \mathcal{N}_L^{(1)}(\mathbf{k}_2)] = 0. \quad (2.29)$$

This condition is the analogue of the *Stosszahlansatz* invoked by Boltzmann to derive his kinetic equation. Under this assumption, all of the *M*-th order correlations that exist will factorize in the large-box limit:

$$\lim_{L \rightarrow \infty} \mathcal{N}_L^{(M)}(\mathbf{k}_1, \dots, \mathbf{k}_M) = \prod_{m=1}^M n(\mathbf{k}_m). \quad (2.30)$$

These observations go back to Lanford (1975, 1976) in his rigorous derivation of the Boltzmann equation. The results that we shall present below suggest that properties (2.25) and (2.29) for the wave field at the initial time, together with the RP property, are sufficient for the validity of the wave-kinetic equation and a LLN for the empirical spectrum at positive times.

RPA fields whose Fourier amplitudes possess the full independence property satisfy an even stronger law of large numbers for the *empirical 1-mode PDF*, which is defined as

$$\hat{P}_L(s; \mathbf{k}) = \left(\frac{2\pi}{L} \right)^d \sum_{\mathbf{k}_1 \in \Lambda_L^*} \delta(s - \tilde{J}_{\mathbf{k}_1}) \delta^d(\mathbf{k} - \mathbf{k}_1). \quad (2.31)$$

CHAPTER 2. MULTI-MODE HIERARCHY EQUATIONS

Assume that the limiting random variables $\tilde{J}_{\mathbf{k}} = \lim_{L \rightarrow \infty} \tilde{J}_{\mathbf{k}_L, L}$ of an RPA field exist and have PDF's $P(s; \mathbf{k})$ which are continuous in \mathbf{k} . Then an analogue of the previous argument implies that the random functions $\hat{P}_L(s; \mathbf{k})$ converge to $P(s; \mathbf{k})$ with probability approaching 1 as $L \rightarrow \infty$. This implies the previous LLN for the spectrum, since $\hat{n}_L(\mathbf{k}) = \int_0^\infty ds \, s \hat{P}_L(s; \mathbf{k})$ and $n(\mathbf{k}) = \int_0^\infty ds \, s P(s; \mathbf{k})$. Although the “empirical PDF” defined in (2.31) is mathematically very convenient, it is not a PDF for finite L . It is therefore more intuitive to use an alternative definition

$$\hat{P}_L(s; \Delta) = \frac{1}{N_L(\Delta)} \sum_{\mathbf{k} \in \Lambda_L^* \cap \Delta} \delta(s - \tilde{J}_{\mathbf{k}}), \quad (2.32)$$

for any open set $\Delta \subset \Lambda^*$ and with $N_L(\Delta)$ the number of elements in $\Lambda_L^* \cap \Delta$. This quantity is nearly the same as $\frac{1}{|\Delta|} \int_{\Delta} d^d k \, \hat{P}_L(s; \mathbf{k})$ for large L but it has the advantage that it defines a probability measure in s for each fixed Δ and L . Definition (2.32) also has a simple intuitive meaning, since it represents the instantaneous distribution of amplitudes of the large number of Fourier modes that reside in the set Δ for large box-size L . Under the same assumptions as above, it follows with probability going to 1 that

$$\lim_{L \rightarrow \infty} \hat{P}_L(s; \Delta) = \frac{1}{|\Delta|} \int_{\Delta} d^d k \, P(s; \mathbf{k}) \equiv P(s; \Delta).$$

As before, the essential property that is required for the above results to hold is a factorization property of *multi-mode PDF's*, defined for $\mathbf{k}_1, \dots, \mathbf{k}_M \in \Lambda^*$ by

$$\mathcal{P}_L^{(M)}(s_1, \dots, s_M; \mathbf{k}_1, \dots, \mathbf{k}_M) = \langle \delta(s_1 - \tilde{J}_{\mathbf{k}_{1,L}, L}) \cdots \delta(s_M - \tilde{J}_{\mathbf{k}_{M,L}, L}) \rangle.$$

The factorization property of the 2-mode PDF's for all pairs of distinct $\mathbf{k}_1, \mathbf{k}_2 \in \Lambda^*$

$$\lim_{L \rightarrow \infty} [\mathcal{P}_L^{(2)}(s_1, s_2; \mathbf{k}_1, \mathbf{k}_2) - \mathcal{P}_L^{(1)}(s_1; \mathbf{k}_1) \mathcal{P}_L^{(1)}(s_2; \mathbf{k}_2)] = 0 \quad (2.33)$$

CHAPTER 2. MULTI-MODE HIERARCHY EQUATIONS

suffices ⁴ to derive the LLN for the empirical PDF and also the factorization of the multi-mode PDF's

$$\lim_{L \rightarrow \infty} \mathcal{P}_L^{(M)}(s_1, \dots, s_M; \mathbf{k}_1, \dots, \mathbf{k}_M) = \prod_{m=1}^M P(s_m; \mathbf{k}_m)$$

for all integers $M \geq 2$ and distinct $\mathbf{k}_1, \dots, \mathbf{k}_M \in \Lambda^*$. The “asymptotic independence” property (2.33) is considerably weaker than strict RPA, permitting statistical dependence between Fourier modes at finite L . We shall discuss natural “microcanonical measures” in section 2.6.2 which satisfy the condition (2.33) but not the more stringent RPA condition.

In sections 2.5 and 2.6 we shall show that the above “generalized RPA” properties (2.30), (2.33) of initial conditions are preserved in time by the limiting wave-kinetic hierarchies.

2.4 Perturbation Expansion and Diagrammatics

Our derivations are quite similar to those of Choi *et al.* (2005a), but our model is somewhat more general in appearance. The major difference between our analysis and theirs, however, lies in a correct accounting of the size of the various terms in the limits as $L \rightarrow \infty$ and $\epsilon \rightarrow 0$.

⁴Since the proof is so similar to the one given previously, we give just a few details here. Because of our assumptions on $\tilde{J}_{\mathbf{k}} = \lim_{L \rightarrow \infty} \tilde{J}_{\mathbf{k}_L, L}$ it is easy to check that the average of the empirical PDF converges as $L \rightarrow \infty$:

$$\langle \hat{P}_L(s; \mathbf{k}) \rangle = \left(\frac{2\pi}{L} \right)^d \sum_{\mathbf{k}' \in \Lambda_L^*} \mathcal{P}_L^{(1)}(s; \mathbf{k}') \delta^d(\mathbf{k}' - \mathbf{k}) \rightarrow P(s; \mathbf{k}).$$

Therefore, in order to prove that $\hat{P}_L(s; \mathbf{k})$ converges in probability to $P(s; \mathbf{k})$, with convergence in the weak- \star topology on regular Borel measures, it is enough to show that

$$\lim_{L \rightarrow \infty} \left\langle \left| \int ds \int_{\Lambda^*} d^d k \varphi(s, \mathbf{k}) \hat{P}_L(s; \mathbf{k}) - \int ds \int_{\Lambda^*} d^d k \varphi(s, \mathbf{k}) \langle \hat{P}_L(s; \mathbf{k}) \rangle \right|^2 \right\rangle = 0$$

for any continuous function $\varphi(s, \mathbf{k})$ on $\mathbb{R}^+ \times \Lambda^*$ which vanishes as $s \rightarrow \infty$. Now a direct calculation of the above average shows that it equals

$$\left(\frac{2\pi}{L} \right)^{2d} \sum_{\mathbf{k}'_1, \mathbf{k}'_2 \in \Lambda_L^*} \int ds_1 \int ds_2 \varphi(s_1, \mathbf{k}'_1) \varphi(s_2, \mathbf{k}'_2) \left[P_L^{(2)}(s_1, s_2; \mathbf{k}'_1, \mathbf{k}'_2) - P_L^{(1)}(s_1; \mathbf{k}'_1) P_L^{(1)}(s_2; \mathbf{k}'_2) \right].$$

The bracketed expression for $\mathbf{k}'_1 = \mathbf{k}'_2$ is found to be

$$P_L^{(2)}(s_1, s_2; \mathbf{k}'_1, \mathbf{k}'_1) - P_L^{(1)}(s_1; \mathbf{k}'_1) P_L^{(1)}(s_2; \mathbf{k}'_1) = \delta(s_1 - s_2) P_L^{(1)}(s_1; \mathbf{k}'_1) - P_L^{(1)}(s_1; \mathbf{k}'_1) P_L^{(1)}(s_2; \mathbf{k}'_1)$$

so that its contribution to the average vanishes as $\sim \left(\frac{2\pi}{L} \right)^d \int_{\Lambda^*} d^d k \left\langle \left| \varphi(\tilde{J}_{\mathbf{k}}, \mathbf{k}) - \langle \varphi(\tilde{J}_{\mathbf{k}}, \mathbf{k}) \rangle \right|^2 \right\rangle$ for $L \rightarrow \infty$. Thus, to prove convergence, it must only be shown that the bracket term for $\mathbf{k}'_1 \neq \mathbf{k}'_2$ vanishes as $L \rightarrow \infty$. This is obviously true for RPA fields, when the bracket term for $\mathbf{k}'_1 \neq \mathbf{k}'_2$ is zero!

CHAPTER 2. MULTI-MODE HIERARCHY EQUATIONS

We shall focus on the multi-mode generating function for finite box-size L , defined as in Choi *et al.* (2005a) by

$$\mathcal{Z}_L[\lambda, \mu, T] = \left\langle \exp \left(\sum_{\mathbf{k} \in \Lambda_L^*} \lambda_{\mathbf{k}} J_{\mathbf{k}}(T) \right) \prod_{\mathbf{k} \in \Lambda^*} \psi_{\mathbf{k}}^{\mu_{\mathbf{k}}}(T) \right\rangle, \quad (2.34)$$

where $\lambda_{\mathbf{k}} \in \mathbb{R}$ and $\mu_{\mathbf{k}} \in \mathbb{Z}$ for all $\mathbf{k} \in \Lambda_{\mathbf{k}}^*$. The time T is free for the moment but will later be chosen to be a time intermediate between the wave-period and the nonlinear time-scale. This generating function is calculated perturbatively in the nonlinearity parameter ϵ at finite L , by expanding the solution of the dynamical equation

$$\dot{a}_1 = \epsilon \sum_{2,3} L_{123} a_2 a_3 e^{i\omega_{23}^1 t} \delta_{23}^1 \quad (2.35)$$

into a power series

$$a_1(T) = a_1(0) + \epsilon a_1^{(1)}(T) + \epsilon^2 a_1^{(2)}(T) + \mathcal{O}(\epsilon^3). \quad (2.36)$$

A straightforward calculation gives

$$a_1^{(0)} = a_1(0), \quad (2.37)$$

$$a_1^{(1)} = \sum_{2,3} L_{123} a_2^{(0)} a_3^{(0)} \Delta_T(\omega_{23}^1) \delta_{23}^1, \quad (2.38)$$

$$a_1^{(2)} = \sum_{2345} L_{123} L_{245} a_3^{(0)} a_4^{(0)} a_5^{(0)} E_T(\omega_{345}^1, \omega_{23}^1) \delta_{23}^1 \delta_{45}^2 + (2 \leftrightarrow 3) \quad (2.39)$$

We employ here the standard definitions (Benney and Newell, 1969):

$$\Delta_T(x) = \int_0^T \exp(ixt) dt, \quad E_T(x, y) = \int_0^T \Delta_t(x - y) \exp(iyt) dt.$$

The terms in this perturbative solution of the equations of motion can be represented by a version of

CHAPTER 2. MULTI-MODE HIERARCHY EQUATIONS

the Wyld diagram expansion (Zakharov and L'vov, 1975). In this technique the various contributions are represented by tree diagrams, as illustrated in Figs. 2.1, 2.2, 2.3 for the zeroth-, first- and second-order terms (eqs.(2.37)-(2.39)). In our conventions, similar to those of Choi *et al.* (2005a), a solid



Figure 2.1: Zeroth-order terms $a_1^{(0)+}$ and $a_1^{(0)-}$.

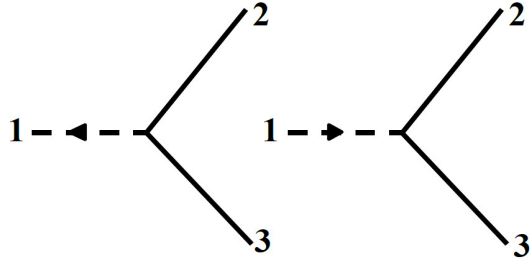


Figure 2.2: First-order terms $a_1^{(1)+}$ and $a_1^{(1)-}$.

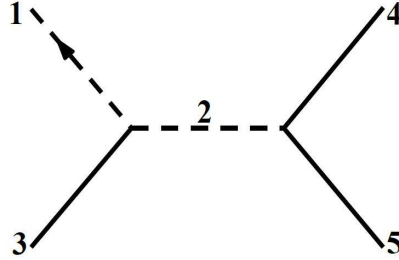


Figure 2.3: Second-order term $a_1^{(2)+}$.

line labeled with an integer j represents a factor $a_j^{(0)}$, whereas a dashed line indicates the absence of such a factor. An arrow is added to a solid line to indicate $\sigma_j = +1$ (“source”) when the arrow is pointed away from j and $\sigma_j = -1$ (“sink”) when the arrow is pointed toward j . The triple vertex labeled 1, 2, 3 represents a factor $L_{\mathbf{k}_1, \mathbf{k}_2, \mathbf{k}_3}^{\sigma_1, \sigma_2, \sigma_3} e^{\omega_{23}^1 t} \delta_{23}^1$ with $\sigma_1 = +1$ when the arrow points out of the vertex and $\sigma_1 = -1$ when the arrow points into the vertex. The times at each vertex are ordered causally, with the latest times at the “root” of the tree, here labeled by 1. When integrations are performed over all times from 0 to T consistent with this ordering, then the various contributions to the perturbative solution result.

CHAPTER 2. MULTI-MODE HIERARCHY EQUATIONS

The generating function is obtained perturbatively by substituting (2.36) and expanding to obtain

$$\mathcal{Z}_L[\lambda, \mu, T] = \mathcal{X}_L\{\lambda, \mu, T\} + \mathcal{X}_L^*\{\lambda, -\mu, T\} \quad (2.40)$$

with

$$\mathcal{X}_L\{\lambda, \mu, T\} = \mathcal{X}_L\{\lambda, \mu, 0\} + \left\langle \prod_{\mathbf{k} \in \Lambda^*} e^{\lambda_{\mathbf{k}} J_{\mathbf{k}}^{(0)}} [\epsilon \mathcal{J}_1 + \epsilon^2 (\mathcal{J}_2 + \mathcal{J}_3 + \mathcal{J}_4 + \mathcal{J}_5)] \right\rangle_J + \mathcal{O}(\epsilon^3), \quad (2.41)$$

where, as in Choi *et al.* (2005a),

$$\mathcal{J}_1 = \left\langle \prod_{\mathbf{k}} \psi_{\mathbf{k}}^{(0)\mu_{\mathbf{k}}} \sum_1 \left(\lambda_1 + \frac{\mu_1}{2J_1^{(0)}} \right) a_1^{(1)} a_1^{(0)*} \right\rangle_{\psi}, \quad (2.42)$$

$$\mathcal{J}_2 = \frac{1}{2} \left\langle \prod_{\mathbf{k}} \psi_{\mathbf{k}}^{(0)\mu_{\mathbf{k}}} \sum_1 \left(\lambda_1 + \lambda_1^2 J_1^{(0)} - \frac{\mu_1^2}{4J_1^{(0)}} \right) |a_1^{(1)}|^2 \right\rangle_{\psi}, \quad (2.43)$$

$$\mathcal{J}_3 = \left\langle \prod_{\mathbf{k}} \psi_{\mathbf{k}}^{(0)\mu_{\mathbf{k}}} \sum_1 \left(\lambda_1 + \frac{\mu_1}{2J_1^{(0)}} \right) a_1^{(2)} a_1^{(0)*} \right\rangle_{\psi}, \quad (2.44)$$

$$\mathcal{J}_4 = \left\langle \prod_{\mathbf{k}} \psi_{\mathbf{k}}^{(0)\mu_{\mathbf{k}}} \sum_1 \left(\frac{1}{2} \lambda_1^2 + \frac{\mu_1}{4J_1^{(0)2}} \left(\frac{\mu_1}{2} - 1 \right) + \frac{\lambda_1 \mu_1}{2J_1^{(0)}} \right) (a_1^{(1)} a_1^{(0)*})^2 \right\rangle_{\psi}, \quad (2.45)$$

$$\begin{aligned} \mathcal{J}_5 = \frac{1}{2} \left\langle \prod_{\mathbf{k}} \psi_{\mathbf{k}}^{(0)\mu_{\mathbf{k}}} \sum_{1 \neq 2} \left(\lambda_1 \lambda_2 (a_1^{(1)} a_1^{(0)*} + a_1^{(1)*} a_1^{(0)}) a_2^{(1)} a_2^{(0)*} \right. \right. \\ \left. \left. + \left(\lambda_1 + \frac{\mu_1}{4J_1^{(0)}} \right) \frac{\mu_2}{J_2^{(0)}} (a_2^{(1)} a_2^{(0)*} - a_2^{(1)*} a_2^{(0)}) a_1^{(1)} a_1^{(0)*} \right) \right\rangle_{\psi}. \end{aligned} \quad (2.46)$$

The various contributions before averaging over phases can be represented by diagrams, combining the tree diagrams for each of the factors by joining the trees with the same “root” indices. Each of the integer labels indicates an index to be summed over independently (except for the constraints imposed by delta-functions at the vertices). We illustrate this representation in Figs. 2.4 and 2.5 below for the first two contributions: The only contributions which survive the average over phases must have all phases summing to zero before averaging. This means that every $a^{(0)}$ factor must either pair with another factor $a^{(0)}$ so that their phases sum to zero or belong to a set of $a^{(0)}$ ’s that pair with a $\psi_{\mathbf{k}}^{(0)\mu_{\mathbf{k}}}$ factor so that the sum of all their phases is zero. The first we call an “internal coupling”, represented graphically by a solid line connecting the paired indices i, j which contributes

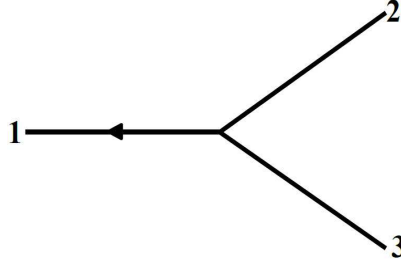


Figure 2.4: First-order term $\sum_1 (\lambda_1 + \frac{\mu_1}{2J_1}) a_1^{(1)} a_1^{(0)*}$.

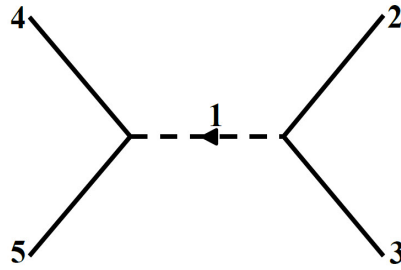


Figure 2.5: Second-order term $\sum_1 (\lambda_1 + \lambda_1^2 J_1 - \frac{\mu_1^2}{4J_1}) |a_1^{(1)}|^2$.

a factor $\delta_{\sigma_i + \sigma_j, 0} \delta_{\mathbf{k}_i, \mathbf{k}_j}$ after phase averaging. The second we call an “external coupling”, represented by joining all of the solid lines for indices i_1, i_2, \dots, i_p to a blob \bullet labelled a that represents the phase $\psi_{\mathbf{k}_a}^{(0)\mu_{\mathbf{k}_a}}$ which contributes a factor $\delta_{\sigma_{i_1} + \dots + \sigma_{i_p} + \mu_a, 0} \prod_{j=1}^p \delta_{\mathbf{k}_j, \mathbf{k}_a}$ after phase averaging. This graphical representation is essentially the same as that employed by Choi *et al.* (2005a). We illustrate the representation in Figs. 2.6 and 2.7 below for the terms in \mathcal{J}_1 and \mathcal{J}_2 which turn out to give the leading-order contributions to those quantities as $L \rightarrow \infty$. Note that solid lines connected to external

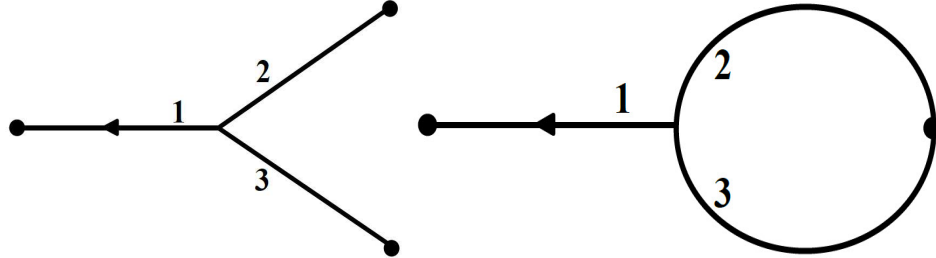


Figure 2.6: Contributions to \mathcal{J}_1 .

blobs have their wavevectors “pinned” at the wavevectors of those blobs, so that those wavevectors are no longer summed over. For simplicity we often omit the labels of the blobs, since those play no

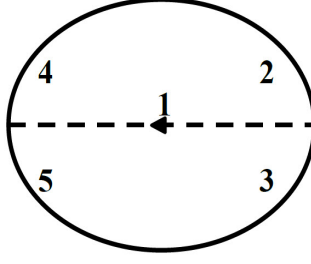


Figure 2.7: Leading contribution to \mathcal{J}_2 .

important role other than the “pinning” described above.

2.5 Spectral Hierarchy

We now consider the first of the possible limits of $\mathcal{Z}_L[\lambda, \mu]$ as $L \rightarrow \infty$ involving *all* of the N modes. This leads to a set of equations for the spectral generating function and the spectral correlation functions. We first sketch the derivation of these equations, with more details in Appendix A, and then analyze their basic properties.

2.5.1 Derivation

The crucial observation which leads to our results differing from Choi *et al.* (2005a) is that one must keep $\tilde{J}_{\mathbf{k}} = O(1)$, *not* $J_{\mathbf{k}} = O(1)$, in order to have a finite spectrum in the limit $L \rightarrow \infty$. Thus, we take in the generating function of Choi *et al.* (2005a).

$$J_{\mathbf{k}} = \left(\frac{2\pi}{L}\right)^d \tilde{J}_{\mathbf{k}}, \quad \lambda_{\mathbf{k}} = i\lambda(\mathbf{k}),$$

where $\lambda(\mathbf{k})$ is a smooth test function and, as before, $\mu_{\mathbf{k}}$ are integers. This leads to

$$\mathcal{Z}_L[\lambda, \mu] = \left\langle \exp \left(i \sum_{\mathbf{k} \in \Lambda_L^*} \left(\frac{2\pi}{L}\right)^d \lambda(\mathbf{k}) \tilde{J}_{\mathbf{k}} \right) \prod_{\mathbf{k} \in \Lambda^*} \psi_{\mathbf{k}}^{\mu_{\mathbf{k}}} \right\rangle, \quad (2.47)$$

CHAPTER 2. MULTI-MODE HIERARCHY EQUATIONS

We consider the large- L asymptotics of the various terms in the perturbation expansion of this quantity, employing the following standard substitutions:

$$\left(\frac{2\pi}{L}\right)^d \sum_{\mathbf{k}} \Rightarrow \int d^d k, \quad \left(\frac{L}{2\pi}\right)^d \delta_{\mathbf{k}, \mathbf{k}'} \Rightarrow \delta^d(\mathbf{k} - \mathbf{k}'), \quad \left(\frac{L}{2\pi}\right)^d \frac{\partial}{\partial \lambda_{\mathbf{k}}} \Rightarrow \frac{\delta}{\delta \lambda(\mathbf{k})} \quad (2.48)$$

From now on, we suppress superscript (0) when there is no confusion.

Calculation of \mathcal{J}_1 : This quantity is represented by the graphs in Fig. 2.6, or analytically:

$$\begin{aligned} \mathcal{J}_1 = & \sum_{1 \neq 2 \neq 3} L_{123} \left(\lambda_1 + \frac{\mu_1}{2J_1} \right) \sqrt{J_1 J_2 J_3} \delta_{\mu_1, 1} \delta_{\mu_2 + \sigma_2, 0} \delta_{\mu_3 + \sigma_3, 0} \Delta(\omega_{23}^1) \delta_{23}^1 \\ & + \sum_{1 \neq 2} L_{122} \left(\lambda_1 + \frac{\mu_1}{2J_1} \right) \sqrt{J_1 J_2} \delta_{\mu_1, 1} \delta_{\mu_2 + 2\sigma_2, 0} \Delta(\omega_{22}^1) \delta_{22}^1 \end{aligned}$$

Note that $\sigma_1 = +1$ in coefficient L_{123} . Taking into account the wavevector delta functions, there are two summations in the first term and one in the second. However, as noted by Choi *et al.* (2005a), these sums contain only a couple of non-zero terms, and then only for special choices of the μ 's. In their terminology, the sums are “pinned” by these choices of μ . Making the substitutions $J_i = (2\pi/L)^{d/2} \tilde{J}_i$ and $\lambda_1 = i\lambda(\mathbf{k}_1)$ into the above gives the leading contribution

$$\begin{aligned} \mathcal{J}_1 = & \left(\frac{2\pi}{L}\right)^{d/2} \sum_{1 \neq 2 \neq 3} L_{123} \frac{1}{2} \mu_1 \sqrt{\frac{\tilde{J}_2 \tilde{J}_3}{\tilde{J}_1}} \delta_{\mu_1, 1} \delta_{\mu_2, -\sigma_2} \delta_{\mu_3, -\sigma_3} \Delta(\omega_{23}^1) \delta_{23}^1 \\ & + \left(\frac{2\pi}{L}\right)^{d/2} \sum_{1 \neq 2} L_{122} \frac{1}{2} \mu_1 \frac{\tilde{J}_2}{\sqrt{\tilde{J}_1}} \delta_{\mu_1, 1} \delta_{\mu_2, -2\sigma_2} \Delta(\omega_{22}^1) \delta_{22}^1 \propto L^{-d/2} \end{aligned}$$

As we shall see, this term first-order in ϵ gives a subleading correction in the limit L large but finite, larger than many of the terms that Choi *et al.* (2005a) retained in their evolution formula for $L \rightarrow \infty$.

Calculation of \mathcal{J}_2 : Averaging over phases, the leading terms are contained in the contribution from Fig. 2.7 and a similar contribution with 2 and 3 interchanged. Because there are no external couplings, all μ' s must vanish. Because of the internal couplings, there are no sums over

CHAPTER 2. MULTI-MODE HIERARCHY EQUATIONS

the wavevectors 4,5 which are the same as wavevectors 2,3. The final contribution to the generating function is:

$$\begin{aligned}
\left\langle e^{\sum_{\mathbf{k}} \lambda_{\mathbf{k}} J_{\mathbf{k}}} \mathcal{J}_2 \right\rangle_J &= \delta_{\mu,0} \sum_{1,2,3} \left\langle (\lambda_1 + \lambda_1^2 J_1) J_2 J_3 e^{\sum_{\mathbf{k}} \lambda_{\mathbf{k}} J_{\mathbf{k}}} \right\rangle_J |L_{\mathbf{k}_1, \mathbf{k}_2, \mathbf{k}_3}^{+, \sigma_2, \sigma_3}|^2 \\
&\quad \times |\Delta(\sigma_2 \omega_2 + \sigma_3 \omega_3 - \omega_1)|^2 \delta_{\mathbf{k}_1, \sigma_2 \mathbf{k}_2 + \sigma_3 \mathbf{k}_3} \\
&= 9 \delta_{\mu,0} \sum_{1,2,3} \left(\lambda_1 + \lambda_1^2 \frac{\partial}{\partial \lambda_1} \right) \frac{\partial^2 \mathcal{Z}}{\partial \lambda_2 \partial \lambda_3} \times |H_{\mathbf{k}_1, \mathbf{k}_2, \mathbf{k}_3}^{-, \sigma_2, \sigma_3}|^2 \\
&\quad \times |\Delta(\sigma_2 \omega_2 + \sigma_3 \omega_3 - \omega_1)|^2 \delta_{\mathbf{k}_1, \sigma_2 \mathbf{k}_2 + \sigma_3 \mathbf{k}_3}. \quad (2.49)
\end{aligned}$$

Jakobsen and Newell (2004) and Choi *et al.* (2005a) retain *both* of the terms in the first factor in (2.49), i.e. both λ_1 and $\lambda_1^2 J_1$. However, with the proper scaling, $\lambda_1 = O(1)$ while $\lambda_1^2 J_1 = (\frac{2\pi}{L})^d \lambda_1 \tilde{J}_1 = O(L^{-d})$. Thus, the second term is even smaller than the contribution from \mathcal{J}_1 in the limit as $L \rightarrow \infty$ and should be neglected. This can be seen also substituting $J_i = (\frac{2\pi}{L})^{d/2} \tilde{J}_i$ and $\lambda_1 = i\lambda(\mathbf{k}_1)$ and taking the limit $L \rightarrow \infty$ using (2.48):

$$\begin{aligned}
\left\langle e^{\sum_{\mathbf{k}} \lambda_{\mathbf{k}} J_{\mathbf{k}}} \mathcal{J}_2 \right\rangle_J &\sim -9i\delta_{\mu,0} \sum_{\underline{\sigma}=(-1, \sigma_2, \sigma_3)} \int d^d k_1 d^d k_2 d^d k_3 \left(\lambda(\mathbf{k}_1) + \left(\frac{2\pi}{L}\right)^d \lambda(\mathbf{k}_1) \frac{\delta}{\delta \lambda(\mathbf{k}_1)} \right) \\
&\quad \times |H_{\mathbf{k}_1, \mathbf{k}_2, \mathbf{k}_3}^{-, \sigma_2, \sigma_3}|^2 |\Delta(\underline{\sigma} \cdot \underline{\omega})|^2 \delta^d(\underline{\sigma} \cdot \underline{\mathbf{k}}) \frac{\delta^2 \mathcal{Z}}{\delta \lambda(\mathbf{k}_2) \delta \lambda(\mathbf{k}_3)}. \quad (2.50)
\end{aligned}$$

The only surviving term in the limit as $L \rightarrow \infty$ is the one proportional to $\lambda(\mathbf{k}_1)$. Verifying our initial estimation, the term proportional to $\lambda(\mathbf{k}_1) \delta / \delta \lambda(\mathbf{k}_1)$ is $O(L^{-d})$ and vanishes in the limit.

A similar analysis may be carried through for the remaining contributions from $\mathcal{J}_3, \mathcal{J}_4$ and \mathcal{J}_5 . Detailed discussion of all the terms is given in Appendix A, where it is shown that only $\mathcal{J}_2, \mathcal{J}_3, \mathcal{J}_5$ give $O(1)$ contributions in the large-box limit $L \rightarrow \infty$:

$$\begin{aligned}
&\mathcal{X}(T) - \mathcal{X}(0) \\
&\sim -9i\delta_{\mu,0} \epsilon^2 \sum_{\underline{\sigma}=(-1, \sigma_2, \sigma_3)} \int d^d k_1 d^d k_2 d^d k_3 \delta^d(\underline{\sigma} \cdot \underline{\mathbf{k}}) |\Delta_T(\underline{\sigma} \cdot \underline{\omega}(\underline{\mathbf{k}}))|^2 \lambda(\mathbf{k}_1) |H_{\underline{\mathbf{k}}}^{\underline{\sigma}}|^2 \frac{\delta^2 \mathcal{Z}}{\delta \lambda(\mathbf{k}_2) \delta \lambda(\mathbf{k}_3)} \\
&\quad + \epsilon^2 \left[18i\delta_{\mu,0} \sum_{\underline{\sigma}=(-1, \sigma_2, \sigma_3)} \sigma_2 \int_{(\mathbb{T}^d)^3} d^d k_1 d^d k_2 d^d k_3 \delta^d(\underline{\sigma} \cdot \underline{\mathbf{k}}) E_T(0, \underline{\sigma} \cdot \underline{\omega}(\underline{\mathbf{k}})) \right.
\end{aligned}$$

CHAPTER 2. MULTI-MODE HIERARCHY EQUATIONS

$$\begin{aligned}
& \times \lambda(\mathbf{k}_1) |H_{\underline{\mathbf{k}}}^\sigma|^2 \frac{\delta^2 \mathcal{Z}}{\delta \lambda(\mathbf{k}_1) \delta \lambda(\mathbf{k}_3)} \\
& - 9 \sum_1 \delta_{\mu_1,1} \delta_{\mu_{-1},1} \prod_{\mathbf{k} \neq \mathbf{k}_1, -\mathbf{k}_1} \delta_{\mu_{\mathbf{k}},0} \sum_{\underline{\sigma}=(-1,\sigma_2,\sigma_3)} \sigma_2 \int d^d k_2 d^d k_3 \delta^d(\underline{\sigma} \cdot \underline{\mathbf{k}}) \\
& \times E_T(\omega(\mathbf{k}_1) + \omega(-\mathbf{k}_1), \underline{\sigma} \cdot \omega(\underline{\mathbf{k}})) H_{\underline{\mathbf{k}}}^\sigma H_{-\mathbf{k}_1, \mathbf{k}_2, \mathbf{k}_3}^{+, \sigma_2, \sigma_3} \left\langle e^{\sum_{\mathbf{k}} \lambda_{\mathbf{k}} J_{\mathbf{k}}} \sqrt{\frac{\tilde{J}_{-1}}{\tilde{J}_1}} \tilde{J}_3 \right\rangle_J + (2 \leftrightarrow 3) \Big] \\
& - \frac{9}{2} \epsilon^2 \sum_1 \delta_{\mu_1,1} \delta_{\mu_{-1},1} \prod_{\mathbf{k} \neq \pm \mathbf{k}_1} \delta_{\mu_{\mathbf{k}},0} \sum_{\underline{\sigma}=(-,\sigma_2,\sigma_3)} \int d^d k_2 d^d k_3 \delta^d(\underline{\sigma} \cdot \underline{\mathbf{k}}) \\
& \times [\Delta_T(\underline{\sigma} \cdot \omega(\underline{\mathbf{k}})) \Delta_T(-\underline{\sigma} \cdot \omega(\underline{\mathbf{k}}'))] H_{\underline{\mathbf{k}}}^\sigma H_{-\mathbf{k}_1, \mathbf{k}_2, \mathbf{k}_3}^{+, \sigma_2, \sigma_3} \left\langle \frac{\tilde{J}_2 \tilde{J}_3}{\sqrt{\tilde{J}_1 \tilde{J}_{-1}}} e^{\sum_{\mathbf{k}} \lambda_{\mathbf{k}} J_{\mathbf{k}}} \right\rangle_J. \tag{2.51}
\end{aligned}$$

The first term is that already found for \mathcal{J}_2 , the second bracketed term is from \mathcal{J}_3 , and the final term is from \mathcal{J}_5 . Note that the expressions proportional to $\delta_{\mu_1,1} \delta_{\mu_{-1},1}$ were missed in Jakobsen and Newell (2004) and Choi *et al.* (2005a) (although they are larger than many extra terms that those authors retained in their final equations which actually vanish as $L \rightarrow \infty$!). The terms proportional to $\delta_{\mu_1,1} \delta_{\mu_{-1},1}$ indeed do not appear in the final equations, not because of the large- L limit but because they are nonsecular.

We therefore consider next the limit of weak nonlinearity. The limit is achieved by choosing the time variable T in the expansion (D.5) to lie between the wave period and nonlinear timescale $O(\epsilon^{-2})$ and by then taking $\epsilon \rightarrow 0$. For this purpose we use the following standard asymptotic relations for $T \rightarrow \infty$ (Benney and Newell, 1969):

$$\begin{aligned}
\Delta_T(x) & \sim \tilde{\Delta}(x) = \pi \delta(x) + iP \left(\frac{1}{x} \right), \quad E_T(x; y) \sim \Delta_T(x) \Delta_T(y) \sim \tilde{\Delta}(x) \tilde{\Delta}(y), \\
|\Delta_T(x)|^2 & \sim 2\pi T \delta(x) + 2P \left(\frac{1}{x} \right) \frac{\partial}{\partial x}, \quad E_T(x; 0) \sim \tilde{\Delta}(x) \left(T - i \frac{\partial}{\partial x} \right), \tag{2.52}
\end{aligned}$$

The terms multiplied by $\delta_{\mu,0}$ contain secular contributions proportional to T , while the terms proportional to $\delta_{\mu_1,1} \delta_{\mu_{-1},1}$ are nonsecular. We now use (2.40) to calculate $\mathcal{Z}(T) - \mathcal{Z}(0)$, with the observation that it is changed by our replacement $\lambda_{\mathbf{k}} = i\lambda(\mathbf{k})$ into

$$\mathcal{Z}[\lambda, \mu, T] = \mathcal{X}\{\lambda, \mu, T\} + \mathcal{X}^*\{-\lambda, -\mu, T\}. \tag{2.53}$$

CHAPTER 2. MULTI-MODE HIERARCHY EQUATIONS

Finally, replacing $(\mathcal{Z}(T) - \mathcal{Z}(0))/T$ by $\dot{\mathcal{Z}}$ and using time variable $\tau = \epsilon^2 t$, one obtains

$$\begin{aligned} \frac{d}{d\tau} \mathcal{Z}[\lambda, \mu, \tau] = & -36i\pi\delta_{\mu,0} \sum_{\underline{\sigma}=(-1, \sigma_2, \sigma_3)} \int d^d k_1 d^d k_2 d^d k_3 \delta^d(\underline{\sigma} \cdot \mathbf{k}) \delta(\underline{\sigma} \cdot \omega(\mathbf{k})) \lambda(\mathbf{k}_1) |H_{\mathbf{k}}^{\underline{\sigma}}|^2 \\ & \times \left\{ \frac{\delta^2 \mathcal{Z}}{\delta \lambda(\mathbf{k}_2) \delta \lambda(\mathbf{k}_3)} - \sigma_2 \frac{\delta^2 \mathcal{Z}}{\delta \lambda(\mathbf{k}_1) \delta \lambda(\mathbf{k}_3)} - \sigma_3 \frac{\delta^2 \mathcal{Z}}{\delta \lambda(\mathbf{k}_1) \delta \lambda(\mathbf{k}_2)} \right\}. \end{aligned} \quad (2.54)$$

Equation (2.54) is the main result of this section.

The validity of (2.54) does not, of course, require an ϵ infinitesimally small or an L infinitely large, but just an ϵ sufficiently small and an L sufficiently large (depending upon ϵ). However, it is worthwhile to stress the precise conditions, largely following the prior discussions of Connaughton *et al.* (2003) and Nazarenko (2011, Chap. 10). In the first place, ϵ must be so small that there is a large separation between the wave period and the nonlinear time

$$\frac{1}{\omega(\mathbf{k})} \ll \epsilon^{-2} \frac{n(\mathbf{k})}{dn(\mathbf{k})/d\tau}, \quad (2.55)$$

with the latter of order $\epsilon^{-2}\gamma_{\mathbf{k}}$. This is required in order to be able to find an intermediate time T so that (2.52) and $(\mathcal{Z}(T) - \mathcal{Z}(0))/T \doteq \dot{\mathcal{Z}}$ are both well-satisfied, e.g. taking $T = O(\epsilon^{-1})$. As emphasized by Connaughton *et al.* (2003), condition (2.55) is almost never uniformly valid for all wavevectors \mathbf{k} , but is typically violated for either low or high k . This means that $\lambda(\mathbf{k})$ in (2.54) must be restricted to be zero for \mathbf{k} outside the interval where (2.55) holds and it is furthermore assumed that the wavevector integrations are sufficient local that no wavevectors outside that range give a substantial contribution. The size of L is determined by the requirement that wavevector summations over $[-\pi/a, \pi/a]^d$ can be approximated as continuous integrals. At the very least, it must be true that $L \gg a$. The most stringent condition seems to arise from the requirement that the approximate delta functions of width $1/T$ in (2.52) contain a large number of frequencies. If $\Delta\omega$ is the spacing of discrete frequencies, then one must have $\Delta\omega \ll 1/T \sim O(\epsilon)$. Estimating $\Delta\omega = |\Delta\mathbf{k}| \cdot |\nabla_{\mathbf{k}}\omega(\mathbf{k})| \sim \frac{2\pi}{L} |\nabla_{\mathbf{k}}\omega(\mathbf{k})|$, the essential requirement is that $L/|\nabla_{\mathbf{k}}\omega(\mathbf{k})| \gg T$, i.e. the

CHAPTER 2. MULTI-MODE HIERARCHY EQUATIONS

time required for a wavepacket traveling at the group velocity to cross the box must be much larger than the time T or, conservatively, the nonlinear interaction time. This requires extremely large boxes in practice, unless ϵ is only moderately small and (2.55) only marginally satisfied. For more discussion of condition (2.55), see Biven *et al.* (2001) and Keldysh (1965, eq.(59)).

2.5.2 Properties

We shall now discuss the most basic properties of eq.(2.54) derived in the previous section. As pointed out by Choi *et al.* (2005a), the factor $\delta_{\mu,0}$ implies that the RP property of the initial conditions is preserved in time. Therefore, without loss of generality, we need only consider the characteristic functional for amplitudes, or $\mathcal{Z}[\lambda, \tau] \equiv \mathcal{Z}[\lambda, \mu = 0, \tau]$. Its evolution equation is

$$\begin{aligned} \dot{\mathcal{Z}}[\lambda, \tau] = & -36i\pi \sum_{\underline{\sigma}=(-1, \sigma_2, \sigma_3)} \int d^d k_1 d^d k_2 d^d k_3 \delta^d(\underline{\sigma} \cdot \underline{\mathbf{k}}) \delta(\underline{\sigma} \cdot \omega(\underline{\mathbf{k}})) \lambda(\mathbf{k}_1) |H_{\underline{\mathbf{k}}}^{\underline{\sigma}}|^2 \\ & \times \left\{ \frac{\delta^2 \mathcal{Z}}{\delta \lambda(\mathbf{k}_2) \delta \lambda(\mathbf{k}_3)} - \sigma_2 \frac{\delta^2 \mathcal{Z}}{\delta \lambda(\mathbf{k}_1) \delta \lambda(\mathbf{k}_3)} - \sigma_3 \frac{\delta^2 \mathcal{Z}}{\delta \lambda(\mathbf{k}_1) \delta \lambda(\mathbf{k}_2)} \right\}. \end{aligned} \quad (2.56)$$

Hereafter we consider only this amplitude characteristic functional. Eq.(2.56) implies a hierarchy of evolution equations for the M -mode spectral correlation functions defined in section 2.3, in the wave-kinetic limit:

$$\mathcal{N}^{(M)}(\mathbf{k}_1, \dots, \mathbf{k}_M, \tau) = \lim_{\epsilon \rightarrow 0} \lim_{L \rightarrow \infty} \mathcal{N}_{L, \epsilon}^{(M)}(\mathbf{k}_1, \dots, \mathbf{k}_M, \epsilon^{-2} \tau).$$

The hierarchy is easiest to derive by using the relation (2.9) between $\mathcal{Z}[\lambda, \tau]$ and the empirical spectrum, which implies that

$$\mathcal{N}^{(M)}(\mathbf{k}_1, \dots, \mathbf{k}_M, \tau) = (-i)^M \frac{\delta^M \mathcal{Z}[\lambda, \tau]}{\delta \lambda(\mathbf{k}_1) \cdots \delta \lambda(\mathbf{k}_M)} \Big|_{\lambda=0}.$$

CHAPTER 2. MULTI-MODE HIERARCHY EQUATIONS

By taking M functional derivatives of (2.56) and setting $\lambda \equiv 0$, one derives for each integer $M = 1, 2, 3, \dots$ the following equation:

$$\begin{aligned} \mathcal{N}^{(M)}(\mathbf{k}_1, \dots, \mathbf{k}_M, \tau) &= 36\pi \sum_{j=1}^M \sum_{\underline{\sigma}=(-1, \sigma_2, \sigma_3)} \int d^d \bar{k}_2 d^d \bar{k}_3 \delta^d(\underline{\sigma} \cdot \underline{\mathbf{k}}_j) \delta(\underline{\sigma} \cdot \omega(\underline{\mathbf{k}}_j)) \lambda(\mathbf{k}_j) |H_{\underline{\mathbf{k}}_j}^{\underline{\sigma}}|^2 \\ &\times \left[\mathcal{N}^{(M+2)}(\mathbf{k}_1, \dots, \mathbf{k}_{j-1}, \mathbf{k}_{j+1}, \dots, \mathbf{k}_M, \bar{\mathbf{k}}_2, \bar{\mathbf{k}}_3, \tau) \right. \\ &\left. - \sigma_2 \mathcal{N}^{(M+1)}(\mathbf{k}_1, \dots, \mathbf{k}_M, \bar{\mathbf{k}}_3, \tau) - \sigma_3 \mathcal{N}^{(M+1)}(\mathbf{k}_1, \dots, \mathbf{k}_M, \bar{\mathbf{k}}_2, \tau) \right]. \end{aligned} \quad (2.57)$$

which couples the M th-order correlation functions to the $(M+1)$ st. We shall refer to the above collection of equations for all $M = 1, 2, 3, \dots$ as the *spectral hierarchy* of wave-kinetic theory. It is exactly analogous to the ‘‘Boltzmann hierarchy’’ derived by Lanford from the BBGKY hierarchy in the low-density limit (Lanford, 1975, 1976). If the spectral correlation functions satisfy bounds on their growth for large orders M that allow them to uniquely characterize the distribution of the empirical spectrum (for example, Carleman’s condition), then the spectral hierarchy (2.57) is not only a consequence of the equation (2.56) but is in fact equivalent to that equation.

An extremely important property of the equations (2.56) or (2.57) is that they possess certain exact solutions. In particular, if the initial functional $\mathcal{Z}[\lambda, 0]$ is of exponential form (2.28), as follows for an initial RP field with uncorrelated amplitudes, then an exact solution of (2.56) is

$$\mathcal{Z}[\lambda, \tau] = \exp \left(i \int d^d \mathbf{k} \lambda(\mathbf{k}) n(\mathbf{k}, \tau) \right), \quad (2.58)$$

where $n(\mathbf{k}, \tau)$ satisfies the standard wave-kinetic equation

$$\begin{aligned} \dot{n}(\mathbf{k}, \tau) &= 36\pi \sum_{\underline{\sigma}=(-1, \sigma_2, \sigma_3)} \int d^d k_2 d^d k_3 |H_{\underline{\mathbf{k}}}^{\underline{\sigma}}|^2 \delta(\underline{\sigma} \cdot \omega(\underline{\mathbf{k}})) \delta^d(\underline{\sigma} \cdot \underline{\mathbf{k}}) \\ &\times \left\{ n(\mathbf{k}_2, \tau) n(\mathbf{k}_3, \tau) - \sigma_2 n(\mathbf{k}, \tau) n(\mathbf{k}_3, \tau) - \sigma_3 n(\mathbf{k}, \tau) n(\mathbf{k}_2, \tau) \right\} \end{aligned} \quad (2.59)$$

with initial condition $n(\mathbf{k}, 0) = n(\mathbf{k})$. This may be checked by direct substitution of (2.58) into (2.56). Equivalently, with factorized M th-order correlation functions (2.30) as initial data, there is

CHAPTER 2. MULTI-MODE HIERARCHY EQUATIONS

a solution of the spectral hierarchy equations (2.57) also of factorized form:

$$\mathcal{N}^{(M)}(\mathbf{k}_1, \dots, \mathbf{k}_M, \tau) = \prod_{m=1}^M n(\mathbf{k}_m, \tau). \quad (2.60)$$

Note that such factorized solutions have only power-law growth for large orders M , so that they uniquely characterize the exponential characteristic functional (2.58). If it can be proved that solutions of the dynamical equations (2.56) or (2.57) are unique for classes of initial data that include the forms (2.28) and (2.30), then the equations we have derived imply that spectral correlation functions initially factorized will remain so for $\tau > 0$. In this sense, therefore, the property of uncorrelated wave amplitudes is preserved in time by our equations. This is an exact analogue of the “propagation of chaos” property for the Boltzmann hierarchy, which implies that the *Stosszahlansatz* is propagated in time (Lanford, 1975, 1976). We shall address ideas and difficulties to solve the well-posedness of solutions of the spectral hierarchy (2.57) in Chap. 5.

The results above have an important implication. As follows from our discussion in section 2.3, the conditions (2.58) or (2.60) imply a law of large numbers for the empirical spectrum at positive times. That is, with probability going to 1 in the wave-kinetic limit (first $L \rightarrow \infty$, then $\epsilon \rightarrow 0$), it follows that

$$\hat{n}_L(\mathbf{k}, \epsilon^{-2}\tau) \simeq n(\mathbf{k}, \tau), \quad \tau > 0$$

where $n(\mathbf{k}, \tau)$ is the solution of the wave-kinetic equation (2.59). The interesting implication for laboratory and numerical experiments is that the wave-kinetic equations will be valid for *typical* initial amplitudes and phases chosen from an RPA ensemble and not just for the spectrum averaged over the RPA ensemble. That is, the empirical spectrum is “self-averaging”. This is the exact analogue of the law of large numbers derived by Lanford for the empirical 1-particle distribution (Klimontovich density) in the low density limit for gases (Lanford, 1975, 1976).

In order to emphasize the close formal analogy of wave-kinetic theory with the kinetic theory of gases, it is worthwhile to make here a few remarks about the role of entropy in both. It is

CHAPTER 2. MULTI-MODE HIERARCHY EQUATIONS

well-known that the wave-kinetic equation (2.59) satisfies an “H-theorem” for the entropy defined, with Boltzmann’s constant k_B , by

$$S[n] = k_B \int_{\Lambda^*} d^d k \ln n(\mathbf{k}). \quad (2.61)$$

That is, $dS/d\tau \geq 0$ for general solutions of (2.59) and $dS/d\tau = 0$ for the thermal equilibrium solutions $n_{\text{eq}}(\mathbf{k}) = k_B T / \omega(\mathbf{k})$ at absolute temperature T , which maximize the entropy (2.61) for fixed energy $E[n] = \int_{\Lambda^*} d^d k \omega(\mathbf{k}) n(\mathbf{k})$. See Zakharov *et al.* (1992, section 2.2.2). This is the exact analogue of the H -theorem originally derived by Boltzmann for his kinetic equation. As pointed out more recently by Spohn (2006), the entropy (2.61) also follows from Boltzmann’s prescription that $S = k_B \log W$ (Boltzmann, 1872), where W is the Liouville measure of the set of microstates (\tilde{J}, ψ) consistent with the given “macrostate” defined by the prescribed spectrum $n(\mathbf{k})$. More precisely, let Δ_i , $i = 1, \dots, P$ be a partition of Λ^* and let $\Gamma_{n, \Delta, \eta, L}$ be the set of microstates $\{(\tilde{J}_{\mathbf{k}}, \psi_{\mathbf{k}}), \mathbf{k} \in \Lambda_L^*\}$ such that $|\hat{n}_L(\Delta_i) - n(\Delta_i)| < \eta$, for $i = 1, \dots, P$ where

$$\hat{n}_L(\Delta_i) = \frac{1}{|\Delta_i|} \int_{\Delta_i} d^d k \hat{n}_L(\mathbf{k}), \quad n(\Delta_i) = \frac{1}{|\Delta_i|} \int_{\Delta_i} d^d k n(\mathbf{k}).$$

Then⁵

$$\lim_{\eta \rightarrow 0} \lim_{L \rightarrow \infty} \left(\frac{2\pi}{L} \right)^d \ln |\Gamma_{n, \Delta, \eta, L}| = \sum_{i=1}^P |\Delta_i| (\ln n(\Delta_i) + 1).$$

The result for each individual cell is the same as the microcanonical entropy $s(e)$ of a system of non-interacting harmonic oscillators or alternatively as the entropy of an ideal gas in a periodic box, thinking of $\tilde{J}_{\mathbf{k}}$ as kinetic energies and $\varphi_{\mathbf{k}}$ as positions of the particles. Furthermore, defining

⁵Note that $\Gamma_{n, \Delta, \eta, L}$ is a Cartesian product set of the form $\otimes_{i=1}^P \{(\tilde{J}_{\mathbf{k}}, \psi_{\mathbf{k}}), \mathbf{k} \in \Lambda_L^* \cap \Delta_i : |\hat{n}_L(\Delta_i) - n(\Delta_i)| < \eta\}$ and for each cell Δ_i of the partition, $\hat{n}_L(\Delta_i) \approx \frac{1}{2N_L(\Delta_i)} \sum_{\mathbf{k} \in \Delta_i \cap \Lambda_L^*} (\tilde{p}_{\mathbf{k}}^2 + \tilde{q}_{\mathbf{k}}^2)$. The stated result then follows using the formula $\frac{\pi^{D/2}}{(D/2)!} R^D$ for the volume of a ball in dimension $D = 2N(\Delta_i)$ of radius $R = (nD)^{1/2}$, dividing by $(2\pi)^{D/2}$ [eq.(2.24)], and applying Stirling’s approximation for the factorial $(D/2)!$ as $D \rightarrow \infty$.

CHAPTER 2. MULTI-MODE HIERARCHY EQUATIONS

$|\Delta| = \max_i |\Delta_i|$, the partition may be refined by taking $|\Delta| \rightarrow 0$, so that

$$\lim_{|\Delta| \rightarrow 0} \lim_{\eta \rightarrow 0} \lim_{L \rightarrow \infty} \left(\frac{2\pi}{L} \right)^d \ln |\Gamma_{n,\Delta,\eta,L}| = \int_{\Lambda^*} d^d k (\ln n(\mathbf{k}) + 1).$$

The result agrees, up to constants, with (2.61). The above argument introduces the “microcanonical measure” obtained by restricting Liouville measure to the set $\Gamma_{n,\Delta,\eta,L}$ and normalizing by $|\Gamma_{n,\Delta,\eta,L}|$ to yield a probability measure. By adapting the arguments of Lanford (1976) it follows that this “microcanonical measure” is a natural example which satisfies asymptotic factorization (2.30) but *not* the RPA property.

Our results so far may appear somewhat disappointing. Equations for the generating function $\mathcal{Z}[\lambda, \tau]$ like our (2.56) have been proposed mainly in the hope of developing theories of intermittency of wave turbulence and of higher-order statistics of the wave-amplitudes. It might be concluded from the discussion above that the correct equation for $\mathcal{Z}[\lambda, \tau]$ —i.e. our equation (2.56)—is equivalent to the wave-kinetic equation (2.59) and has no more physical content. However, this is not entirely correct. To clarify this point, we now classify all of the realizable solutions of (2.56). That is, we characterize the solutions of the equation (2.56) for the most general possible initial conditions that can be physically attained in the kinetic limit, assuming RP but *no* form of RPA. For this purpose, note that the characteristic functional $\mathcal{Z}_L(\lambda, 0)$ defined in (2.9) is a positive-definite functional, i.e.

$$\sum_{i,j=1}^n c_i c_j^* \mathcal{Z}_L(\lambda_i - \lambda_j, 0) \geq 0$$

for any set of n fields $\lambda_1, \dots, \lambda_n$ and complex numbers c_1, \dots, c_n . It is also normalized so that $\mathcal{Z}_L(\lambda = 0, 0) = 1$. Since these properties are preserved under pointwise limits, the physical initial condition

$$\mathcal{Z}(\lambda, 0) = \lim_{L \rightarrow \infty} \mathcal{Z}_L(\lambda, 0)$$

for our eq.(2.56) also satisfies them. We must assume that the above limit exists, if eq.(2.56) is to

CHAPTER 2. MULTI-MODE HIERARCHY EQUATIONS

have any validity at all, and we shall assume furthermore that the limiting $\mathcal{Z}(\lambda, 0)$ is a continuous functional of the λ fields⁶. By the Bochner-Minlos theorem, it therefore has the form

$$\mathcal{Z}(\lambda, 0) = \int d\rho(n_0) \exp \left(i \int d^d \mathbf{k} \lambda(\mathbf{k}) n_0(\mathbf{k}) \right)$$

for some probability measure ρ ; e.g. see Yamasaki (1985). That is, the initial condition $\mathcal{Z}(\lambda, 0)$ is a statistical superposition of exponential initial conditions of the form (2.28) that arise from RPA fields. Since equation (2.56) is linear in \mathcal{Z} , a solution for such superposed initial data is

$$\mathcal{Z}(\lambda, \tau) = \int d\rho(n_0) \exp \left(i \int d^d \mathbf{k} \lambda(\mathbf{k}) n(\mathbf{k}, \tau) \right)$$

where $n(\mathbf{k}, \tau)$ solves the kinetic equation with initial condition $n_0(\mathbf{k})$. This is the only solution if the uniqueness of solutions holds for (2.56). The conclusion of this argument is that *the most general, statistically realizable solutions⁷ of eq.(2.56) correspond to ensembles of solutions of the wave-kinetic equation with random initial conditions $n_0(\mathbf{k})$.*

The above argument is a formal analogue of a rigorous result of Spohn for the Boltzmann hierarchy in the kinetic theory of gases (Spohn, 1984). With appropriate technical assumptions, his argument can be carried over to our spectral hierarchy (2.57), with the conclusion that its general realizable solutions are statistical superpositions of factorized solutions, that is,

$$\mathcal{N}^{(M)}(\mathbf{k}_1, \dots, \mathbf{k}_M, \tau) = \int d\rho(n_0) \prod_{m=1}^M n(\mathbf{k}_m, \tau),$$

where again $n(\mathbf{k}, \tau)$ solves the kinetic equation with initial condition $n_0(\mathbf{k})$. We shall refer to such solutions of the spectral hierarchy (2.57) or of the equivalent equation (2.56) as “super-statistical

⁶We shall not attempt to identify here the precise topologies on the spaces of λ 's and n 's that would permit a rigorous formulation and proof of our results.

⁷It should be noted that there may be non-realizable solutions of eq.(2.56) that do not have this form. In general, statistical moment equations may have “parasitic” solutions that do not correspond to realizable solutions of the underlying statistical problem. For an example of this phenomenon in the Kraichnan passive scalar model, see Eyink and Xin (2000).

CHAPTER 2. MULTI-MODE HIERARCHY EQUATIONS

solutions”, since they correspond to random ensembles of solutions of the spectral closure equation. As we shall discuss at length in section 2.7, such “super-statistical solutions” offer a possibility to explain intermittency and non-Gaussian statistics previously little discussed in the wave turbulence literature. However, we shall first consider the alternative approach based on closed equations for the PDF’s of the wave amplitudes.

2.6 PDF Hierarchy

We now consider a second possible limit involving only a fixed number M of modes $a_{\mathbf{k}_m}$, $m = 1, \dots, M$ as the total number $N \rightarrow \infty$. As before, one must keep $\tilde{J}_{\mathbf{k}} = O(1)$ for all modes. We thus define the joint characteristic function:

$$\mathcal{Z}_L^{(M)}(\lambda_1, \dots, \lambda_M, \mu_1, \dots, \mu_M, T; \mathbf{k}_1, \dots, \mathbf{k}_M) = \left\langle \exp \left(i \sum_{m=1}^M \lambda_m \tilde{J}_{\mathbf{k}_m}(T) \right) \prod_{m=1}^M \psi_{\mathbf{k}_m}^{\mu_m}(T) \right\rangle, \quad (2.62)$$

This is the generating function (2.34) of Choi *et al.* (2005a) with

$$\lambda_{\mathbf{k}_m} = i \left(\frac{L}{2\pi} \right)^d \lambda_m, \quad J_{\mathbf{k}_m} = \left(\frac{2\pi}{L} \right)^d \tilde{J}_{\mathbf{k}_m}, \quad m = 1, \dots, M \quad (2.63)$$

and all other $\lambda_{\mathbf{k}} = 0$. We use the shorthand $\mathcal{Z}_L^{(M)}(\lambda, \mu, T)$ when there is no possibility of confusion. As we shall see, the limit $L \rightarrow \infty$, $\epsilon \rightarrow 0$ of this object leads to a *hierarchy* of equations connecting different values of M . We sketch the derivation of these equations, with more details in Appendix B, and then analyze their basic properties.

2.6.1 Derivation

The method is the same as before. We use the perturbation expansion in ϵ giving the formula (2.40) for the generating functions, with the definitions (2.41) of $\mathcal{X}_L(\lambda, \mu)$ and (2.42)-(2.46) of the \mathcal{J} ’s. As a consequence of (2.63) all separate terms in the prefactors of the \mathcal{J} ’s are of the same

CHAPTER 2. MULTI-MODE HIERARCHY EQUATIONS

order:

$$\lambda_{\mathbf{k}_1} + \frac{\mu_{\mathbf{k}_1}}{2J_{\mathbf{k}_1}}, \quad \lambda_{\mathbf{k}_1} + \lambda_{\mathbf{k}_1}^2 J_{\mathbf{k}_1} - \frac{\mu_{\mathbf{k}_1}^2}{4J_{\mathbf{k}_1}} = O(L^d)$$

$$\frac{1}{2}\lambda_{\mathbf{k}_1}^2 + \frac{\mu_{\mathbf{k}_1}}{4J_{\mathbf{k}_1}^2}(\frac{\mu_{\mathbf{k}_1}}{2} - 1) + \frac{\lambda_{\mathbf{k}_1}\mu_{\mathbf{k}_1}}{2J_{\mathbf{k}_1}}, \quad \lambda_{\mathbf{k}_1}\lambda_{\mathbf{k}_2}, \quad (\lambda_{\mathbf{k}_1} + \frac{\mu_{\mathbf{k}_1}}{4J_{\mathbf{k}_1}})\frac{\mu_{\mathbf{k}_2}}{J_{\mathbf{k}_2}} = O(L^{2d}).$$

Hence, we only need to calculate the leading-order graphical contributions. We already analyzed these in the previous section and this discussion carries over here, except that now some wavevectors are discrete and take on only M values (mode 1 for $\mathcal{J}_1 - \mathcal{J}_4$ and modes 1,2 for \mathcal{J}_5) whereas all others are continuous in the infinite-box limit. One must consider carefully whether free wavevectors in graphical summations are discrete or continuous to see whether their contribution is $O(M)$ or $O(L^d)$. This analysis is carried out in Appendix B. It is found that $\mathcal{X}_L^{(M)}(\lambda, \mu, T)$ in the large-box limit gets no contributions from $\mathcal{J}_1, \mathcal{J}_4$ and $O(1)$ contributions from $\mathcal{J}_2, \mathcal{J}_3, \mathcal{J}_5$. The result is

$$\begin{aligned} & \mathcal{X}^{(M)}(\lambda, \mu, T) - \mathcal{X}^{(M)}(\lambda, \mu, 0) \\ \sim & -9\epsilon^2 i \delta_{\mu,0} \sum_{j=1}^M \sum_{\underline{\sigma}=(-1, \sigma_2, \sigma_3)} \int d^d \bar{k}_2 d^d \bar{k}_3 \delta^d(\underline{\sigma} \cdot \underline{\mathbf{k}}_j) |\Delta_T(\underline{\sigma} \cdot \omega(\underline{\mathbf{k}}_j))|^2 \\ & \times |H_{\underline{\mathbf{k}}_j}^{\underline{\sigma}}|^2 (\lambda_{\mathbf{k}_j} + \lambda_{\mathbf{k}_j}^2 \frac{\partial}{\partial \lambda_{\mathbf{k}_j}}) \frac{\partial^2 \mathcal{Z}^{(M+2)}}{\partial \bar{\lambda}_2 \partial \bar{\lambda}_3} \Big|_{\bar{\lambda}_2 = \bar{\lambda}_3 = 0} \\ & + \epsilon^2 \left[18i \delta_{\mu,0} \sum_{j=1}^M \sum_{\underline{\sigma}=(-1, \sigma_2, \sigma_3)} \sigma_2 \int d^d k_2 d^d k_3 \delta^d(\underline{\sigma} \cdot \underline{\mathbf{k}}_j) E_T(0, \underline{\sigma} \cdot \omega(\underline{\mathbf{k}}_j)) \right. \\ & \times |H_{\underline{\mathbf{k}}_j}^{\underline{\sigma}}|^2 \lambda_{\mathbf{k}_j} \frac{\partial^2 \mathcal{Z}^{(M+1)}}{\partial \bar{\lambda}_3 \partial \lambda_j} \Big|_{\bar{\lambda}_3 = 0} + (2 \leftrightarrow 3) \\ & - 9 \sum_{j=1}^M \delta_{\mu_j,1} \delta_{\mu-j,1} \prod_{m \neq j, -j} \delta_{\mu_m,0} \sum_{\underline{\sigma}=(-1, \sigma_2, \sigma_3)} \sigma_2 \int d^d \bar{k}_2 \int d^d \bar{k}_3 \delta^d(\underline{\sigma} \cdot \underline{\mathbf{k}}_j) \\ & \times E_T(\omega(\underline{\mathbf{k}}_j) + \omega(-\underline{\mathbf{k}}_j), \underline{\sigma} \cdot \omega(\underline{\mathbf{k}}_j)) H_{\underline{\mathbf{k}}_j, \bar{\mathbf{k}}_2, \bar{\mathbf{k}}_3}^{-, \sigma_2, \sigma_3} H_{-\underline{\mathbf{k}}_j, \bar{\mathbf{k}}_2, \bar{\mathbf{k}}_3}^{+, \sigma_2, \sigma_3} \left\langle e^{\sum_m i \lambda_m \tilde{J}_m} \sqrt{\frac{\tilde{J}_{-1}}{\tilde{J}_1}} \tilde{J}_3 \right\rangle_J + (2 \leftrightarrow 3) \Big] \\ & + 18\epsilon^2 \sum_{j=1}^M \delta_{\mu_j,1} \delta_{\mu-j,1} \prod_{m \neq 1, -1} \delta_{\mu_m,0} \left(\lambda_1 \lambda_{-1} - i \frac{\lambda_1}{\tilde{J}_{-1}} - \frac{1}{4 \tilde{J}_1 \tilde{J}_{-1}} \right) \sum_{\underline{\sigma}=(-, \sigma_2, \sigma_3)} \int d^d \bar{k}_2 d^d \bar{k}_3 \delta^d(\underline{\sigma} \cdot \underline{\mathbf{k}}_j) \\ & \times \Delta_T(\underline{\sigma} \cdot \omega(\underline{\mathbf{k}}_j)) \Delta_T(-\underline{\sigma} \cdot \omega(\underline{\mathbf{k}}'_j)) H_{\underline{\mathbf{k}}_j, \bar{\mathbf{k}}_2, \bar{\mathbf{k}}_3}^{-, \sigma_2, \sigma_3} H_{-\underline{\mathbf{k}}_j, \bar{\mathbf{k}}_2, \bar{\mathbf{k}}_3}^{+, \sigma_2, \sigma_3} \left\langle \sqrt{\tilde{J}_1 \tilde{J}_{-1}} \tilde{J}_2 \tilde{J}_3 e^{i \sum_m \lambda_m \tilde{J}_m} \right\rangle_J. \end{aligned} \quad (2.64)$$

Here $\underline{\mathbf{k}}_j = (\mathbf{k}_j, \bar{\mathbf{k}}_2, \bar{\mathbf{k}}_3)$ and $\underline{\mathbf{k}}'_j = (-\mathbf{k}_j, \bar{\mathbf{k}}_2, \bar{\mathbf{k}}_3)$. Taking the small- ϵ limit using the asymptotic formulas (2.52), one finds the terms proportional to $\delta_{\mu,0}$ contain secular contributions while the terms

CHAPTER 2. MULTI-MODE HIERARCHY EQUATIONS

proportional to $\delta_{\mu_j,1}\delta_{\mu-j,1}$ are nonsecular. Using (2.53) to calculate $\mathcal{Z}^{(M)}(T) - \mathcal{Z}^{(M)}(0)$, replacing $(\mathcal{Z}^{(M)}(T) - \mathcal{Z}^{(M)}(0))/T$ by $\dot{\mathcal{Z}}^{(M)}$ and using time variable $\tau = \epsilon^2 t$, one finally obtains

$$\begin{aligned} \frac{d}{d\tau} \mathcal{Z}^{(M)}(\lambda, \mu, \tau) = & -36i\pi\delta_{\mu,0} \sum_{j=1}^M \sum_{\underline{\sigma}=(-1,\bar{\sigma}_2,\bar{\sigma}_3)} \int d^d \bar{k}_2 d^d \bar{k}_3 \delta^d(\underline{\sigma} \cdot \underline{\mathbf{k}}_j) \delta(\underline{\sigma} \cdot \omega(\underline{\mathbf{k}}_j)) \left| H_{\underline{\mathbf{k}}_j}^{\underline{\sigma}} \right|^2 \\ & \left\{ (\lambda_j + \lambda_j^2 \frac{\partial}{\partial \lambda_j}) \frac{\partial^2 \mathcal{Z}^{(M+2)}}{\partial \bar{\lambda}_2 \partial \bar{\lambda}_3} \Big|_{\bar{\lambda}_2=\bar{\lambda}_3=0} - \bar{\sigma}_2 \lambda_j \frac{\partial \mathcal{Z}^{(M+1)}}{\partial \bar{\lambda}_3 \partial \lambda_j} \Big|_{\bar{\lambda}_3=0} - \bar{\sigma}_3 \lambda_j \frac{\partial \mathcal{Z}^{(M+1)}}{\partial \bar{\lambda}_2 \partial \lambda_j} \Big|_{\bar{\lambda}_2=0} \right\}. \end{aligned} \quad (2.65)$$

Equation (2.65) is the main result of this section.

2.6.2 Properties

We now consider the important properties of the multi-mode equations (2.65). As for the spectral characteristic functional in the previous section, the factors $\delta_{\mu,0}$ imply that the RP property is preserved in time. Therefore, we can consider the generating functions for the amplitudes alone, obtained by setting $\mu = 0$. These form a *hierarchy* of equations, for $M = 1, 2, 3, \dots$

$$\begin{aligned} \frac{d}{d\tau} \mathcal{Z}^{(M)}(\lambda, \tau) = & -36i\pi \sum_{j=1}^M \sum_{\underline{\sigma}=(-1,\bar{\sigma}_2,\bar{\sigma}_3)} \int d^d \bar{k}_2 d^d \bar{k}_3 \delta^d(\underline{\sigma} \cdot \underline{\mathbf{k}}_j) \delta(\underline{\sigma} \cdot \omega(\underline{\mathbf{k}}_j)) \left| H_{\underline{\mathbf{k}}_j}^{\underline{\sigma}} \right|^2 \\ & \times \left\{ (\lambda_j + \lambda_j^2 \frac{\partial}{\partial \lambda_j}) \frac{\partial^2 \mathcal{Z}^{(M+2)}}{\partial \bar{\lambda}_2 \partial \bar{\lambda}_3} \Big|_{\bar{\lambda}_2=\bar{\lambda}_3=0} - \bar{\sigma}_2 \lambda_j \frac{\partial \mathcal{Z}^{(M+1)}}{\partial \bar{\lambda}_3 \partial \lambda_j} \Big|_{\bar{\lambda}_3=0} - \bar{\sigma}_3 \lambda_j \frac{\partial \mathcal{Z}^{(M+1)}}{\partial \bar{\lambda}_2 \partial \lambda_j} \Big|_{\bar{\lambda}_2=0} \right\}. \end{aligned} \quad (2.66)$$

By straightforward Fourier transformation in the λ variables, one can obtain an equivalent hierarchy of equations for the joint PDF's $\mathcal{P}^{(M)}(s_1, \dots, s_M; \mathbf{k}_1, \dots, \mathbf{k}_M)$. For each $M = 1, 2, 3, \dots$ these are equations for conservation of probability

$$\dot{\mathcal{P}}^{(M)} + \sum_{m=1}^M \frac{\partial}{\partial s_m} \mathcal{F}_m^{(M)} = 0, \quad (2.67)$$

CHAPTER 2. MULTI-MODE HIERARCHY EQUATIONS

with the probability flux

$$\begin{aligned} \mathcal{F}_m^{(M)} = & -36\pi s_m \sum_{\underline{\sigma}=(-1,\sigma_2,\sigma_3)} \int d^d \bar{k}_2 d^d \bar{k}_3 \delta^d(\underline{\sigma} \cdot \mathbf{k}_m) \delta(\underline{\sigma} \cdot \omega(\mathbf{k}_m)) |H_{\mathbf{k}_m}^{\underline{\sigma}}|^2 \\ & \left[\int d\bar{s}_2 d\bar{s}_3 \frac{\partial \mathcal{P}^{(M+2)}}{\partial s_m}(s_1, \dots, s_M, \bar{s}_2, \bar{s}_3) \bar{s}_2 \bar{s}_3 \right. \\ & \left. + \sigma_2 \int d\bar{s}_3 \mathcal{P}^{(M+1)}(s_1, \dots, s_M, \bar{s}_3) \bar{s}_3 + \sigma_3 \int d\bar{s}_2 \mathcal{P}^{(M+1)}(s_1, \dots, s_M, \bar{s}_2) \bar{s}_2 \right]. \quad (2.68) \end{aligned}$$

We obtain no closed equations for $\mathcal{P}^{(M)}$ with any choice of M but instead an infinite hierarchy, in which the evolution equation for $\mathcal{P}^{(M)}$ contains $\mathcal{P}^{(M+1)}$ and $\mathcal{P}^{(M+2)}$, for $M = 1, 2, 3, \dots$. Our results are therefore not in agreement with previously proposed closed equations for $\mathcal{P}^{(2)}$ with $M = 2$ (Choi *et al.*, 2009).

We do, however, recover the equations for $\mathcal{P}^{(1)}$ and $\mathcal{Z}^{(1)}$ with $M = 1$ which were previously obtained (Jakobsen and Newell, 2004; Choi *et al.*, 2005a,b), under appropriate conditions. Namely, assume that the initial data for the hierarchy (2.66) are factorized

$$\mathcal{Z}^{(M)}(\lambda_1, \dots, \lambda_M, 0; \mathbf{k}_1, \dots, \mathbf{k}_M) = \prod_{m=1}^M Z(\lambda_m, 0; \mathbf{k}_m),$$

as would follow from RPA initial conditions, for example. It is then easy to show by substitution into (2.66) that there are solutions which remain factorized

$$\mathcal{Z}^{(M)}(\lambda_1, \dots, \lambda_M, \tau; \mathbf{k}_1, \dots, \mathbf{k}_M) = \prod_{m=1}^M Z(\lambda_m, \tau; \mathbf{k}_m), \quad \tau > 0,$$

where the factors $Z(\lambda, \tau; \mathbf{k})$ satisfy the closed equations

$$\frac{\partial}{\partial \tau} Z(\lambda; \mathbf{k}) = i\eta_{\mathbf{k}} \lambda \left(1 + \lambda \frac{\partial}{\partial \lambda} \right) Z(\lambda; \mathbf{k}) - \gamma_{\mathbf{k}} \lambda \frac{\partial Z}{\partial \lambda}(\lambda; \mathbf{k}) \quad (2.69)$$

CHAPTER 2. MULTI-MODE HIERARCHY EQUATIONS

with

$$\eta_{\mathbf{k}} = 36\pi \sum_{\underline{\sigma}=(-1,\sigma_2,\sigma_3)} \int d^d k_2 d^d k_3 \delta^d(\underline{\sigma} \cdot \underline{\mathbf{k}}) \delta(\underline{\sigma} \cdot \omega(\underline{\mathbf{k}})) |H_{\underline{\mathbf{k}}}^{\underline{\sigma}}|^2 n(\mathbf{k}_2) n(\mathbf{k}_3) \geq 0, \quad (2.70)$$

$$\gamma_{\mathbf{k}} = 36\pi \sum_{\underline{\sigma}=(-1,\sigma_2,\sigma_3)} \int d^d k_2 d^d k_3 \delta^d(\underline{\sigma} \cdot \underline{\mathbf{k}}) \delta(\underline{\sigma} \cdot \omega(\underline{\mathbf{k}})) |H_{\underline{\mathbf{k}}}^{\underline{\sigma}}|^2 [\sigma_3 n(\mathbf{k}_2) + \sigma_2 n(\mathbf{k}_3)]. \quad (2.71)$$

These results are equivalent to the existence of solutions of the PDF hierarchy (2.67),(2.68) that remain factorized

$$\mathcal{P}^{(M)}(s_1, \dots, s_M, \tau; \mathbf{k}_1, \dots, \mathbf{k}_M) = \prod_{m=1}^M P(s_m, \tau; \mathbf{k}_m), \quad \tau > 0$$

where the 1-mode pdfs $P(s, \tau; \mathbf{k})$ satisfy

$$\frac{\partial}{\partial \tau} P = \frac{\partial}{\partial s} \left[s \left(\eta_{\mathbf{k}} \frac{\partial P}{\partial s} + \gamma_{\mathbf{k}} P \right) \right]. \quad (2.72)$$

Preservation of RPA therefore follows if one can prove uniqueness of solutions of the hierarchy (2.66) or, equivalently, (2.67),(2.68). The equations for the factors agree with previous results for the 1-mode equations obtained by Jakobsen and Newell (2004) and Choi *et al.* (2005a,b).

The equations (2.72) are not simple linear Fokker-Planck equations, however, but are instead *nonlinear* Markov evolution equations in the sense of McKean (1966). That is, the solutions must satisfy a set of self-consistency conditions,

$$n(\mathbf{k}, \tau) = \int ds s P(s, \tau; \mathbf{k}) \quad (2.73)$$

where $n(\mathbf{k}, \tau)$ is the same spectrum that appears in the formulas for the coefficients (2.70),(2.71).

These equations are the exact solutions of a model of “self-consistent Langevin equations”, like those for the DIA turbulence closure (Kraichnan, 1970; Leith, 1971). Here the model equations take the

CHAPTER 2. MULTI-MODE HIERARCHY EQUATIONS

form of the stochastic differential equations

$$ds_{\mathbf{k}} = (\eta_{\mathbf{k}} - \gamma_{\mathbf{k}} s_{\mathbf{k}}) d\tau + \sqrt{2\eta_{\mathbf{k}} s_{\mathbf{k}}} dW_{\mathbf{k}}, \quad (2.74)$$

interpreted in the Ito sense and with self-consistent determination of $n(\mathbf{k}, \tau)$ via (2.73). Solutions of this stochastic model can be realized by a Monte Carlo procedure of McKean (1966), with (2.74) generalized to

$$ds_{\mathbf{k}}^{(n)} = (\eta_{\mathbf{k}} - \gamma_{\mathbf{k}} s_{\mathbf{k}}^{(n)}) dt + \sqrt{2\eta_{\mathbf{k}} s_{\mathbf{k}}^{(n)}} dW_{\mathbf{k}}^{(n)}, \quad \mathbf{k} \in \Lambda_L^*, n = 1, \dots, N,$$

with the spectrum obtained by an N -sample average

$$n_{\mathbf{k}} = \frac{1}{N} \sum_{n=1}^N s_{\mathbf{k}}^{(n)},$$

and with $\gamma_{\mathbf{k}}, \eta_{\mathbf{k}}$ given by formulas (2.70),(2.71) in which wavevector integrals are discretized as sums. Taking first $N \gg 1$ and then $L \gg a$ yields a solution of the PDF equations (2.72). This procedure works as well to solve the general hierarchy equations (2.67),(2.68), without assuming factorized initial data. For the factorized case, a far simpler procedure is to solve first the wave-kinetic equation (2.59) for $n(\mathbf{k}, \tau)$ and then, using this as input, to solve the 1-mode equation (2.72) in order to obtain $P(s, \tau; \mathbf{k})$ for any wavevector mode \mathbf{k} of interest. As initial condition one may take any $P(s, 0; \mathbf{k})$ which satisfies the consistency condition (2.73) at $\tau = 0$, since this condition is preserved in time by the 1-mode equation.

It is interesting that, independent of the initial condition $P(s, 0; \mathbf{k})$, the solution $P(s, \tau; \mathbf{k})$ relaxes as τ increases to a Rayleigh distribution

$$Q(s, \tau; \mathbf{k}) = \frac{1}{n(\mathbf{k}, \tau)} \exp(-s/n(\mathbf{k}, \tau)), \quad (2.75)$$

CHAPTER 2. MULTI-MODE HIERARCHY EQUATIONS

which corresponds to a Gaussian distribution of the Fourier coefficient $\tilde{a}_{\mathbf{k}}(\tau)$. It is easy to check that, for any solution $n(\mathbf{k}, \tau)$ of the wave-kinetic equation (2.59), $Q(s, \tau; \mathbf{k})$ defined above solves the 1-mode PDF equation (2.72). (Since wavevector \mathbf{k} appears only as a parameter in our argument, we suppress its appearance for the rest of this paragraph.) The relaxation of a general solution P to Q is indicated by an H -theorem for the *relative entropy*⁸

$$H(P|Q) = \int ds P(s) \ln \left(\frac{P(s)}{Q(s)} \right) = \int ds P(s) \ln P(s) + \ln n + 1.$$

This is a convex function of P , non-negative, and vanishing only for $P = Q$ (Cover and Thomas, 1991). Taking the time-derivative using (2.72), it is straightforward to derive

$$\frac{d}{d\tau} H(P(\tau)|Q(\tau)) = -\eta \int ds \frac{s|\partial_s P(s, \tau)|^2}{P(s, \tau)} + \frac{\eta}{n(\tau)},$$

where

$$\int -s\partial_s P(s, \tau) ds = \int P(s, \tau) ds = 1 \quad (2.76)$$

was used to cancel terms involving the γ coefficient. But note the self-consistency condition $n(\tau) = \int s P(s, \tau) ds$ implies

$$\frac{d}{d\tau} H(P(\tau)|Q(\tau)) = -\eta \left(\int ds \frac{s|\partial_s P(s, \tau)|^2}{P(s, \tau)} - \frac{1}{\int s P(s, \tau) ds} \right) \leq 0.$$

The inequality follows from the Cauchy-Schwartz inequality applied to (2.76)

$$1 = \int \sqrt{sP} \cdot \sqrt{\frac{s}{P}} (-\partial_s P) ds \leq \sqrt{\int sP(s) ds \cdot \int \frac{s|\partial_s P|^2}{P} ds}.$$

Equality holds and entropy production vanishes if and only if $\sqrt{sP} = c\sqrt{\frac{s}{P}}(-\partial_s P)$ for some constant c , or $P = -c\partial_s P$. The solution of this latter equation gives $P = Q$ with $n = c$. We thus see that

⁸A related set of observations were made in Jakobsen and Newell (2004, section 9).

CHAPTER 2. MULTI-MODE HIERARCHY EQUATIONS

$P(\tau)$ should relax to $Q(\tau)$ as τ increases. For the purpose of later discussion, we emphasize that this argument assumes that the kinetic theory is valid over the entire range of amplitudes $s \in (0, \infty)$ and it could otherwise fail.

Let us remark that the relative entropy has a simple probabilistic meaning, similar to that discovered by Boltzmann for his entropy function, which involves the empirical PDF $\hat{P}_L(s; \Delta)$ defined in (2.32). For a single cell Δ in wavevector space Λ^* , let $\mu_{\Delta, n, \eta}$ be the microcanonical measure on the set of microstates $\Gamma_{\Delta, n, \eta} = \{(\tilde{J}, \psi) : |\hat{n}_L(\Delta) - n(\Delta)| < \eta\}$. Then, with respect to this microcanonical measure, the most probable value of $\hat{P}_L(s; \Delta)$ as first $L \rightarrow 0$, then $\eta \rightarrow 0$ is $Q(s; \Delta) = e^{-s/n(\Delta)}/n(\Delta)$. However, the probability of observing another PDF P as a rare fluctuation is

$$\lim_{\eta \rightarrow 0} \lim_{L \rightarrow \infty} \frac{1}{N_L(\Delta)} \ln \mu_{\Delta, n, \eta}(\{\hat{P}_L \approx P\}) = -H(P|Q). \quad (2.77)$$

This can be shown heuristically by adapting the original argument of Boltzmann (1872). Let $P(s)$ be a probability density function over possible values of s , let $\Sigma = \{\Sigma_j, j = 1, \dots, R\}$ be a finite partition of the positive reals into intervals with s_j the midpoint values and define the integers $N_j = \left\lfloor N \int_{\Sigma_j} P(s) ds \right\rfloor$ where $\lfloor \cdot \rfloor$ denotes integer part and $N = N_L(\Delta)$. (Since Δ is fixed in this argument, we hereafter omit explicit reference to that quantity in the remainder of this paragraph.) Note that $\sum_{j=1}^R N_j = N$ for large enough L . Now let \hat{N}_j denote the number of modes $\mathbf{k} \in \Lambda_L^* \cap \Delta$ such that $\tilde{\mathbf{k}} \in \Sigma_j$ and define the set $\Gamma_{P, \Sigma, L} = \{(\tilde{J}, \psi) : \hat{N}_j = N_j, j = 1, \dots, R\}$. The Liouville measure of this set is $|\Gamma_{P, \Sigma, L}| = \frac{N!}{N_1! \dots N_R!} |\Sigma_1|^{N_1} \dots |\Sigma_R|^{N_R} \sim \exp\left(-N \sum_j |\Sigma_j| P_j \ln P_j\right)$ with $P_j = N_j/N|\Sigma_j|$ and using Stirling's approximation for the factorials, exactly as in the original argument of Boltzmann. Then

$$\lim_{|\Sigma| \rightarrow 0} \lim_{L \rightarrow \infty} \frac{1}{N} \ln |\Gamma_{P, \Sigma, L}| = - \int ds P(s) \ln P(s).$$

Now consider the set $\Gamma_{n, \eta, L} = \cup_{\{P: |n - \sum_j |\Sigma_j| s_j P_j| < \eta\}} \Gamma_{P, \Sigma, L}$. Its Liouville measure $|\Gamma_{n, \eta, L}|$ is dominated in the limits $L \rightarrow \infty$, $\eta \rightarrow 0$, $|\Sigma| \rightarrow 0$ by $|\Gamma_{P, \Sigma, L}|$ for the pdf P satisfying $\int ds s P(s) = n$ with the largest entropy $-\int ds P(s) \ln P(s)$. As is well-known, this maximum entropy distribution is the

CHAPTER 2. MULTI-MODE HIERARCHY EQUATIONS

Rayleigh pdf $Q(s) = e^{-s/n}/n$. Thus,

$$\lim_{|\Sigma| \rightarrow 0} \lim_{\eta \rightarrow 0} \lim_{L \rightarrow \infty} \frac{1}{N} \ln |\Gamma_{n,\eta,L}| = - \int ds Q(s) \ln Q(s) = \ln n + 1.$$

Taking $\mu_{n,\eta}(\{\hat{P}_L \approx P\}) = \frac{|\Gamma_{P,\Sigma,L}|}{|\Gamma_{n,\eta,L}|}$, then $\lim_{|\Sigma| \rightarrow 0} \lim_{\eta \rightarrow 0} \lim_{L \rightarrow \infty} \frac{1}{N} \ln \frac{|\Gamma_{P,\Sigma,L}|}{|\Gamma_{n,\eta,L}|} = -(\int ds P(s) \ln P(s) + \ln n + 1)$, as claimed. The result (2.77) becomes the standard Sanov theorem (Cover and Thomas, 1991), if the measure $\mu_{\Delta,n,\eta}$ is replaced by the RPA measure for which each mode $\tilde{J}_{\mathbf{k}}$, $\mathbf{k} \in \Lambda_L^* \cap \Delta$ has the independent density $Q(s; \Delta)$.

The above argument motivates a microcanonical measure $\mu_{P,\Delta,\Sigma,\eta,L}$ defined for a given $P(s; \mathbf{k})$ by normalizing Liouville measure on the set

$$\Gamma_{P,\Delta,\Sigma,\eta,L} = \left\{ (\tilde{J}, \psi) : \left| \int_{\Sigma_j} ds \hat{P}_L(s, \Delta_i) - \int_{\Sigma_j} ds P(s, \Delta_i) \right| < \eta, i = 1, \dots, P, j = 1, \dots, R \right\}$$

for partitions Δ of Λ^* and Σ of \mathbb{R}^+ . This measure satisfies the RP property, as it contains no dependence on the phases. One can define for this measure the M -mode correlation functions of the empirical PDF, $\hat{P}_L(\varphi) = \left(\frac{2\pi}{L}\right)^d \sum_{\mathbf{k} \in \Lambda_L^*} \varphi(\tilde{J}_{\mathbf{k}}, \mathbf{k})$:

$$\mathcal{P}_{P,\Delta,\Sigma,\eta,L}^{(M)}(\varphi_1, \dots, \varphi_M) = \mu_{P,\Delta,\Sigma,\eta,L} \left(\hat{P}_L(\varphi_1) \cdots \hat{P}_L(\varphi_M) \right)$$

for any choice of continuous functions $\varphi_1, \dots, \varphi_M$ on $\mathbb{R}^+ \times \Lambda^*$ vanishing at infinity. The arguments of Lanford (1976) can be adapted to show that

$$\lim_{|\Delta|, |\Sigma| \rightarrow 0} \lim_{\eta \rightarrow 0} \lim_{L \rightarrow \infty} \mathcal{P}_{P,\Delta,\Sigma,\eta,L}^{(M)}(\varphi_1, \dots, \varphi_M) = P(\varphi_1) \cdots P(\varphi_M)$$

where $P(\varphi) = \int_0^\infty ds \int_{\Lambda^*} d^d k \varphi(s, \mathbf{k}) P(s; \mathbf{k})$. Thus the factorization property of the M -mode PDFs holds asymptotically for the microcanonical measure $\mu_{P,\Delta,\Sigma,\eta,L}$, although it does not satisfy the strict RPA property. Our derivation of the PDF hierarchy equations (2.67), (2.68) assumed existence

CHAPTER 2. MULTI-MODE HIERARCHY EQUATIONS

of the M -mode PDF's in a somewhat stronger sense in the limit as $L \rightarrow \infty$ (i.e. for fixed values of $\mathbf{k}_1, \dots, \mathbf{k}_M$), but it is reasonable to expect that they remain valid for such “generalized RPA” initial conditions.

Lastly, we can ask what are the solutions of the PDF hierarchy for general initial data which are RP but which are not factorized even asymptotically. One must assume at least that

$$\begin{aligned} \lim_{L \rightarrow \infty} \langle \hat{P}_L(\varphi_1, 0) \cdots \hat{P}_L(\varphi_M, 0) \rangle &= \int_0^\infty ds_1 \cdots \int_0^\infty ds_M \int d^d k_1 \cdots d^d k_M \\ &\quad \times \varphi_1(s_1, \mathbf{k}_1) \cdots \varphi_M(s_M, \mathbf{k}_M) \mathcal{P}_0^{(M)}(s_1, \dots, s_M; \mathbf{k}_1, \dots, \mathbf{k}_M), \end{aligned}$$

in order to provide suitable initial data $\mathcal{P}_0^{(M)}(s_1, \dots, s_M; \mathbf{k}_1, \dots, \mathbf{k}_M)$ for the hierarchy. However, with appropriate technical assumptions, it follows by the argument of Spohn (1984) that

$$\mathcal{P}_0^{(M)}(s_1, \dots, s_M; \mathbf{k}_1, \dots, \mathbf{k}_M) = \int d\rho_0(P) P(s_1; \mathbf{k}_1) \cdots P(s_M; \mathbf{k}_M),$$

where ρ_0 is a probability measure on the PDF's. Since the PDF hierarchy equations (2.67),(2.68) are linear in the $\mathcal{P}^{(M)}$'s, a solution will be provided by

$$\mathcal{P}^{(M)}(s_1, \dots, s_M, \tau; \mathbf{k}_1, \dots, \mathbf{k}_M) = \int d\rho_0(P) P(s_1, \tau; \mathbf{k}_1) \cdots P(s_M, \tau; \mathbf{k}_M).$$

This will be the only solution if existence and uniqueness of solutions holds for the PDF hierarchy. Thus, the most general realizable solutions of the PDF hierarchy equations are again expected to be “super-statistical solutions” that correspond to ensembles of solutions of the 1-mode PDF equations (2.72) with random initial conditions.

2.7 Intermittency in Kinetic Wave Turbulence

One of the important potential applications of multi-mode equations in wave kinetics is the explanation of observed intermittency and anomalous scaling in wave turbulence (Falcon *et al.*, 2007; Nazarenko *et al.*, 2010; Yokoyama, 2004). On the face of it, wave-kinetic theory appears to have few resources to explain such phenomena and instead has all the attributes of a “mean-field theory” (Goldenfeld, 1992). As we have seen in previous sections, it is a theory which ignores fluctuations and in which important quantities in fact become deterministic. All interactions of the infinite collection of modes are through a mean-field $n(\mathbf{k}, \tau)$. Furthermore, scaling exponents in the Kolmogorov solutions of the wave-kinetic equations are given by dimensional analysis (Connaughton *et al.*, 2003). These are the hallmarks of a mean-field theory, which generally cannot predict anomalous scaling.

Nevertheless, there are at least two approaches based on wave kinetics which seem to have some promise to explain intermittency and non-Gaussian statistics. One is the idea of a “cascade in amplitude space” that was proposed by Choi *et al.* (2005b) and Nazarenko *et al.* (2010), based on the 1-mode PDF equation (2.72). Another is the idea of a “super-turbulence” in wave-kinetics, advanced in the present work. We shall now discuss both of these possibilities.

2.7.1 Cascade in Amplitude Space?

It is well-known that wave-kinetic equations generally cannot be uniformly valid over the whole range of wavenumbers, but must break down in either low or high wavenumbers where non-linearity become strong (Connaughton *et al.*, 2003). Choi *et al.* (2005b) and Nazarenko *et al.* (2010) have proposed that there is a similar non-uniformity in amplitude space, with equation (2.72) for the 1-mode PDF $P(s, \tau; \mathbf{k})$ restricted in validity to $s < s_{nl}$, where s_{nl} is the amplitude for which nonlinear interactions become strong at wavevector \mathbf{k} . [For the remainder of this section we shall assume that the wavevector \mathbf{k} is fixed and drop it as an explicit label.] For amplitudes $s > s_{nl}$ strong-interaction processes such as “wave-breaking”, “crested”, etc. are assumed to occur which

CHAPTER 2. MULTI-MODE HIERARCHY EQUATIONS

are beyond the description of wave kinetics. The hope is that the effects of such nonlinear processes can be modeled by supplementing the equation (2.72) with suitable boundary conditions and forcing terms. We find this a very intriguing suggestion but, as we now argue, it seems to us to have as yet no successful formulation, either analytically or physically.

Let us review the specific proposals of Choi *et al.* (2005b) and Nazarenko *et al.* (2010). They note that eq.(2.72) is a probability conservation law

$$\partial_t P + \partial_s F = 0 \quad (2.78)$$

with probability flux in amplitude space given by

$$F(s) = -s(\gamma P + \eta \partial_s P). \quad (2.79)$$

The general time-independent solution of (2.78) with constant flux $F(s) = F_*$ was observed by Choi *et al.* (2005b) to be

$$P(s) = C e^{-s/\nu} - \frac{F_*}{\eta} \text{Ei}(s/\nu) e^{-s/\nu}$$

with $\nu \equiv \eta/\gamma$ and with $\text{Ei}(x) = \text{P} \int_{-\infty}^x e^t \frac{dt}{t}$ the standard exponential integral. The first term has zero flux $F(s) \equiv 0$ while the second term has non-vanishing flux $F(s) \equiv F_*$. Since $\text{Ei}(x) > 0$ for $x > x_* \doteq 0.3725$, positivity of $P(s)$ for $s \gg \nu$ requires $F_* \leq 0$. When $F_* = 0$ then $P(s) = Q(s)$, the Rayleigh distribution with spectral density $n = \nu$. Not noted in Choi *et al.* (2005b) is the fact that one must more generally make a distinction between ν and n given by the self-consistency condition

$$n = \int ds s P(s),$$

which are only the same when $P = Q$. The above integral diverges for $F_* \neq 0$, if the upper limit extends to infinity, because $P(s) \sim \frac{|F_*|}{\gamma s}$ due to the asymptotics $\text{Ei}(x) \sim \frac{e^x}{x} \left(1 + \frac{1!}{x} + \frac{2!}{x^2} + \dots\right)$ for

CHAPTER 2. MULTI-MODE HIERARCHY EQUATIONS

$x \gg 1$. The integral is finite if it is cut off at the upper limit s_{nl} . This assumes that whatever nonlinear processes such as “wave-breaking” occur at $s > s_{nl}$ lead to a PDF which decays very rapidly for $s \gtrsim s_{nl}$.

Choi *et al.* (2005b) and Nazarenko *et al.* (2010) propose to model the nonlinear effects at $s > s_{nl}$ by a negative flux $F(s_{nl}) = F_* < 0$, which represents a flow of samples back into the kinetic range $s < s_{nl}$, at least in some range of wavenumbers. For example, this might occur at low-wavenumbers as wavecaps and cusps in the nonlinear range break up and feed back into the weak, incoherent background. However, the equation (2.78) will then no longer conserve probability but instead satisfies $\frac{d}{dt} \int_0^{s_{nl}} ds P(s) = |F_*| > 0$. Choi *et al.* (2005b) propose to add to the equation a constant “drag” D

$$\partial_t P + \partial_s F = -D, \quad s < s_{nl} \quad (2.80)$$

to represent the dilution in the weight of samples at $s < s_{nl}$ by the flux F_* of new samples into the ensemble at $s = s_{nl}$. It is easy to see that one must choose $D = |F_*|/s_{nl}$ to conserve total probability⁹. Choi *et al.* (2005b) then claim that the general solution to the modified equation is $P(s) = Ce^{-s/n} + \frac{|F_*|}{\eta} \text{Ei}(s/n - \log(s/n))e^{-s/n}$. The picture proposed in Choi *et al.* (2005b) and Nazarenko *et al.* (2010) is one of an “inverse probability cascade” with flux $F_* < 0$ in amplitude space, coexisting with the usual forward energy cascade in wavevector space. The power-law tails $P(s) \sim \frac{|F_*|}{\gamma s}$ for $s \gg \nu$ are a source of non-Gaussianity and intermittency in wave turbulence if $F_* \neq 0$. A “critical balance” argument is used in Nazarenko *et al.* (2010) to estimate that $|F_*| \sim \gamma n/s_{nl}$.

It is easy to see, however, that the proposed cascade picture cannot be correct for the specific model in Choi *et al.* (2005b) and Nazarenko *et al.* (2010), on both physical and mathematical grounds. A constant “drag” D is not localized at small and large s but has effects felt over the whole range of s . Thus, one would not expect a constant-flux “inertial range” to exist for such a drag. In

⁹In fact, Choi *et al.* (2005b) proposed to take $D = -\gamma P(s_{nl})/s_{nl}$, which does not conserve probability and which is not even dimensionally correct.

CHAPTER 2. MULTI-MODE HIERARCHY EQUATIONS

fact, for any choice of D , a particular solution of the inhomogeneous equation (2.80) is

$$P_{part}(s) = D/\gamma.$$

The general solution $P(s)$ of (2.80) is a superposition of $P_{part}(s)$ with any solution of the homogeneous equation (2.78):

$$P(s) = \frac{D}{\gamma} + \frac{C_1}{\nu} e^{-s/\nu} + \frac{C_2}{\nu} e^{-s/\nu} \text{Ei}\left(\frac{s}{\nu}\right).$$

This has flux $F(s) = -Ds - C_2\gamma$. With the boundary condition $F(s_{nl}) = F_*$ and the unique probability-conserving choice $D = |F_*|/s_{nl}$ one finds $C_2 = 0$ and thus

$$P(s) = \frac{|F_*|}{\gamma} \cdot \frac{1}{s_{nl}} + \left(1 - \frac{|F_*|}{\gamma}\right) \frac{e^{-s/\nu}}{\nu(1 - e^{-s_{nl}/\nu})}, \quad (2.81)$$

using normalization. Note the requirement $|F_*| < \gamma$ for positivity of this solution, which is then a superposition of a Rayleigh distribution and a uniform distribution. As expected, it has not constant flux but instead $F(s) = F_*s/s_{nl}$.

We claim that (2.81) is the correct solution of the model formulated in Choi *et al.* (2005b). It gives an alternative possibility to explain intermittency and non-Rayleigh distributions, with constant tails $P(s) \propto s^0$ for $s \gg \nu$ rather than $P(s) \propto s^{-1}$. Using the estimate $|F_*| \sim \gamma n/s_{nl}$ of Nazarenko *et al.* (2010) one finds that the realizability inequality $|F_*| < \gamma$ is satisfied whenever $n \lesssim s_{nl}$. However, it is unclear to us that the flux b.c. and constant drag D give a physically correct model of wave-breaking. Constant-flux solutions as originally proposed in Choi *et al.* (2005b) could be relevant with a more general model of strong nonlinear effects, in which the constant D is replaced with a function $D(s)$ such that $\int_0^{s_{nl}} ds D(s) = |F_*|$ but for which $D(s)$ nearly vanishes except at the upper and lower limits. This would provide a “transparency window” that would allow constant probability-flux solutions to exist.

Whatever may be the correct model of the strong nonlinear effects at $s > s_{nl}$, an important

CHAPTER 2. MULTI-MODE HIERARCHY EQUATIONS

general point is that any modification of the 1-mode PDF eq.(2.78) requires that the wave-kinetic equation must also be modified. This can be illustrated for the specific model in (2.80) with $D = |F_*|/s_{nl}$. Taking the time-dervative of $n = \int_0^{s_{nl}} ds sP(s)$ gives

$$\dot{n} = -\gamma n + \eta - \eta s_{nl} P(s_{nl}) + \frac{1}{2}|F_*|s_{nl}, \quad (2.82)$$

which differs from the standard kinetic equation $\dot{n} = -\gamma n + \eta$. The stationary form of the “modified kinetic equation” (2.82) is easily checked to be valid for our solution (2.81) by calculating $n = \int_0^{s_{nl}} ds sP(s)$ to be

$$\begin{aligned} n &= \nu - \nu s_{nl} P(s_{nl}) + \frac{|F_*|}{2\gamma} s_{nl} \\ &\simeq \nu \left(1 - \frac{|F_*|}{\gamma}\right) + \frac{|F_*|}{2\gamma} s_{nl}, \end{aligned} \quad (2.83)$$

with the latter approximation valid for $s_{nl} \gg \nu$. The correction to the usual value $n = \nu$ predicted by the kinetic equation need not be small. If we use the estimate $|F_*| \sim \gamma n/s_{nl}$ from “critical balance” (Nazarenko *et al.*, 2010) then the second term in (2.83) is comparable to the first term, or even much larger if $\nu \ll n$. If such changes in $n(\mathbf{k})$ occur for a large set of wavevectors \mathbf{k} , then the coefficients γ and η defined through the integrals (2.70),(2.71) may also be strongly modified. These remarks make clear the nontriviality of constructing a self-consistent hybrid model of wave kinetics and of the strong nonlinear effects.

2.7.2 Super-Turbulence of Wave Kinetics?

A second possibility to explain intermittency and anomalous scaling entirely within the framework of wave kinetics is by “super-turbulence”. We shall discuss this mechanism here, mainly at a general, qualitative level.

It is useful to begin with a review of the work of Spohn (1984), who already discussed turbulence in gas dynamics as a natural motivation for ensembles of Boltzmann solutions. This is

CHAPTER 2. MULTI-MODE HIERARCHY EQUATIONS

easiest to understand in the hydrodynamic regime where length-scale of variations in local equilibrium parameters (temperature, density, velocity) is much larger than the mean-free-path length. The Boltzmann equation reduces then to a hydrodynamic description and one can appeal to the extensive literature on turbulent solutions of hydrodynamic equations. The specific example discussed in Spohn (1984) is the Rayleigh-Bernard system, considered as a many-particle system subject to thermal boundary conditions. In such a situation driven by the boundary conditions, Boltzmann's original H -theorem is no longer valid and the stationary solution of the Boltzmann equation for the pure conducting state is no longer purely Maxwellian but has a small correction corresponding to thermal non-equilibrium (Esposito *et al.*, 1998). In the turbulent regime at sufficiently high Reynolds and Rayleigh numbers, the laminar purely conducting state is unstable and turbulent convection develops. The temporal dynamics is chaotic so that long-time-averages, for example, are described naturally by invariant measures corresponding to ensembles of Boltzmann solutions.

Such a statistical description is natural also for turbulent situations without driving by body forces or boundaries and with time-dependent statistics. For example, a single realization of decaying, statistically homogeneous turbulence is very spatially complex and heterogeneous. Averages over large volumes —by space-ergodicity— are again described by ensembles of solutions. Note in this example that Boltzmann's H -theorem applies, with a monotonic increase of entropy due to heating of the fluid. There is eventual approach to global thermodynamic equilibrium and a space-independent Maxwellian 1-particle distribution, but the turbulent state with strong spatial variations exists as a long transient for an intermediate range of times. The previous examples are in the hydrodynamic regime, but there should be similar turbulence in the fully kinetic regime. For example, in compressible turbulence in gases at sufficiently high Mach numbers the thickness of shocks should be of the order of the mean-free-path length (Griffith, 1981) and, for a quantitative description, the Boltzmann equation should be used rather than hydrodynamic equations.

These ideas can carry over from the Boltzmann equation to the wave-kinetic equation. As noted in the introduction, Zakharov *et al.* (1992, section 4.2.2) had already pointed out that strong

CHAPTER 2. MULTI-MODE HIERARCHY EQUATIONS

instability of the Kolmogorov solutions to the wave-kinetic equation could lead to such a “secondary turbulence”. The statistical distribution of wave amplitudes that would be obtained in a long time-series from experiment or simulation would then correspond to a random ensemble of solutions of the 1-mode PDF equation (2.72):

$$\mathcal{P}^{(1)}(s; \mathbf{k}) = \int d\rho(P) P(s; \mathbf{k}).$$

Even if the individual solutions $P(s; \mathbf{k})$ were close to Rayleigh distributions, the measurable distributions $\mathcal{P}^{(1)}(s; \mathbf{k})$ could be arbitrarily far from Rayleigh, depending upon the “super-statistical” measure ρ . To determine this measure becomes a very difficult problem, as daunting as the corresponding problem for Navier-Stokes turbulence! Here we can only identify some of the sources of randomness, including instability, random forcing, and boundary conditions. We consider these in turn.

Instability of the Kolmogorov solution is a natural origin for “super-turbulence”. As a related example, consider the GOY shell model of turbulence, a dynamical system with a stationary Kolmogorov solution supporting a constant energy flux with dimensional scaling (Biferale, 2003). This solution, however, is subject to a rich array of instabilities (Biferale *et al.*, 1995; Kadanoff *et al.*, 1997) and the statistical behavior of the GOY model shows strong intermittency and anomalous scaling. There is a detailed theory of linear stability of the Kolmogorov solutions of wave-kinetic theory (Falkovich and Shafarenko, 1987; Balk and Zakharov, 1988a,b, 1998), reviewed in Zakharov *et al.* (1992, Chap. 4). This theory studies perturbations to a scale-homogeneous Kolmogorov solution which, strictly speaking, requires an infinitely long inertial interval. The conclusion of this theory is that, for most common cases, the Kolmogorov solution is linearly stable. However, the theory, although sophisticated, is not quite definitive. Quoting from Zakharov *et al.* (1992):

“It should be noted that a more consistent formulation of the problem of the stability of the Kolmogorov spectrum should be as follows. First of all, the kinetic equation should be supplemented by terms describing the isotropic pumping and damping regions and a stationary solution of this equation should be found that is close to the Kolmogorov

CHAPTER 2. MULTI-MODE HIERARCHY EQUATIONS

spectrum in an interval (k_1, k_2) ; outside this interval the solution may strongly differ from the Kolmogorov spectrum. Then the kinetic equation must be linearized in the vicinity of this stationary solution and expanded in angular harmonics. . . . Having examined the behavior of the solutions equation, one should clarify the changes that occur when the ranges of the source and sink in k -space go to zero or to infinity and examine the behavior of the perturbations established in the interval (k_1, k_2) . Finally, one should analyze in which situations this behavior is independent of the specific type of the source and sink.

This program for examining the stability of Kolmogorov spectra turns out to be too complex. Currently there exists no strict proof of the fact that in general the kinetic equation with a source and sink has a stationary solution close to the Kolmogorov spectrum in some interval.”

In fact, the situation is even less certain than this statement implies. There are hydrodynamic flows such as plane Couette and pipe Poiseuille which, despite being linearly stable for all Reynolds numbers, become turbulent in laboratory experiments and in numerical simulations at moderate Reynolds number (Schmid and Henningson, 2001). The usual understanding is that these flows are unstable to finite amplitude perturbations, e.g. Dubrulle and Zahn (1991). Thus, linear stability does not rule out transition to turbulence. For these reasons, we must regard “super-turbulence” as a viable possibility in wave kinetics.

As emphasized in the previous quote, external forcings are required to maintain a stationary energy cascade state. It is important to consider more deeply the origin and role of such forces. Zakharov *et al.* (1992) consider the necessary conditions on the force for the existence of a stationary distribution (section 2.2.3) and how to match the Kolmogorov solutions to the wavevector regions of the force (section 3.4). This discussion assumes a particular idealized model for the forcing, in which to the collision integral $I(\mathbf{k}, \tau)$ of the wave-kinetic equation there is added an additional term:

$$\dot{n}(\mathbf{k}, \tau) = \Gamma(\mathbf{k}, \tau)n(\mathbf{k}, \tau) + I(\mathbf{k}, \tau).$$

This model describes “pumping” for wavevectors at which $\Gamma(\mathbf{k}, \tau) > 0$ and “damping” for $\Gamma(\mathbf{k}, \tau) < 0$. Validity of this model requires a suitably weak, slowly-changing force in the equations of motion

CHAPTER 2. MULTI-MODE HIERARCHY EQUATIONS

(2.21):

$$\frac{d}{dt} A_{\mathbf{k}}^{\sigma} = \frac{1}{2} \epsilon^2 \Gamma(\mathbf{k}, \epsilon^2 t) A_{\mathbf{k}}^{\sigma} + \dots$$

Here \dots denotes the original terms in (2.21). The addition of this term to the dynamics can be easily accommodated into our derivations, with a new term appearing in eq.(2.39)

$$a_{\mathbf{k}}^{(2)}(T) = \frac{1}{2} T \cdot \Gamma_{\mathbf{k}} a_{\mathbf{k}}^{(0)} + \dots,$$

in eq.(2.44)

$$\mathcal{J}_3 = \frac{1}{2} T \delta_{\mu,0} \sum_1 \Gamma_1 \lambda_1 J_1 + \dots,$$

in eq.(2.56)

$$\frac{d\mathcal{Z}}{d\tau} = \int d^d k \Gamma(\mathbf{k}, \tau) \lambda(\mathbf{k}) \frac{\delta \mathcal{Z}}{\delta \lambda(\mathbf{k})} + \dots,$$

in eq.(2.65)

$$\frac{d\mathcal{Z}^{(M)}}{d\tau} = \sum_{m=1}^M \Gamma(\mathbf{k}_m, \tau) \lambda_m \frac{\partial \mathcal{Z}^{(M)}}{\partial \lambda_m} + \dots$$

and in eq.(2.68)

$$\mathcal{F}_m^{(M)} = \Gamma(\mathbf{k}_m, \tau) s_m + \dots$$

Thus, the standard forcing model from Zakharov *et al.* (1992) is obtained. All of our previous results, e.g. on preservation of factorized solutions, law of large numbers, etc., still carry over. In general, forced wave turbulence can be described by kinetic equations only for suitable assumptions on the forcing, like those above. In the above derivation, the only randomness was in the phases and amplitudes of the waves. However, the forcing amplitudes $\Gamma(\mathbf{k}, \tau)$ may be chosen to be a realization of a stationary and time-ergodic random process. In that case, long-time averages in the statistical steady-state can be described by averages over ensembles of solutions of the wave-kinetic equations with different realizations of the force. In fact, Falcon *et al.* (2008) find that in their experiments the forcing is well modelled by an Ornstein-Uhlenbeck process with large fluctuations in the energy

CHAPTER 2. MULTI-MODE HIERARCHY EQUATIONS

input rate. Even without chaos or turbulence in the wave-kinetic equations, this will yield “super-randomness”, since the Kolmogorov solution is neutrally stable to change in the energy flux rate (Zakharov *et al.*, 1992).

In addition to pumping by an external force, hydrodynamic turbulence may also be (in fact, more commonly, is) driven by boundary conditions. Such a situation can also occur in wave kinetics, as we have discussed in the previous section 2.7.1, where strongly nonlinear effects such as wave-breaking can provide both sinks and sources to kinetic wave turbulence. These effects restrict the validity of wave kinetics to a “bounded domain” in wavevectors and amplitudes and could provide suitable forcings at the boundaries to represent those nonlinear effects. In this setting, Kolmogorov cascade solutions which are stable when considered without restriction, might become unstable and “super-turbulence” develop. The two scenarios in this section and the previous one are thus not completely exclusive.

2.8 Conclusion

We summarize the major contributions of this chapter here:

1. We have derived by formal asymptotics the correct multi-mode equations for wave kinetics in Hamiltonian systems with 3-wave resonances.
2. We have shown formally that these equations possess factorized solutions for factorized initial conditions, corresponding to “propagation of chaos” or preservation of “random phases & amplitudes”.
3. We introduced the “empirical spectrum” and “empirical 1-mode PDF” and showed that the above factorization implies a law of large numbers, so that these quantities are self-averaging and satisfy the wave-kinetic equations for nearly every initial realization of random phases and amplitudes.

CHAPTER 2. MULTI-MODE HIERARCHY EQUATIONS

4. We have demonstrated the close formal relations of wave-kinetic theory with the kinetic theory of gases, especially regarding the role of entropy and the 2nd law of thermodynamics in both theories.
5. We have completely classified all realizable solutions of our multi-mode equations and have shown that they correspond to an ensemble of “super-statistical solutions”, or ensembles of the wave-kinetic equations with either random initial conditions or random forces.
6. We have exploited our results to discuss the possibilities to explain intermittency and non-Gaussian statistics of wave turbulence within the kinetic description, in particular by a super-turbulence corresponding to ensembles of chaotic or stochastic solutions of the wave-kinetic equations.

Chapter 3

Resonance Van Hove Singularities: Case Studies

3.1 Introduction

In the last chapter, we have formally derived the multi-mode hierarchy equations and discussed some of their properties. Our analysis is based on multi-scale perturbation analysis with no rigorous bounds on the error terms. Indeed, many questions remain about the validity of these equations, in particular, in which wavenumber regimes they hold and under what precise assumptions on the underlying wave dynamics. It has been cogently argued by Newell and Rumpf (2011) and Spohn (2006) that one can relax the RPA assumption to dispersivity of the waves. In this and the following chapter we shall argue that the dispersivity requirement is more stringent than what has commonly been understood. In particular, a wave system that is generally dispersive can experience a breakdown of dispersivity locally in the N -wave phase space which renders the wave-kinetic equation ill-defined. Consider, for example, a general 3-wave equation for the evolution of the wave-action

CHAPTER 3. RESONANCE VAN HOVE SINGULARITIES: CASE STUDIES

spectrum, $n(\mathbf{k}, t)$:

$$\begin{aligned} \partial_\tau n(\mathbf{k}, \tau) = & 36\pi \sum_{\underline{\sigma}=(-1, \sigma_2, \sigma_3)} \int d^d k_2 \int d^d k_3 |H_{\underline{\mathbf{k}}}^{\underline{\sigma}}|^2 \delta(\underline{\sigma} \cdot \omega(\underline{\mathbf{k}})) \delta^d(\underline{\sigma} \cdot \underline{\mathbf{k}}) \\ & \times \left\{ n(\mathbf{k}_2) n(\mathbf{k}_3) - \sigma_2 n(\mathbf{k}) n(\mathbf{k}_3) - \sigma_3 n(\mathbf{k}) n(\mathbf{k}_2) \right\}. \end{aligned} \quad (3.1)$$

Here we use the shorthand notations $\underline{\mathbf{k}} = (\mathbf{k}, \mathbf{k}_2, \mathbf{k}_3)$, $\underline{\sigma} = (\sigma, \sigma_2, \sigma_3)$ with $\underline{a} \cdot \underline{b} = ab + a_2 b_2 + a_3 b_3$. The integer σ labels the degree of degeneracy of the waves, or the number of frequencies ω_σ corresponding to a given wavevector \mathbf{k} . We have assumed above that $\sigma = \pm 1$ and $\omega_\sigma(\mathbf{k}) = \sigma \omega(\mathbf{k})$, appropriate for systems second-order in time where there are two waves traveling in opposite directions. Because of the Dirac delta functions, the collision integral is restricted to the *resonant manifold*:

$$\mathcal{R}_{\mathbf{k}}^{\sigma_2 \sigma_3} = \left\{ \mathbf{k}_2 : \sigma \omega(\mathbf{k}) + \sigma_2 \omega(\mathbf{k}_2) + \sigma_3 \omega(\mathbf{k}_3) \Big|_{\mathbf{k}_3 = -\sigma_3(\sigma \mathbf{k} + \sigma_2 \mathbf{k}_2)} = 0 \right\}.$$

An immediate issue in making sense of the kinetic equation is the well-definedness of the measure on $\mathcal{R}_{\mathbf{k}}$:

$$\int d^d k_2 \int d^d k_3 \delta(\underline{\sigma} \cdot \omega(\underline{\mathbf{k}})) \delta^d(\underline{\sigma} \cdot \underline{\mathbf{k}}) = \int_{\mathcal{R}_{\mathbf{k}}} \frac{dS(\mathbf{k}_2)}{|\nabla \omega(\mathbf{k}_2) - \nabla \omega(\mathbf{k}_3)|}. \quad (3.2)$$

In the last equality we have used a standard formula to express the measure in terms of the surface area S on the imbedded manifold in Euclidean space (e.g. see Hörmander (1983, theorem 6.1.5)). The difficulty occurs at critical points where

$$\nabla \omega(\mathbf{k}_2) = \nabla \omega(\mathbf{k}_3)$$

and the denominator vanishes. Since $\nabla \omega(\mathbf{k})$ is the group velocity of wavepackets, such points correspond physically to wavevector triads at which the dispersivity of the wave system breaks down locally and for which two distinct wavepackets from the triad propagate together for all times

CHAPTER 3. RESONANCE VAN HOVE SINGULARITIES: CASE STUDIES

with the same velocity. The kinetic equation may be ill-defined for \mathbf{k} at which the denominator produces a non-integrable singularity.

An exactly analogous problem was studied in 1953 by Van Hove (1953) for the phonon density of states in a crystalline solid, which is the function defined by

$$g(\omega) = L^d \sum_{\sigma} \int d^d k \, \delta^d(\omega - \omega_{\sigma}(\mathbf{k})) = \frac{L^d}{(2\pi)^d} \sum_{\sigma} \int_{\omega_{\sigma}(\mathbf{k})=\omega} \frac{dS(\mathbf{k})}{|\nabla \omega_{\sigma}(\mathbf{k})|}$$

where the sum σ is over the branches of phonon frequencies and the \mathbf{k} -integral is over a Brillouin zone of the crystal. Critical points of the phonon dispersion relations, where the group velocity $\nabla \omega_{\sigma}(\mathbf{k})$ vanishes, may lead to singularities in the density of states. Indeed, by a beautiful application of the Morse inequalities (Milnor, 1963), Van Hove showed that the homology groups of the Brillouin zone (topologically a d -torus) make such critical points inevitable. He showed further by a local analysis of the critical points using the Morse Lemma (Milnor, 1963; Lang, 2012) that the resulting singularities are non-integrable for space dimension $d = 2$, giving rise to a logarithmic divergence in the density of states, and are integrable for $d = 3$, producing divergences only in the derivative (cusps). As we shall see in the following, the local analysis of Van Hove carries over to the corresponding point singularities in the measures (3.2) on the resonant manifolds, which we propose to call *resonance Van Hove singularities* because of their close physical and mathematical analogies with the singularities considered by Van Hove.

It is important to emphasize that the global topological argument for existence of critical points given by Van Hove does not carry over to the wave-kinetic problem, even when there is a spatial lattice and the reciprocal wavevector space is a d -torus. The most essential difference is that the density of states function involves all level sets of the dispersion relation, whereas only the zero level sets are relevant for wave kinetics. Nevertheless, topological criteria for existence of singularities can be sometimes exploited in wave kinetics. For example, in the absence of singular points, the resonant manifold can deform continuously from $\mathcal{R}_{\mathbf{k}_1}$ to $\mathcal{R}_{\mathbf{k}_2}$ for any \mathbf{k}_1 and \mathbf{k}_2 . It is

CHAPTER 3. RESONANCE VAN HOVE SINGULARITIES: CASE STUDIES

thus sufficient to establish the existence of singularity if one can find certain topological invariants of two manifolds $\mathcal{R}_{\mathbf{k}_1}$ and $\mathcal{R}_{\mathbf{k}_2}$ for $\mathbf{k}_1 \neq \mathbf{k}_2$, e.g., the fundamental group or the homology group, which are different. We shall not develop general criteria along this line but instead show by many concrete examples below that critical points often appear on the resonant manifold in practice. Figure 3.1 plots a simple example ¹ in which physical space is a cubic lattice and wavevector space is a 3-torus, which can have relevance for numerical simulations of wave turbulence on a rectangular grid (for more discussion, see section 3.2.2). This example illustrates the general geometric feature of resonant Van Hove singularities that the “resonant manifold” is no longer a true manifold, locally diffeomorphic to Euclidean space. When zero is a regular value of the resonance condition, then the Regular Value Theorem/Submersion Theorem (Guillemin and Pollack, 1974) guarantees that the “resonant manifold” is indeed a smooth manifold. This is not usually the case when zero is a critical value. If the dispersion relation is not a Morse function (i.e. a smooth function with only non-degenerate critical points), then the singularities can occur also along critical lines and surfaces within the resonant manifold.

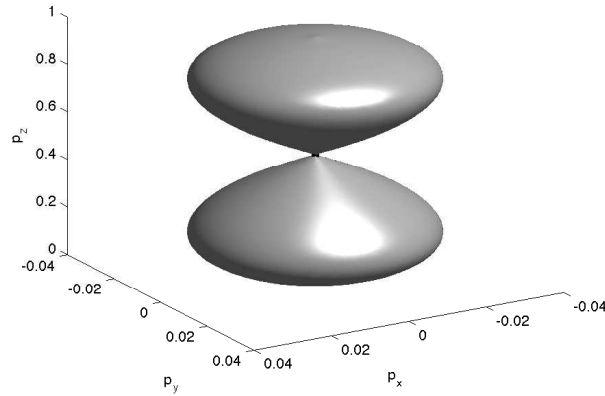


Figure 3.1: Three-wave resonant manifold $\mathcal{R}_{\mathbf{k}} = \{\mathbf{p} : \omega(\mathbf{p}) + \omega(\mathbf{k} - \mathbf{p}) - \omega(\mathbf{k}) = 0\}$ for dispersion relation $\omega(\mathbf{k}) = \left[4 \sum_{i=1}^3 \sin^2\left(\frac{k_i}{2}\right)\right]^{\alpha/2}$, $\alpha = \frac{1}{1+\log_2 \cos(1/4)}$, on the 3-torus $[-\pi, \pi]^3$, and for the specific wavevector $\mathbf{k} = (0, 0, 1)$. There is a critical point (black dot) at $\mathbf{p} = \mathbf{k}/2$.

¹All of the resonant manifolds exhibited in this chapter are plotted with MATLAB, using `contour` for $D = 2$ and `isosurface` for $D \geq 3$

CHAPTER 3. RESONANCE VAN HOVE SINGULARITIES: CASE STUDIES

The critical set on the singular manifold may have effects on the wave-kinetic theory either little or drastic, depending on their character. As in the analysis of Van Hove, isolated critical points have only very mild consequences for 3-wave resonances in space dimensions $d \geq 3$, but lead to divergences for $d = 1, 2$, which may alter the naive predictions of the wave-kinetic theory or vitiate the theory entirely. For higher-order wave resonances and in higher space dimensions, critical lines and surfaces can have similar effects. We shall give below examples of resonance Van Hove singularities for many concrete systems, including acoustic waves in compressible fluids, helical waves in rotating incompressible fluids, capillary-gravity waves on free fluid surfaces, one-dimensional optical waves, electron-hole matter waves in graphene, etc. A pioneering study of acoustic wave turbulence by Newell and Aucoin (1971) argued that the breakdown of dispersivity of sound waves on the resonant manifold leads to a different long-time asymptotics and a modified kinetic equation. The breakdown for acoustic waves is extremely severe, in that all points on the resonant manifold are critical (for more discussion, see section 3.2.1). As we shall discuss in this work, even a single critical point on the resonant manifold can lead to breakdown of standard wave kinetics, which then must be replaced with a new *singular kinetic equation* with a collision integral resulting only from resonant interactions in the critical set.

In this chapter, we want to consider singularities that occur for various dispersion relations commonly discussed in the literature. We begin with the simplest case of 3-wave resonances.

3.2 Triplet Resonances

The conditions of resonance for triplet interaction can be written, without loss of generality, as

$$\sigma_2\omega(\mathbf{p}) + \sigma_3\omega(\mathbf{q}) = \omega(\mathbf{k}) \quad (3.3)$$

$$\sigma_2\mathbf{p} + \sigma_3\mathbf{q} = \mathbf{k} \quad (3.4)$$

CHAPTER 3. RESONANCE VAN HOVE SINGULARITIES: CASE STUDIES

by taking $\sigma'_i = -\sigma_i\sigma \rightarrow \sigma_i$, and the condition for singularity as

$$\nabla\omega(\mathbf{p}) = \nabla\omega(\mathbf{q}). \quad (3.5)$$

3.2.1 Isotropic Power Law

In wave turbulence literature, the most commonly considered dispersion relation is an isotropic power-law:

$$\omega(\mathbf{k}) = Ck^\alpha. \quad (3.6)$$

Resonance requires $\alpha \geq 1$ (Nazarenko, 2011). The singularity condition (3.5) becomes

$$p^{\alpha-2}\mathbf{p} = q^{\alpha-2}\mathbf{q} \quad (3.7)$$

and thus

$$p^{\alpha-1} = q^{\alpha-1}. \quad (3.8)$$

We treat first the case $\alpha > 1$, where clearly (3.8) implies $p = q$ and (3.7) then implies $\mathbf{p} = \mathbf{q}$. Substituting back into (3.3),(3.4) gives

$$k^\alpha = (\sigma_2 + \sigma_3)p^\alpha, \quad \mathbf{k} = (\sigma_2 + \sigma_3)\mathbf{q}.$$

If $p = q = 0$, then also $k = 0$, which is the trivial resonance with all members of the triad zero. If $p = q > 0$, then we can have either $\sigma_2 + \sigma_3 = 2$ or $\sigma_2 + \sigma_3 = 0$. However, $\sigma_2 + \sigma_3 = 2$ implies both $k^\alpha = 2p^\alpha$ and $k = 2p$, which requires $\alpha = 1$, a contradiction. If instead $\sigma_2 + \sigma_3 = 0$, then $\mathbf{k} = \mathbf{0}$ and any $\mathbf{p} = \mathbf{q}$ are allowed. The “resonant manifold” is here all of space. However, for any dynamics which preserves the space average of the wave field, the interaction leaves the zero-wavenumber Fourier amplitude invariant. The dynamics of the $\mathbf{k} = 0$ mode is then null and there is no interest

CHAPTER 3. RESONANCE VAN HOVE SINGULARITIES: CASE STUDIES

in the kinetic equation for that wavenumber. (This conclusion is, however, a bit too glib, as we shall discuss further in section 3.2.3 below.) Thus, no singularities of a nontrivial type are allowed for $\alpha > 1$.

The case $\alpha = 1$ is different, as has been long understood (Zakharov and Sagdeev, 1970; Newell and Aucoin, 1971). For this situation, the condition (3.8) gives no restriction on p, q and (3.7) is the condition of collinearity:

$$\hat{\mathbf{p}} = \hat{\mathbf{q}}. \quad (3.9)$$

For $\sigma_2 = \sigma_3 = 1$, the conditions

$$k = p + q, \quad \mathbf{k} = \mathbf{p} + \mathbf{q}$$

are satisfied by

$$\mathbf{p} = \beta \mathbf{k}, \quad \mathbf{q} = \mathbf{k} - \mathbf{p} = (1 - \beta) \mathbf{k}, \quad \beta \in [0, 1]$$

For $\sigma_2 = -\sigma_3 = 1$, the conditions

$$p = k + q, \quad \mathbf{p} = \mathbf{k} + \mathbf{q}$$

are satisfied by

$$\mathbf{p} = \gamma \mathbf{k}, \quad \mathbf{q} = \mathbf{p} - \mathbf{k} = (\gamma - 1) \mathbf{k}, \quad \gamma \in [1, \infty)$$

Finally, for $-\sigma_2 = \sigma_3 = 1$, we just reverse $\mathbf{p} \leftrightarrow \mathbf{q}$ in the last two equations. Because of our initial choice $\sigma = -1$, all of the above solutions have $\mathbf{p} \cdot \mathbf{k} > 0$. Taking $\mathbf{k} \rightarrow -\mathbf{k}$, $|\mathbf{k}| = k \rightarrow |-\mathbf{k}| = k$ gives solutions with $\mathbf{p} \cdot \mathbf{k} < 0$. Note that the resonant “manifolds” where

$$E^{\sigma_2 \sigma_3}(\mathbf{p}; \mathbf{k}) = \sigma_2 \omega(\mathbf{p}) + \sigma_3 \omega(\sigma_3(\mathbf{k} - \sigma_2 \mathbf{p})) - \omega(\mathbf{k}) = 0 \quad (3.10)$$

are now straight line segments or rays, and not manifolds at all. The entire “manifold” is in the critical set where $\nabla_{\mathbf{p}} E^{\sigma_2 \sigma_3}(\mathbf{p}; \mathbf{k}) = \mathbf{0}$. It is a consequence of the Morse Lemma that non-degenerate critical points must be isolated, but the critical points here form a continuum. In fact, these

CHAPTER 3. RESONANCE VAN HOVE SINGULARITIES: CASE STUDIES

critical points are all one-dimensionally degenerate, since the Hessian $\nabla \otimes \nabla E^{\sigma_2 \sigma_3}(\mathbf{p}; \mathbf{k})$ has $\hat{\mathbf{k}}$ as an eigenvector with eigenvalue 0.

The dispersion law (3.6) with $\alpha = 1$ occurs physically, for example for sound waves, and all of the above facts have been noted in previous discussions of acoustic wave turbulence (Zakharov and Sagdeev, 1970; Newell and Aucoin, 1971). This was termed a “semidispersive” wave system, since sound waves are nondispersive on the resonant manifolds, along the direction of propagation, but there is lateral dispersion due to angular separation of wave packets. The usual wave-kinetic equation is no longer applicable, as the standard phase measure on the resonant manifold becomes ill-defined. Various proposals have been made to derive related kinetic equations by generalizing the arguments for strictly dispersive waves (Newell and Aucoin, 1971) or by taking into account nonlinear broadening of the resonance (L’vov *et al.*, 1997). The breakdown of dispersivity is quite severe for sound waves, but, as we have seen, it is an isolated phenomenon for wave systems with power dispersion laws, occurring only for $\alpha = 1$. This may have led to an expectation that dispersivity breakdown and the associated singularity of the resonant manifold is otherwise absent. However, we shall now show by further examples that it occurs more widely, although in generally less severe forms than for sound waves.

3.2.2 Lattice Regularization of Power Laws

The work of Van Hove suggests that the presence of a spatial lattice could facilitate the appearance of resonance singularities. We show that this expectation is correct, by considering a “lattice regularization” of the power-law dispersion of the previous section. If physical space is a cubic lattice $a\mathbb{Z}^d$, then Fourier space is the d -torus $\frac{2\pi}{a}\mathbb{T}^d = [-\frac{\pi}{a}, \frac{\pi}{a}]^d$. The dispersion law must be a periodic function on $\Lambda^* = [-\frac{\pi}{a}, \frac{\pi}{a}]^d$. A natural replacement for k^2 is therefore $\frac{4}{a^2} \sum_{i=1}^d \sin^2(\frac{k_i a}{2})$, the discrete Fourier transform of the lattice Laplacian $-\Delta_a$ defined by 2nd-order differences. We

CHAPTER 3. RESONANCE VAN HOVE SINGULARITIES: CASE STUDIES

thus consider

$$\omega(\mathbf{k}) = C \left[\frac{4}{a^2} \sum_{i=1}^d \sin^2\left(\frac{k_i a}{2}\right) \right]^{\alpha/2}. \quad (3.11)$$

This dispersion law is a toy model that does not describe any physical system but that we use as the simplest example of the effect of a lattice. It could appear in a computational algorithm to solve a wave equation with a power-law dispersion relation on a regular space grid. A lattice formulation of the equations can also be useful for theoretical purposes as an “ultraviolet regularization” to avoid high-wavenumber divergences, a mathematically cleaner alternative to the Fourier-Galerkin truncation of the wave dynamics employed in Nazarenko (2011). Of course, lattices exist physically in nature, e.g. in crystalline solids, and similar singularities must exist in certain cases on the resonant manifolds in the quantum Boltzmann equations which describe particle transport in crystals. Since this is a 4-wave resonance, we discuss it in more detail in section 3.3 below. It would be interesting to investigate whether such resonance singularities exist more widely for quantum transport in crystals.

We now turn to our simple example. Without loss of generality, we take lattice constant $a = 1$. We first show that, as for the continuous case, nontrivial resonance requires $\alpha > 1$:

Proposition 3.2.1 *If $\alpha \leq 1$, the resonant manifolds $\mathcal{R}_{\mathbf{k}}^{\sigma_2 \sigma_3} = \{\mathbf{p} : E^{\sigma_2 \sigma_3}(\mathbf{p}; \mathbf{k}) = 0\}$ contain only two points $\mathbf{0}$ and \mathbf{k} .*

Proof We introduce the notation

$$|\mathbf{k}|_{\Lambda^*} = \left[4 \sum_{i=1}^d \sin^2(k_i/2) \right]^{1/2}, \quad \mathbf{k} \in 2\pi\mathbb{T}^d$$

for the “vector norm” on the torus. We see that this function satisfies the triangle inequality, $|\mathbf{p} + \mathbf{q}|_{\Lambda^*} \leq |\mathbf{p}|_{\Lambda^*} + |\mathbf{q}|_{\Lambda^*}$, with equality only for $\mathbf{p} = \mathbf{0}$ or $\mathbf{q} = \mathbf{0} \pmod{\Lambda^*}$, because of an observation of Spohn (2006) that $|\mathbf{k}|_{\Lambda^*} = |\mathbf{z}(\mathbf{k})|$ for $\mathbf{z}(\mathbf{k}) \in \mathbb{C}^d$ defined by $z_j(\mathbf{k}) = 1 - e^{ik_j}$ with $z_j(\mathbf{p} + \mathbf{q}) = z_j(\mathbf{p}) + e^{ip_j} z_j(\mathbf{q})$. In particular note that $e^{-ip_j} z_j(\mathbf{p}) = \lambda \cdot z_j(\mathbf{q})$ for some real $\lambda \in [0, \infty]$ if and only

CHAPTER 3. RESONANCE VAN HOVE SINGULARITIES: CASE STUDIES

if either $p_j = 0$ or $q_j = 0 \pmod{2\pi}$. It follows from this fact that the standard proof of lack of resonances for \mathbf{k} in Euclidean space (Nazarenko, 2011) carries over. For completeness we give the details.

Consider first $\sigma_2 = \sigma_3 = 1$, so that $\mathbf{k} = \mathbf{p} + \mathbf{q}$. Then,

$$|\mathbf{k}|_{\Lambda^*} = |\mathbf{p} + \mathbf{q}|_{\Lambda^*} \leq |\mathbf{p}|_{\Lambda^*} + |\mathbf{q}|_{\Lambda^*} \leq [|\mathbf{p}|_{\Lambda^*}^\alpha + |\mathbf{q}|_{\Lambda^*}^\alpha]^{1/\alpha}, \text{ for } \alpha \leq 1.$$

so that $\omega(\mathbf{k}) = |\mathbf{k}|_{\Lambda^*}^\alpha \leq |\mathbf{p}|_{\Lambda^*}^\alpha + |\mathbf{q}|_{\Lambda^*}^\alpha = s_2\omega(\mathbf{p}) + s_3\omega(\mathbf{q})$ with equality only for $\mathbf{p} = \mathbf{0}$ or $\mathbf{p} = \mathbf{k}$.

Now consider $\sigma_2 + \sigma_3 = 0$, for example $\sigma_2 = -\sigma_3 = 1$. In that case $\mathbf{p} = \mathbf{k} + \mathbf{q}$ and the previous argument shows that $|\mathbf{k}|_{\Lambda^*}^\alpha + |\mathbf{q}|_{\Lambda^*}^\alpha \geq |\mathbf{p}|_{\Lambda^*}^\alpha$, or

$$\omega(\mathbf{k}) = |\mathbf{k}|_{\Lambda^*}^\alpha \geq |\mathbf{p}|_{\Lambda^*}^\alpha - |\mathbf{q}|_{\Lambda^*}^\alpha = \sigma_2\omega(\mathbf{p}) + \sigma_3\omega(\mathbf{q}),$$

with inequality only for $\mathbf{p} = \mathbf{k}$ or $\mathbf{p} = \mathbf{q}$. The second possibility requires $\mathbf{k} = \mathbf{0}$, however, and is not of interest. Repeating the argument for $\sigma_3 = -\sigma_2 = 1$ leads to the same conclusion with $2, \mathbf{p} \leftrightarrow 3, \mathbf{q}$ so that equality requires $\mathbf{q} = \mathbf{k}$ or $\mathbf{q} = \mathbf{p}$. The first possibility is equivalent to $\mathbf{p} = \mathbf{0}$ and the second to $\mathbf{k} = \mathbf{0}$, again not of interest. \square

We now establish results on existence of critical points, separately for the cases $\sigma_2 \cdot \sigma_3 = 1$ and $\sigma_2 \cdot \sigma_3 = -1$:

Proposition 3.2.2 *For any $\alpha > 1$, there always exists \mathbf{k} for which the resonant manifold $\mathcal{R}_{\mathbf{k}}^{++}$ contains nontrivial critical points.*

Proof The singularity condition

$$|\mathbf{p}|_{\Lambda^*}^{\alpha-2} \sin(p_i) = |\mathbf{q}|_{\Lambda^*}^{\alpha-2} \sin(q_i) \quad \text{for } i = 1, \dots, d. \quad (3.12)$$

is solved by either $\mathbf{p} = \mathbf{q} = \frac{1}{2}\mathbf{k}$ or by $\mathbf{p} = \mathbf{q} = \frac{1}{2}\mathbf{k} + \boldsymbol{\pi}$, where $\boldsymbol{\pi} = (\pi, \pi, \dots, \pi)$. Observe that the

CHAPTER 3. RESONANCE VAN HOVE SINGULARITIES: CASE STUDIES

notation “ $\mathbf{k}/2$ ” is actually ambiguous, because changing the components of \mathbf{k} by integer multiples of 2π yield different points depending on whether the integer is odd or even. We remove that ambiguity by requiring that $-\pi < k_j \leq \pi$, $j = 1, \dots, d$ so that both $\frac{1}{2}\mathbf{k}$ and $\frac{1}{2}\mathbf{k} + \boldsymbol{\pi}$ are well-defined (mod Λ^*). In either case, $\mathbf{p} + \mathbf{q} = \mathbf{k}$ (mod Λ^*).

The resonance condition $\omega(\mathbf{p}) + \omega(\mathbf{q}) = \omega(\mathbf{k})$ then yields for $\mathbf{q} = \mathbf{p} = \frac{1}{2}\mathbf{k}$

$$\begin{aligned} & 2 \left| \frac{\mathbf{k}}{2} \right|_{\Lambda^*}^\alpha = |\mathbf{k}|_{\Lambda^*}^\alpha \\ \Rightarrow & 2 \left[\sum_{i=1}^d \sin^2 \left(\frac{k_i}{4} \right) \right]^{\alpha/2} = \left[\sum_{i=1}^d \sin^2 \left(\frac{k_i}{2} \right) \right]^{\alpha/2} = 2^\alpha \left[\sum_{i=1}^d \sin^2 \left(\frac{k_i}{4} \right) \cos^2 \left(\frac{k_i}{4} \right) \right]^{\alpha/2} \\ \Rightarrow & 2^{2/\alpha-2} = \left\langle \cos^2 \left(\frac{\mathbf{k}}{4} \right) \right\rangle \end{aligned} \quad (3.13)$$

where we define the average $\langle f(\mathbf{k}) \rangle = \sum_{i=1}^d f(k_i) \sin^2(k_i/4) / [\sum_{i=1}^d \sin^2(k_i/4)]$. Note $\langle \cos^2(\mathbf{k}/4) \rangle = \frac{1}{2}$ when $\mathbf{k} = \boldsymbol{\pi}$ and approaches 1 when $\mathbf{k} \rightarrow \mathbf{0}$. Thus for any $1 < \alpha \leq 2$, there always exists \mathbf{k} that solves the condition (3.13) by the intermediate value theorem.

On the other hand, for $\mathbf{p} = \mathbf{q} = \frac{1}{2}\mathbf{k} + \boldsymbol{\pi}$, the resonance condition $\omega(\mathbf{p}) + \omega(\mathbf{q}) = \omega(\mathbf{k})$ yields

$$\begin{aligned} & 2 \left| \frac{\mathbf{k}}{2} + \boldsymbol{\pi} \right|_{\Lambda^*}^\alpha = |\mathbf{k}|_{\Lambda^*}^\alpha \\ \Rightarrow & 2 \left[\sum_{i=1}^d \cos^2 \left(\frac{k_i}{4} \right) \right]^{\alpha/2} = \left[\sum_{i=1}^d \sin^2 \left(\frac{k_i}{2} \right) \right]^{\alpha/2} = 2^\alpha \left[\sum_{i=1}^d \sin^2 \left(\frac{k_i}{4} \right) \cos^2 \left(\frac{k_i}{4} \right) \right]^{\alpha/2} \\ \Rightarrow & 2^{2/\alpha-2} = \left\langle \sin^2 \left(\frac{\mathbf{k}}{4} \right) \right\rangle \end{aligned} \quad (3.14)$$

where we now define $\langle f(\mathbf{k}) \rangle = \sum_{i=1}^d f(k_i) \cos^2(k_i/4) / [\sum_{i=1}^d \cos^2(k_i/4)]$. Note $\langle \sin^2(\mathbf{k}/4) \rangle = 0$ for $\mathbf{k} = \mathbf{0}$ and equals $\frac{1}{2}$ for $\mathbf{k} = \boldsymbol{\pi}$. Thus for any $\alpha \geq 2$, there always exists \mathbf{k} that solves the condition (3.14).

Note that in the borderline case $\alpha = 2$, the singularity condition becomes simply

$$\sin(p_i) = \sin(k_i - p_i) \quad \text{for } i = 1, \dots, d. \quad (3.15)$$

CHAPTER 3. RESONANCE VAN HOVE SINGULARITIES: CASE STUDIES

and one can easily check that there are only resonant solutions for $\mathbf{k} = \boldsymbol{\pi}$. For this choice, every point of Λ^* is in the resonant manifold, since

$$\sin^2\left(\frac{p_i}{2}\right) + \sin^2\left(\frac{q_i}{2}\right) = \sin^2\left(\frac{p_i}{2}\right) + \cos^2\left(\frac{p_i}{2}\right) = 1 = \sin^2\left(\frac{k_i}{2}\right).$$

Every point of the torus is a degenerate critical point in this case. \square

The condition (3.13) provides the example in section 3.1. For $\mathbf{k} = (0, 0, 1)$, one gets $\langle \cos^2(\mathbf{k}/4) \rangle = \cos^2(1/4)$, which reduces (3.13) to $2^{2/\alpha-2} = \cos^2(1/4)$, or $\alpha = 1/(1 + \log_2 \cos(1/4)) \doteq 1.0477$. One can likewise use condition (3.14) to construct examples for $\alpha > 2$. For instance, if one chooses $\mathbf{k} = (3, 3, 3)$, then $\langle \sin^2(\mathbf{k}/4) \rangle = \sin^2(3/4)$, and one obtains from (3.14) that $\alpha = 1/(1 + \log_2 \sin(3/4)) \doteq 2.2367$. This example is plotted in Fig. 3.2.

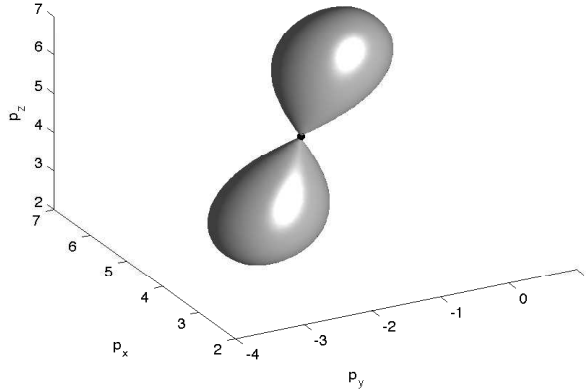


Figure 3.2: Resonant manifold $\mathcal{R}_{\mathbf{k}}^{++} = \{\mathbf{p} : \omega(\mathbf{p}) + \omega(\mathbf{k} - \mathbf{p}) - \omega(\mathbf{k}) = 0\}$ for dispersion relation $\omega(\mathbf{k}) = \left[4 \sum_{i=1}^3 \sin^2\left(\frac{k_i}{2}\right)\right]^{\alpha/2}$, $\alpha = \frac{1}{1 + \log_2 \sin(3/4)}$, on the 3-torus $[\frac{1}{2}\pi, \frac{5}{2}\pi] \times [-\frac{3}{2}\pi, \frac{1}{2}\pi] \times [\frac{1}{2}\pi, \frac{5}{2}\pi]$, and for the specific wavevector $\mathbf{k} = (3, 3, 3)$. There is a critical point (black dot) at $\mathbf{p} = \mathbf{k}/2 - \boldsymbol{\pi}$.

We finally discuss briefly the case $\sigma_2 \cdot \sigma_3 = -1$, or, without loss of generality, $\sigma_2 = 1, \sigma_3 = -1$. We present here no construction of critical points for all values of $\alpha > 1$, but we can establish their existence in specific instances. A simple example is provided by exploiting a general criterion for the existence of critical points, namely, that there be a pair of distinct wavevectors \mathbf{k}_1 and \mathbf{k}_2

CHAPTER 3. RESONANCE VAN HOVE SINGULARITIES: CASE STUDIES

such that the topological invariants of $\mathcal{R}_{\mathbf{k}_1}$ and $\mathcal{R}_{\mathbf{k}_2}$ are different. For example, in the case $\alpha = 5/2$, critical points must be present because there is a change of topological invariants of the resonant manifold as \mathbf{k} is varied, see Fig. 3.3. The manifold for $\mathbf{k}_1 = (.2, -.2)$ is connected and belongs to the trivial 1st homology class on the 2-torus, while the manifold for $\mathbf{k}_2 = (.18, -.2)$ has two connected components in the same non-trivial 1st homology class (both winding around the same hole of the 2-torus). Thus, as the wavevector is changed continuously from \mathbf{k}_1 to \mathbf{k}_2 , a critical point in $\mathcal{R}_{\mathbf{k}}$ must occur at some intermediate value of \mathbf{k} . Such a critical point is shown in the bottom subplot of Fig. 3.3.

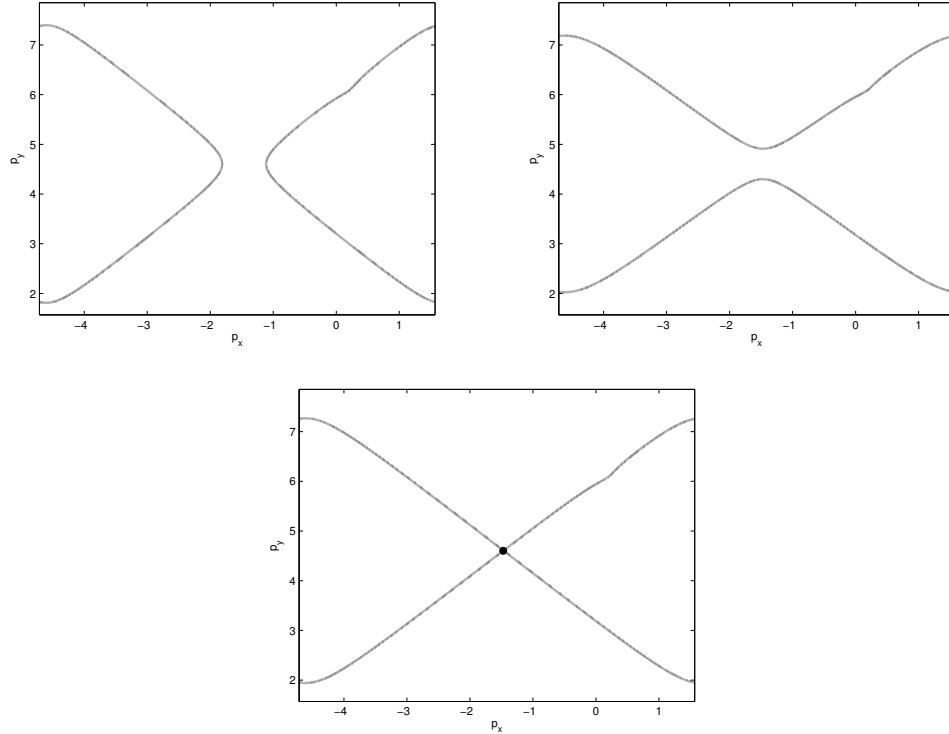


Figure 3.3: Resonant manifold $\mathcal{R}_{\mathbf{k}}^{+-}$ for dispersion relation $\omega(\mathbf{k}) = \left[4 \sum_{i=1}^2 \sin^2\left(\frac{k_i}{2}\right)\right]^{\alpha/2}$ with $\alpha = 2.5$, on the 2-torus $[-\pi/2, 3/2\pi] \times [\pi/2, 5/2\pi]$, and for the specific wavevector $\mathbf{k} = (.2, -.2)$ on the top left and $\mathbf{k} = (.18, -.2)$ on the top right. For the specific numerically approximated wavevector $\mathbf{k} = (.1887713, -.2)$ (bottom figure), there is a critical point (black dot) at $\mathbf{p} = (-1.4716, 4.6016)$.

The examples in this section are only toy problems meant to provide some analytical insight. In Chap. 4 we shall show that non-degenerate singularities at a single point, like those in

the examples of this section, can lead in appropriate circumstances to an infinite phase measure on the resonant manifolds. For 3-wave resonances, the phase measure is finite for dimensions $d > 2$ but logarithmically divergent for $d = 2$. We see below that such non-degenerate singularities can arise from dispersion laws in physically relevant models.

3.2.3 Anisotropic Dispersion Relations

Many wave dispersion relations in physical systems are anisotropic, either power-laws or more general forms. Here we show by several examples that anisotropy can lead to critical points on the resonant manifolds. A simple class of examples are systems whose dispersion relation has the form

$$\omega(\mathbf{k}) = k_1 \varphi(k)$$

where $k = |\mathbf{k}|$ is the Euclidean norm and k_1 is a component in a distinguished direction. In cases such as this, for any “slow mode” \mathbf{k} with $k_1 = 0$,

$$\mathcal{R}_{\mathbf{k}}^{++} = \{\mathbf{p} : E^{++}(\mathbf{p}; \mathbf{k}) = p_1(\varphi(p) - \varphi(q)) = 0, \ q = |\mathbf{k} - \mathbf{p}|\}.$$

Since

$$\nabla_{\mathbf{p}} E^{++}(\mathbf{p}; \mathbf{k}) = (\varphi(p) - \varphi(q))\hat{\mathbf{e}}_1 + p_1 \left(\varphi'(p)\hat{\mathbf{p}} + \varphi'(q)\hat{\mathbf{q}} \right),$$

it follows that the subset

$$\mathcal{R}_{\mathbf{k}}^{++*} = \{\mathbf{p} : p_1 = 0 \ \& \ \varphi(p) = \varphi(q), \ q = |\mathbf{k} - \mathbf{p}|\} \subset \mathcal{R}_{\mathbf{k}}^{++}$$

consists of critical points satisfying $\nabla \omega(\mathbf{p}) = \nabla \omega(\mathbf{q}) \propto \hat{\mathbf{e}}_1$. Note also that when $p_1 = 0$ the Hessian matrix becomes

$$\nabla \otimes \nabla E^{++}(\mathbf{p}; \mathbf{k}) = \varphi'(p)(\hat{\mathbf{e}}_1 \otimes \hat{\mathbf{p}} + \hat{\mathbf{p}} \otimes \hat{\mathbf{e}}_1) + (\mathbf{p} \leftrightarrow \mathbf{q})$$

CHAPTER 3. RESONANCE VAN HOVE SINGULARITIES: CASE STUDIES

so that the critical points $\mathbf{p} \in \mathcal{R}_{\mathbf{k}}^{++*}$ with $\varphi'(p), \varphi'(q) \neq 0$ are non-degenerate for $d = 2$, while for $d > 2$ the Hessian matrix is degenerate. A null eigenvector of the Hessian for any $d > 2$ when $\hat{\mathbf{p}}, \hat{\mathbf{q}}$ are non-parallel is given by the vector $\varphi'(p)\hat{\mathbf{q}}^\perp - \varphi'(q)\hat{\mathbf{p}}^\perp$, where $\hat{\mathbf{p}}^\perp$ is the component of $\hat{\mathbf{p}}$ perpendicular to $\hat{\mathbf{q}}$ and vice versa for $\hat{\mathbf{q}}^\perp$. When $\hat{\mathbf{p}} \parallel \hat{\mathbf{q}}$, then any vector orthogonal to both $\hat{\mathbf{e}}_1$ and \mathbf{p} (or \mathbf{q}) is a null eigenvector. For $d > 3$, furthermore, any vector orthogonal to all three vectors $\hat{\mathbf{e}}_1$, \mathbf{p} , and \mathbf{q} (or \mathbf{k}) is a null eigenvector.

Rossby/drift waves

A well-known example of an isotropic dispersion relation occurs for Rossby/drift waves, where $d = 2$, the 1-direction is zonal, $\varphi(k) = -\beta\rho^2/(1+\rho^2k^2)$ with β the beta parameter (meridional gradient of the Coriolis frequency) and ρ the Rossby radius (Balk *et al.*, 1990). In that case, the condition $\varphi(p) = \varphi(q)$ can be easily solved to give $\mathbf{k} \cdot (\mathbf{p} - \mathbf{k}/2) = 0$. For a general “slow” wavevector $\mathbf{k} = (0, k_y)$, the resonant manifold $\mathcal{R}_{\mathbf{k}}^{++}$ is the union of the two lines $p_x = 0$ and $p_y = k_y/2$, see Fig. 3.4, bottom panel. The point of intersection $(0, k_y/2)$ is a nondegenerate resonance Van Hove singularity. Note that for generic \mathbf{k} , the manifold $\mathcal{R}_{\mathbf{k}}^{++}$ for the system of Rossby waves is instead diffeomorphic to a circle, as shown in Fig. 3.4, top left and top right panels.

It is easy in this example to exhibit explicitly the logarithmic divergence in the phase measure $dS/|\nabla E|$ on the resonant manifold, which is expected for $d = 2$. A simple calculation gives

$$\nabla_{\mathbf{p}} E^{++}(\mathbf{p}; \mathbf{k}) = \frac{2\beta\rho^4 k_y}{(1 + \rho^2 p^2)(1 + \rho^2 q^2)} \left[\left(p_y - \frac{k_y}{2} \right) \hat{\mathbf{x}} + p_x \hat{\mathbf{y}} \right]$$

on the resonant manifold for $\mathbf{k} = (0, k_y)$, vanishing approaching the singular point. Since $E^{++}(\mathbf{p}; \mathbf{k}) \propto p_x(p_y - k_y/2)$, the divergence has the general form of the integral

$$\iint dx dy \delta(xy) = \iint dx dy \left[\frac{1}{|x|} \delta(y) + \frac{1}{|y|} \delta(x) \right].$$

One might dismiss this singularity as dynamically irrelevant, since the zonal flows with $k_x = 0$ have

CHAPTER 3. RESONANCE VAN HOVE SINGULARITIES: CASE STUDIES

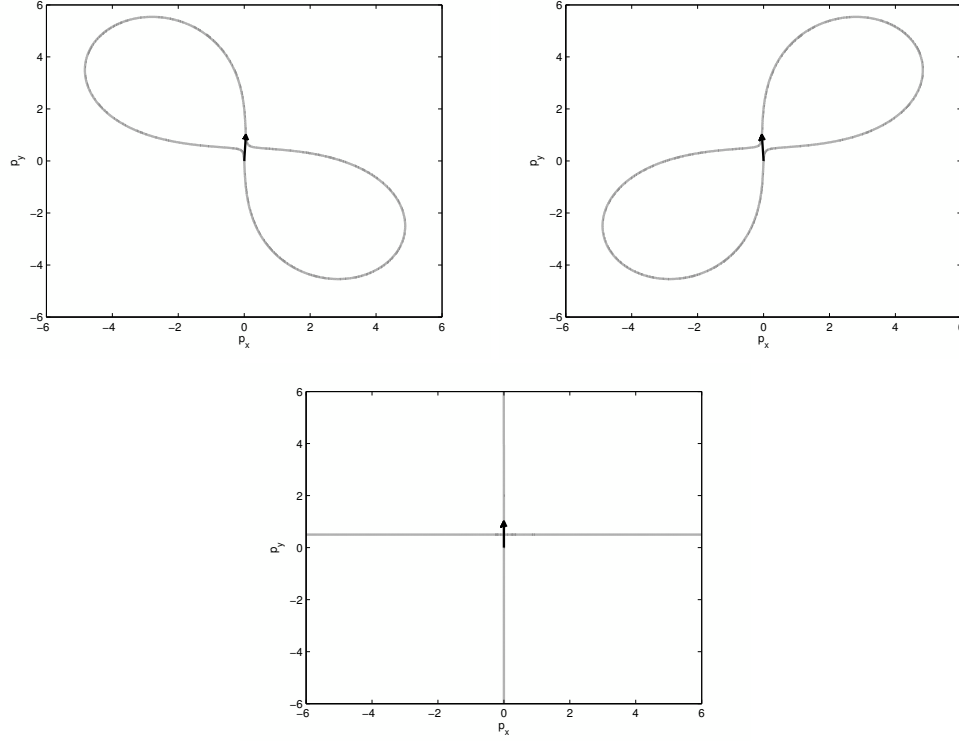


Figure 3.4: Resonant manifold $\mathcal{R}_{\mathbf{k}}^{++}$, $\mathbf{k} = (\cos \theta, \sin \theta)$ for Rossby/drift waves, plotted as gray lines. The black arrow is the vector \mathbf{k} . Here $\theta = \frac{\pi}{2} - 0.05$ for the top left panel, $\theta = \frac{\pi}{2} + 0.05$ for the top right panel, and $\theta = \frac{\pi}{2}$ for the bottom panel.

vanishing nonlinearity. This may be easily verified for the Charney-Hasegawa-Mima equation (Balk *et al.*, 1990),

$$\partial_t(\rho^2 \triangle \psi - \psi) - \beta \partial_x \psi + AJ(\psi, \rho^2 \triangle \psi) = 0,$$

with $J(f, g) = f_x g_y - f_y g_x$ the Jacobian, which vanishes whenever one of the functions is independent of x (or of y). This argument is correct, but must be made carefully.

The delicate point is that the critical point for the resonant manifold $\mathcal{R}_{\mathbf{k}}^{++}$ with $k_x = 0$ implies not only divergent phase measure on that manifold but also extremely large phase measures on adjacent manifolds with k_x very small. Note for such k_x that the resonant manifold locally for \mathbf{p}

CHAPTER 3. RESONANCE VAN HOVE SINGULARITIES: CASE STUDIES

near $(0, k_y/2)$ is a hyperbola whose equation is, to leading order,

$$(p_x - \frac{k_x}{2})(p_y - \frac{k_y}{2}) = \frac{3}{8}k_x k_y \frac{1 + \frac{1}{4}\rho^2 k_y^2}{1 + \rho^2 k_y^2}.$$

Near $\mathbf{p} = (0, k_y/2)$, to leading order,

$$\nabla E^{++}(\mathbf{p}; \mathbf{k}) = \frac{\beta \rho^4}{(1 + \frac{\rho^2}{4}k_y^2)^2} \left[(3k_x(2p_x - k_x) + k_y(2p_y - k_y)) \hat{\mathbf{x}} + (k_x(2p_y - k_y) + k_y(2p_x - k_x)) \hat{\mathbf{y}} \right]$$

Therefore on the resonant manifold

$$|\nabla E^{++}(\mathbf{p}; \mathbf{k})| \geq \frac{\beta \rho^4}{(1 + \frac{\rho^2}{4}k_y^2)^2} \sqrt{16|k_x k_y (k_y - 2p_y)(k_x - 2p_x)|} = \frac{\beta \rho^4}{(1 + \frac{\rho^2}{4}k_y^2)^2} \sqrt{6k_x^2 k_y^2 \frac{1 + \frac{1}{4}\rho^2 k_y^2}{1 + \rho^2 k_y^2}},$$

which implies a phase measure which is $O(|k_x|^{-1})$. Fortunately, however, all of the standard dynamical models of Rossby/drift waves (Balk *et al.*, 1990) have interaction coefficients $H_{\mathbf{k}, \mathbf{p}, \mathbf{q}}^{\sigma, \sigma_1, \sigma_2}$ vanishing proportional to $|k_x p_x q_x|^{1/2}$ for any of the three wavevectors in the “slow” set. In these models, the singularity in the phase measure for small k_x is cancelled by the interaction coefficient $|H_{\mathbf{k}, \mathbf{p}, \mathbf{q}}|^2 \sim |k_x p_x q_x|$, rendering the collision integral finite even as k_x tends to zero. If the interaction coefficient had vanished more slowly than $|k_x|^{1/2}$ in the limit, then the collision integral for near-zonal flows could become large, threatening the validity of the kinetic description (Newell *et al.*, 2001; Biven *et al.*, 2001; Nazarenko, 2011). These considerations apply more generally, e.g. to the isotropic power-law dispersion relations discussed in section 3.2.1².

²In the case of an isotropic power-law dispersion relation for $|\mathbf{k}| \ll |\mathbf{p}|$

$$\nabla_{\mathbf{p}} E^{+-}(\mathbf{p}; \mathbf{k}) = \alpha |\mathbf{p}|^{\alpha-2} \mathbf{p} - \alpha |\mathbf{p} - \mathbf{k}|^{\alpha-2} (\mathbf{p} - \mathbf{k}) \approx \alpha |\mathbf{p}|^{\alpha-2} [\mathbf{k}^\perp + (\alpha - 1)k_\parallel],$$

where $\mathbf{k}^\perp, k_\parallel$ are components of \mathbf{k} perpendicular and parallel to \mathbf{p} , resp. A lower bound follows that $|\nabla_{\mathbf{p}} E^{+-}(\mathbf{p}; \mathbf{k})| \geq \text{const.} |\mathbf{p}|^{\alpha-2} |\mathbf{k}|$ and the limit $\mathbf{k} \rightarrow \mathbf{0}$ gives a finite collision integral if the interaction coefficient vanishes no slower than $|\mathbf{k}|^{1/2}$

Inertial waves

Another example is inertial waves, where $d = 3$, the 1-direction is the rotation axis, and $\varphi(k) = 2\Omega/k$ with Ω the rotation rate (Galtier, 2003). This case is geometrically quite similar to the case of Rossby waves, but extended to $d = 3$. For a generic wavevector \mathbf{k} the resonant manifold $\mathcal{R}_{\mathbf{k}}^{++}$ is diffeomorphic to a sphere. For a “slow” mode with $\mathbf{k} \cdot \boldsymbol{\Omega} = 0$, however, the resonant manifold $\mathcal{R}_{\mathbf{k}}^{++}$ is a union of two planes, one orthogonal to $\boldsymbol{\Omega}$ and one orthogonal to \mathbf{k} . For example, if $\boldsymbol{\Omega} = \Omega \hat{\mathbf{z}}$ and $\mathbf{k} = (k_x, 0, 0)$, these are the planes $p_z = 0$ and $p_x = k_x/2$. See Fig. 3.5. Consistent with our general

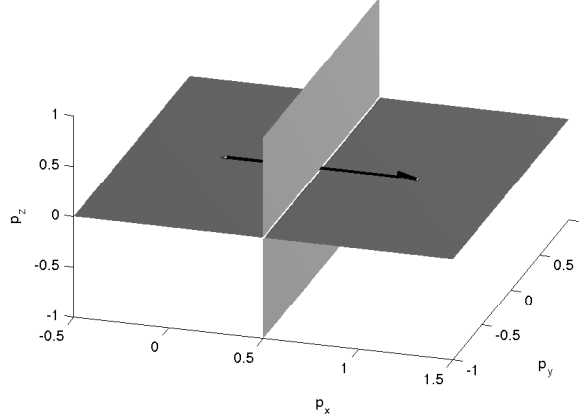


Figure 3.5: Resonant manifold $\mathcal{R}_{\mathbf{k}}^{++}$, $\mathbf{k} = (1, 0, 0)$ for inertial waves with rotation about the z -axis. The black arrow is the vector \mathbf{k} .

discussion for $d = 3$, the critical subset of the resonant manifold is 1-dimensionally degenerate, given here by the intersection of the two planes. The phase measure on the resonant manifold is logarithmically divergent in the vicinity of the singular line. This result shows by example that, while non-degenerate critical points produce integrable singularities for $d > 2$, line singularities can lead to divergences in three dimensions. Although geometrically quite similar to the case of drift waves, the situation is dynamically very different. While for drift waves the nonlinearity vanishes for the “slow” modes, in the case of inertial waves the “slow” modes with $\mathbf{k} \cdot \boldsymbol{\Omega} = 0$ correspond to a strongly interacting system described by 2D Navier-Stokes dynamics. It has been argued convincingly that the kinetic theory for inertial waves must break down in the vicinity of this 2D

CHAPTER 3. RESONANCE VAN HOVE SINGULARITIES: CASE STUDIES

plane of “slow” modes, as there is there no separation of time scales between fast linear and slow nonlinear dynamics (Galtier, 2003). Here we see that there is also a breakdown in the fundamental assumption of dispersivity of waves. There is an infinite set of wavevector pairs of “slow” modes with identical group velocities along the rotation axis and triads formed from these pairs produce a diverging contribution to the phase measure. Thus, the kinetic equation for inertial waves is not even well-defined for wave action non-zero in the vicinity of the “slow” 2D modes.

Internal gravity waves

A third example of an anisotropic dispersion law in $d = 3$ of a slightly different sort is internal gravity waves, where the 1-direction is vertical (the direction of gravity), and $\omega(\mathbf{k}) = Nk_H/k$, with $k_H = \sqrt{k^2 - k_1^2}$ the magnitude of the horizontal component and N the Brunt-Väisälä frequency (Caillol and Zeitlin, 2000). In this case

$$\nabla\omega(\mathbf{k}) = \frac{Nk_1}{k_H k} \hat{\mathbf{k}} \times (\hat{\mathbf{k}} \times \hat{\mathbf{e}}_1).$$

For a “slow mode” with only vertical variation ($k_H = 0$), it is straightforward to see that $\mathcal{R}_{\mathbf{k}}^{++} = \{\mathbf{p} : p_H = 0\}$, i.e. the resonant manifold is the 1-axis or the set of slow modes. Since in that case $\mathbf{p} \parallel \hat{\mathbf{e}}_1$, $\nabla\omega(\mathbf{p}) = \mathbf{0}$ and the entire resonant set $\mathcal{R}_{\mathbf{k}}^{++}$ consists of (degenerate) critical points. As in the case of Rossby waves, however, the nonlinear interaction coefficient of the Euler-Boussinesq system vanishes rapidly near the set of slow modes (see Caillol and Zeitlin (2000), eqs.(62) and (63)) and this singular manifold is not dynamically relevant in wave kinetics.

Another interesting phenomenon is seen in the resonant manifold of internal gravity waves when \mathbf{k} is a 2D mode, with $k_1 = 0$. It is easy to show in that case that the only possible critical points in $\mathcal{R}_{\mathbf{k}}^{++}$ are also 2D modes and, because of the restriction $p_H/p + q_H/q = 1$, the only allowed values are $\mathbf{p} = \mathbf{0}$ and $\mathbf{p} = \mathbf{k}$. A plot of the resonant manifold for $\mathbf{k} = \mathbf{e}_1$ in Fig. 3.6 below shows that geometric singularities indeed occur at $\mathbf{p} = \mathbf{0}, \mathbf{k}$. However, these do not correspond to ordinary

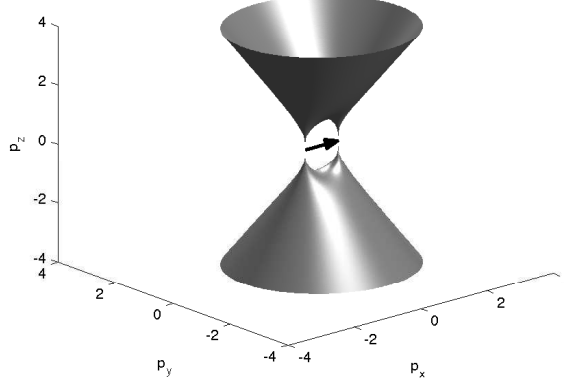


Figure 3.6: Resonant manifold $\mathcal{R}_{\mathbf{k}}^{++}$, $\mathbf{k} = (1, 0, 0)$ for internal gravity waves with vertical direction along the z -axis. The black arrow is the vector \mathbf{k} .

critical points where $\nabla_{\mathbf{p}} E^{++}(\mathbf{p}; \mathbf{k}) = \mathbf{0}$ but to points \mathbf{p} instead where $|\nabla_{\mathbf{p}} E^{++}(\mathbf{p}; \mathbf{k})| = \infty$. In this example, the singularities are cube-root cusps, since the equation for the resonant manifold is given near $\mathbf{p} = \mathbf{0}$ in cylindrical coordinates by $p_1 = \pm(2k^2 p_H)^{1/3}$, to leading order. Although we have considered here a 2D mode \mathbf{k} , the resonant manifold $\mathcal{R}_{\mathbf{k}}^{++}$ of internal gravity waves exhibits similar cusps at $\mathbf{p} = \mathbf{0}$ and $\mathbf{p} = \mathbf{k}$ for generic \mathbf{k} , because of the divergence of $\nabla\omega$ at the origin.

In general, we shall use the term “pseudo-critical point” for any point \mathbf{p} on a resonant manifold $\mathcal{R}_{\mathbf{k}}^{\sigma_1\sigma_2}$ where $E^{\sigma_1\sigma_2}(\mathbf{p}; \mathbf{k})$ is non-smooth in \mathbf{p} . Although such points may give rise to geometric singularities, they do not usually produce an infinite phase measure. In fact, the density of the phase measure with respect to surface area (Hausdorff measure) vanishes at points where $|\nabla_{\mathbf{p}} E^{++}(\mathbf{p}; \mathbf{k})| = \infty$, and thus the phase measure is locally finite whenever the Hausdorff measure is locally finite. The latter condition may easily be checked for the pseudo-critical points in Fig. 3.6 by using the standard formula for element of surface area in cylindrical coordinates to obtain near $\mathbf{p} = \mathbf{0}$ that $dA = 2\pi(2k^2)^{1/3} p_H^{1/3} dp_H$, which has locally a finite integral. Note furthermore for the Euler-Boussinesq system that the pseudo-critical points are not dynamically relevant in wave kinetics, since the nonlinear interaction coefficient vanishes when all modes in the triad have zero vertical wavenumber (Caillol and Zeitlin, 2000).

Summary

As these examples show, anisotropy—whether power-law or other type—can readily lead to critical points. In most of the common cases that we have examined, the singularities in the resonant manifold are protected by vanishing nonlinearity from having any dynamical effects. Such protection is by no means guaranteed. The case of inertial waves presents an opposite case, where the singularity is associated to strong nonlinearity and a breakdown of the wave-kinetic theory. More generally, the singularities can have intermediate effects between none at all and complete breakdown of wave kinetics. We shall present examples of this in the next section.

3.3 Quartet Resonances

Resonance Van Hove singularities also occur in 4-wave systems, for which the collision integral has the standard form:

$$C_{\mathbf{k}}[n] = \int d^d p d^d q d^d \ell \delta^d(\mathbf{p} + \mathbf{q} - \mathbf{k} - \ell) \delta(\omega(\mathbf{p}) + \omega(\mathbf{q}) - \omega(\mathbf{k}) - \omega(\ell)) |H_{\mathbf{p}, \mathbf{q}}^{\mathbf{k}, \ell}|^2 \times n(\mathbf{p})n(\mathbf{q})n(\ell)n(\mathbf{k}) \left[\frac{1}{n(\ell)} + \frac{1}{n(\mathbf{k})} - \frac{1}{n(\mathbf{p})} - \frac{1}{n(\mathbf{q})} \right] \quad (3.16)$$

When the wave dynamics is Hamiltonian and 3-wave resonances are absent, the collision integral can be brought to the above form by a canonical transformation of the Hamiltonian system (Zakharov *et al.*, 1992). The resonant manifold is now $\mathcal{R}_{\mathbf{k}}^{(4)} = \{(\mathbf{p}, \mathbf{q}) : E^{(4)}(\mathbf{p}, \mathbf{q}; \mathbf{k}) = 0\}$, with

$$E^{(4)}(\mathbf{p}, \mathbf{q}; \mathbf{k}) = \omega(\mathbf{p}) + \omega(\mathbf{q}) - \omega(\mathbf{k}) - \omega(\mathbf{p} + \mathbf{q} - \mathbf{k}). \quad (3.17)$$

Thus $\mathcal{R}^{(4)}$ can be expected to be a $(2d - 1)$ -dimensional surface embedded in a Euclidean space of dimension $D = 2d$. As a matter of fact, this is only true if one disregards the “trivial” part $\mathcal{R}_{\text{triv}}^{(4)} = \{(\mathbf{p}, \mathbf{q}) : \mathbf{p} = \mathbf{k} \text{ or } \mathbf{q} = \mathbf{k}\}$, which is the union of two d -dimensional hyperplanes. This “trivial” part gives a vanishing direct contribution to the collision integral (3.25) because either

CHAPTER 3. RESONANCE VAN HOVE SINGULARITIES: CASE STUDIES

$n(\mathbf{p}) = n(\mathbf{k}), n(\mathbf{q}) = n(\ell)$ or $n(\mathbf{p}) = n(\ell), n(\mathbf{q}) = n(\mathbf{k})$, and it is thus generally ignored. However, we shall see below that it may be of indirect importance because any intersection of the “non-trivial” part with $\mathcal{R}_{\text{triv}}^{(4)}$ leads to sets of critical points, generically of dimension $d-1$, and possible divergences.

The condition for a critical point on the 4-wave resonant manifold is

$$\nabla\omega(\mathbf{p}) = \nabla\omega(\mathbf{q}) = \nabla\omega(\ell) \quad (3.18)$$

with the group velocity of all three wavevectors $\mathbf{p}, \mathbf{q}, \ell$ the same. Degeneracy depends upon the rank of the $D \times D$ Hessian matrix

$$\nabla \otimes \nabla E^{(4)} = \begin{pmatrix} \nabla \otimes \nabla\omega(\mathbf{p}) - \nabla \otimes \nabla\omega(\ell) & -\nabla \otimes \nabla\omega(\ell) \\ -\nabla \otimes \nabla\omega(\ell) & \nabla \otimes \nabla\omega(\mathbf{q}) - \nabla \otimes \nabla\omega(\ell) \end{pmatrix}, \quad (3.19)$$

the critical point being non-degenerate if this matrix has full rank and otherwise degenerate.

It is worth discussing the case of a general isotropic dispersion law $\omega(k)$, as a preliminary to some specific examples below. The condition for a critical point

$$\omega'(p)\hat{\mathbf{p}} = \omega'(q)\hat{\mathbf{q}} = \omega'(\ell)\hat{\ell}$$

can be met in one of two ways:

(i) $|\omega'(p)| = |\omega'(q)| = |\omega'(\ell)| \neq 0$ and the vectors $\hat{\mathbf{p}}, \hat{\mathbf{q}}, \hat{\ell}$ are all collinear with $\hat{\mathbf{k}}$ (parallel or anti-parallel depending on the sign of ω'),

(ii) $\omega'(p) = \omega'(q) = \omega'(\ell) = 0$ and no restriction on the vectors $\hat{\mathbf{p}}, \hat{\mathbf{q}}, \hat{\ell}$.

We shall refer to the first case as a *non-null critical point* with non-vanishing group velocity of the waves and to the second as a *null critical point* with zero group velocities. We include for completeness the third case

(iii) At least one of $\omega'(p), \omega'(q), \omega'(\ell)$ is infinite.

CHAPTER 3. RESONANCE VAN HOVE SINGULARITIES: CASE STUDIES

This is what we earlier termed a *pseudo-critical point*. These present generally no difficulty since the density of the phase measure with respect to surface area on the resonant manifold vanishes at pseudo-critical points, with an infinite gradient. Note also for the isotropic dispersion that

$$\nabla \otimes \nabla \omega(\mathbf{k}) = \omega''(k) \hat{\mathbf{k}} \otimes \hat{\mathbf{k}} + \frac{\omega'(k)}{k} (\mathbf{I} - \hat{\mathbf{k}} \otimes \hat{\mathbf{k}}),$$

from which it is easy to determine the rank of the Hessian matrix (3.19).

We now consider several concrete examples:

3.3.1 Surface gravity-capillary waves

An illustrative example is surface gravity-capillary waves with dispersion relation $\omega(k) = \sqrt{gk + \sigma k^3}$, where g is the acceleration due to gravity and $\sigma = S/\rho$, where S is surface tension. The physically most relevant case is $d = 2$, but it turns out that most of the relevant features appear already for the idealized one-dimensional case $d = 1$.

Consider first pure surface gravity waves with dispersion law $\omega = \sqrt{gk}$. This case has no null critical points. Because any non-null critical points must have wavevectors all parallel to $\hat{\mathbf{k}}$, we may check for their existence in the simplest case $d = 1$. As a matter of fact, the resonant manifold is analytically known and explicitly parameterized for $d = 1$, and consists of points for which one of the wavenumbers out of p, q, k, ℓ has an opposite sign from the others (Dyachenko and Zakharov, 1994). There are thus also no non-null critical points in $d = 1$ and therefore none for $d > 1$. There are, however, pseudo-critical points in $d = 1$ where the nontrivial portion of the resonant manifold intersects the trivial parts, as seen in Fig. 3.7 below. These occur at the points where either $p = 0$ or $q = 0$ and ω' diverges. The non-trivial part of the resonant manifold is a union of three smooth pieces, joined at the pseudo-critical points, but the phase measure on it is locally finite (and the 4-wave interaction coefficient zero (Dyachenko and Zakharov, 1994)).

However, if the surface tension effect is included, there will be critical points as well as

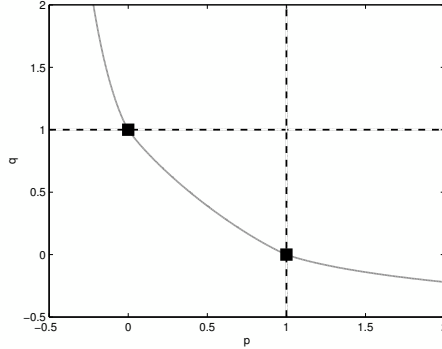


Figure 3.7: Resonant manifold $\mathcal{R}_k^{(4)}$, $k = 1$ for surface gravity waves in $d = 1$, with the non-trivial part plotted in gray and the trivial part in dashed black. Here ■ indicates pseudo-critical points.

pseudo-critical points, as seen in Fig. 3.8, due to the inflection point of $\omega(k)$ at $k = k_* := \sqrt{\frac{2-\sqrt{3}}{\sqrt{3}}} \frac{g}{\sigma}$ where $\omega''(k_*) = 0$. Again, null critical points are not present. However, for $k \neq k_*$ there is a distinct wavenumber $\ell \neq k$ satisfying $\omega'(k) = \omega'(\ell)$, implying that there are two non-null critical points for $\mathbf{p} = \mathbf{k}, \mathbf{q} = \ell$ and $\mathbf{q} = \mathbf{k}, \mathbf{p} = \ell$ with $\ell = \ell \hat{\mathbf{k}}$. To determine their degeneracy, we again examine the Hessian (3.19). At least one of the diagonal term vanishes and the off-diagonal term $-\nabla \otimes \nabla \omega(\ell)$ has eigenvalue $-\omega''(\ell)$ with multiplicity 1 and $-\omega'(\ell)/\ell$ with multiplicity $d - 1$. If $k \neq k_*$ such that $\omega''(k) \neq 0$, then $\omega''(\ell) \neq 0$ and there exist two non-degenerate critical points; if $k = k_*$ such that $\omega''(k) = 0$, then $\omega''(\ell) = 0$ and there exists one degenerate critical point. In Fig. 3.8, we show for $d = 1$ the typical resonant manifold $\mathcal{R}_k^{(4)}$ for $k < k_*$ (top left panel), $k = k_*$ (bottom panel), and $k > k_*$ (top right panel). In general, the degeneracy $\delta = 0$ for $k \neq k_*$ and $\delta = 1$ for $k = k_*$. As we shall discuss in Chap. 4, this implies that the phase measure remains finite for the physically relevant case $d = 2$.

It should be noted that the wavenumber $k_* \approx 0.4(g/\sigma)^{1/2}$ is expected to lie in the transition range between two energy cascades, one at low wavenumbers driven by quartet resonances of gravity waves and another at high wavenumbers driven by triplet resonances of capillary waves (Biven *et al.*, 2001; Newell *et al.*, 2001; Newell and Zakharov, 2008). The quartet at the critical points in Fig. 3.8 has two wavevectors with each magnitude k, ℓ , and one of the magnitudes k, ℓ is always $< k_*$

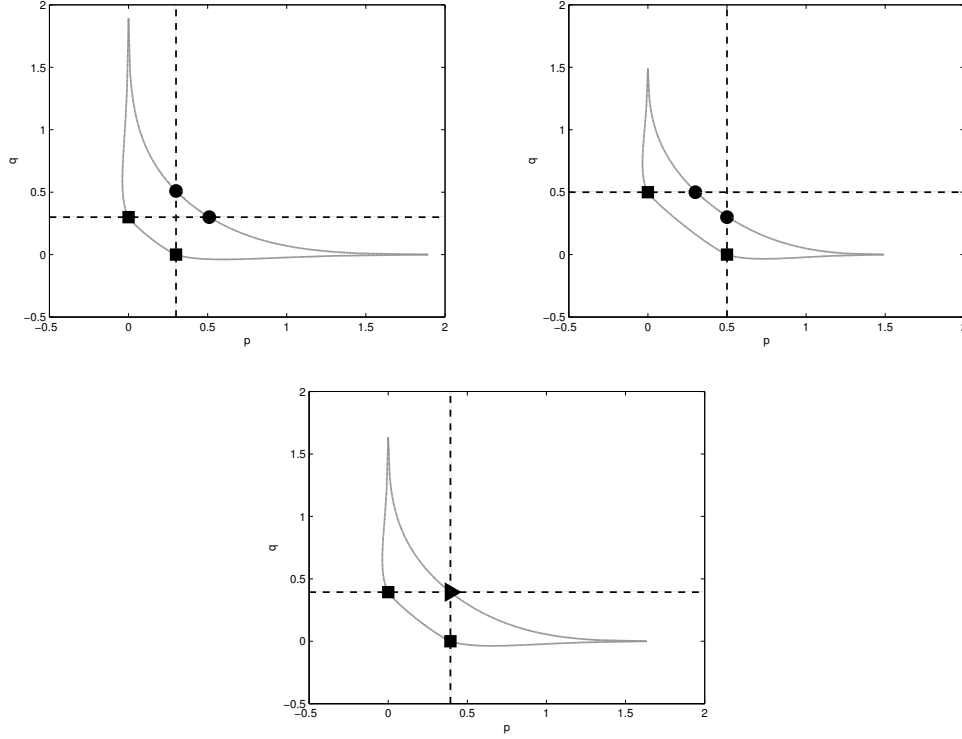


Figure 3.8: The figures show the resonant manifold $\mathcal{R}_k^{(4)}$ for surface gravity waves in $d = 1$ for $g = \sigma$, with the non-trivial part plotted in gray and the trivial part in dashed black. Here $k = 0.3$ for the top left panel; $k = \sqrt{(2 - \sqrt{3})/\sqrt{3}}$ for the bottom panel; $k = 0.5$ for the top right panel. \blacksquare indicates pseudo-critical points; \bullet indicates non-degenerate critical points; \blacktriangleright indicates degenerate critical points.

and the other $> k_*$. Thus, any possible observable effect of the critical points would presumably be found in the transition region where $k \simeq k_*$, perhaps in laboratory experiments where there is no large scale-separation between the gravity and capillary wave regimes. However, finiteness of the phase measure for $d = 2$ makes it unlikely that there are any appreciable effects.

3.3.2 Wave propagation along an optical fiber

A very similar situation to the previous one, but where the physical case corresponds to $d = 1$, occurs for optical wave propagation along a fiber, modeled by a 1D nonlinear Schrödinger (NLS) equation with third-order dispersion (Michel *et al.*, 2011; Suret *et al.*, 2010). The dispersion

CHAPTER 3. RESONANCE VAN HOVE SINGULARITIES: CASE STUDIES

law is³

$$\omega(k) = sk^2 + \alpha k^3, \quad (3.20)$$

for $s = \pm 1$, with an inflection point at $k_* = -s/3\alpha$. The collision integral is

$$\begin{aligned} C_k[n] &= \frac{1}{\pi} \int dp dq d\ell \delta(p + q - k - \ell) \delta(\omega(p) + \omega(q) - \omega(k) - \omega(\ell)) \\ &\quad \times n(k)n(\ell)n(p)n(q) \left[\frac{1}{n(k)} + \frac{1}{n(\ell)} - \frac{1}{n(p)} - \frac{1}{n(q)} \right]. \end{aligned} \quad (3.21)$$

It can be easily shown here that

$$E^{(4)}(p, q; k) \equiv \omega(p) + \omega(q) - \omega(k) - \omega(p + q - k) = 3\alpha(p + q - 2k_*)(p - k)(q - k).$$

The non-trivial part of the resonant manifold $\mathcal{R}_k^{(4)}$ is the straight line $p + q = 2k_*$ in the pq -plane, independent of k , and there are non-null critical points at the intersections with the trivial part, at $(p, q) = (k, 2k_* - k)$ and $(2k_* - k, k)$. The collision integral on the non-trivial part becomes

$$\begin{aligned} C_k[n] &= \frac{1}{3\pi|\alpha|} \int dp \frac{n(k)n(2k_* - k)n(p)n(2k_* - p)}{|p - k||p + k - 2k_*|} \\ &\quad \times \left[\frac{1}{n(k)} + \frac{1}{n(2k_* - k)} - \frac{1}{n(p)} - \frac{1}{n(2k_* - p)} \right]. \end{aligned} \quad (3.22)$$

As expected for $D = 2d = 2$, these critical points produce logarithmic divergences in the phase measure at the points $p = k, 2k_* - k$. For the special choice $k = k_*$, there is a double pole at $p = k_*$ when $\nabla \otimes \nabla E^{(4)}$ becomes identically zero at the critical point $(p, q) = (k_*, k_*)$. This degenerate critical point corresponds to a triple intersection between all three smooth pieces of the resonant manifold; see Fig. 3.9 below.

Because the critical points correspond to intersections with the trivial part of the resonant

³As usual in application of the NLS equation to optics, the space variable z and the time variable t have their roles exchanged, and thus also the roles of wavenumber k and frequency ω . However, here we revert to the notations used elsewhere in this dissertation.

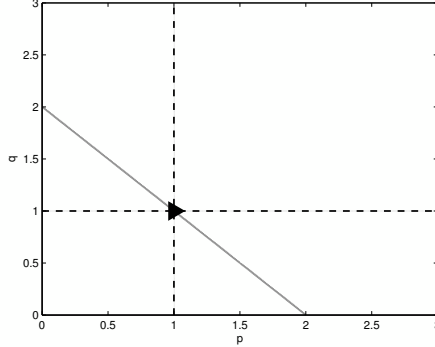


Figure 3.9: Resonant manifold $\mathcal{R}_k^{(4)}$, $k = 1$ of one-dimensional 3rd-order dispersive optical waves for $s = -1$, $\alpha = 3$, so that $k_* = 1$, with the non-trivial part of the manifold plotted in gray and the trivial part in dashed black. The triple intersection is a degenerate critical point, indicated by ►.

manifold, the integrand of the collision integral vanishes at those points and thus the integrals may be finite. For example, assume that $n(p)$ is twice-differentiable in the vicinity of k and let δp be the scale of variation of $n(p)$ near that point. Then one easily finds by Taylor expansion that the contribution to $C_k[n]$ from integrating over $|p - k| < \delta p$ is

$$C_k^{(p \approx k)}[n] = \frac{1}{6\pi|\alpha|} \left[\left(\frac{n''(k)n^2(2k_* - k)}{2} - \frac{(n'(k))^2 n^2(2k_* - k)}{n(k)} \right) + (k \leftrightarrow 2k_* - k) \right] \frac{(\delta p)^2}{|k - k_*|} \quad (3.23)$$

with a similar contribution coming from $p \approx 2k_* - k$. When $|k - k_*| < \delta p$ this is replaced by a contribution from the double pole:

$$C_{k \approx k_*}^{(p \approx k_*)}(n) = \frac{1}{3\pi|\alpha|} [n''(k_*)n^2(k_*) - 2(n'(k_*))^2 n^2(k_*)] (\delta p). \quad (3.24)$$

These contributions are finite as long as $n(p)$ is twice continuously differentiable near the poles. More generally, the contribution to the collision integral is finite if $n(p)$ has cusp-like singularities near $p = k_*$, $n(p) - n(k_*) \sim A|p - k_*|^c$ with $c > 1$.

Although the collision integral remains finite under the assumptions stated above, it may nevertheless become large, in the sense that the nonlinear frequency $\Gamma_k(n) = C_k(n)/n(k)$ could be of the same order as (or greater than) the linear frequency $\omega(k)$. If so, this violates the condition

CHAPTER 3. RESONANCE VAN HOVE SINGULARITIES: CASE STUDIES

$\Gamma_k(n) \ll \omega(k)$ required for validity of the kinetic equation (Newell *et al.*, 2001; Biven *et al.*, 2001; Nazarenko, 2011). Indeed, it was shown in the numerical study of Michel *et al.* (2011) that, for certain values of the cubic coefficient α , the ratio $\Gamma_k(n)/\omega(k)$ exceeded 1 near $k = k_*$ and, in that case, there was no longer quantitative agreement between the predictions of the kinetic equation and ensemble-averaged solutions of the NLS equation (see Figs.2 and 5 in Michel *et al.* (2011)). This is a physically interesting example which shows that resonance Van Hove singularities can lead to a breakdown in validity of kinetic theory, even when the collision integral remains finite.

3.3.3 Electrons and holes in graphene

We have so far considered classical 4-wave systems, but resonance Van Hove singularities can also occur in quantum wave kinetics. The collision integral of the quantum kinetic equation has the typical form

$$\begin{aligned}
 C_{\mathbf{k}s}[n] = & \sum_{s', s'', s'''} \int d^d p d^d q d^d \ell \delta^d(\mathbf{k} + \boldsymbol{\ell} - \mathbf{p} - \mathbf{q}) \delta(\omega_s(\mathbf{k}) + \omega_{s'}(\boldsymbol{\ell}) - \omega_{s''}(\mathbf{p}) - \omega_{s'''}(\mathbf{q})) \\
 & \times R_{\mathbf{k}\boldsymbol{\ell}\mathbf{p}\mathbf{q}}^{ss's''s'''} \left[(1 \pm n_s(\mathbf{k}))(1 \pm n_{s'}(\boldsymbol{\ell}))n_{s''}(\mathbf{p})n_{s'''}(\mathbf{q}) \right. \\
 & \left. - n_s(\mathbf{k})n_{s'}(\boldsymbol{\ell})(1 \pm n_{s''}(\mathbf{p}))(1 \pm n_{s'''}(\mathbf{q})) \right]
 \end{aligned} \tag{3.25}$$

with \pm for Bose/Fermi particles, respectively. (E.g. see section 2.1.6 of Zakharov *et al.* (1992)). The presence or not of resonance Van Hove singularities in the quantum case is thus governed by the same considerations as for classical wave kinetics.

A concrete example of physical interest is the dispersion law $\omega_s(k) = csk$, $s = \pm 1$ which for $d = 2$ describes the band energies of electron-hole excitations in graphene near the Dirac points. The quantum kinetic equation has been used to predict electron transport properties of pure, undoped samples of graphene (Kashuba, 2008; Fritz *et al.*, 2008; Müller *et al.*, 2009). The resonant manifold is a three-dimensional surface embedded in the Euclidean space of dimension $D = 2d = 4$. Any critical points are clearly non-null with all wavevectors collinear. Because $\omega''(k) \equiv 0$, the Hessian

CHAPTER 3. RESONANCE VAN HOVE SINGULARITIES: CASE STUDIES

matrix (3.19) has null eigenvectors $(\hat{\mathbf{k}}, \mathbf{0})$, $(\mathbf{0}, \hat{\mathbf{k}})$ and is co-rank at least 2. Thus the critical points are all doubly degenerate. In fact, the critical points lie on a 2-dimensional surface. For example, if $\mathbf{k} = (k, 0)$ with $k > 0$, then the critical set for $s, s', s'', s''' = 1$ consists of $\mathbf{p} = (p_1, 0)$, $\mathbf{q} = (q_1, 0)$ satisfying $p_1 > 0$, $q_1 > 0$, and $p_1 + q_1 > k$.

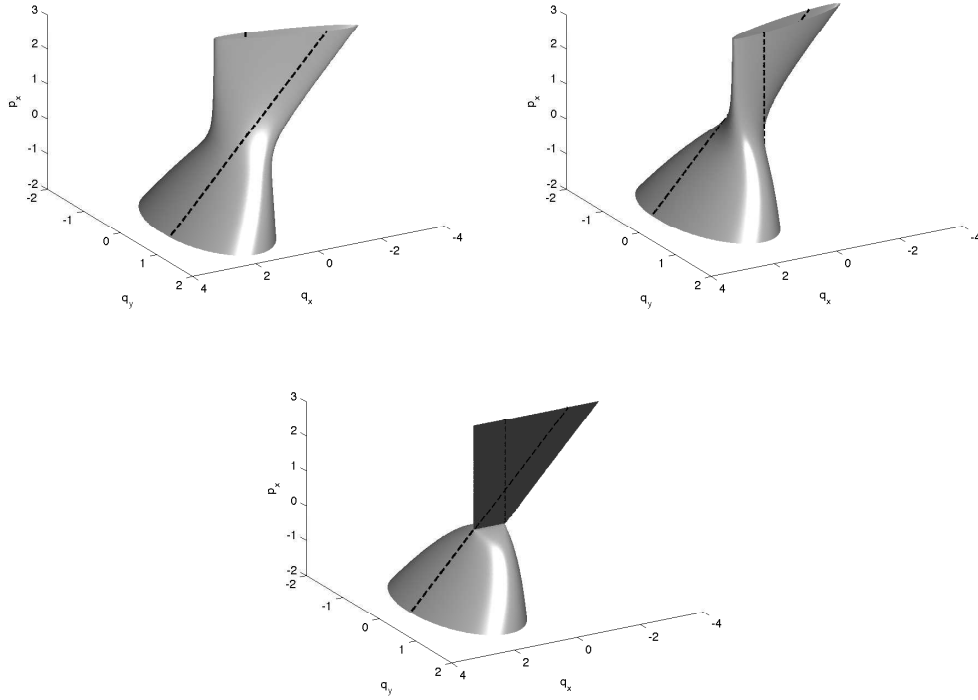


Figure 3.10: The section of the resonant manifold $\mathcal{R}_{\mathbf{k}}^{++++}$, $\mathbf{k} = (1, 0)$ for fixed p_y ($p_y < 0$ for the top left panel; $p_y = 0$ for the bottom panel; $p_y > 0$ for the top right panel), with the non-trivial part plotted in gray and the trivial part in dashed black. The 2D critical set in the bottom panel is plotted in dark gray. For $p_y \neq 0$ the horizontal sections of the resonant manifold at fixed p_x -values are ellipses, but for $p_y = 0$ and $p_x \geq 0$ these sections are line-segments.

In Fig. 3.10, we plot the resonant manifold $\mathcal{R}_{\mathbf{k}}^{++++}$, $\mathbf{k} = \mathbf{e}_1$ for 4-wave interactions in graphene. For visualization, we employ the notation in (Sachdev, 1998; Kashuba, 2008; Fritz *et al.*, 2008) that the four resonant wave vectors $\mathbf{k}, \ell, \mathbf{p}, \mathbf{q}$ are instead denoted by $\mathbf{k}, \mathbf{p}, \mathbf{k} + \mathbf{q}, \mathbf{p} - \mathbf{q}$. The resonance condition in these variables becomes $|\mathbf{q} + \mathbf{k}| + |\mathbf{q} - \mathbf{p}| = k + p$, which, as noted in (Sachdev, 1998), corresponds at fixed \mathbf{p} values to ellipses in the \mathbf{q} -planes, with foci at $-\mathbf{k}$ and $+\mathbf{p}$. When $\mathbf{k} \parallel \mathbf{p}$, these ellipses degenerate to line-segments $[-\mathbf{k}, +\mathbf{p}]$, whose set union comprises the critical set. In

CHAPTER 3. RESONANCE VAN HOVE SINGULARITIES: CASE STUDIES

Fig. 3.10 we plot 2D sections of the resonant manifold in the 3D space (q_x, q_y, p_x) at three different values of p_y . For the chosen value of $\mathbf{k} = \mathbf{e}_1$, the 2D critical set is located on the $p_y = 0$ section, as shown in the middle panel.

For graphene with $D = 4$, this 2-dimensional critical surface produces a logarithmic singularity in the phase measure, as has been previously noted by Sachdev (1998), Kashuba (2008), and Fritz *et al.* (2008). For example, for $\mathbf{k} = k\mathbf{e}_1$, $k > 0$, using the notation $\mathbf{k}, \mathbf{p}, \mathbf{k} + \mathbf{q}, \mathbf{p} - \mathbf{q}$ for the wavenumber quartet, and writing $\mathbf{p} = (p_1, p_\perp)$, $\mathbf{q} = (q_1, q_\perp)$, it was pointed out in Fritz *et al.* (2008) that to quadratic order in the transverse variables near the critical set

$$\begin{aligned} k + p - |\mathbf{q} + \mathbf{k}| - |\mathbf{q} - \mathbf{p}| &\simeq \frac{p_\perp^2}{2p} - \frac{q_\perp^2}{2(k+p)} - \frac{(p_\perp - q_\perp)^2}{2(p-q)} \\ &= -\frac{k+p}{2(k+q)(p-q)}(q_\perp - \zeta_1 p_\perp)(q_\perp - \zeta_2 p_\perp) \end{aligned} \quad (3.26)$$

where $\zeta_{1,2}$ are the roots of the quadratic polynomial in q_\perp/p_\perp defined by the first line. At each fixed value of p_1, q_1 that corresponds to points in the critical set, the integral over the transverse variables p_\perp, q_\perp is logarithmically divergent. This can be seen most easily by changing variables to

$$r_\perp = q_\perp - \zeta_1 p_\perp, \quad s_\perp = q_\perp - \zeta_2 p_\perp$$

with the Jacobian of transformation

$$\left| \frac{\partial(r_\perp, s_\perp)}{\partial(q_\perp, p_\perp)} \right| = |\zeta_1 - \zeta_2| = \frac{2}{k+p} \sqrt{\frac{k(k+q)(p-q)}{p}}.$$

Thus,

$$\int dp_\perp \int dq_\perp \delta(k+p - |\mathbf{q} + \mathbf{k}| - |\mathbf{q} - \mathbf{p}|) = \sqrt{\frac{p(k+q)(p-q)}{k}} \int dr_\perp \int ds_\perp \delta(r_\perp s_\perp)$$

and the latter integral exhibits, for each fixed value of p_1, q_1 corresponding to points in the critical set,

CHAPTER 3. RESONANCE VAN HOVE SINGULARITIES: CASE STUDIES

the same type of logarithmic divergence that was observed for Rossby/drift waves in $d = 2$. However, electron-hole interactions do not vanish near the critical set, unlike the case for Rossby/drift waves, so that the divergence is unregulated.

The local logarithmic divergence can be removed by resonance-broadening of the delta function (e.g. Nazarenko (2011, section 6.5.2)). Assuming for simplicity a constant resonance width γ , the delta function $\delta(r_\perp s_\perp)$ is replaced by the Lorentzian (Cauchy distribution)

$$\delta_\gamma(r_\perp s_\perp) = \frac{\gamma}{\pi} \frac{1}{r_\perp^2 s_\perp^2 + \gamma^2}.$$

Since $\delta_\gamma(r_\perp s_\perp) \sim 1/\pi\gamma$ for $r_\perp s_\perp \ll \gamma$, an integral over a small neighborhood of $r_\perp = s_\perp = 0$ is now finite. The quantitative behavior can be seen from the following integral

$$I = \int_{-a}^a dr_\perp \int_{-b}^b ds_\perp \delta_\gamma(r_\perp s_\perp) = 2 \int_0^a \frac{dr_\perp}{r_\perp} \left[\frac{\gamma/r_\perp}{\pi} \int_{-b}^b \frac{ds_\perp}{s_\perp^2 + (\gamma/r_\perp)^2} \right],$$

with cutoffs a, b . The region of integration $r_\perp \ll \gamma/b$ gives a γ -independent contribution, whereas for values $r_\perp \gg \gamma/b$ the inner integral is $\simeq 1$ and thus

$$I \sim 2 \ln(ab/\gamma), \quad \gamma \ll ab.$$

This asymptotic evaluation can easily be made rigorous by noting that $I = \frac{4}{\pi} \text{Ti}_2(ab/\gamma)$ where $\text{Ti}_2(x) = \int_0^x du \frac{\arctan u}{u}$ is the inverse tangent integral (Lewin (1981), Ch.VII, §1.2). The cutoffs a, b may come from limits to the magnitude of all wavevectors, e.g. the size of the Brillouin zone in graphene. The cutoffs a, b may also be associated to the maximum size of the region where $E(\mathbf{p}, \mathbf{q}; \mathbf{k}) \propto r_\perp s_\perp$. We shall discuss in further detail in section 4.3 how the logarithmic singularity is understood to affect the electron-hole kinetics in graphene.

3.4 Conclusion

This chapter has shown by various concrete examples that critical points in the resonance condition (resonance Van Hove singularities) occur in many common wave-kinetic equations. They lead to geometric singularities in the “resonant manifold”, which is thus no longer a true manifold. The singularities may furthermore lead to local non-finiteness of the phase measure appearing in the collision integral, which is associated physically to the infinite scattering time for locally non-dispersive waves. Such a diverging phase measure may nevertheless produce a finite collision integral, e.g. due to a vanishing interaction coefficient (Rossby/drift waves, $d = 2$) or due to cancellations between terms in the collision integrand (waves in an optical fiber, $d = 1$). When the collision integral itself diverges or even if it is finite but large, standard kinetic theory may break down (optical waves, $d = 1$; electron-holes in graphene, $d = 2$). Before we discuss this latter situation in section 4.3, we first discuss in section 4.2 more generally the conditions under which a critical point leads to a locally infinite phase measure at the singularity.

Chapter 4

Resonance Van Hove Singularities: Physical Consequences

4.1 Introduction

In this chapter, we first develop some quite general results about the effect of critical points on the local finiteness of phase measures in section 4.2. For the case of non-degenerate critical points we can carry over essentially unchanged the considerations of the classic study by Van Hove (1953). Thereafter we discuss briefly the case of degenerate critical points. We then discuss in section 4.3 electron-hole systems in graphene, where we have already seen in section 3.3.3 that the local phase measure is infinite. We employ the multi-scale perturbation approach from Newell and Aucoin (1971) on acoustic waves to derive a different asymptotic closure equation that governs the singular wave kinetics. We find via a local H-theorem that the local equilibrium solution is, along each ray, a generalized Fermi-Dirac distribution. Our analysis provides a simple picture of three time-scale process.

We begin with a mathematical issue that we have neglected until now: the resonance

CHAPTER 4. RESONANCE VAN HOVE SINGULARITIES: PHYSICAL CONSEQUENCES

function $E(\underline{\mathbf{p}}; \mathbf{k})$ is generally not smooth enough in the phase-space variable $\underline{\mathbf{p}} = (\mathbf{p}_1, \dots, \mathbf{p}_{N-2})$ in order to make the delta-function $\delta(E(\underline{\mathbf{p}}; \mathbf{k}))$ meaningful in any naive sense. Thus, the phase measure that we have defined formally by $d\mu = d^D \underline{p} \delta(E(\underline{\mathbf{p}}; \mathbf{k}))$ has no actual mathematical meaning. To give it a proper definition, one must return to the derivation of the wave kinetic equation. The standard multi-scale perturbation argument in Chap. 2 shows that what appears in the kinetic equation is actually an approximate delta function of the form

$$\delta_T(E(\underline{\mathbf{p}}; \mathbf{k})) = \frac{T}{2\pi} \text{sinc}^2 \left(\frac{T}{2} E(\underline{\mathbf{p}}; \mathbf{k}) \right), \quad (4.1)$$

for a time T chosen so that $\omega(\mathbf{k}) \gg 1/T \gg \Gamma_{\mathbf{k}}(n)$, where “sinc” denotes the cardinal sine function $\text{sinc}(x) = \sin x/x$. A physically motivated definition of the phase measure is thus as a suitable limit

$$d\mu = \lim_{T \rightarrow \infty} d^D \underline{p} \delta_T(E(\underline{\mathbf{p}}; \mathbf{k})). \quad (4.2)$$

We rigorously construct the phase measure $d\mu = d^D \underline{p} \delta(E(\underline{\mathbf{p}}; \mathbf{k}))$ in Appendix C through a suitable limiting process for the approximate delta function (4.1). This measure satisfies

$$d\mu = \frac{d\mathcal{H}^{D-1}(\underline{\mathbf{p}})}{|\nabla E(\underline{\mathbf{p}}; \mathbf{k})|}. \quad (4.3)$$

In this chapter we shall simply assume the phase measure is well-defined, appealing to the results in Appendix C. An alternative approach is suggested by field-theoretic derivations of wave kinetics (L’vov *et al.*, 1997), which instead yield an approximate delta function of Lorentzian (Cauchy) form:

$$\delta_\gamma(E(\underline{\mathbf{p}}; \mathbf{k})) = \frac{\gamma}{\pi} \frac{1}{E^2(\underline{\mathbf{p}}; \mathbf{k}) + \gamma^2}, \quad (4.4)$$

and which suggests to take a similar limit $\gamma \rightarrow 0$. This was the starting point of Lukkarinen and Spohn (2007) to define the phase measure, in a slightly different context. We also compare this

alternate approach with our direct approach in Appendix C.

4.2 Local Finiteness of the Phase Measure

Now using the relation (4.3) we study the local finiteness of the phase measure μ in the neighborhood of a non-degenerate critical point, following the basic idea of Van Hove (1953), who analyzed this question for the energy density of states using the Morse Lemma. Since \mathbf{k} appears as a parameter in the argument, we omit it and write simply $E(\underline{\mathbf{p}})$. We recall here the statement of the Morse Lemma (Milnor, 1963; Lang, 2012): if $E(\underline{\mathbf{p}})$ has a non-degenerate critical point $\underline{\mathbf{p}}_*$ such that E is C^{k+2} , $k \geq 1$ with respect to $\underline{\mathbf{p}}$ in a neighborhood of $\underline{\mathbf{p}}_*$, then there is a C^k diffeomorphism φ of a neighborhood U of $\underline{\mathbf{p}}_*$ with a neighborhood V of $\underline{\mathbf{0}} = \varphi(\underline{\mathbf{p}}_*)$ such that $\tilde{E}(\underline{\mathbf{q}}) = E(\varphi^{-1}(\underline{\mathbf{q}}))$ has the canonical form

$$\tilde{E}(\underline{\mathbf{q}}) = E(\underline{\mathbf{p}}_*) - |\underline{\mathbf{q}}^-|^2 + |\underline{\mathbf{q}}^+|^2$$

where $(\underline{\mathbf{q}}^-, \underline{\mathbf{q}}^+) = \underline{\mathbf{q}} = \varphi(\underline{\mathbf{p}})$ with $\underline{\mathbf{q}}^\pm \in \mathbb{R}^{D_\pm}$ and $D_- + D_+ = D$. It is possible that $D_- = 0$, in which case $\tilde{E}(\underline{\mathbf{q}}) = E(\underline{\mathbf{p}}_*) + |\underline{\mathbf{q}}|^2$ or that $D_+ = 0$, in which case $\tilde{E}(\underline{\mathbf{q}}) = E(\underline{\mathbf{p}}_*) - |\underline{\mathbf{q}}|^2$. Note that D_\pm are just the number of positive/negative eigenvalues of the Hessian of E at $\underline{\mathbf{p}}_*$. Van Hove assumed further that φ can be chosen to preserve D -dimensional volume (Lebesgue measure), in which case

$$I = \int_U d^D \underline{\mathbf{p}} \delta(E(\underline{\mathbf{p}})) = \int_V d^D \underline{\mathbf{q}} \delta(\tilde{E}(\underline{\mathbf{q}})),$$

and the righthand side can then be shown to be finite/infinite by a direct calculation. It has indeed been proved subsequently by de Verdiere and Vey (1979) that such a volume-preserving (“isochoric”) choice of φ is possible, if E is a C^∞ function. However, even if E is only C^{k+2} , the neighborhoods U, V can always be chosen so that the Jacobian determinant of φ satisfies

$$0 < c \leq |\det(D\varphi)(\underline{\mathbf{p}})| \leq C < \infty, \quad \underline{\mathbf{p}} \in U$$

CHAPTER 4. RESONANCE VAN HOVE SINGULARITIES: PHYSICAL CONSEQUENCES

and since

$$\int_V d^D \underline{q} \, \delta(\tilde{E}(\underline{q})) = \int_U d^D \underline{p} \, |\det(D\varphi)(\underline{p})| \, \delta(E(\underline{p}))$$

the two integrals $J = \int_V d^D \underline{q} \, \delta(\tilde{E}(\underline{q}))$, $I = \int_U d^D \underline{p} \, \delta(E(\underline{p}))$ are either both finite or both infinite.

Thus, the question again reduces to an elementary calculation of the integral J .

Taking therefore a critical point \underline{p}_* on the resonant manifold, satisfying $E(\underline{p}_*) = 0$, the condition for the resonant manifold \mathcal{R} in the \underline{q} -coordinates in V becomes simply

$$|\underline{q}^-| = |\underline{q}^+|.$$

When either $D_- = 0$ or $D_+ = 0$, the resonant manifold reduces to the isolated point $\underline{q} = \underline{0}$, and one can easily show that $J = 0$. Thus we assume $D_{\pm} \neq 0$. We use

$$J = \int_V d^D \underline{q} \, \delta(\tilde{E}(\underline{q})) = \int_{V \cap \mathcal{R}} \frac{d\mathcal{H}^{D-1}(\underline{q})}{|\nabla \tilde{E}(\underline{q})|}$$

and $\nabla \tilde{E}(\underline{q}) = 2(-\underline{q}^-, \underline{q}^+)$, so that $|\nabla \tilde{E}(\underline{q})| = 2\sqrt{2}|\underline{q}^-|$ on \mathcal{R} . To simplify the calculation, without loss of generality, we take the neighborhood V to be a Cartesian product of two balls of radius η , $V = B(\underline{0}^-, \eta) \times B(\underline{0}^+, \eta)$. Using hyperspherical coordinates for both \underline{q}^- and \underline{q}^+ , the calculation reduces to ¹

$$J = \int_{B(\underline{0}^-, \eta)} d\mathcal{H}^{D-1}(\underline{q}^-) \frac{1}{2\sqrt{2}q_-} \int_{q_+ = q_-} d\mathcal{H}^{D_+-1}(\underline{q}^+) = (const.) \int_0^\eta q_-^{D-3} dq_-,$$

where a factor $\propto q_-^{D_+-1}$ arises from the $(D_+ - 1)$ -dimensional Hausdorff measure of the \underline{q}^+ -sphere of radius q_- . Clearly, $J < \infty$ if $D > 2$ and $J = \infty$ if $D \leq 2$, exactly as had been concluded by Van

¹The Fubini-like theorem that we use here follows from the co-area formula of geometric measure theory. E.g. see Federer (1969, Theorem 3.2.22): For any $W \subset \mathbb{R}^M$ which is M -rectifiable and \mathcal{H}^M -measurable, $Z \subset \mathbb{R}^N$, $N < M$ which is N -rectifiable and \mathcal{H}^N -measurable, a Lipschitz map $f : W \rightarrow Z$, and any non-negative, \mathcal{H}^M -measurable function $g : W \rightarrow \mathbb{R}$, $\int_W g(w)(Jf)(w) d\mathcal{H}^M(w) = \int_Z d\mathcal{H}^N(z) \int_{f^{-1}(z)} g(w') d\mathcal{H}^{M-N}(w')$. We apply that theorem with $M = D - 1$, $N = D_-$, $W = V \cap \mathcal{R}$, $V = Z \times Y$, $Z = B(\underline{0}^-, \eta)$, $Y = B(\underline{0}^+, \eta)$, $f : W \rightarrow Z$ is the restriction to W of $\pi : V \rightarrow Z$, the projection onto the first factor of V , and $g = 1/|\nabla \tilde{E}|$. Note that for each $\underline{q}^- \in Z$, $f^{-1}(\underline{q}^-) = S(\underline{0}^+, q_-)$, the \underline{q}^+ -sphere of radius q_- centered at $\underline{0}^+$, and that the Jacobian $Jf \equiv 1$. Finally, W is obviously $(D - 1)$ -rectifiable and Z is D_- -rectifiable. Thus, $\int_{V \cap \mathcal{R}} d\mathcal{H}^{D-1}(\underline{q})/|\nabla \tilde{E}(\underline{q})| = \int_{B(\underline{0}^-, \eta)} d\mathcal{H}^{D-1}(\underline{q}^-) \int_{S(\underline{0}^+, q_-)} d\mathcal{H}^{D_+-1}(\underline{q}^+)/|\nabla \tilde{E}(\underline{q})|$.

CHAPTER 4. RESONANCE VAN HOVE SINGULARITIES: PHYSICAL CONSEQUENCES

Hove for the energy density of states.

In particular, we find a logarithmic divergence for $D = 2$, when one can write simply $\underline{\mathbf{q}} = (q_-, q_+)$. Introducing the new coordinates

$$r = q_+ - q_-, \quad s = q_+ + q_-$$

with Jacobian of transformation $\left| \frac{\partial(r,s)}{\partial(q_+, q_-)} \right| = 2$ one can write

$$\tilde{E} = q_+^2 - q_-^2 = rs$$

and thus

$$J = \int_{|\underline{\mathbf{q}}| < \eta} dq_+ dq_- \delta(q_+^2 - q_-^2) = \frac{1}{2} \int_{r^2 + s^2 < 2\eta^2} dr ds \delta(rs).$$

We see from this formula that our previous considerations on the effect of resonance broadening for graphene carry over to the general case, with the local divergence removed and replaced by a logarithmically large value $\propto \ln(ab/\gamma)$ for resonance width γ .

We have thus obtained quite general results on the local finiteness of the phase measure in the vicinity of a non-degenerate critical point. These general considerations explain the specific results we found in Chap. 3, such as the logarithmically divergent phase measure for 3-wave resonance of Rossby/drift waves in $d = 2$ ($D = 2$) and the finite phase measure for 4-wave resonance of capillary-gravity waves in $d = 2$ ($D = 4$).

Let us now consider briefly the effect of degeneracy. The simplest situation is when the critical points lie on a δ -dimensional submanifold where $\nabla E(\underline{\mathbf{p}}) = \mathbf{0}$, which immediately implies a degeneracy degree of at least δ at each such critical point. This corresponds to the situation where in a neighborhood U of each critical point $\underline{\mathbf{p}}_*$, with $E(\underline{\mathbf{p}}_*) = 0$, there is a diffeomorphism φ with a

CHAPTER 4. RESONANCE VAN HOVE SINGULARITIES: PHYSICAL CONSEQUENCES

neighborhood V of $\underline{\mathbf{0}} = \varphi(\underline{\mathbf{p}}_*)$ such that

$$\tilde{E}(\underline{\mathbf{q}}) = -|\underline{\mathbf{q}}^-|^2 + |\underline{\mathbf{q}}^+|^2$$

where $(\underline{\mathbf{q}}^0, \underline{\mathbf{q}}^-, \underline{\mathbf{q}}^+) = \underline{\mathbf{q}} = \varphi(\underline{\mathbf{p}})$ with $\underline{\mathbf{q}}^\pm \in \mathbb{R}^{D^\pm}$ and $\underline{\mathbf{q}}^0 \in \mathbb{R}^\delta$. In this case, $D_+ + D_- = D - \delta \equiv D'$.

One can take the neighborhood V , without loss of generality, to be of the form $V = V_0 \times V'$, where V_0 is a neighborhood of $\underline{\mathbf{0}}^0 \in \mathbb{R}^\delta$ and V' is a neighborhood of $(\underline{\mathbf{0}}^-, \underline{\mathbf{0}}^+) \in \mathbb{R}^{D'}$. In this case, it is seen that

$$J = \mathcal{L}^\delta(V_0)J', \quad J' = \int_{V'} d^{D'} \underline{q}' \delta(\tilde{E}(\underline{\mathbf{q}}'))$$

with $\underline{\mathbf{q}}' = (\underline{\mathbf{q}}^-, \underline{\mathbf{q}}^+)$ and \mathcal{L}^δ the δ -dimensional Lebesgue measure (volume). Here J' has the same form as did J for the non-degenerate case, but with D' replacing D . Thus, the measure is locally finite at each critical point for $D' > 2$ but locally infinite for $D' \leq 2$.

This analysis explains the results we obtained in several concrete examples in Chap. 3, such as the logarithmically divergent phase measures for 3-wave resonance of inertial waves in $d = 3$ ($D = 3, \delta = 1$) and for 4-wave resonance of electron-hole excitations of graphene in $d = 2$ ($D = 4, \delta = 2$), both with $D' = 2$.

Another case of interest is an isolated critical point with degeneracy degree δ (co-rank of the Hessian matrix). The classification of isolated critical points for differentiable functions E belongs to the field of singularity theory; see Arnold *et al.* (2012). We shall not discuss such a classification in detail here, but we briefly mention in this light the doubly degenerate critical point obtained for wave propagation along an optical fiber, from section 3.3.2. For the distinguished value $k = k_*$ (known as the “zero-dispersion frequency” in the nonlinear optics community) one can express $E(p, q; k_*)$ locally at the degenerate critical point (k_*, k_*) in terms of the deviation variables $\delta p = p - k_*, \delta q = q - k_*$ as

$$E(\delta p, \delta q; k_*) = 3\alpha(\delta p + \delta q) \delta p \delta q.$$

CHAPTER 4. RESONANCE VAN HOVE SINGULARITIES: PHYSICAL CONSEQUENCES

After a linear transformation $\delta p = (x - y)/(6\alpha)^{1/3}$, $\delta q = -(x + y)/(6\alpha)^{1/3}$ this becomes

$$E(x, y; k_*) = x^2 y - y^3.$$

The latter is the normal form for the family D_4^- in the classification of “simple” singularities for differentiable real functions in Arnold *et al.* (2012). The general possibilities are quite rich and complex, and still the subject of mathematical investigation. However, we note from the optics example that the effect of degeneracy is again to worsen the divergence of the phase measure, whose density now exhibits a double pole rather than the simple poles (leading to logarithmic divergences) found for the non-degenerate critical points when $k \neq k_*$.

The cases of degenerate points that we have discussed here are by no means exhaustive. For example, one could have a set of critical points with degeneracy degree δ comprising a D_0 -dimensional submanifold with $1 < D_0 < \delta$. There is also the possibility of pseudo-critical points, but, as discussed earlier, these will produce no divergence of phase measure unless the geometric singularity is so severe that the resonant manifold develops a locally infinite Hausdorff measure.

The general morals to be drawn from our discussion are as follows. Pseudo-critical points should usually yield a locally finite phase measure and are “harmless” for kinetic theory. True critical points are potentially “dangerous” and can lead to locally infinite phase measure, especially in situations of low dimensions d , low-order N of resonance, and/or high degeneracy degree δ . The divergence of phase measure due to such singularities can be rendered harmless by vanishing interaction coefficients or by cancellations in the collision integral.

4.3 Singular Wave Kinetics: Electron-Hole Plasma in Graphene

We have seen several examples in Chap. 3 (inertial waves in $d = 3$ fluids, optical wave propagation along a $d = 1$ fiber, and Dirac electron-hole excitations in $d = 2$ graphene) where an “unprotected” resonance Van Hove singularity leads to a breakdown of standard wave kinetics. This

CHAPTER 4. RESONANCE VAN HOVE SINGULARITIES: PHYSICAL CONSEQUENCES

is analogous to the situation in the theory of low-amplitude acoustic wave turbulence, except that now the breakdown of dispersivity of the waves occurs only locally on the resonant manifold rather than for all resonances. In the case of acoustic waves, generalized equations were derived to describe the “singular wave kinetics” of semi-dispersive waves, both by multiple time-scale perturbation theory (Newell and Aucoin, 1971) and by field-theoretic methods (L’vov *et al.*, 1997). One can expect that such singular kinetic theories will apply more generally, even when the critical set is only a subset of the entire resonant manifold. We shall illustrate this situation with the example of electron-hole kinetics in graphene.

4.3.1 Derivation of the Singular Kinetic Equation

We first discuss graphene from the point of view of multiple time-scale perturbation theory, as originally developed in Newell and Aucoin (1971). It should be stressed at the outset that the applicability of perturbation theory is itself a nontrivial result, because electron-hole excitations in graphene on most substrates are not weakly coupled (nor infinitely-strongly coupled). It is instead believed that the coupling becomes weak for sufficiently low wavenumbers because of a globally attractive, asymptotically-free renormalization-group (RG) fixed point. See González *et al.* (1999), Son (2007), and Hofmann *et al.* (2014) for discussions of this issue. Thus, the perturbation theory argument must be applied to a low-wavenumber renormalized theory. A further very significant complication is that the Coloumb interaction is long-range and many-electron effects such as dynamical screening are expected in graphene (Kotov *et al.*, 2012), and these effects do not appear at any finite order in naive weak-coupling perturbation theory. Although such a naive perturbation theory analysis is therefore very incomplete, we find that it provides useful insight.

The perturbative derivation of the quantum Boltzmann equation is much the same as the derivation of the kinetic equation for weakly-coupled classical waves, e.g. see Spohn (2006) and

CHAPTER 4. RESONANCE VAN HOVE SINGULARITIES: PHYSICAL CONSEQUENCES

Zakharov *et al.* (1992). Start with a general quantum Hamiltonian $H = H_0 + H_1$ with free part

$$H_0 = \sum_{s,a} \int d^d k \, \omega_s(k) \gamma_{sa}^\dagger(\mathbf{k}) \gamma_{sa}(\mathbf{k}), \quad (4.5)$$

where

$$\omega_s(k) = s v_F k, \quad s = \pm 1, \quad (4.6)$$

and interaction part

$$\begin{aligned} H_1 = & \frac{\alpha}{2} \sum_{s_1, s_2, s_3, s_4} \sum_{a,b} \int d^d k_1 d^d k_2 d^d k_3 d^d k_4 \delta^d(\mathbf{k}_1 + \mathbf{k}_2 - \mathbf{k}_3 - \mathbf{k}_4) \\ & \times T_{\mathbf{k}_1 \mathbf{k}_2 \mathbf{k}_3 \mathbf{k}_4}^{s_1 s_2 s_3 s_4} \gamma_{s_4 b}^\dagger(\mathbf{k}_4) \gamma_{s_3 a}^\dagger(\mathbf{k}_3) \gamma_{s_2 a}(\mathbf{k}_2) \gamma_{s_1 b}(\mathbf{k}_1), \end{aligned} \quad (4.7)$$

where $\gamma_{sa}^\dagger(\mathbf{k}), \gamma_{sa}(\mathbf{k})$ are standard creation/annihilation operators. We assume here that these operators obey canonical anti-commutation relations, as appropriate for fermionic electron & hole excitations. The indices $s = \pm 1$ represent electrons and holes, respectively. The indices a, b are summed over integers $1, \dots, N$, to incorporate a possible N -fold degeneracy of the fermions. The interaction coefficient

$$T_{\mathbf{k}_1 \mathbf{k}_2 \mathbf{k}_3 \mathbf{k}_4}^{s_1 s_2 s_3 s_4} = \frac{1}{|\mathbf{k}_4 - \mathbf{k}_1|} \left(1 + s_1 s_4 \frac{\mathbf{K}_4^* \mathbf{K}_1}{k_4 k_1} \right) \left(1 + s_2 s_3 \frac{\mathbf{K}_3^* \mathbf{K}_2}{k_3 k_2} \right) \quad (4.8)$$

arises from Coulomb interaction (cf. Fritz *et al.* (2008)), with $\mathbf{K} = k_x + i k_y$. The physical dimensions require a bit of discussion. The 1-particle energies in the free part of the Hamiltonian are $E_s(\mathbf{k}) = \hbar \omega_s(\mathbf{k})$, so our units correspond to $\hbar = 1$. The Coulomb potential is $V(\mathbf{r}) = e^2 / \kappa r$, where κ is the background dielectric constant. Hence, the parameter α in the interaction Hamiltonian for graphene corresponds to the dimensionless “fine-structure constant” $\alpha = e^2 / \kappa \hbar v_F$, in units where $v_F = 1$. We have kept the factor v_F in the dispersion relation, although it is strictly just 1 in our units.

For an infinite-volume system, define the mean occupation number $n_s(\mathbf{k}, t)$ by $\langle \gamma_{sa}^\dagger(\mathbf{k}, t) \gamma_{s'a'} \rangle$

CHAPTER 4. RESONANCE VAN HOVE SINGULARITIES: PHYSICAL CONSEQUENCES

$(\mathbf{k}', t)\rangle = n_s(\mathbf{k}, t)\delta_{ss'}\delta_{aa'} \delta^d(\mathbf{k} - \mathbf{k}')$. Perturbation theory in the small parameter α yields the result that

$$\begin{aligned} & n_{s_1}(\mathbf{k}_1, t) - n_{s_1}(\mathbf{k}_1, 0) \\ &= -\alpha^2 \sum_{s_2, s_3, s_4} \int d^d k_2 d^d k_3 d^d k_4 \delta^d(\mathbf{k}_1 + \mathbf{k}_2 - \mathbf{k}_3 - \mathbf{k}_4) \frac{2 \left(1 - \cos(E_{\mathbf{k}_1 \mathbf{k}_2 \mathbf{k}_3 \mathbf{k}_4}^{s_1 s_2 s_3 s_4} t)\right)}{(E_{\mathbf{k}_1 \mathbf{k}_2 \mathbf{k}_3 \mathbf{k}_4}^{s_1 s_2 s_3 s_4})^2} \\ & \quad \times R_{\mathbf{k}_1 \mathbf{k}_2 \mathbf{k}_3 \mathbf{k}_4}^{s_1 s_2 s_3 s_4} [n_{s_1}(\mathbf{k}_1) n_{s_2}(\mathbf{k}_2) \tilde{n}_{s_3}(\mathbf{k}_3) \tilde{n}_{s_4}(\mathbf{k}_4) - \tilde{n}_{s_1}(\mathbf{k}_1) \tilde{n}_{s_2}(\mathbf{k}_2) n_{s_3}(\mathbf{k}_3) n_{s_4}(\mathbf{k}_4)] \end{aligned} \quad (4.9)$$

where

$$\begin{aligned} E_{\mathbf{k}_1 \mathbf{k}_2 \mathbf{k}_3 \mathbf{k}_4}^{s_1 s_2 s_3 s_4} &= \omega_{s_1}(\mathbf{k}_1) + \omega_{s_2}(\mathbf{k}_2) - \omega_{s_3}(\mathbf{k}_3) - \omega_{s_4}(\mathbf{k}_4), \\ R_{\mathbf{k}_1 \mathbf{k}_2 \mathbf{k}_3 \mathbf{k}_4}^{s_1 s_2 s_3 s_4} &= \frac{1}{2} |T_{\mathbf{k}_1 \mathbf{k}_2 \mathbf{k}_3 \mathbf{k}_4}^{s_1 s_2 s_3 s_4} - T_{\mathbf{k}_1 \mathbf{k}_2 \mathbf{k}_4 \mathbf{k}_3}^{s_1 s_2 s_4 s_3}|^2 + \frac{N-1}{2} |T_{\mathbf{k}_1 \mathbf{k}_2 \mathbf{k}_3 \mathbf{k}_4}^{s_1 s_2 s_3 s_4}|^2 + \frac{N-1}{2} |T_{\mathbf{k}_1 \mathbf{k}_2 \mathbf{k}_4 \mathbf{k}_3}^{s_1 s_2 s_4 s_3}|^2. \end{aligned} \quad (4.10)$$

and

$$\tilde{n}_s(\mathbf{k}, t) = 1 - n_s(\mathbf{k}, t). \quad (4.12)$$

See Appendix D for the details of the derivation. An elementary calculation gives

$$\frac{1 - \cos(Et)}{E^2} = \pi t \delta_t(E)$$

where $\delta_t(E)$ is the approximate delta function in eq.(4.1). When the condition $E_{\mathbf{k}_1 \mathbf{k}_2 \mathbf{k}_3 \mathbf{k}_4}^{s_1 s_2 s_3 s_4} = 0$ defines a non-degenerate resonance, the righthand side of (4.9) exhibits a secular growth $\propto \alpha^2 t$. This secular behavior is removed by choosing the occupation number to satisfy the quantum kinetic equation on the slow time scale $\tau = \alpha^2 t$, with collision integral (3.25).

This standard derivation fails for electron-hole kinetics in graphene , when $d = 2$ and

$$\omega_s(k) = s v_F k, \quad s = \pm 1.$$

CHAPTER 4. RESONANCE VAN HOVE SINGULARITIES: PHYSICAL CONSEQUENCES

The index $N = 4$, for the two electron spins and two Dirac points (valleys) in the Brillouin zone. The degeneracy of the condition $E_{\mathbf{k}_1 \mathbf{k}_2 \mathbf{k}_3 \mathbf{k}_4}^{s_1 s_2 s_3 s_4} = 0$ changes the asymptotics of the integral in eq.(4.9). Note that momentum and energy conservation allow non-trivial resonances only for electron-electron/hole-hole collisions (all s 's of the same sign) or electron-hole collisions (one $s = +1$ and one $s = -1$ in both incoming and outgoing states). For simplicity, we discuss explicitly here only the first case. To obtain the long-time asymptotics, it is useful to take two derivatives with respect to time, to obtain the contribution with all $s_i = s$:

$$\frac{d^2}{dt^2} [n_s(\mathbf{k}, t) - n_s(\mathbf{k}, 0)] = -2\alpha^2 \int d^2 k_3 d^2 k_4 \cos(E_{\mathbf{k} \mathbf{k}_2 \mathbf{k}_3 \mathbf{k}_4}^{++++} t) M^{++++}(\mathbf{k}_3, \mathbf{k}_4), \quad (4.13)$$

where $\mathbf{k}_2 = \mathbf{k}_3 + \mathbf{k}_4 - \mathbf{k}$ and

$$M^{++++}(\mathbf{k}_3, \mathbf{k}_4) = R_{\mathbf{k} \mathbf{k}_2 \mathbf{k}_3 \mathbf{k}_4}^{++++} [n_s(\mathbf{k}) n_s(\mathbf{k}_2) \tilde{n}_s(\mathbf{k}_3) \tilde{n}_s(\mathbf{k}_4) - \tilde{n}_s(\mathbf{k}) \tilde{n}_s(\mathbf{k}_2) n_s(\mathbf{k}_3) n_s(\mathbf{k}_4)], \quad (4.14)$$

with

$$R_{\mathbf{k} \mathbf{k}_2 \mathbf{k}_3 \mathbf{k}_4}^{++++} = \frac{1}{2} |T_{\mathbf{k} \mathbf{k}_2 \mathbf{k}_3 \mathbf{k}_4}^{++++} - T_{\mathbf{k} \mathbf{k}_2 \mathbf{k}_4 \mathbf{k}_3}^{++++}|^2 + (N - 1) |T_{\mathbf{k} \mathbf{k}_2 \mathbf{k}_3 \mathbf{k}_4}^{++++}|^2. \quad (4.15)$$

Using polar coordinates $\mathbf{k} = k(\cos \theta, \sin \theta)$ with fixed direction angle θ of wavevector \mathbf{k} and $\mathbf{k}_i = k_i(\cos(\theta + \theta_i), \sin(\theta + \theta_i))$, $i = 3, 4$, this can be rewritten as

$$\begin{aligned} & \frac{d^2}{dt^2} [n_s(\mathbf{k}, t) - n_s(\mathbf{k}, 0)] \\ &= -\frac{\alpha^2}{2\pi^2} \text{Re} \int_0^\infty k_3 dk_3 \int_0^\infty k_4 dk_4 \int_{-\pi}^\pi d\theta_3 \int_{-\pi}^\pi d\theta_4 e^{it E_{\mathbf{k}, \mathbf{k}_3 + \mathbf{k}_4 - \mathbf{k}, \mathbf{k}_3, \mathbf{k}_4}^{++++}} M^{++++}(k_3, k_4, \theta_3, \theta_4), \end{aligned} \quad (4.16)$$

where a simple calculation gives

$$\begin{aligned} E_{\mathbf{k}, \mathbf{k}_3 + \mathbf{k}_4 - \mathbf{k}, \mathbf{k}_3, \mathbf{k}_4}^{++++} &= k_3 + k_4 - k \\ &- \sqrt{(k_3 + k_4 - k)^2 - 2k_3 k_4 (1 - \cos(\theta_3 + \theta_4)) + 2k_3 k (1 - \cos \theta_3) + 2k_4 k (1 - \cos \theta_4)} \end{aligned}$$

$$\simeq \boldsymbol{\theta}^\top H \boldsymbol{\theta} \quad (4.17)$$

to quadratic order in $\boldsymbol{\theta} = (\theta_3, \theta_4)$, with the 2×2 matrix

$$H = \frac{1}{2(k_3 + k_4 - k)} \begin{pmatrix} k_3(k_4 - k) & k_3 k_4 \\ k_3 k_4 & k_4(k_3 - k) \end{pmatrix}. \quad (4.18)$$

Using $\det H = \frac{k k_3 k_4}{4(k - k_3 - k_4)}$, the integral over angles in eq.(4.16) is then evaluated asymptotically for $t \rightarrow \infty$ by the method of stationary phase (Fedoryuk, 1971), giving

$$\begin{aligned} & \frac{d^2}{dt^2} [n_s(\mathbf{k}, t) - n_s(\mathbf{k}, 0)] \\ &= -\frac{\alpha^2}{2\pi^2} \operatorname{Re} \left[\frac{2\pi}{t} \iint_{k_3 > 0, k_4 > 0, k_3 + k_4 > k} k_3 k_4 \, dk_3 \, dk_4 \, |\det H|^{-1/2} M^{++++}(\theta_3 = \theta_4 = 0) \right. \\ & \quad \left. + \frac{2\pi}{t} e^{\frac{\pi}{2}i} \iint_{k_3 > 0, k_4 > 0, k_3 + k_4 < k} k_3 k_4 \, dk_3 \, dk_4 \, |\det H|^{-1/2} M^{++++}(\theta_3 = \theta_4 = 0) \right] + O(t^{-2}) \\ &= -\frac{2\alpha^2}{\pi} \frac{1}{t} \iint_{k_3 > 0, k_4 > 0, k_3 + k_4 > k} dk_3 \, dk_4 \, \sqrt{\frac{(k_3 + k_4 - k)k_3 k_4}{k}} M^{++++}(\theta_3 = \theta_4 = 0) + O(t^{-2}). \end{aligned} \quad (4.19)$$

This integrates to

$$n_s(\mathbf{k}, t) - n_s(\mathbf{k}, 0) \sim -\frac{2\alpha^2}{\pi} t \ln t \iint_{k_3 > 0, k_4 > 0, k_3 + k_4 > k} dk_3 \, dk_4 \sqrt{\frac{(k_3 + k_4 - k)k_3 k_4}{k}} M^{++++}(\theta_3 = \theta_4 = 0) \quad (4.20)$$

as $t \rightarrow \infty$. The crucial point is that the leading secular growth is now faster than t by a logarithmic factor $\ln t$, as a consequence of the degeneracy of resonance. Note that the entire contribution arises from the critical subset of the resonant manifold, with all quartet wavevectors parallel to \mathbf{k} .

Taking into account the electron-hole scattering changes this result only by appearance of an additional term, which is obtained by a very similar calculation. The complete asymptotics is

CHAPTER 4. RESONANCE VAN HOVE SINGULARITIES: PHYSICAL CONSEQUENCES

given by

$$n_s(\mathbf{k}, t) - n_s(\mathbf{k}, 0) \sim -\frac{2\alpha^2}{\pi} t \ln t \iint_{k_3 > 0, k_4 > 0, k_3 + k_4 > k} dk_3 dk_4 \sqrt{\frac{(k_3 + k_4 - k)k_3 k_4}{k}} M(\theta_3 = \theta_4 = 0) \quad (4.21)$$

with

$$M(\mathbf{k}_3, \mathbf{k}_4) = M^{++++}(\mathbf{k}_3, \mathbf{k}_4) + M^{+--+}(\mathbf{k}_3, \mathbf{k}_4)$$

and the electron-hole scattering contribution

$$M^{+--+}(\mathbf{k}_3, \mathbf{k}_4) = R_{\mathbf{k}, -\mathbf{k}_4, \mathbf{k}_3, -\mathbf{k}_2}^{+--+} \times [n_s(\mathbf{k})n_{-s}(-\mathbf{k}_4)\tilde{n}_s(\mathbf{k}_3)\tilde{n}_{-s}(-\mathbf{k}_2) - \tilde{n}_s(\mathbf{k})\tilde{n}_{-s}(-\mathbf{k}_4)n_s(\mathbf{k}_3)n_{-s}(-\mathbf{k}_2)], \quad (4.22)$$

with

$$R_{\mathbf{k}\mathbf{k}_2\mathbf{k}_3\mathbf{k}_4}^{+--+} = |T_{\mathbf{k}\mathbf{k}_2\mathbf{k}_3\mathbf{k}_4}^{+--+} - T_{\mathbf{k}\mathbf{k}_2\mathbf{k}_4\mathbf{k}_3}^{+--+}|^2 + (N-1)|T_{\mathbf{k}\mathbf{k}_2\mathbf{k}_3\mathbf{k}_4}^{+--+}|^2 + (N-1)|T_{\mathbf{k}\mathbf{k}_2\mathbf{k}_4\mathbf{k}_3}^{+--+}|^2. \quad (4.23)$$

We have made a change of variables $\mathbf{k}_2 \rightarrow -\mathbf{k}_4$, $\mathbf{k}_4 \rightarrow -\mathbf{k}_2$ in the integral for the electron-hole contribution so that the range of integration is the same as for the electron-electron contribution. The physics of the electron-hole scattering term is easy to understand, if one recalls that a hole excitation with wavevector \mathbf{k} has a group velocity $\nabla\omega_{-}(\mathbf{k}) = -v_F\hat{\mathbf{k}}$ which is opposite to the group velocity $\nabla\omega_{+}(\mathbf{k}) = +v_F\hat{\mathbf{k}}$ for an electron excitation with the same wavevector \mathbf{k} . Hence, non-dispersive interactions with identical group velocities for a quartet of modes requires that the holes have wavevectors anti-parallel to the wavevectors for the electrons. The fact that electron-hole scattering couples occupation numbers for anti-parallel wavevectors will be seen below to have interesting consequences.

The leading secular growth in (4.21) can be removed, following the ideas in Newell and

CHAPTER 4. RESONANCE VAN HOVE SINGULARITIES: PHYSICAL CONSEQUENCES

Aucoin (1971), by allowing the occupation numbers to evolve on the time-scale $\tau_1 = \alpha^2 t \ln t$ according to the *singular kinetic equation*:

$$\begin{aligned}
 dn_s(\mathbf{k})/d\tau_1 = & -\frac{2}{\pi} \iint_{k_3 > 0, k_4 > 0, k_3 + k_4 > k} d\mathbf{k}_3 d\mathbf{k}_4 \sqrt{\frac{(k_3 + k_4 - k)k_3 k_4}{k}} \\
 & \times \left\{ R_{\mathbf{k}\mathbf{k}_2\mathbf{k}_3\mathbf{k}_4}^{++++} [n_s(\mathbf{k})n_s(\mathbf{k}_2)\tilde{n}_s(\mathbf{k}_3)\tilde{n}_s(\mathbf{k}_4) - \tilde{n}_s(\mathbf{k})\tilde{n}_s(\mathbf{k}_2)n_s(\mathbf{k}_3)n_s(\mathbf{k}_4)] \right. \\
 & \left. + R_{\mathbf{k},-\mathbf{k}_4,\mathbf{k}_3,-\mathbf{k}_2}^{+-+-} [n_s(\mathbf{k})n_{-s}(-\mathbf{k}_4)\tilde{n}_s(\mathbf{k}_3)\tilde{n}_{-s}(-\mathbf{k}_2) - \tilde{n}_s(\mathbf{k})\tilde{n}_{-s}(-\mathbf{k}_4)n_s(\mathbf{k}_3)n_{-s}(-\mathbf{k}_2)] \right\}
 \end{aligned} \tag{4.24}$$

where in the collision integral all wavevectors $\mathbf{k}_i = k_i \hat{\mathbf{k}}$ are parallel to \mathbf{k} and $k_2 = k_3 + k_4 - k$. Similarly as in the work of Newell and Aucoin (1971) on acoustic turbulence, this new kinetic equation is actually a continuum of uncoupled equations, one for each line along $\pm \hat{\mathbf{k}}$. Whereas the usual quantum kinetic equation holds on a time-scale $\tau_2 = \alpha^2 t$, the singular kinetic equation is valid at logarithmically shorter times. Put another way, for $\tau_1 = O(1)$, $\tau_2 = O(1)$ one finds $t \approx \tau_1/\alpha^2 \ln(1/\alpha) \ll \tau_2/\alpha^2$, when $\ln(1/\alpha) \gg 1$. It is important to note that the singular kinetic equation (4.24) coincides (up to a constant of proportionality) with the result previously derived for electron-hole kinetics in graphene by Kashuba (2008) and Fritz *et al.* (2008), who made a leading-logarithm approximation to the divergent collision integral in the standard quantum Boltzmann equation. However, such a “derivation” of (4.24) is inconsistent, taken literally, because it employs the quantum Boltzmann equation in a regime outside its validity. We discuss further below the derivation of Kashuba (2008) and Fritz *et al.* (2008), which must be consistently understood within a proper field-theoretic framework. Both our derivation and that of Kashuba (2008) and Fritz *et al.* (2008) have also made an *ad hoc* assumption that the Coulomb interaction is dynamically screened at very low waveumbers, in order to eliminate an infrared divergence of the collision integral ², but a proper derivation of this effect requires a more sophisticated many-body theory.

²This divergence due to unscreened Coulomb interaction is simply exhibited in the coordinates used in Fig. 3.10, with $\mathbf{k}_1 = \mathbf{k}$, $\mathbf{k}_2 = \mathbf{p}$, $\mathbf{k}_3 = \mathbf{k} + \mathbf{q}$, $\mathbf{k}_4 = \mathbf{p} - \mathbf{q}$, for which the singular collision integral is with respect to the measure $\sqrt{\frac{p(k+q)(p-q)}{k}} dp dq$ over the range $p > 0$ and $p > q > -k$. Since the $d = 2$ Fourier transform of the $d = 3$ Coulomb potential is $\propto 1/q$, the interaction coefficients $R^{++++}, R^{+-+-} \propto 1/q^2$, leading to an integral over dq/q^2 divergent at $q = 0$.

4.3.2 Properties of the Singular Kinetic Equation

At a time $t = \tau_1/\alpha^2 \ln(1/\alpha)$ with $\tau_1 \gg 1$ (but with $t \ll \tau_2/\alpha^2$), the solutions of the singular kinetic equation should be expected to approach a *local equilibrium* separately along each line in directions $\pm \hat{\mathbf{k}}$. This is what occurs in the singular kinetics for acoustic turbulence (Newell and Aucoin, 1971) and was also argued to occur for electron-hole kinetics in graphene in Kashuba (2008) and Fritz *et al.* (2008).

The local entropy along each ray $\pm \hat{\mathbf{k}}$ is given by

$$S(\hat{\mathbf{k}}) = -k_B \sum_s \int_0^\infty k \, dk [n_s(\mathbf{k}) \ln n_s(\mathbf{k}) + \tilde{n}_s(\mathbf{k}) \ln \tilde{n}_s(\mathbf{k})]. \quad (4.25)$$

By a direct calculation, we have

$$\begin{aligned} dS/d\tau_1 = & -\frac{2k_B}{\pi} \iint_{k_3>0, k_4>0, k_3+k_4>k} dk_3 \, dk_4 \sqrt{k(k_3+k_4-k)k_3k_4} \\ & \times \left\{ R_{\mathbf{k}\mathbf{k}_2\mathbf{k}_3\mathbf{k}_4}^{++++} G(n_s(\mathbf{k})n_s(\mathbf{k}_2)\tilde{n}_s(\mathbf{k}_3)\tilde{n}_s(\mathbf{k}_4), \tilde{n}_s(\mathbf{k})\tilde{n}_s(\mathbf{k}_2)n_s(\mathbf{k}_3)n_s(\mathbf{k}_4)) \right. \\ & \left. + R_{\mathbf{k},-\mathbf{k}_4,\mathbf{k}_3,-\mathbf{k}_2}^{+-+-} G(n_s(\mathbf{k})n_{-s}(-\mathbf{k}_4)\tilde{n}_s(\mathbf{k}_3)\tilde{n}_{-s}(-\mathbf{k}_2), \tilde{n}_s(\mathbf{k})\tilde{n}_{-s}(-\mathbf{k}_4)n_s(\mathbf{k}_3)n_{-s}(-\mathbf{k}_2)) \right\}_{\mathbf{k} \parallel \mathbf{k}_2 \parallel \mathbf{k}_3 \parallel \mathbf{k}_4} \end{aligned} \quad (4.26)$$

with

$$G(x, y) = (x - y) \log \left(\frac{x}{y} \right). \quad (4.27)$$

The H-theorem $dS/d\tau_1 \geq 0$ follows from $G(x, y) \geq 0$. The equality holds if and only if

$$n_s(\mathbf{k})n_s(\mathbf{k}_2)\tilde{n}_s(\mathbf{k}_3)\tilde{n}_s(\mathbf{k}_4) = \tilde{n}_s(\mathbf{k})\tilde{n}_s(\mathbf{k}_2)n_s(\mathbf{k}_3)n_s(\mathbf{k}_4), \quad (4.28)$$

$$n_s(\mathbf{k})n_{-s}(-\mathbf{k}_4)\tilde{n}_s(\mathbf{k}_3)\tilde{n}_{-s}(-\mathbf{k}_2) = \tilde{n}_s(\mathbf{k})\tilde{n}_{-s}(-\mathbf{k}_4)n_s(\mathbf{k}_3)n_{-s}(-\mathbf{k}_2) \quad (4.29)$$

for any $\mathbf{k} \parallel \mathbf{k}_2 \parallel \mathbf{k}_3 \parallel \mathbf{k}_4$ and $k + k_2 = k_3 + k_4$. From eq.(4.28) we have $\log(\tilde{n}_s(\mathbf{k})/n_s(\mathbf{k})) =$

CHAPTER 4. RESONANCE VAN HOVE SINGULARITIES: PHYSICAL CONSEQUENCES

$\beta_s(\hat{\mathbf{k}})k + \mu_s(\hat{\mathbf{k}})$ assuming ψ is continuous³. Plugging this into eq.(4.29), we have $\beta_s(\hat{\mathbf{k}}) = -\beta_{-s}(-\hat{\mathbf{k}})$.

Hence the local equilibria of (4.24) is of a generalized Fermi-Dirac form

$$n_s(\mathbf{k}) = \frac{1}{\exp[(\beta_s(\hat{\mathbf{k}})k + \mu_s(\hat{\mathbf{k}}))] + 1}, \quad s = \pm 1, \quad (4.30)$$

where

$$\beta_s(\hat{\mathbf{k}}) = \beta_o(\hat{\mathbf{k}}) + \beta_e(\hat{\mathbf{k}})s, \quad \mu_s(\hat{\mathbf{k}}) = \mu(\hat{\mathbf{k}}) + \chi(\hat{\mathbf{k}})s$$

are distinct inverse temperatures and chemical potentials, independently specified for each direction $\hat{\mathbf{k}}$ and for electrons ($s = 1$) and holes ($s = -1$), subject to the conditions that $\beta_e(\hat{\mathbf{k}})$ must be even and $\beta_o(\hat{\mathbf{k}})$ odd:

$$\beta_e(-\hat{\mathbf{k}}) = \beta_e(\hat{\mathbf{k}}), \quad \beta_o(-\hat{\mathbf{k}}) = -\beta_o(\hat{\mathbf{k}}). \quad (4.31)$$

Physically, this last restriction arises from the vanishing of the electron-hole contribution to the collision integral in (4.24), whereas the same local Fermi-Dirac distribution (4.30) causes the electron-electron/hole-hole term to vanish without any restriction on parameters. Note that $\beta_o(\hat{\mathbf{k}})$ is the temperature asymmetry between electrons and holes, and $\chi(\hat{\mathbf{k}})$ is the chemical potential asymmetry. If one confines attention to solutions satisfying particle-hole symmetry appropriate to zero doping, $\tilde{n}_{-s}(\mathbf{k}) = n_s(\mathbf{k})$, then the possible equilibria are reduced to

$$n_s(\mathbf{k}) = \frac{1}{\exp[(\beta_e(\hat{\mathbf{k}})k + \chi(\hat{\mathbf{k}})s] + 1]}, \quad s = \pm 1. \quad (4.32)$$

Nonzero values of symmetric chemical potential $\mu(\hat{\mathbf{k}})$ or of temperature asymmetry $\beta_o(\hat{\mathbf{k}})$ explicitly break particle-hole symmetry. The results (4.30),(4.31),(4.32) do not seem to have been given earlier in the literature, although they are implicit in the papers (Kashuba, 2008; Fritz *et al.*, 2008; Müller

³This follows from the fact that if $\psi(x_1) + \psi(x_2) = \psi(x_3) + \psi(x_4)$ for some continuous function ψ and any $x_1 + x_2 = x_3 + x_4$, then $\psi(x)$ is a linear function of x . The proof is standard. We give the details here. Note first $\psi(2x) = 2\psi(x) - \psi(0)$. Then by induction $\psi(nx) = n\psi(x) - (n-1)\psi(0)$. Let $x = \frac{1}{n}$ we have $\psi(1) = n\psi(\frac{1}{n}) - (n-1)\psi(0)$; and thus $\psi(\frac{1}{n}) = \frac{1}{n}\psi(1) + (1 - \frac{1}{n})\psi(0)$. Let $x = \frac{1}{m}$ we have $\psi(\frac{n}{m}) = n\psi(\frac{1}{m}) - (n-1)\psi(0) = \frac{n}{m}\psi(1) + (1 - \frac{n}{m})\psi(0)$. Then for any real x , we can write it as $\lim_{n \rightarrow \infty} x_n$ with x_n rational. Therefore by continuity of ψ we have $\psi(x) = \lim_{n \rightarrow \infty} x_n\psi(1) + (1 - x_n)\psi(0) = x\psi(1) + (1 - x)\psi(0)$.

CHAPTER 4. RESONANCE VAN HOVE SINGULARITIES: PHYSICAL CONSEQUENCES

et al., 2009) on dissipative transport by electrons in graphene. These local equilibrium solutions are not only stationary solutions of (4.24) but in fact should be global attractors.

Until now our discussion has been quite parallel to the case of acoustic turbulence (Newell and Aucoin, 1971), but we now encounter a difference, because the critical set which dominates the singular kinetic equation (4.24) is not the entire resonant manifold for electrons in graphene, unlike the situation for acoustic waves. Thus, there are additional secular terms $\propto \alpha^2 t$ in eq.(4.9) which arise from integration over the remainder of the resonant manifold. To remove those secularities, one should impose an additional dependence upon the time variable τ_2 , equivalent to the condition that n_s satisfies the ordinary quantum Boltzmann equation on time-scales $\tau_2 = O(1)$, or that $dn_s(\mathbf{k})/d\tau_2 = C_{ks}(n)$ with the collision integral in (3.25). This collision integral diverges for general distributions $n_s(\mathbf{k})$, but it is finite for local Fermi-Dirac distributions of the form (4.30). To see this, again using polar coordinates $k = k(\cos\theta, \sin\theta)$ with fixed direction angle θ of wavevector \mathbf{k} and $\mathbf{k}_i = k_i(\cos(\theta + \theta_i), \sin(\theta + \theta_i))$ for $i = 2, 3, 4$, we write the kinetic equation as

$$\begin{aligned} \partial_{\tau_2} n_s(\mathbf{k}, \tau_2) = & -\frac{1}{4\pi} \int_0^\infty k_3 dk_3 \int_0^\infty k_4 dk_4 \int_{-\pi}^\pi d\theta_3 \int_{-\pi}^\pi d\theta_4 \delta(k + k_2 - k_3 - k_4) \\ & \times \left\{ R_{\mathbf{k}\mathbf{k}_2\mathbf{k}_3\mathbf{k}_4}^{++++} [n_s(\mathbf{k})n_s(\mathbf{k}_2)\tilde{n}_s(\mathbf{k}_3)\tilde{n}_s(\mathbf{k}_4) \right. \\ & \quad \left. - \tilde{n}_s(\mathbf{k})\tilde{n}_s(\mathbf{k}_2)n_s(\mathbf{k}_3)n_s(\mathbf{k}_4)] \right. \\ & \quad \left. + R_{\mathbf{k},-\mathbf{k}_4,\mathbf{k}_3,-\mathbf{k}_2}^{+-+-} [n_s(\mathbf{k})n_{-s}(-\mathbf{k}_4)\tilde{n}_s(\mathbf{k}_3)\tilde{n}_{-s}(-\mathbf{k}_2) \right. \\ & \quad \left. - \tilde{n}_s(\mathbf{k})\tilde{n}_{-s}(-\mathbf{k}_4)n_s(\mathbf{k}_3)n_{-s}(-\mathbf{k}_2)] \right\}_{\mathbf{k}_2=\mathbf{k}_3+\mathbf{k}_4-\mathbf{k}}. \end{aligned} \quad (4.33)$$

On the one hand, the phase measure has a logarithmic divergence that comes from $\delta(k_1 + k_2 - k_3 - k_4)$.

Note for $\theta_3, \theta_4 \approx 0$

$$\begin{aligned} & k + |\mathbf{k}_3 + \mathbf{k}_4 - \mathbf{k}| - k_3 - k_4 \\ = & k + [k_3^2 + k_4^2 + k^2 - 2\mathbf{k} \cdot \mathbf{k}_3 - 2\mathbf{k} \cdot \mathbf{k}_4 + 2\mathbf{k}_3 \cdot \mathbf{k}_4]^{1/2} - k_3 - k_4 \\ = & k - k_3 - k_4 \end{aligned}$$

CHAPTER 4. RESONANCE VAN HOVE SINGULARITIES: PHYSICAL CONSEQUENCES

$$\begin{aligned}
 & + [(k_3 + k_4 - k)^2 + 2kk_3(1 - \cos \theta_3) + 2kk_4(1 - \cos \theta_4) + 2k_3k_4(\cos(\theta_3 - \theta_4) - 1)]^{1/2} \\
 \approx & \frac{kk_4\theta_4^2 + kk_3\theta_3^2 - k_3k_4(\theta_3 - \theta_4)^2}{2(k_3 + k_4 - k)} = \frac{(k - k_4)k_3}{2(k_3 + k_4 - k)}(\theta_3 - \zeta_1\theta_4)(\theta_3 - \zeta_2\theta_4),
 \end{aligned} \tag{4.34}$$

where

$$\zeta_{1,2} = \frac{-k_3k_4 \pm \sqrt{k(k_3 + k_4 - k)k_3k_4}}{(k - k_4)k_3}. \tag{4.35}$$

Hence the collision integral near $\theta_3 = \theta_4 = 0$ is given by

$$\begin{aligned}
 & \int k_3 \, dk_3 \int k_4 \, dk_4 \int d\theta_3 \int d\theta_4 \, \delta(k + k_2 - k_3 - k_4) (M^{++++}(\theta_3, \theta_4) + M^{+-+-}(\theta_3, \theta_4)) \\
 = & \int dk_3 \int dk_4 \sqrt{\frac{(k_3 + k_4 - k)k_3k_4}{k}} \int \frac{d\theta_4}{\theta_4} \left[M^{++++}(\theta_3 = \zeta_1\theta_4, \theta_4) + M^{++++}(\theta_3 = \zeta_2\theta_4, \theta_4) \right. \\
 & \left. + M^{+-+-}(\theta_3 = \zeta_1\theta_4, \theta_4) + M^{+-+-}(\theta_3 = \zeta_2\theta_4, \theta_4) \right].
 \end{aligned} \tag{4.36}$$

On the other hand, assume parameters $\beta_s(\hat{\mathbf{k}}), \mu_s(\hat{\mathbf{k}})$ are C^1 , then M^{++++}, M^{+-+-} are $O(\theta_4)$ and thus fortuitously suppressed the singularity. To see this, note

$$\begin{aligned}
 & n_s(\mathbf{k})n_s(\mathbf{k}_2)\tilde{n}_s(\mathbf{k}_3)\tilde{n}_s(\mathbf{k}_4) - \tilde{n}_s(\mathbf{k})\tilde{n}_s(\mathbf{k}_2)n_s(\mathbf{k}_3)n_s(\mathbf{k}_4) \\
 = & n_s(\mathbf{k})n_s(\mathbf{k}_2)\tilde{n}_s(\mathbf{k}_3)\tilde{n}_s(\mathbf{k}_4) \left[1 - \exp(\beta_s(\hat{\mathbf{k}})k + \beta_s(\hat{\mathbf{k}}_2)k_2 - \beta_s(\hat{\mathbf{k}}_3)k_3 - \beta_s(\hat{\mathbf{k}}_4)k_4) \right. \\
 & \left. \times \exp(\mu_s(\hat{\mathbf{k}}) + \mu_s(\hat{\mathbf{k}}_2) - \mu_s(\hat{\mathbf{k}}_3) - \mu_s(\hat{\mathbf{k}}_4)) \right],
 \end{aligned} \tag{4.37}$$

and

$$\begin{aligned}
 & n_s(\mathbf{k})n_{-s}(-\mathbf{k}_4)\tilde{n}_s(\mathbf{k}_3)\tilde{n}_{-s}(-\mathbf{k}_2) - \tilde{n}_s(\mathbf{k})\tilde{n}_{-s}(-\mathbf{k}_4)n_s(\mathbf{k}_3)n_{-s}(-\mathbf{k}_2) \\
 = & n_s(\mathbf{k})n_{-s}(-\mathbf{k}_4)\tilde{n}_s(\mathbf{k}_3)\tilde{n}_{-s}(-\mathbf{k}_2) \left[1 - \exp(\beta_s(\hat{\mathbf{k}})k + \beta_{-s}(-\hat{\mathbf{k}}_4)k_4 - \beta_s(\hat{\mathbf{k}}_3)k_3 - \beta_{-s}(-\hat{\mathbf{k}}_2)k_2) \right. \\
 & \left. \times \exp(\mu_s(\hat{\mathbf{k}}) + \mu_{-s}(-\hat{\mathbf{k}}_4) - \mu_s(\hat{\mathbf{k}}_3) - \mu_{-s}(-\hat{\mathbf{k}}_2)) \right]
 \end{aligned} \tag{4.38}$$

are $O(\theta_4)$ since $\theta_2 = O(\theta_3) + O(\theta_4)$ ⁴ for small θ_3 and θ_4 .

⁴From $\mathbf{k} + \mathbf{k}_2 = \mathbf{k}_3 + \mathbf{k}_4$ we have $(k + k_2)^2 + 2kk_2(\cos \theta_2 - 1) = (k_3 + k_4)^2 + 2k_3k_4(\cos^2(\theta_3 - \theta_4) - 1)$. Using the resonance condition $k + k_2 = k_3 + k_4$, we have $\theta_2 \sim \pm \sqrt{k_3k_4/kk_2}(\theta_3 - \theta_4)$.

CHAPTER 4. RESONANCE VAN HOVE SINGULARITIES: PHYSICAL CONSEQUENCES

A simple picture thus arises for electron kinetics in graphene as a *three time-scale problem*.

At the shortest times $t = \tau_0$ of order the linear wave period, the dynamics is dominated by the free part of the Hamiltonian, whose dispersive character drives the system into a locally quasi-free state completely characterized by the occupation numbers $n_s(\mathbf{k})$. Cf. the discussion in Spohn (2006), section 9. At times $t = \tau_1/\alpha^2 \ln(1/\alpha) \gg \tau_0$ the occupation numbers evolve further into the local Fermi-Dirac form (4.30), completely characterized by the local thermodynamic parameters $\beta_o(\hat{\mathbf{k}}), \beta_e(\hat{\mathbf{k}}), \mu(\hat{\mathbf{k}}), \chi(\hat{\mathbf{k}})$ along each wavevector direction. Finally, at times $t = \tau_2/\alpha^2 \gg \tau_1/\alpha^2 \ln(1/\alpha)$ the distribution further relaxes according to the standard quantum Boltzmann equation. Because the ratio of times t with $\tau_2 = O(1)$ and $\tau_1 = O(1)$ is only logarithmically large, it is possible that the occupation numbers will not fully relax to a local Fermi-Dirac form (4.30) for times $\tau_2 = O(1)$ and there may be corrections of order $1/\ln(1/\alpha)$. If there is no external driving or boundary conditions to keep the system in a dissipative non-equilibrium state, the subsequent evolution by the standard quantum Boltzmann equation will relax the system at times $\tau_2 \gg 1$ to a global Fermi-Dirac equilibrium

$$n_s(\mathbf{k}) = \frac{1}{\exp(\beta s k + \mu) + 1}, \quad s = \pm 1,$$

with uniform values of inverse temperature β and chemical potential μ .

So far we have discussed electron kinetics in graphene from the multi-time perturbation theory viewpoint developed by Newell and Aucoin (1971) to describe semi-dispersive acoustic turbulence. There is however another point of view on singular kinetics for acoustic waves which was developed by L'vov *et al.* (1997), based on a Martin-Siggia-Rose field-theoretic formulation. In this approach, the starting point is a set of Schwinger-Dyson integrodifferential equations, which are exact and non-perturbative but non-closed. By a set of rational approximations based on weak non-linearity and self-consistency, L'vov *et al.* (1997) showed that the Schwinger-Dyson equations for acoustic wave turbulence can be simplified to a *generalized kinetic equation*. This has a form

CHAPTER 4. RESONANCE VAN HOVE SINGULARITIES: PHYSICAL CONSEQUENCES

similar to the standard 3-wave kinetic equation

$$\begin{aligned} \partial_\tau n(\mathbf{k}, t) = & 36\pi \sum_{\underline{s}=(-1, s_2, s_3)} \int d^d k_2 \int d^d k_3 |H_{\underline{\mathbf{k}}}^{\underline{s}}|^2 \delta_{\Gamma(\underline{\mathbf{k}})}(\underline{s} \cdot \omega(\underline{\mathbf{k}})) \delta^d(\underline{s} \cdot \underline{\mathbf{k}}) \\ & \times \left\{ n(\mathbf{k}_2)n(\mathbf{k}_3) - s_2 n(\mathbf{k})n(\mathbf{k}_3) - s_3 n(\mathbf{k})n(\mathbf{k}_2) \right\}. \end{aligned} \quad (4.39)$$

but with $\delta_{\Gamma(\underline{\mathbf{k}})}(\omega)$ a resonance-broadened delta-function or Lorentzian of the form (4.4), where

$$\Gamma(\underline{\mathbf{k}}) = \gamma(\mathbf{k}) + \gamma(\mathbf{k}_2) + \gamma(\mathbf{k}_3)$$

is a triad-interaction decay rate. The individual rate $\gamma(\mathbf{k})$ is given by the imaginary part of the self-energy function $\Sigma(\mathbf{k})$, so that it must be determined self-consistently in terms of the solution $n(\mathbf{k})$ of the generalized kinetic equation and is $O(\epsilon^2)$ in the nonlinear interaction strength ϵ . See eq.(B13) of L’vov *et al.* (1997). The collision integral of this generalized kinetic equation remains finite and free of any divergences due to the Van Hove-type singularities in the “manifold” of exact resonances for acoustic waves.

This field-theoretic point of view is very closely related to the previous derivations of the quantum Boltzmann equation for electron kinetics in graphene (Kashuba, 2008; Fritz *et al.*, 2008), which were based on a nonequilibrium Schwinger-Keldysh field-theory approach (the quantum analogue of the Martin-Siggia-Rose field-theory for classical dynamics). In fact, Kashuba (2008) and Fritz *et al.* (2008) assumed that self-energy corrections will cut off the divergence of the standard collision integral due to the resonance Van Hove singularity, but without assuming an explicit form for these corrections. It is likely that the self-consistent approach of L’vov *et al.* (1997) can be carried over to electron kinetics in graphene, e.g. with a wavevector-dependent broadening corresponding to a quartet-interaction time

$$\Gamma(\underline{\mathbf{k}}) = \gamma(\mathbf{k}) + \gamma(\mathbf{k}_2) + \gamma(\mathbf{k}_3) + \gamma(\mathbf{k}_4).$$

CHAPTER 4. RESONANCE VAN HOVE SINGULARITIES: PHYSICAL CONSEQUENCES

As discussed in section 3.3.3, such a broadening should cure the logarithmic divergence, if the resonance width is non-zero in the vicinity of the critical set. There is considerable interest in investigating explicit self-energy regularizations, since it has been estimated that corrections to the leading-logarithm approximation may make a 30% change to the electrical conductivity of defectless graphene at experimentally realizable temperatures (Kashuba, 2008). In addition to the interest for potential electronic applications of graphene, such a study would also help to assess the validity of theoretical approximations for acoustic turbulence which, to our knowledge, have never been subjected to experimental test. More generally, electron kinetics in graphene is a problem which should illuminate the subject of singular wave kinetics, with applications to a wide variety of systems.

4.4 Conclusion

The effects of the singularities on the kinetic theory can range from none at all, to moderate, to quite destructive. As a general rule of thumb, the singularities are more threatening in low dimensions ($d = 1, 2$). For example, the non-degenerate critical points for the gravity-capillary wave system in $d = 1$ illustrated in Fig. 3.8 produce a logarithmic divergence in the phase measure, whereas the same system for the physical dimension $d = 2$ has a locally finite phase measure near the critical points. Likewise, the singularities will generally be less important for N -wave resonances with N large, since what matters is the size of the phase-space dimension $D = (N - 2)d$. The cautionary remark to these general rules of thumb is that degeneracy degree $\delta > 0$ can lead to a stronger singularity at the critical set, and this may result in a divergence even when D is larger than 2. This is what occurs in the cases of three-dimensional inertial-waves and electron-hole excitations in two-dimensional graphene, for example.

With the general results in section 4.2, we are now ready to collect our case studies in Table 4.1. The table shows space dimension d , order of resonance N , geometry of the critical set, degree of degeneracy δ , effective dimensionality $D' = d(N - 2) - \delta$ of the phase space, local finiteness

CHAPTER 4. RESONANCE VAN HOVE SINGULARITIES: PHYSICAL CONSEQUENCES

of the phase measure at the singularity (if any), and divergence or not of the standard collision integral. Note that we consider only genuine critical points, not pseudo-critical points (which are usually harmless). When the critical set is empty, we take $\delta = 0$ in the definition of D' . If the phase measure is locally infinite near the singularity, we indicate the nature of the divergence. The diligent reader will recognize that the table is a simplification of the discussion in the text and glosses over some of the finer points. (For example, a degenerate critical point with $\delta = 1$ is possible for gravity-capillary waves at the inflection point of the dispersion relation when $k = k_*$.) Nevertheless, the results presented in the table support the general lessons educed above. In particular, there tend to be serious consequences for the standard kinetic description when the critical set is non-empty and $D' \leq 2$. In such cases, closer examination of the problem is warranted, to see whether there are any ameliorating circumstances (vanishing interaction coefficients, cancellations in the collision integral, etc.) or whether the standard kinetic equation indeed breaks down. Resonance Van Hove singularities and their potential effects should be generally recognized as a possibility in wave kinetics.

Table 4.1: Summary

Wave system	d	N	critical set	δ	D'	phase measure	collision integral
Isotropic power-law, $\alpha > 1$	≥ 2	3	\emptyset	$-$	d	finite	finite
Acoustic waves	3	3	line	1	2	ill-defined	divergent
Rossby/drift waves	2	3	point	0	2	log-divergent	finite
Inertial waves	3	3	line	1	2	log-divergent	divergent
Internal gravity waves	3	3	\emptyset	$-$	3	finite	finite
Surface gravity waves	2	4	\emptyset	$-$	4	finite	finite
Surface gravity-capillary waves	2	4	point	0	4	finite	finite
Light waves in optical fiber	1	4	point	1	1	linear divergent	finite (but large)
Electrons & holes in graphene	2	4	surface	2	2	log-divergent	divergent

Chapter 5

Conclusion

We have found that the equation (2.2) originally obtained by Peierls (1929) and many subsequent authors (Brout and Prigogine, 1956; Zaslavskii and Sagdeev, 1967; Choi *et al.*, 2005a,b; Jakobsen and Newell, 2004) is not the leading-order, asymptotically valid equation in the wave-kinetic limit. The Peierls equation contains additional terms which vanish as $L \rightarrow \infty$ and which do not appear in our limit equations. It should be stressed that the derivation of the Peierls equation in Choi *et al.* (2005a,b) and Jakobsen and Newell (2004) and also earlier derivations of Peierls (1929), Brout and Prigogine (1956), Zaslavskii and Sagdeev (1967), etc. are *not* systematic in the limit $L \rightarrow \infty$. At present, the Peierls equation has no established validity (or even a precise meaning) in the large-volume limit. Although the Peierls equation does not have any obvious asymptotic validity, it does serve as a “generating equation”¹ from which all of our simpler equations can be obtained in the limit $L \rightarrow \infty$. The virtue of our new equations (2.54) and (2.65) is that they contain all and only the leading-order terms and thus allow us to clarify the structure of that limit. We have completely characterized the solutions of the limiting hierarchies and shown them to consist of random ensembles of solutions of the wave-kinetic equation (2.59) and 1-mode PDF equation (2.72). This should permit a better evaluation of the theory by simulation and experiment. In particular, our most subversive

¹This terminology was suggested to us by S. Nazarenko (private communication).

CHAPTER 5. CONCLUSION

conclusion is that the “mean-field” scaling of the Kolmogorov-Zakharov solutions may not be the true prediction of kinetic theory for scaling exponents of spectra and higher-order statistics in wave turbulence and that wave kinetics may instead allow for intermittency and anomalous scaling.

Our work solves the problem posed in Newell and Rumpf (2011, section 5.2.5) on the continuum limit of wave turbulence to show “how the natural closure arises in taking the limit $L \rightarrow \infty$ ”. Although we only derived the multi-mode hierarchy equations for 3-wave resonant models, we expect that analogous results should hold also for other closely related wave systems, e.g. those whose first nontrivial resonances are 4-wave. A natural generalization of our derivation is to consider the Wigner function, which, unlike the spectrum, has spatial dependence. See Appendix E for detailed definitions. The Wigner function $W(\mathbf{k}, \boldsymbol{\xi}, t)$ is expected to satisfy the generalized wave-kinetic equation

$$\begin{aligned} & \partial_t W(\mathbf{k}, \boldsymbol{\xi}, t) - \frac{1}{L} \nabla_{\mathbf{k}} \omega(\mathbf{k}, \boldsymbol{\xi}) \cdot \nabla_{\boldsymbol{\xi}} W(\mathbf{k}, \boldsymbol{\xi}, t) + \frac{1}{L} \nabla_{\boldsymbol{\xi}} \omega(\mathbf{k}, \boldsymbol{\xi}) \cdot \nabla_{\mathbf{k}} W(\mathbf{k}, \boldsymbol{\xi}, \tau) \\ = & 36\pi\epsilon^2 \sum_{\sigma=(-1, \sigma_2, \sigma_3)} \int_{(\Lambda^*)^2} d^d \bar{k}_2 d^d \bar{k}_3 |H_{\underline{\mathbf{k}}}^{\sigma}|^2 \delta(\underline{\sigma} \cdot \omega(\underline{\mathbf{k}})) \delta_{\Lambda^*}(\underline{\sigma} \cdot \underline{\mathbf{k}}) \\ & \times \left\{ W(\bar{\mathbf{k}}_2, \boldsymbol{\xi}, t) W(\bar{\mathbf{k}}_3, \boldsymbol{\xi}, t) - \sigma_2 W(\mathbf{k}, \boldsymbol{\xi}, t) W(\bar{\mathbf{k}}_3, \boldsymbol{\xi}, t) - \sigma_3 W(\mathbf{k}, \boldsymbol{\xi}, t) W(\bar{\mathbf{k}}_2, \boldsymbol{\xi}, t) \right\}. \end{aligned} \quad (5.1)$$

See Spohn (2006) and Newell *et al.* (2012). For the wave-kinetic hierarchy, it is expected that the following equations hold for the n -point Wigner function (defined in Appendix E)

$$\begin{aligned} & \partial_t W^{(n)}(\mathbf{k}_1, \boldsymbol{\xi}_1, \dots, \mathbf{k}_n, \boldsymbol{\xi}_n) - \frac{1}{L} \sum_{j=1}^n \left[\nabla_{\mathbf{k}_j} \omega(\mathbf{k}_j, \boldsymbol{\xi}_j) \cdot \nabla_{\boldsymbol{\xi}_j} W^{(n)}(\mathbf{k}_1, \boldsymbol{\xi}_1, \dots, \mathbf{k}_n, \boldsymbol{\xi}_n, t) \right. \\ & \quad \left. - \nabla_{\boldsymbol{\xi}_j} \omega(\mathbf{k}_j, \boldsymbol{\xi}_j) \cdot \nabla_{\mathbf{k}_j} W^{(n)}(\mathbf{k}_1, \boldsymbol{\xi}_1, \dots, \mathbf{k}_n, \boldsymbol{\xi}_n, t) \right] \\ = & 36\pi\epsilon^2 \sum_{j=1}^n \sum_{\sigma=(-1, \sigma_2, \sigma_3)} \int d^d \bar{k}_2 \int d^d \bar{k}_3 \delta^d(\underline{\sigma} \cdot \underline{\mathbf{k}}_j) \delta(\underline{\sigma} \cdot \omega(\underline{\mathbf{k}}_j)) |H_{\underline{\mathbf{k}}_j}^{\sigma}|^2 \\ & \times \left[W^{(n+1)}(\mathbf{k}_1, \boldsymbol{\xi}_1, \dots, \mathbf{k}_{j-1}, \boldsymbol{\xi}_{j-1}, \mathbf{k}_{j+1}, \boldsymbol{\xi}_{j+1}, \dots, \mathbf{k}_n, \boldsymbol{\xi}_n, \bar{\mathbf{k}}_2, \boldsymbol{\xi}_j, \bar{\mathbf{k}}_3, \boldsymbol{\xi}_j, t) \right. \\ & \quad \left. - \sigma_3 W^{(n+1)}(\mathbf{k}_1, \boldsymbol{\xi}_1, \dots, \mathbf{k}_n, \boldsymbol{\xi}_n, \bar{\mathbf{k}}_2, \boldsymbol{\xi}_j, t) - \sigma_2 W^{(n+1)}(\mathbf{k}_1, \boldsymbol{\xi}_1, \dots, \mathbf{k}_n, \boldsymbol{\xi}_n, \bar{\mathbf{k}}_3, \boldsymbol{\xi}_j, t) \right]. \end{aligned} \quad (5.2)$$

CHAPTER 5. CONCLUSION

There are physical situations where one has to consider these generalized equations. For example, the dispersion relation may have a spatial dependence due to boundary conditions. Long (1973) considered the shallow-water surface gravity waves where the bottom topography is varying in space. Another case is when the solutions of the kinetic equation are unstable to spatially inhomogeneous perturbations as found by Newell *et al.* (2012) for the MMT model (Majda *et al.*, 1997). Spohn (2006) derived the generalized wave-kinetic equation assuming a Gaussian ensemble of waves with a slow variation of covariance in physical space. However, this derivation does not start in finite volume, like most other works in the literature (see also Marcià (2004), Mielke (2006), and Lukkarinen and Spohn (2007)). To fill this gap in the literature, we discuss in Appendix E the definition and the properties of the Wigner function, both in finite-volume and in the infinite-volume limit. As a first step to understand how the generalized wave-kinetic equation arises in the infinite-volume limit, particularly for systems with a spatial-dependent dispersion relation (note the derivation of Spohn (2006) considers only dispersion relation with no spatial dependence), we present in Appendix F a formal derivation of the linear transport equation for the Wigner function and discuss conditions for the generalized wave-kinetic equation to be valid.

It is perhaps important to emphasize that we have not provided a rigorous mathematical proof of wave-kinetic theory. At this time, no set of sufficient conditions are known that would imply the validity of wave kinetics for any general class of systems (Newell and Rumpf, 2011, section 5.2.6). Our derivations fail to constitute a proof in particular because we have made no attempt to rigorously bound the $O(\epsilon^3)$ remainder term and higher order terms in the perturbation expansion (2.41). In principle, there exist methods to calculate the collision integral in the wave-kinetic equation formally to any order in the small parameter ϵ (Benney and Newell, 1969, 1967; Erofeev and Malkin, 1989). As a matter of fact, there are reasons to expect that the collision integral is non-analytic in ϵ , if the kinetic theory of gases is any guide. The multi-scale asymptotic formalism devised by Bogolyubov (1946) to calculate systematic corrections to the Boltzmann equation in powers of gas density is closely analogous to the methods employed to derive the wave-kinetic equation perturbatively in ϵ .

CHAPTER 5. CONCLUSION

However, it was discovered in the mid-1960's that the 4th- and higher-order terms in Bogolyubov's density expansion of the collision operator for gases are divergent and the true dependence appears to be non-analytic in density (Cohen, 1993). Even for gas kinetics, many fundamental issues regarding higher-order corrections remain unresolved. The rigorous works of Lanford (1975, 1976) imply that these higher-order terms are asymptotically negligible in the low-density limit for gases, but only for one-third of a mean-free time. Similar mathematical study of wave kinetics is only just begun.

As we have seen in the second part of this dissertation, there is one more complication in wave-kinetic theory – the phase measure. It is for this reason that it is not trivial to even establish the local-in-time well-posedness of the wave-kinetic hierarchies, which is the one missing piece to make rigorous our arguments in Chap. 2 on the property “propagation of chaos”. For this proof, one may wish to refer to a similar problem studied by Lanford in the kinetic theory of gases. The landmark work of Lanford (1975, 1976) laid down the fundamental ideas to rigorously derive the Boltzmann equation as the Boltzmann-Grad limit of systems of Newtonian particles with a short-range potential. We refer the readers to Gallagher *et al.* (2013) for a recent review, which also filled in the detailed rigorous study of pathological trajectories that involves recollisions. However, Lanford's construction of function spaces for solutions of the Boltzmann hierarchy involves L^∞ -norm and cannot naively carry over to the case of the wave-kinetic hierarchies. The reason is that the phase measure in the Boltzmann equation is absolutely continuous with respect to the Lebesgue measure, whereas for the wave-kinetic equations, the phase measure is generally singularly supported on the resonant manifold (a lower dimensional set with zero Lebesgue measure).

We did, however, construct the phase measure in the collision integral for many physically relevant dispersion relations, which an earlier construction by Lukkarinen and Spohn (2007) did not achieve. Our construction exhibits directly the importance of the resonance Van Hove singularities and allows us to develop some rather general results on the local finiteness of the phase measure. While we have developed no comprehensive theory for existence of resonance Van Hove singularities, the examples presented in Chap. 3 indicate that they occur rather commonly. Their presence may

CHAPTER 5. CONCLUSION

be due to disparate causes, including periodicity of Fourier space, anisotropy of the wave dispersion relation, or intersection of the trivial and non-trivial parts of the resonant manifold for 4-wave resonances. The basic requirement for such critical points is that there are distinct wavevectors with the same group velocity, which is facilitated by dispersion laws with segments strictly linear in wavenumber or with inflection points. Our examples have presumably not exhausted the possible mechanisms to produce such resonance singularities but they already demonstrate the varying effects of resonance Van Hove singularities.

Perhaps the most dramatic consequence of the resonance Van Hove singularities is exhibited in electron-hole systems in graphene. The logarithmic divergence in the standard quantum Boltzmann equation actually leads to a different scaling in the multi-scale perturbation analysis. As a result, the typical two time-scale process in wave-kinetic theory becomes a three time-scale process. The transient states governed by the singular kinetic equation should be relatively short-lived since the difference in two time-scales are only logarithmic. They serve to prepare the initial condition of the standard quantum Boltzmann equation to be the generalized Fermi-Dirac distribution so that it may suppress the divergence that comes from the resonance Van Hove singularity. It is interesting whether these transient states can be maintained with suitable forcings to result in a different electrical conductivity as predicted from the leading-logarithmic approximation of the quantum Boltzmann equation by Kashuba (2008) and Fritz *et al.* (2008). Another prospect study is to carry over the Schwinger-Keldysh field-theoretic approach of L'vov *et al.* (1997), who studied the problem of acoustic wave turbulence, to electron kinetics in graphene. It is then of considerable interest to see whether the explicit self-energy regularizations can account for the corrections to the leading-logarithm approximation of electrical conductivity of defectless graphene at experimentally realizable temperatures, which is estimated by Kashuba (2008) to be about 30%. Such a study would in turn help to assess the validity of theoretical approximations for acoustic wave turbulence.

Appendix A

Derivation of the Spectral Hierarchy

As discussed in the text, we have verified the results of Choi *et al.* (2005a) for the \mathcal{J} -terms in eqs.(2.42)-(2.49), up to minor corrections. The contributions to the spectral generating functional are obtained by making the substitutions $J_i = (2\pi/L)^d \tilde{J}_i$ and $\lambda_1 = i\lambda(\mathbf{k}_1)$ and taking the limit $L \rightarrow \infty$. The asymptotics of the various terms can be summarized in the following general rule: each action variable J changes the order by L^{-d} and each free sum over wavevectors by L^d . We illustrate this rule in our detailed calculations below.

Calculation of \mathcal{J}_1 : Substituting the definition (D.5) of $a_1^{(1)}$, one obtains

$$\mathcal{J}_1 = \sum_{1,2,3} \left(\lambda_1 + \frac{\mu_1}{2J_1} \right) L_{\mathbf{k}_1, \mathbf{k}_2, \mathbf{k}_3}^{+, \sigma_2, \sigma_3} \sqrt{J_1 J_2 J_3} \left\langle \psi_1^{-1} \psi_2^{\sigma_2} \psi_3^{\sigma_3} \prod_{\mathbf{k}} \psi_{\mathbf{k}}^{\mu_{\mathbf{k}}} \right\rangle_{\psi} \Delta_T(\sigma_2 \omega_2 + \sigma_3 \omega_3 - \omega_1) \delta_{\mathbf{k}_1, \sigma_2 \mathbf{k}_2 + \sigma_3 \mathbf{k}_3},$$

which has the following diagram pre-phase-averaged; see Fig. A.1. After phase averaging, there are two contributions represented by the diagrams in Fig. A.2, or explicitly written as

APPENDIX A. DERIVATION OF THE SPECTRAL HIERARCHY

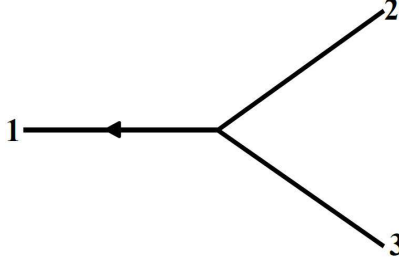


Figure A.1: Terms in \mathcal{J}_1 before phase averaging.

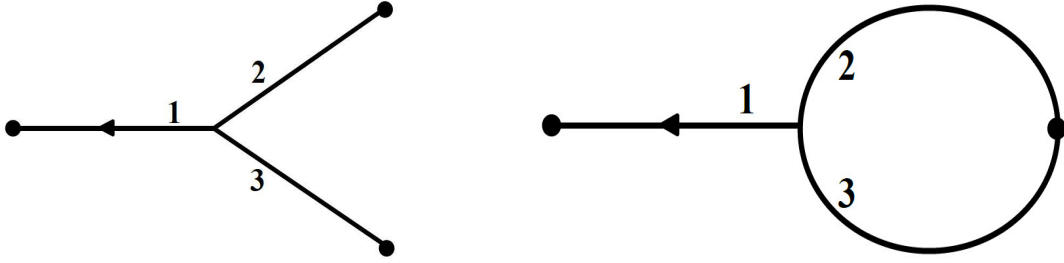


Figure A.2: Contributions in \mathcal{J}_1 after phase averaging.

$$\begin{aligned}
 \mathcal{J}_1 = & \sum'_{1,2,3} \left(\lambda_1 + \frac{\mu_1}{2J_1} \right) L_{\mathbf{k}_1, \mathbf{k}_2, \mathbf{k}_3}^{+, \sigma_2, \sigma_3} \sqrt{J_1 J_2 J_3} \Delta_T (\sigma_2 \omega_2 + \sigma_3 \omega_3 - \omega_1) \delta_{\mathbf{k}_1, \sigma_2 \mathbf{k}_2 + \sigma_3 \mathbf{k}_3} \\
 & \times \delta_{\mu_1, 1} \delta_{\mu_2, -\sigma_2} \delta_{\mu_3, -\sigma_3} \prod_{m \neq 1, 2, 3} \delta_{\mu_m, 0} \\
 & + \sum'_{1,2} \left(\lambda_1 + \frac{\mu_1}{2J_1} \right) L_{\mathbf{k}_1, \mathbf{k}_2, \mathbf{k}_2}^{+, \sigma_2, \sigma_2} \sqrt{J_1 J_2} \Delta_T (2\sigma_2 \omega_2 - \omega_1) \delta_{\mathbf{k}_1, 2\sigma_2 \mathbf{k}_2} \\
 & \times \delta_{\mu_1, 1} \delta_{\mu_2, -2\sigma_2} \prod_{m \neq 1, 2} \delta_{\mu_m, 0}. \tag{A.1}
 \end{aligned}$$

Note that a prime $'$ on a sum indicates that all wavevectors must be distinct. Here all of the summations are “pinned.” Now making the substitutions $J_i = (2\pi/L)^d \tilde{J}_i$ and $\lambda_1 = i\lambda(\mathbf{k}_1)$ into the above and taking the limit $L \rightarrow \infty$ gives

$$\begin{aligned}
 \mathcal{J}_1 = & \frac{1}{2} \left(\frac{2\pi}{L} \right)^{d/2} \sum_{\underline{\sigma} = (-1, \sigma_2, \sigma_3)} \sum_{\underline{\mathbf{k}}} \sum' L_{\mathbf{k}_1, \mathbf{k}_2, \mathbf{k}_3}^{+, \sigma_2, \sigma_3} \sqrt{\frac{\tilde{J}_2 \tilde{J}_3}{\tilde{J}_1}} \Delta_T (\underline{\sigma} \cdot \omega(\underline{\mathbf{k}})) \delta_{\underline{\sigma} \cdot \underline{\mathbf{k}}, 0} \delta_{\underline{\mu}, -\underline{\sigma}} \prod_{m \neq 1, 2, 3} \delta_{\mu_m, 0} \\
 & + \frac{1}{2} \left(\frac{2\pi}{L} \right)^{d/2} \sum_{\underline{\sigma} = (-1, 2\sigma_2)} \sum_{\underline{\mathbf{k}}'} \sum' L_{\mathbf{k}_1, \mathbf{k}_2, \mathbf{k}_2}^{+, \sigma_2, \sigma_2} \frac{\tilde{J}_2}{\sqrt{\tilde{J}_1}} \Delta_T (\underline{\sigma} \cdot \omega(\underline{\mathbf{k}}')) \delta_{\underline{\sigma} \cdot \underline{\mathbf{k}}', 0} \delta_{\underline{\mu}', -\underline{\sigma}} \prod_{m \neq 1, 2} \delta_{\mu_m, 0}, \tag{A.2}
 \end{aligned}$$

where $\underline{\mu}' = (\mu_1, \mu_2)$ and $\underline{\mathbf{k}}' = (\mathbf{k}_1, \mathbf{k}_2)$. Hence \mathcal{J}_1 is $O(L^{-d/2})$ in the large box limit. In fact, the result easily follows from the aforementioned asymptotic rules. The amplitude factor $\sqrt{J_1 J_2 J_3}$ changes the

APPENDIX A. DERIVATION OF THE SPECTRAL HIERARCHY

order of \mathcal{J}_1 by $L^{-3d/2}$. Since there is no free sum here, the contribution of the term proportional to λ_1 is at most $O(L^{-3d/2})$. The term proportional to μ_1 introduces an additional action variable $1/J_1$ and thus gives the leading contribution $O(L^{-d/2})$.

Calculation of \mathcal{J}_2 : Again substituting the definition (2.38) of $a_1^{(1)}$, one obtains

$$\mathcal{J}_2 = \frac{1}{2} \sum_{1,2,3,4,5} \left(\lambda_1 + \lambda_1^2 J_1 - \frac{\mu_1^2}{4J_1} \right) L_{\mathbf{k}_1, \mathbf{k}_2, \mathbf{k}_3}^{+, \sigma_2, \sigma_3} L_{\mathbf{k}_1, \mathbf{k}_4, \mathbf{k}_5}^{-, \sigma_4, \sigma_5} \sqrt{J_2 J_3 J_4 J_5} \left\langle \psi_2^{\sigma_2} \psi_3^{\sigma_3} \psi_4^{\sigma_4} \psi_5^{\sigma_5} \prod_{\mathbf{k}} \psi_{\mathbf{k}}^{\mu_{\mathbf{k}}} \right\rangle_{\psi} \quad (\text{A.3})$$

$$\Delta_T(\sigma_2 \omega_2 + \sigma_3 \omega_3 - \omega_1) \Delta_T(\sigma_4 \omega_4 + \sigma_5 \omega_5 + \omega_1) \delta_{\mathbf{k}_1, \sigma_2 \mathbf{k}_2 + \sigma_3 \mathbf{k}_3} \delta_{-\mathbf{k}_1, \sigma_4 \mathbf{k}_4 + \sigma_5 \mathbf{k}_5},$$

which can be represented by the diagram in Fig. A.3 before phase-averaging. After phase averaging,

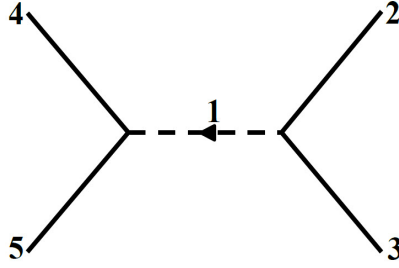


Figure A.3: Terms in \mathcal{J}_2 before phase averaging.

\mathcal{J}_2 has three types of contributions. The leading contributions are two type I diagrams with no external couplings. We show one such diagram in Fig. A.4 (the other one is obtained by the exchange $2 \leftrightarrow 3$). These contain three distinct wavevectors and two vertices, but the wavevector

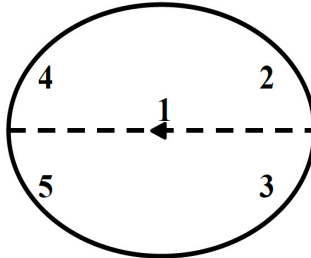


Figure A.4: Type I diagram in \mathcal{J}_2 .

delta-functions at the two vertices turn out to give the same constraint. Thus the type I diagrams contain two free wavevectors corresponding to unconstrained sums. Subleading contributions are

APPENDIX A. DERIVATION OF THE SPECTRAL HIERARCHY

given by type II diagrams with two wavevectors externally coupled. We show one diagram in Fig. A.5 with the wavevectors 2 and 4 coupled to distinct external blobs. The three others can

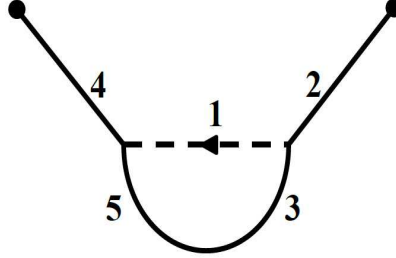


Figure A.5: Type II diagram in \mathcal{J}_2 .

be obtained by exchanging $4 \leftrightarrow 5$ and $2 \leftrightarrow 3$. These subleading contributions contain only one free wavevector. The two delta functions $\delta_{\mathbf{k}_1, \sigma_2 \mathbf{k}_2 + \sigma_3 \mathbf{k}_3}$ and $\delta_{-\mathbf{k}_1, \sigma_4 \mathbf{k}_4 + \sigma_5 \mathbf{k}_5}$ along with the internal connection $\delta_{\mathbf{k}_3, \mathbf{k}_5} \delta_{\sigma_3, -\sigma_5}$ require $\sigma_2 \mathbf{k}_2 = -\sigma_4 \mathbf{k}_4$. Therefore, $\mathbf{k}_2 = -\mathbf{k}_4$ (since \mathbf{k}_1 and \mathbf{k}_4 must be distinct) and $\sigma_2 = \sigma_4$ in this diagram. In principle, another type II contribution could exist with two wavevectors coupled to the same external blob as shown in Fig. A.6, together with diagrams

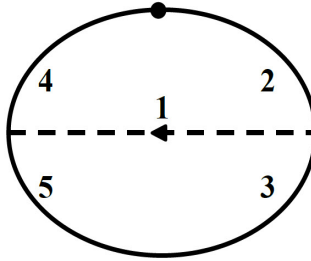


Figure A.6: Type II diagram in \mathcal{J}_2 .

resulting from $4 \leftrightarrow 5$ and $2 \leftrightarrow 3$. However, the condition $\sigma_2 \mathbf{k}_2 = -\sigma_4 \mathbf{k}_4$ in this case requires that $\mathbf{k}_2 = \mathbf{k}_4$, $\sigma_2 = -\sigma_4$, and $\mu_2 = 0$, which coincides with the type I diagram.

All other contributions are type III where all wavevectors are pinned; see the diagram in Fig. A.7. Now consider large L . The amplitude factor $\sqrt{\mathcal{J}_2 \mathcal{J}_3 \mathcal{J}_4 \mathcal{J}_5}$ changes the order by L^{-2d} . Now consider the contributions proportional to the three terms in the prefactor $\lambda_1 + \lambda_1^2 J_1 - \frac{\mu_1^2}{4J_1}$. In the term proportional to λ_1 the type I diagrams provide two free sums that increase the order by L^{2d} , giving an $O(1)$ contribution. The next order contributions from type II diagrams have only one free

APPENDIX A. DERIVATION OF THE SPECTRAL HIERARCHY

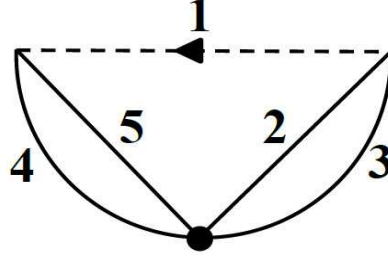


Figure A.7: Type III diagram in \mathcal{J}_2 .

wavevector and thus are at most $O(L^{-d})$. The term proportional to $\lambda_1^2 J_1$ is at most $O(L^{-d})$ because of the additional action variable J_1 . For the term proportional to $\frac{\mu_1^2}{4J_1}$, we note for both type I and type II diagrams \mathbf{k}_1 is not pinned, which requires μ_1 to be zero. Thus the only nonzero contribution here must come from type III graphs, which is at most $O(L^{-d})$. Therefore we can conclude that the leading contributions in \mathcal{J}_1 are $O(1)$, or explicitly

$$\mathcal{J}_2 \sim 9\delta_{\mu,0} \sum_{1,2,3} \lambda_1 J_2 J_3 |H_{\mathbf{k}_1, \mathbf{k}_2, \mathbf{k}_3}^{-, \sigma_2, \sigma_3}|^2 |\Delta_T(\sigma_2 \omega_2 + \sigma_3 \omega_3 - \omega_1)|^2 \quad (\text{A.4})$$

Substituting $J_i = (2\pi/L)^d \tilde{J}_i$ and $\lambda_1 = i\lambda(\mathbf{k}_1)$ and taking the limit $L \rightarrow \infty$ using (2.48), one finds

$$\begin{aligned} \left\langle e^{\sum_{\mathbf{k}} \lambda_{\mathbf{k}} J_{\mathbf{k}}} \mathcal{J}_2 \right\rangle_J &\sim -9i\delta_{\mu,0} \sum_{\underline{\sigma}=(-1, \sigma_2, \sigma_3)} \int d^d k_1 d^d k_2 d^d k_3 \delta^d(\underline{\sigma} \cdot \underline{\mathbf{k}}) |\Delta_T(\underline{\sigma} \cdot \omega(\underline{\mathbf{k}}))|^2 \\ &\quad \times \lambda(\mathbf{k}_1) |H_{\mathbf{k}_1, \mathbf{k}_2, \mathbf{k}_3}^{-, \sigma_2, \sigma_3}|^2 \frac{\delta^2 \mathcal{Z}}{\delta \lambda(\mathbf{k}_2) \delta \lambda(\mathbf{k}_3)} \end{aligned} \quad (\text{A.5})$$

It is worth mentioning here that the term proportional to λ_1^2 kept in Choi *et al.* (2005a) gives only an $O(L^{-d})$ contribution in the large box limit, which can be calculated exactly as

$$\begin{aligned} 9i \left(\frac{2\pi}{L} \right)^d \delta_{\mu,0} \sum_{\underline{\sigma}=(-1, \sigma_2, \sigma_3)} \int d^d k_1 d^d k_2 d^d k_3 \lambda^2(\mathbf{k}_1) \frac{\delta^3 \mathcal{Z}}{\delta \lambda(\mathbf{k}_1) \delta \lambda(\mathbf{k}_2) \delta \lambda(\mathbf{k}_3)} |H_{\mathbf{k}_1, \mathbf{k}_2, \mathbf{k}_3}^{-, \sigma_2, \sigma_3}|^2 \\ \times |\Delta_T(\underline{\sigma} \cdot \omega(\underline{\mathbf{k}}))|^2 \delta^d(\underline{\sigma} \cdot \underline{\mathbf{k}}), \end{aligned} \quad (\text{A.6})$$

which is even smaller than the $O(L^{-d/2})$ correction from \mathcal{J}_1 which we calculated before.

APPENDIX A. DERIVATION OF THE SPECTRAL HIERARCHY

Calculation of \mathcal{J}_3 : Substituting the definition (2.39) of $a_1^{(2)}$ we have

$$\mathcal{J}_3 = \sum_{1,2,3,4,5} \left(\lambda_1 + \frac{\mu_1}{2J_1} \right) L_{\mathbf{k}_1, \mathbf{k}_2, \mathbf{k}_3}^{+, \sigma_2, \sigma_3} L_{\mathbf{k}_2, \mathbf{k}_4, \mathbf{k}_5}^{\sigma_2, \sigma_4, \sigma_5} \sqrt{J_1 J_3 J_4 J_5} \langle \psi_1^{-1} \psi_3^{\sigma_3} \psi_4^{\sigma_4} \psi_5^{\sigma_5} \prod_{\mathbf{k}} \psi_{\mathbf{k}}^{\mu_{\mathbf{k}}} \rangle_{\psi} \\ E_T(\omega_{345}^1, \omega_{23}^1) \delta_{23}^1 \delta_{45}^2 \big|_{\sigma_1=1} + (2 \leftrightarrow 3). \quad (\text{A.7})$$

By symmetry, we only need to consider the first part, which has the following diagram pre-phase-averaged, see Fig. A.8. After phase averaging, there are three types of contributions. The type

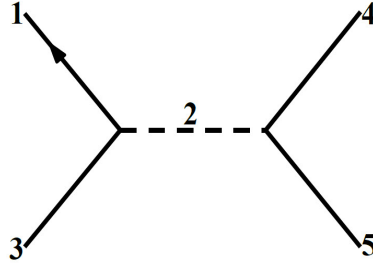


Figure A.8: Terms in \mathcal{J}_3 before phase averaging.

I diagrams are two leading contributions which contain two free wavevectors. We show only one diagram here; see Fig. A.9. The other obtained by exchanging $4 \leftrightarrow 5$. The type II diagrams are four

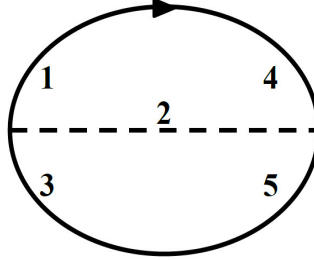


Figure A.9: Type I diagram in \mathcal{J}_3 .

subleading contributions which contain one free wavevector. Again we only show one diagram here, with mode 1 externally coupled; see Fig. A.10. It turns out that the graphs with mode 1 externally coupled are the most important type II contributions to \mathcal{J}_3 . The delta functions require $\mathbf{k}_4 = -\mathbf{k}_1$ and $\sigma_4 = -1$ in this diagram. Additional type II graphs can be obtained by symmetry. All other contributions are type III where all wavevectors are pinned.

APPENDIX A. DERIVATION OF THE SPECTRAL HIERARCHY

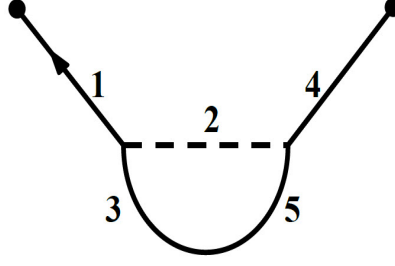


Figure A.10: Type II diagram in \mathcal{J}_3 .

Now consider large L . The amplitude factor $\sqrt{J_1 J_3 J_4 J_5}$ changes the order of \mathcal{J}_3 by L^{-2d} . In the term proportional to λ_1 , the type I diagrams increase the order by L^{2d} since they contain two free sums, giving an $O(1)$ contribution to \mathcal{J}_1 . In the term proportional to $\frac{\mu_1}{2J_1}$, the type I diagrams give zero contribution because they require μ_1 to vanish. The leading $O(1)$ contribution now comes from the type II diagrams with mode 1 externally coupled and $\mu_1 = 1$. The type III diagrams contain no free wavevector and give contributions at most $O(L^{-d})$. The leading contribution to \mathcal{J}_3 in the large-box limit is thus:

$$\begin{aligned} \mathcal{J}_3 \sim & 2 \sum_{\sigma_2, \sigma_3} \prod_{\mathbf{k}} \delta_{\mu_{\mathbf{k}}, 0} \sum_{1, 2, 3} \lambda_1 L_{\mathbf{k}_1, \mathbf{k}_2, \mathbf{k}_3}^{+, \sigma_2, \sigma_3} L_{\mathbf{k}_2, \mathbf{k}_1, \mathbf{k}_3}^{\sigma_2, -1, -\sigma_3} J_1 J_3 E_T(0, \sigma_2 \omega_2 + \sigma_3 \omega_3 - \omega_1) \delta_{\mathbf{k}_1, \sigma_2 \mathbf{k}_2 + \sigma_3 \mathbf{k}_3} \\ & + \sum_{\sigma_2, \sigma_3} \sum_{1, 2, 3} \delta_{\mu_1, 1} \delta_{\mu_{-1}, 1} \prod_{\mathbf{k} \neq \mathbf{k}_1, -\mathbf{k}_1} \delta_{\mu_{\mathbf{k}}, 0} \frac{\mu_1}{2J_1} L_{\mathbf{k}_1, \mathbf{k}_2, \mathbf{k}_3}^{+, \sigma_2, \sigma_3} L_{\mathbf{k}_2, -\mathbf{k}_1, \mathbf{k}_3}^{\sigma_2, -1, -\sigma_3} \sqrt{J_1 J_{-1} J_3} \\ & \times E_T(\omega_1 + \omega_{-1}, \omega_1 - \sigma_2 \omega_2 - \sigma_3 \omega_3) \delta_{\mathbf{k}_1, \sigma_2 \mathbf{k}_2 + \sigma_3 \mathbf{k}_3} + (2 \leftrightarrow 3) \end{aligned} \quad (\text{A.8})$$

Substituting $J_i = (2\pi/L)^d \tilde{J}_i$ and $\lambda_1 = i\lambda(\mathbf{k}_1)$ and taking the limit $L \rightarrow \infty$ using (2.48), one finds

$$\begin{aligned} & \left\langle e^{\sum_{\mathbf{k}} \lambda_{\mathbf{k}} J_{\mathbf{k}}} \mathcal{J}_3 \right\rangle_J \\ \sim & 18i\delta_{\mu, 0} \sum_{\underline{\sigma} = (-1, \sigma_2, \sigma_3)} \sigma_2 \int d^d k_1 \int d^d k_2 \int d^d k_3 \delta^d(\underline{\sigma} \cdot \underline{\mathbf{k}}) \\ & \times E_T(\underline{\sigma} \cdot \omega(\underline{\mathbf{k}}), 0) \lambda(\mathbf{k}_1) |H_{\mathbf{k}_1, \mathbf{k}_2, \mathbf{k}_3}^{-, \sigma_2, \sigma_3}|^2 \frac{\delta^2 \mathcal{Z}}{\delta \lambda(\mathbf{k}_1) \delta \lambda(\mathbf{k}_3)} \\ & - 9 \sum_1 \delta_{\mu_1, 1} \delta_{\mu_{-1}, 1} \prod_{\mathbf{k} \neq \mathbf{k}_1, -\mathbf{k}_1} \delta_{\mu_{\mathbf{k}}, 0} \sum_{\underline{\sigma} = (-1, \sigma_2, \sigma_3)} \sigma_2 \int d^d k_2 \int d^d k_3 \delta^d(\underline{\sigma} \cdot \underline{\mathbf{k}}) \\ & \times E_T(\omega(\mathbf{k}_1) + \omega(-\mathbf{k}_1), \underline{\sigma} \cdot \omega(\underline{\mathbf{k}})) H_{\mathbf{k}_1, \mathbf{k}_2, \mathbf{k}_3}^{-, \sigma_2, \sigma_3} H_{-\mathbf{k}_1, \mathbf{k}_2, \mathbf{k}_3}^{+, \sigma_2, \sigma_3} \left\langle e^{\sum_{\mathbf{k}} \lambda_{\mathbf{k}} J_{\mathbf{k}}} \sqrt{\frac{\tilde{J}_{-1}}{\tilde{J}_1}} \tilde{J}_3 \right\rangle_J \\ & + (2 \leftrightarrow 3). \end{aligned} \quad (\text{A.9})$$

APPENDIX A. DERIVATION OF THE SPECTRAL HIERARCHY

Calculation of \mathcal{J}_4 : Similarly, substituting (2.38) for $a_1^{(1)}$

$$\begin{aligned} \mathcal{J}_4 = & \sum_{1,2,3,4,5} \left(\frac{1}{2} \lambda_1^2 + \frac{\mu_1}{4J_1^2} \left(\frac{\mu_1}{2} - 1 \right) + \frac{\lambda_1 \mu_1}{2J_1} \right) L_{\mathbf{k}_1, \mathbf{k}_2, \mathbf{k}_3}^{+, \sigma_2, \sigma_3} L_{\mathbf{k}_1, \mathbf{k}_4, \mathbf{k}_5}^{+, \sigma_4, \sigma_5} \left\langle \psi_1^{-2} \psi_2^{\sigma_2} \psi_3^{\sigma_3} \psi_4^{\sigma_4} \psi_5^{\sigma_5} \prod_{\mathbf{k}} \psi_{\mathbf{k}}^{\mu_{\mathbf{k}}} \right\rangle_{\psi} \\ & \times J_1 \sqrt{J_2 J_3 J_4 J_5} \Delta_T(\sigma_2 \omega_2 + \sigma_3 \omega_3 - \omega_1) \Delta_T(\sigma_4 \omega_4 + \sigma_5 \omega_5 - \omega_1) \delta_{\mathbf{k}_1, \sigma_2 \mathbf{k}_2 + \sigma_3 \mathbf{k}_3} \delta_{\mathbf{k}_1, \sigma_4 \mathbf{k}_4 + \sigma_5 \mathbf{k}_5} \quad (\text{A.10}) \end{aligned}$$

which can be represented by the following diagram before phase-averaging; see Fig. A.11. After phase

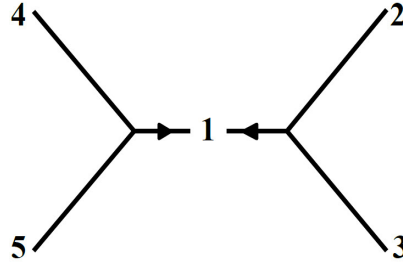


Figure A.11: Terms in \mathcal{J}_4 before phase averaging.

averaging, there are two types of contributions. Type I diagrams have only the 1 mode externally coupled, corresponding to the following diagram and its partner with $2 \leftrightarrow 3$; see Fig. A.12. These

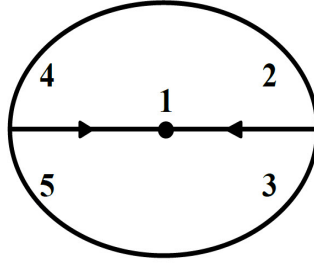


Figure A.12: Type I diagram in \mathcal{J}_4 .

are formally the leading contributions, with one free wavevector. However, the wavevector delta functions require $\mathbf{k}_1 = \mathbf{0}$ and thus this graph vanishes identically. All other nonzero contributions are type II where there are no free wavevectors.

Now consider large L . The amplitude factor $J_1 \sqrt{J_2 J_3 J_4 J_5}$ in \mathcal{J}_4 changes the order by L^{-3d} . The largest possible contribution comes from the term proportional to $\frac{\mu_1}{4J_1^2} \left(\frac{\mu_1}{2} - 1 \right)$, which is a large factor of $O(L^{2d})$. However, such contributions are still only $O(L^{-d})$. Hence \mathcal{J}_4 is negligible in the

APPENDIX A. DERIVATION OF THE SPECTRAL HIERARCHY

large box limit.

Calculation of \mathcal{J}_5 : Write $\mathcal{J}_5 \equiv \sum_{1 \neq 2} \left\{ \lambda_1 \lambda_2 (\mathcal{B}_1 + \mathcal{B}_2) + (\lambda_1 + \frac{\mu_1}{4J_1}) \frac{\mu_2}{J_2} (\mathcal{B}_1 - \mathcal{B}_3) \right\}$, where (2.38) gives

$$\begin{aligned}
\mathcal{B}_1 &\equiv \left\langle \prod_{\mathbf{k}} \psi_{\mathbf{k}}^{(0)\mu_{\mathbf{k}}} a_1^{(1)} a_1^{(0)*} a_2^{(1)} a_2^{(0)*} \right\rangle_{\psi} \\
&= \sum_{3,4,5,6} L_{\mathbf{k}_1, \mathbf{k}_3, \mathbf{k}_4}^{+, \sigma_3, \sigma_4} L_{\mathbf{k}_2, \mathbf{k}_5, \mathbf{k}_6}^{+, \sigma_5, \sigma_6} \sqrt{J_1 J_2 J_3 J_4 J_5 J_6} \left\langle \psi_1^{-1} \psi_2^{-1} \psi_3^{\sigma_3} \psi_4^{\sigma_4} \psi_5^{\sigma_5} \psi_6^{\sigma_6} \prod_{\mathbf{k}} \psi_{\mathbf{k}}^{\mu_{\mathbf{k}}} \right\rangle_{\psi} \\
&\quad \times \Delta(\sigma_3 \omega_3 + \sigma_4 \omega_4 - \omega_1) \Delta(\sigma_5 \omega_5 + \sigma_6 \omega_6 - \omega_2) \delta_{\mathbf{k}_1, \sigma_3 \mathbf{k}_3 + \sigma_4 \mathbf{k}_4} \delta_{\mathbf{k}_2, \sigma_5 \mathbf{k}_5 + \sigma_6 \mathbf{k}_6} \\
\mathcal{B}_2 &\equiv \left\langle \prod_{\mathbf{k}} \psi_{\mathbf{k}}^{\mu_{\mathbf{k}}} a_1^{(1)*} a_1^{(0)*} a_2^{(1)} a_2^{(0)*} \right\rangle_{\psi} = \sum_{3,4,5,6} L_{\mathbf{k}_1, \mathbf{k}_3, \mathbf{k}_4}^{-, \sigma_3, \sigma_4} L_{\mathbf{k}_2, \mathbf{k}_5, \mathbf{k}_6}^{+, \sigma_5, \sigma_6} \sqrt{J_1 J_2 J_3 J_4 J_5 J_6} \\
&\quad \times \Delta(\sigma_3 \omega_3 + \sigma_4 \omega_4 + \omega_1) \Delta(\sigma_5 \omega_5 + \sigma_6 \omega_6 - \omega_2) \delta_{-\mathbf{k}_1, \sigma_3 \mathbf{k}_3 + \sigma_4 \mathbf{k}_4} \delta_{\mathbf{k}_2, \sigma_5 \mathbf{k}_5 + \sigma_6 \mathbf{k}_6} \\
&\quad \times \left\langle \psi_1^{+1} \psi_2^{-1} \psi_3^{\sigma_3} \psi_4^{\sigma_4} \psi_5^{\sigma_5} \psi_6^{\sigma_6} \prod_{\mathbf{k}} \psi_{\mathbf{k}}^{\mu_{\mathbf{k}}} \right\rangle_{\psi} \\
\mathcal{B}_3 &\equiv \left\langle \prod_{\mathbf{k}} \psi_{\mathbf{k}}^{\mu_{\mathbf{k}}} a_1^{(1)} a_1^{(0)*} a_2^{(1)*} a_2^{(0)} \right\rangle_{\psi} = \sum_{3,4,5,6} L_{\mathbf{k}_1, \mathbf{k}_3, \mathbf{k}_4}^{+, \sigma_3, \sigma_4} L_{\mathbf{k}_2, \mathbf{k}_5, \mathbf{k}_6}^{-, \sigma_5, \sigma_6} \sqrt{J_1 J_2 J_3 J_4 J_5 J_6} \\
&\quad \times \Delta(\sigma_3 \omega_3 + \sigma_4 \omega_4 - \omega_1) \Delta(\sigma_5 \omega_5 + \sigma_6 \omega_6 + \omega_2) \delta_{\mathbf{k}_1, \sigma_3 \mathbf{k}_3 + \sigma_4 \mathbf{k}_4} \delta_{-\mathbf{k}_2, \sigma_5 \mathbf{k}_5 + \sigma_6 \mathbf{k}_6} \\
&\quad \times \left\langle \psi_1^{-1} \psi_2^{+1} \psi_3^{\sigma_3} \psi_4^{\sigma_4} \psi_5^{\sigma_5} \psi_6^{\sigma_6} \prod_{\mathbf{k}} \psi_{\mathbf{k}}^{\mu_{\mathbf{k}}} \right\rangle_{\psi}. \tag{A.11}
\end{aligned}$$

Note under the interchanges $1 \leftrightarrow 2$, $3 \leftrightarrow 5$, $4 \leftrightarrow 6$, that $\mathcal{B}_2 \leftrightarrow \mathcal{B}_3$. All three of the \mathcal{B} 's contain the same amplitude factor $\sqrt{J_1 J_2 J_3 J_4 J_5 J_6}$ that changes the order by L^{-3d} . We list their diagrams as follows; see Fig. A.13. After phase averaging, there are three types of diagrams for the \mathcal{B} 's. The type I diagrams are leading contributions with no external couplings. Shown here is one type I diagram for \mathcal{B}_1 ; see Fig. A.14. with others obtained by $3 \leftrightarrow 4$ and $5 \leftrightarrow 6$. These contain two free wavevectors. For $\mathcal{B}_2, \mathcal{B}_3$ there are additional type I contributions with 1 and 2 coupled, but these do not contribute to \mathcal{J}_5 because of the restriction that $1 \neq 2$. The type II diagrams are subleading contributions which contain one free wavevector. Shown here is one such contribution for \mathcal{B}_1 with both 1 and 2 externally coupled; see Fig. A.15. The delta functions here require $\mathbf{k}_2 = -\mathbf{k}_1$. In the corresponding diagrams for $\mathcal{B}_2, \mathcal{B}_3$ the delta functions instead require $\mathbf{k}_1 = \mathbf{k}_2$, so these do not exist. (Contributions to $\mathcal{B}_2, \mathcal{B}_3$ with 1 and 2 coupled to the *same* external blob coincide with the

APPENDIX A. DERIVATION OF THE SPECTRAL HIERARCHY

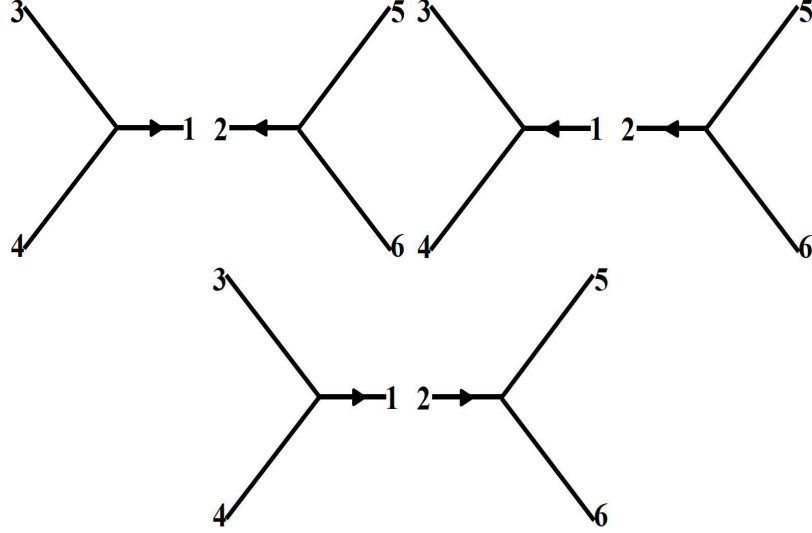


Figure A.13: Terms in \mathcal{J}_5 before phase averaging.

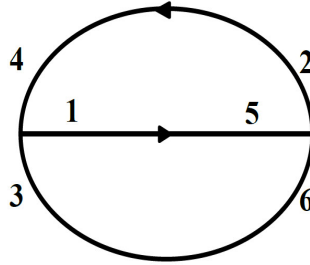


Figure A.14: Type I diagram for \mathcal{B}_1 in \mathcal{J}_5 .

type I diagrams that do not contribute to \mathcal{J}_5 .) There are also type II contributions for the \mathcal{B} 's with only one of 1 or 2 externally coupled. For example, one such contribution is obtained for \mathcal{B}_1 by exchanging $1 \leftrightarrow 4$ in the above graph and then the delta functions require that $\mathbf{k}_2 = \sigma_4 \mathbf{k}_4$ so that $\mathbf{k}_2 = -\mathbf{k}_4$, $\sigma_4 = -1$. Similar type II contributions exist for $\mathcal{B}_2, \mathcal{B}_3$. Other type II contributions with neither 1 nor 2 externally coupled must have both $\mu_1 = \mu_2 = 0$ and do not contribute at non-vanishing order to \mathcal{J}_5 . Type III contributions with additional external couplings have no free wavevectors.

Now consider the size of the various terms for large L . For $\sum_{1 \neq 2} \lambda_1 \lambda_2 (\mathcal{B}_1 + \mathcal{B}_2)$, the leading contribution comes from type I diagrams and is $O(L^{-d})$. For $\sum_{1 \neq 2} \frac{\lambda_1 \mu_2}{J_2} (\mathcal{B}_1 - \mathcal{B}_3)$, the type I diagrams give zero contribution since $\mu_2 = 0$ and type II diagrams are at most $O(L^{-d})$.

APPENDIX A. DERIVATION OF THE SPECTRAL HIERARCHY

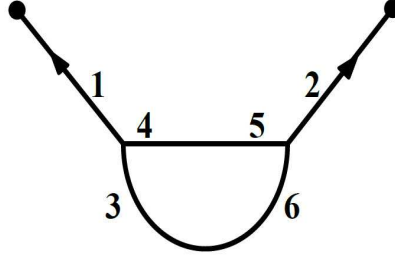


Figure A.15: Type II diagram for \mathcal{B}_1 in \mathcal{J}_5 .

For $\sum_{1 \neq 2} \frac{\mu_1 \mu_2}{4J_1 J_2} \mathcal{B}_1$, type I diagrams give zero contribution and type II diagrams with both 1 and 2 externally coupled give an $O(1)$ contribution. The corresponding term $\sum_{1 \neq 2} \frac{\mu_1 \mu_2}{4J_1 J_2} \mathcal{B}_3 = O(L^{-d})$ from type III diagrams, since, as noted above, there do not exist type II diagrams for \mathcal{B}_3 with 1 and 2 externally coupled to distinct blobs. In large box limit, the term \mathcal{J}_5 is given, to leading order, by

$$\begin{aligned} \mathcal{J}_5 \sim & -\frac{9}{2} \sum_1 \delta_{\mu_1,1} \delta_{\mu_{-1},1} \prod_{\mathbf{k} \neq \pm \mathbf{k}_1} \delta_{\mu_{\mathbf{k}},0} \sum_{\underline{\sigma} = (-1, \sigma_2, \sigma_3)} \int d^d k_2 \int d^d k_3 \delta^d(\underline{\sigma} \cdot \underline{\mathbf{k}}) \Delta_T(\underline{\sigma} \cdot \omega(\underline{\mathbf{k}})) \Delta_T(\underline{\sigma} \cdot \omega(\underline{\mathbf{k}}')) \\ & \times H_{\mathbf{k}_1, \mathbf{k}_2, \mathbf{k}_3}^{-, \sigma_2, \sigma_3} H_{-\mathbf{k}_1, \mathbf{k}_2, \mathbf{k}_3}^{+, \sigma_2, \sigma_3} \left\langle \frac{\tilde{J}_2 \tilde{J}_3}{\sqrt{\tilde{J}_1 \tilde{J}_{-1}}} e^{\sum_{\mathbf{k}} \lambda_{\mathbf{k}} J_{\mathbf{k}}} \right\rangle_J, \end{aligned} \quad (\text{A.12})$$

where $\underline{\mathbf{k}} = (\mathbf{k}_1, \mathbf{k}_2, \mathbf{k}_3)$ and $\underline{\mathbf{k}}' = (-\mathbf{k}_1, \mathbf{k}_2, \mathbf{k}_3)$. Now making the substitution $\lambda_{\mathbf{k}} = i\lambda(\mathbf{k})$ and taking the limit, one obtains,

$$\begin{aligned} \left\langle e^{\sum_{\mathbf{k}} \lambda_{\mathbf{k}} J_{\mathbf{k}}} \mathcal{J}_5 \right\rangle_J \sim & -\frac{9}{2} \sum_1 \delta_{\mu_1,1} \delta_{\mu_{-1},1} \prod_{\mathbf{k} \neq \pm \mathbf{k}_1} \delta_{\mu_{\mathbf{k}},0} \sum_{\underline{\sigma} = (-, \sigma_2, \sigma_3)} \int d^d k_2 d^d k_3 \delta^d(\underline{\sigma} \cdot \underline{\mathbf{k}}) \\ & \times \Delta_T(\underline{\sigma} \cdot \omega(\underline{\mathbf{k}})) \Delta_T(-\underline{\sigma} \cdot \omega(\underline{\mathbf{k}}')) \times H_{\mathbf{k}_1, \mathbf{k}_2, \mathbf{k}_3}^{-, \sigma_2, \sigma_3} H_{-\mathbf{k}_1, \mathbf{k}_2, \mathbf{k}_3}^{+, \sigma_2, \sigma_3} \left\langle \frac{\tilde{J}_2 \tilde{J}_3}{\sqrt{\tilde{J}_1 \tilde{J}_{-1}}} e^{\sum_{\mathbf{k}} \lambda_{\mathbf{k}} J_{\mathbf{k}}} \right\rangle_J. \end{aligned} \quad (\text{A.13})$$

Appendix B

Derivation of the PDF Hierarchy

We here evaluate the \mathcal{J} -terms that contribute to $\mathcal{X}^{(M)}(\lambda, \mu, T)$. Most of the essential work has already been done in A. As discussed in the text, the main difference is that mode 1 is now discrete for $\mathcal{J}_1 - \mathcal{J}_4$ and assumes only M values, while for \mathcal{J}_5 modes 1,2 are both discrete. All other modes are continuous in the infinite-box limit. One must consider carefully whether free wavevectors in graphical summations are discrete or continuous to see whether their contribution is $O(M)$ or $O(L^d)$.

\mathcal{J}_1 : The graphs contain no free wavevectors, so that \mathcal{J}_1 is still $O(L^{-d/2})$.

\mathcal{J}_2 : The leading order $O(1)$ contribution comes again from the type I diagrams, which contain two free wavevectors. One of these free wavevectors is mode 1 which is discrete, but this is compensated by the extra factor of L^d from the prefactors $\lambda_{\mathbf{k}_1}$ and $\lambda_{\mathbf{k}_1}^2 J_{\mathbf{k}_1}$, which now contribute equally. One thus obtains by substituting $\lambda_{\mathbf{k}_m} = i(L/2\pi)^d \lambda_m$ and $J_m = (2\pi/L)^d \tilde{J}_m$ the result

$$\begin{aligned} \left\langle e^{\sum_{\mathbf{k}} \lambda_{\mathbf{k}} J_{\mathbf{k}}} \mathcal{J}_2 \right\rangle_J &\sim 9\delta_{\mu,0} \sum_{j=1}^M \sum_{\underline{\sigma}=(-1,\sigma_2,\sigma_3)} \int d^d \bar{k}_2 d^d \bar{k}_3 \delta^d(\underline{\sigma} \cdot \underline{\mathbf{k}}_j) |\Delta_T(\underline{\sigma} \cdot \omega(\underline{\mathbf{k}}_j))|^2 |H_{\underline{\mathbf{k}}_j}^{\underline{\sigma}}|^2 \\ &\quad \times \left\langle (i\lambda_j - \lambda_j^2 \tilde{J}_j) \tilde{J}_2 \tilde{J}_3 e^{\sum_m i\lambda_m \tilde{J}_m} \right\rangle_J \\ &= -9i\delta_{\mu,0} \sum_{j=1}^M \sum_{\underline{\sigma}=(-1,\sigma_2,\sigma_3)} \int d^d \bar{k}_2 d^d \bar{k}_3 \delta^d(\underline{\sigma} \cdot \underline{\mathbf{k}}_j) |\Delta_T(\underline{\sigma} \cdot \omega(\underline{\mathbf{k}}_j))|^2 |H_{\underline{\mathbf{k}}_j}^{\underline{\sigma}}|^2 \end{aligned}$$

APPENDIX B. DERIVATION OF THE PDF HIERARCHY

$$\times (\lambda_j + \lambda_j^2 \frac{\partial}{\partial \lambda_j}) \frac{\partial^2 \mathcal{Z}^{(M+2)}}{\partial \bar{\lambda}_2 \partial \bar{\lambda}_3} \Big|_{\bar{\lambda}_2 = \bar{\lambda}_3 = 0}. \quad (\text{B.1})$$

Here $\underline{\mathbf{k}}_j = (\mathbf{k}_j, \bar{\mathbf{k}}_2, \bar{\mathbf{k}}_3)$.

\mathcal{J}_3 : There are two contributions, from the two terms in the prefactor, $\lambda_{\mathbf{k}_1}$ and $\mu_{\mathbf{k}_1}/2J_{\mathbf{k}_1}$. For the $\lambda_{\mathbf{k}_1}$ term, the leading $O(1)$ contribution comes from the type I diagrams, just as for \mathcal{J}_2 . One of the two free wavevectors is discrete mode 1, but this is compensated by the $O(L^d)$ prefactor $\lambda_{\mathbf{k}_1}$. For the $\mu_{\mathbf{k}_1}/2J_{\mathbf{k}_1}$ term, the leading $O(1)$ contribution comes from the type II diagrams with modes 1 and -1 externally coupled, so that $\mu_{\mathbf{k}_1} = \mu_{-\mathbf{k}_1} = 1$. The type II diagram has one free continuous wavevector. Thus, its contribution is also $O(1)$ if the set of M wavevectors includes at least one pair of opposite wavevectors. Assuming this is not so, the final result is:

$$\begin{aligned} \left\langle e^{\sum_{\mathbf{k}} \lambda_{\mathbf{k}} J_{\mathbf{k}}} \mathcal{J}_3 \right\rangle_J^{(I)} &\sim -18\delta_{\mu,0} \sum_{j=1}^M \sum_{\underline{\sigma}=(-1,\sigma_2,\sigma_3)} \sigma_2 \int d^d \bar{k}_2 d^d \bar{k}_3 \delta^d(\underline{\sigma} \cdot \underline{\mathbf{k}}_j) E_T(0, \underline{\sigma} \cdot \omega(\underline{\mathbf{k}}_j)) |H_{\underline{\mathbf{k}}_j}^{\underline{\sigma}}|^2 \\ &\quad \times \left\langle i\lambda_j \tilde{J}_j \tilde{J}_3 e^{\sum_m i\lambda_m \tilde{J}_m} \right\rangle_J + (2 \leftrightarrow 3). \\ &= 18i\delta_{\mu,0} \sum_{j=1}^M \sum_{\underline{\sigma}=(-1,\sigma_2,\sigma_3)} \sigma_2 \int d^d \bar{k}_2 d^d \bar{k}_3 \delta^d(\underline{\sigma} \cdot \underline{\mathbf{k}}_j) E_T(0, \underline{\sigma} \cdot \omega(\underline{\mathbf{k}}_j)) \\ &\quad \times \lambda_j |H_{\underline{\mathbf{k}}_j}^{\underline{\sigma}}|^2 \frac{\partial^2 \mathcal{Z}^{(M+1)}}{\partial \bar{\lambda}_3 \partial \lambda_j} \Big|_{\bar{\lambda}_3=0} + (2 \leftrightarrow 3). \end{aligned} \quad (\text{B.2})$$

However, if the M wavevectors include pairs of opposites, then there is an additional contribution

$$\begin{aligned} \left\langle e^{\sum_{\mathbf{k}} \lambda_{\mathbf{k}} J_{\mathbf{k}}} \mathcal{J}_3 \right\rangle_J^{(II)} &\sim -9 \sum_{j=1}^M \delta_{\mu_j,1} \delta_{\mu_{-j},1} \prod_{m \neq j, -j} \delta_{\mu_m,0} \sum_{\underline{\sigma}=(-1,\sigma_2,\sigma_3)} \sigma_2 \int d^d \bar{k}_2 \int d^d \bar{k}_3 \delta^d(\underline{\sigma} \cdot \underline{\mathbf{k}}_j) \\ &\quad \times E_T(\omega(\mathbf{k}_j) + \omega(-\mathbf{k}_j), \underline{\sigma} \cdot \omega(\underline{\mathbf{k}}_j)) H_{\mathbf{k}_j, \bar{\mathbf{k}}_2, \bar{\mathbf{k}}_3}^{-,\sigma_2,\sigma_3} H_{-\mathbf{k}_j, \bar{\mathbf{k}}_2, \bar{\mathbf{k}}_3}^{+,\sigma_2,\sigma_3} \left\langle e^{\sum_m i\lambda_m \tilde{J}_m} \sqrt{\frac{\tilde{J}_{-1}}{\tilde{J}_1}} \tilde{J}_3 \right\rangle_J \\ &\quad + (2 \leftrightarrow 3). \end{aligned} \quad (\text{B.3})$$

\mathcal{J}_4 : The type I contribution vanishes and the leading contribution from type II diagrams with no free sums remains $O(L^{-d})$.

\mathcal{J}_5 : The amplitude factors contribute $O(L^{-3d})$ while the prefactors are $O(L^{2d})$. Thus, to

APPENDIX B. DERIVATION OF THE PDF HIERARCHY

give an overall $O(1)$ contribution, the \mathcal{B} factors must contain a free continuous wavevector. For \mathcal{B}_1 the type I diagrams have two free discrete wavevectors and type II diagrams with mode 2 only pinned have one free discrete wavevector, but type II diagrams with both 1 and 2 pinned have one free continuous wavevector. For $\mathcal{B}_2, \mathcal{B}_3$, there are no graphs with modes 1 and 2 distinct, contributing to \mathcal{J}_5 , that have a free continuous wavevector. Type I diagrams have two free wavevectors, both discrete if 1 and 2 are uncoupled. Type II diagrams with only one of the modes 1 or 2 externally coupled have one discrete free wavevector.

Thus, the only $O(1)$ contribution to \mathcal{J}_5 is from $\sum_{1 \neq 2} \left\{ \lambda_{\mathbf{k}_1} \lambda_{\mathbf{k}_2} + \frac{\lambda_{\mathbf{k}_1} \mu_{\mathbf{k}_2}}{J_{\mathbf{k}_2}} + \frac{\mu_{\mathbf{k}_1} \mu_{\mathbf{k}_2}}{4J_{\mathbf{k}_1} J_{\mathbf{k}_2}} \right\} \mathcal{B}_1$ and type II diagrams for \mathcal{B}_1 with both 1 and 2 pinned. Corrections are at most $O(M/L^d)$. The $O(1)$ contribution is thus like that obtained before for \mathcal{J}_5 , except that the mode-1 sum is over just M discrete values and all terms in the prefactor contribute equally. This gives

$$\begin{aligned}
& \left\langle e^{\sum_{\mathbf{k}} \lambda_{\mathbf{k}} J_{\mathbf{k}}} \mathcal{J}_5 \right\rangle_J \\
& \sim 18 \sum_{j=1}^M \delta_{\mu_j, 1} \delta_{\mu_{-j}, 1} \prod_{m \neq 1, -1} \delta_{\mu_m, 0} \left(\lambda_1 \lambda_{-1} - i \frac{\lambda_1}{\tilde{J}_{-1}} - \frac{1}{4\tilde{J}_1 \tilde{J}_{-1}} \right) \sum_{\underline{\sigma} = (-, \sigma_2, \sigma_3)} \int d^d \bar{k}_2 d^d \bar{k}_3 \delta^d(\underline{\sigma} \cdot \underline{\mathbf{k}}_j) \\
& \quad \times \Delta_T(\underline{\sigma} \cdot \omega(\underline{\mathbf{k}}_j)) \Delta_T(-\underline{\sigma} \cdot \omega(\underline{\mathbf{k}}'_j)) H_{\mathbf{k}_j, \bar{\mathbf{k}}_2, \bar{\mathbf{k}}_3}^{-, \sigma_2, \sigma_3} H_{-\mathbf{k}_j, \bar{\mathbf{k}}_2, \bar{\mathbf{k}}_3}^{+, \sigma_2, \sigma_3} \left\langle \sqrt{\tilde{J}_1 \tilde{J}_{-1} \tilde{J}_2 \tilde{J}_3} e^{i \sum_m \lambda_m \tilde{J}_m} \right\rangle_J. \quad (\text{B.4})
\end{aligned}$$

Appendix C

Construction of the Phase Measure

In this appendix, we rigorously construct the phase measure $d\mu = d^D \underline{p} \, \delta(E(\underline{\mathbf{p}}; \mathbf{k}))$ for the resonance function $E(\underline{\mathbf{p}}; \mathbf{k})$ through a proper limiting process for the approximate delta function (4.1). Since \mathbf{k} serves as a parameter, we shall omit it throughout this appendix and simply write $E(\mathbf{p})$. Lukkarinen and Spohn (2007, Appendix A) has studied a similar problem. They constructed the phase measure for E that is a Morse function (C^2 with only isolated, non-degenerate critical points) in dimension $d = 3$. By using the Fourier transform of an approximate delta function of Lorentzian form (4.4), they proved the bound for the limiting measure $d\mu = d^D p \, \delta(E(\mathbf{p}))$ that

$$\int_{\mathbb{T}^D} d^D p \, \delta(E(\mathbf{p})) \leq C_E \quad (\text{C.1})$$

where C_E is a constant dependent on E . The measure they constructed is in fact a finite Borel measure. However, many examples we considered in Chap. 3 yield measures that are not even locally finite. To make proper sense of the integral

$$I_0[f] := \int_{\{\mathbf{p}: E(\mathbf{p})=0\}} \frac{d\mathcal{H}^{D-1}(\mathbf{p})}{|\nabla E(\mathbf{p})|} f(\mathbf{p}) \quad (\text{C.2})$$

APPENDIX C. CONSTRUCTION OF THE PHASE MEASURE

such that

$$I_0[f] = \lim_{T \rightarrow \infty} \int d^D p \, \delta_T(E(\mathbf{p})) f(\mathbf{p}), \quad (\text{C.3})$$

we can no longer consider the weak limit for Radon measures, i.e. convergence for f in the class of continuous functions that are compactly supported (we shall denote this space as $\mathcal{C}_c(\mathbb{R}^D)$). Instead we have to consider a “slightly weaker” limit such that f is in a proper subset of $\mathcal{C}_c(\mathbb{R}^D)$.

Our strategy is to employ the coarea formula proved by Federer (1959), which states that for any $W \subset \mathbb{R}^M$ which is M -rectifiable and \mathcal{H}^M -measurable, $Z \subset \mathbb{R}^N$, $N < M$ which is N -rectifiable and \mathcal{H}^N -measurable, a Lipschitz map $E : W \rightarrow Z$, and any \mathcal{H}^M -measurable function $g : W \rightarrow \mathbb{R}$ such that $g(w)(JE)(w)$ is \mathcal{H}^M -integrable, then the relation $\int_W g(w)(JE)(w) d\mathcal{H}^M(w) = \int_Z d\mathcal{H}^N(z) \int_{E^{-1}(z)} g(w') d\mathcal{H}^{M-N}(w')$ holds. Here $JE(w)$ is the so-called N -dimensional Jacobian. See Federer (1969, section 3.2.1). We apply the theorem for $M = D$, $N = 1$, $W = \mathbb{R}^D$, $Z = \mathbb{R}$, and $g = \delta_T(E)f/|\nabla E|$. With the 1-dimensional Jacobian $JE = |\nabla E|$, we have

$$\int d^D p \, \delta_T(E(\mathbf{p})) f(\mathbf{p}) = \int d\varepsilon \, \delta_T(\varepsilon) I_\varepsilon[f]. \quad (\text{C.4})$$

with

$$I_\varepsilon[f] = \int_{\{\mathbf{p}: E(\mathbf{p})=\varepsilon\}} \frac{d\mathcal{H}^{D-1}(\mathbf{p})}{|\nabla E(\mathbf{p})|} f(\mathbf{p}). \quad (\text{C.5})$$

All the dispersion relations we considered in Chap. 3 are Lipschitz continuous except for those with pseudo-critical points. There are many stronger results that do not require Lipschitz continuity. We refer the readers to Malý *et al.* (2003) for the subject. These weaker conditions do not, however, cover any examples in Chap. 3 that are not already covered by the Lipschitz condition. Here $I_\varepsilon[f]$ is well-defined and finite for almost all ε because f is continuous with compact support and thus by coarea formula with $g = f/|\nabla E|$

$$\int_{-\infty}^{\infty} d\varepsilon \, I_\varepsilon[f] = \int d^D p \, f(\mathbf{p}) < \infty. \quad (\text{C.6})$$

APPENDIX C. CONSTRUCTION OF THE PHASE MEASURE

We still need additional conditions on E for $I_0[f]$ to be well-defined. For that, we assume the critical set for E defined as

$$\mathcal{M}_{crit} = \{\mathbf{p} : E \text{ is not differentiable at } \mathbf{p}, \text{ or } E \text{ is differentiable with } \nabla E(\mathbf{p}) = \mathbf{0}\} \quad (\text{C.7})$$

has only a \mathcal{H}^{D-1} -null part on the resonant manifold $E^{-1}(\{0\})$. This condition is also true for nearly all of the examples in Chap. 3 (except for acoustic turbulence for all wavevectors \mathbf{k} and some other examples for special choices of \mathbf{k}). In that case, the integrand in (C.2) is well-defined except for a \mathcal{H}^{D-1} -null set and $d\mu = \mathcal{H}^{D-1}(\mathbf{p})/|\nabla E(\mathbf{p})|$ restricted to $E^{-1}(\{0\})$ is a well-defined Borel measure. Note this still does not guarantee (C.2) to be finite for all $f \in \mathcal{C}_c(\mathbb{R}^D)$. We now summarize the above discussion in the following definition of $\mathcal{C}_c^E(\mathbb{R}^D)$, the class of functions for which we shall define the limit of the approximate delta functions as a Borel measure.

Definition C.1 $f \in \mathcal{C}_c^E(\mathbb{R}^D)$ if and only if the following conditions are met

- 1) $f \in \mathcal{C}_c(\mathbb{R}^D)$;
- 2) $I_0[f]$ is finite;
- 3) $I_\varepsilon[f]$ is continuous at 0, i.e.,

$$\lim_{\varepsilon \rightarrow 0} I_\varepsilon[f] = I_0[f]. \quad (\text{C.8})$$

We are now ready to prove the following result on the limiting measure.

Theorem C.2 If E is Lipschitz continuous and $\mathcal{H}^{D-1}(\mathcal{M}_{crit} \cap E^{-1}(\{0\})) = 0$, then

$$\lim_{T \rightarrow \infty} \int d^D p \, \delta_T(E(\mathbf{p})) f(\mathbf{p}) = I_0[f]. \quad (\text{C.9})$$

for $f \in \mathcal{C}_c^E(\mathbb{R}^D)$.

Proof Upon decomposing into positive and negative parts, we assume $f \geq 0$ and is supported on a

APPENDIX C. CONSTRUCTION OF THE PHASE MEASURE

compact set K . By condition (C.8), there exists δ such that $I_\varepsilon[f] \leq I_0[f] + 1$ for any $|\varepsilon| \leq \delta$. Note

$$\int_{|E|>\delta} d^D p \, \delta_T(E(\mathbf{p})) f(\mathbf{p}) \leq \max(f) \frac{\lambda(K)}{T\delta^2} \xrightarrow{T \rightarrow \infty} 0, \quad (\text{C.10})$$

where λ is the Lebesgue measure on \mathbb{R}^D . By Lipschitz continuity of E , we have from the coarea formula that

$$\int_{|E|\leq\delta} d^D p \, \delta_T(E(\mathbf{p})) f(\mathbf{p}) = \int_{-\delta}^{\delta} d\varepsilon \, \delta_T(\varepsilon) I_\varepsilon[f] = \int_{-\delta T}^{\delta T} d\varepsilon \, \delta_1(\varepsilon) I_{\varepsilon/T}[f] \xrightarrow{T \rightarrow \infty} I_0[f]. \quad (\text{C.11})$$

The last limit follows from condition (C.8) and the dominated convergence theorem. \square

Remark C.3 The specific form of approximate delta functions does not matter in this proof.

Now that we have proved the theorem that constructs the limiting measure $\lim_{T \rightarrow \infty} d^D p \, \delta_T(E(\mathbf{p}))$ when integrated against $f \in \mathcal{C}_c^E(\mathbb{R}^D)$, we have to investigate how large the set $\mathcal{C}_c^E(\mathbb{R}^D)$ is. We demonstrate the characteristics of $\mathcal{C}_c^E(\mathbb{R}^D)$ with the following examples.

Example C.4 When E is everywhere C^1 and $|\nabla E| > 0$ on the set $E^{-1}(\{0\})$, we have $\mathcal{C}_c^E(\mathbb{R}^D) = \mathcal{C}_c(\mathbb{R}^D)$. This is already proven by Hörmander (1983, theorem 6.1.2, 6.1.5).

Example C.5 We consider $E(\mathbf{p}) = p_x p_y$. This is the simplest case yielding a phase measure that is not locally finite. Also any C^2 Morse function E in 2D (with only isolated, non-degenerate critical points) can be written into the above form in the vicinity of the critical points (see section 4.2). If $f \in \mathcal{C}_c(\mathbb{R}^2)$ and further satisfies the mild regularity condition that near the origin

$$|f(\mathbf{p})| \leq C |\ln |\mathbf{p}||^{-1-\alpha} \quad (\text{C.12})$$

for some constants $\alpha > 0$ and $C > 0$, then $f \in \mathcal{C}_c^E(\mathbb{R}^2)$.

APPENDIX C. CONSTRUCTION OF THE PHASE MEASURE

Proof First of all, note

$$I_0[f] = \int_{-\infty}^{\infty} dp_x \frac{f(p_x, 0)}{|p_x|} + \int_{-\infty}^{\infty} dp_y \frac{f(0, p_y)}{|p_y|} \quad (\text{C.13})$$

is finite for $f \in \mathcal{C}_c(\mathbb{R}^2)$ that satisfies (C.12). Note $I_\varepsilon[f]$ can be written as

$$I_\varepsilon[f] = \int_{-\infty}^{\infty} \frac{dx}{|x|} f(x, \frac{\varepsilon}{x}). \quad (\text{C.14})$$

We assume, upon decomposing into positive and negative parts, $f \geq 0$. For some $\delta > 0$, we decompose the above integral into four parts

$$\text{I} := \int_{|x| \geq \delta} \frac{dx}{|x|} f(x, \frac{\varepsilon}{x}) \quad (\text{C.15})$$

$$\text{II} := \int_{|x| \leq \frac{\varepsilon}{\delta}} \frac{dx}{|x|} f(x, \frac{\varepsilon}{x}) \quad (\text{C.16})$$

$$\text{III} := \int_{\sqrt{\varepsilon} \leq |x| \leq \delta} \frac{dx}{|x|} f(x, \frac{\varepsilon}{x}) \quad (\text{C.17})$$

$$\text{IV} := \int_{\frac{\varepsilon}{\delta} \leq |x| \leq \sqrt{\varepsilon}} \frac{dx}{|x|} f(x, \frac{\varepsilon}{x}) \quad (\text{C.18})$$

We now take the limit $\varepsilon \rightarrow 0$. (I) converges to $\int_{|x| \geq \delta} \frac{dx}{|x|} f(x, 0)$ by uniform continuity of the integrand.

(II) can be rewritten via the change of variable $y = \varepsilon/x$ to

$$\text{II} = \int_{|y| \geq \delta} \frac{dy}{|y|} f(\frac{\varepsilon}{y}, y) \xrightarrow{\varepsilon \rightarrow 0} \int_{|y| \geq \delta} \frac{dy}{|y|} f(0, y). \quad (\text{C.19})$$

For (III), note for δ small enough and $\varepsilon \leq \delta^2$, on the region $\sqrt{\varepsilon} \leq |x| \leq \delta$

$$f(x, \frac{\varepsilon}{x}) \leq C \left| \ln \left(\sqrt{x^2 + \frac{\varepsilon^2}{x^2}} \right) \right|^{-1-\alpha} \leq C \left| 2 \ln |x| \right|^{-1-\alpha}. \quad (\text{C.20})$$

Thus

$$\text{III} \leq \frac{C}{2} \int_{|x| \leq \delta} \frac{dx}{|x|} \left| \ln |x| \right|^{-1-\alpha} \leq \frac{C}{\alpha} \left| \ln |\delta| \right|^{-\alpha}. \quad (\text{C.21})$$

APPENDIX C. CONSTRUCTION OF THE PHASE MEASURE

The result for (IV) is similar via the change of variable $y = \varepsilon/x$. We can now conclude by taking the limit δ goes to 0. \square

Remark C.6 There are well behaved functions that are continuous and compactly supported but do not satisfy the condition (C.12), e.g. any smooth function that is nonzero at the origin. Thus, $\mathcal{C}_c^E(\mathbb{R}^2)$ is strictly contained in $\mathcal{C}_c(\mathbb{R}^2)$ for this example.

Remark C.7 For degenerate critical points that have a faster divergence (for example, see section 3.3.2), the regularity conditions also become more stringent.

Appendix D

Perturbative Derivation of the Quantum Boltzmann Equation

The Heisenberg equation of motion for the Hamiltonian (4.5),(4.7) are

$$i\dot{\gamma}_{sa}(\mathbf{k}) = \omega_s(k)\gamma_{sa}(\mathbf{k}) + \frac{\alpha}{2} \sum_b \sum_{s_2 s_3 s_4} \int d^d k_2 d^d k_3 d^d k_4 \delta^d(\mathbf{k}_1 + \mathbf{k}_2 - \mathbf{k}_3 - \mathbf{k}_4) \\ \times [T_{\mathbf{k}_4 \mathbf{k}_3 \mathbf{k}_2 \mathbf{k}}^{s_4 s_3 s_2 s} \gamma_{s_2 b}^\dagger(\mathbf{k}_2) \gamma_{s_3 b}(\mathbf{k}_3) \gamma_{s_4 a}(\mathbf{k}_4) - T_{\mathbf{k}_4 \mathbf{k}_3 \mathbf{k} \mathbf{k}_2}^{s_4 s_3 s s_2} \gamma_{s_2 b}^\dagger(\mathbf{k}_2) \gamma_{s_3 a}(\mathbf{k}_3) \gamma_{s_4 b}(\mathbf{k}_4)]. \quad (\text{D.1})$$

We shall write this using a self-explanatory shorthand notation as

$$i\dot{\gamma}_{1a} = \omega_1 \gamma_{1a} + \frac{\alpha}{2} \sum_b \int d_{234} \delta_{34}^{12} \left[T_{4321} \gamma_{2b}^\dagger \gamma_{3b} \gamma_{4a} - T_{4312} \gamma_{2b}^\dagger \gamma_{3a} \gamma_{4b} \right]. \quad (\text{D.2})$$

Hermiticity of the interaction Hamiltonian requires

$$T_{1234}^* = T_{4321}$$

APPENDIX D. PERTURBATIVE DERIVATION OF THE QUANTUM BOLTZMANN EQUATION

and, using the canonical anti-commutation relations, one can also impose the symmetry

$$T_{1234} = T_{2143}.$$

One can check that these relations are satisfied for the coefficient T_{1234} arising from the Coulomb interaction between electrons & holes in graphene by means of the explicit expression given in (Fritz *et al.*, 2008), Eq.(3.9). Using these symmetries, we have

$$i\dot{\gamma}_{1a} = \omega_1 \gamma_{1a} + \frac{\alpha}{2} \sum_b \int d_{234} \delta_{34}^{12} \left[T_{1234}^* \gamma_{2b}^\dagger \gamma_{3b} \gamma_{4a} + (3 \leftrightarrow 4) \right]. \quad (\text{D.3})$$

Introducing $\tilde{\gamma}_{1a} = e^{i\omega_1 t} \gamma_{1a}$, we have

$$i \frac{d}{dt} \tilde{\gamma}_{1a} = \frac{\alpha}{2} \sum_b \int d_{234} \delta_{34}^{12} e^{i\omega_{34}^{12} t} \left[T_{1234}^* \tilde{\gamma}_{2b}^\dagger \tilde{\gamma}_{3b} \tilde{\gamma}_{4a} + (3 \leftrightarrow 4) \right]. \quad (\text{D.4})$$

Here $\omega_{34}^{12} = \omega_{s_1}(k_1) + \omega_{s_2}(k_2) - \omega_{s_3}(k_3) - \omega_{s_4}(k_4)$. For simplicity, we shall omit the tilde “ \sim ” from now on. We shall calculate the mean occupation number n_1 perturbatively by expanding the creation/annihilation operators into a power series

$$\gamma_{1a} = \gamma_{1a}^{(0)} + \alpha \gamma_{1a}^{(1)} + \alpha^2 \gamma_{1a}^{(2)} + o(\alpha^2). \quad (\text{D.5})$$

A straightforward calculation gives

$$\gamma_{1a}^{(0)} = \gamma_{1a}(0) \quad (\text{D.6})$$

$$\gamma_{1a}^{(1)} = -\frac{i}{2} \sum_b \int d_{234} \delta_{34}^{12} \Delta_t(\omega_{34}^{12}) \left[T_{1234}^* \gamma_{2b}^\dagger \gamma_{3b} \gamma_{4a} + (3 \leftrightarrow 4) \right]. \quad (\text{D.7})$$

$$\begin{aligned} \gamma_{1a}^{(2)} &= \frac{1}{4} \sum_{b,c} \int d_{234567} \delta_{34}^{12} T_{1234}^* \\ &\times \left[E_t(\omega_{345}^{167}; \omega_{34}^{12}) \delta_{67}^{25} T_{2567} \gamma_{7b}^\dagger \gamma_{6c}^\dagger \gamma_{5c} \gamma_{3b} \gamma_{4a} - E_t(\omega_{467}^{125}; \omega_{34}^{12}) \delta_{67}^{35} T_{3567}^* \gamma_{2b}^\dagger \gamma_{5c}^\dagger \gamma_{6c} \gamma_{7b} \gamma_{4a} \right] \end{aligned}$$

APPENDIX D. PERTURBATIVE DERIVATION OF THE QUANTUM BOLTZMANN EQUATION

$$- \left[E_t(\omega_{367}^{125}; \omega_{34}^{12}) \delta_{67}^{45} T_{4567}^* \gamma_{2b}^\dagger \gamma_{3b}^\dagger \gamma_{5c}^\dagger \gamma_{6c}^\dagger \gamma_{7a} + (6 \leftrightarrow 7) + (3 \leftrightarrow 4) + (3 \leftrightarrow 4, 6 \leftrightarrow 7) \right] \quad (\text{D.8})$$

where we employ the standard definitions (Benney and Newell, 1969):

$$\Delta_t(x) = \int_0^t \exp(ixs) ds, \quad E_t(x, y) = \int_0^t \Delta_s(x - y) \exp(isy) ds. \quad (\text{D.9})$$

We shall omit (0)-superscript below, when there is no possibility of confusion. The mean occupation number is obtained perturbatively by substituting (D.5) into $\langle \gamma_{1'a}^\dagger \gamma_{1a} \rangle$.

$$\langle \gamma_{1'a}^\dagger \gamma_{1a} \rangle = \langle \gamma_{1'a}^{(0)\dagger} \gamma_{1a}^{(0)} \rangle + \alpha \left(\langle \gamma_{1'a}^{(0)\dagger} \gamma_{1a}^{(1)} \rangle + c.c \right) + \alpha^2 \left(\langle \gamma_{1'a}^{(0)\dagger} \gamma_{1a}^{(2)} \rangle + c.c + \langle \gamma_{1'a}^{(1)\dagger} \gamma_{1a}^{(1)} \rangle \right). \quad (\text{D.10})$$

We assume as initial condition a fermionic quasi-free state with the 2nd-order correlations $\langle \gamma_{1'a}^\dagger \gamma_{1b} \rangle = n_1 \delta_{1'}^1 \delta_{s_1'}^{s_1} \delta_b^a$, $\langle \gamma_{1'a}^\dagger \gamma_{1b}^\dagger \rangle = \tilde{n}_1 \delta_{1'}^1 \delta_{s_1'}^{s_1} \delta_b^a$ and $\tilde{n}_1 = 1 - n_1$. Substituting (D.6)-(D.8) into (D.10), we have

$$\langle \gamma_{1'a}^{(0)\dagger} \gamma_{1a}^{(1)} \rangle = -\frac{i}{2} \sum_b \int d_{234} \Delta_t(\omega_{34}^{12}) \left[T_{1234}^* \langle \gamma_{1'a}^\dagger \gamma_{2b}^\dagger \gamma_{3b}^\dagger \gamma_{4a} \rangle + (3 \leftrightarrow 4) \right] \quad (\text{D.11})$$

$$\begin{aligned} \langle \gamma_{1'a}^{(0)\dagger} \gamma_{1a}^{(2)} \rangle &= \frac{1}{4} \sum_{b,c} \int d_{234567} \delta_{34}^{12} T_{1234}^* \\ &\times \left[\begin{aligned} &E_t(\omega_{345}^{167}; \omega_{34}^{12}) \delta_{67}^{25} T_{2567} \langle \gamma_{1'a}^\dagger \gamma_{7b}^\dagger \gamma_{6c}^\dagger \gamma_{5c}^\dagger \gamma_{3b}^\dagger \gamma_{4a} \rangle \\ &- E_t(\omega_{467}^{125}; \omega_{34}^{12}) \delta_{67}^{35} T_{3567}^* \langle \gamma_{1'a}^\dagger \gamma_{2b}^\dagger \gamma_{5c}^\dagger \gamma_{6c}^\dagger \gamma_{7b}^\dagger \gamma_{4a} \rangle \\ &- E_t(\omega_{367}^{125}; \omega_{34}^{12}) \delta_{67}^{45} T_{4567}^* \langle \gamma_{1'a}^\dagger \gamma_{2b}^\dagger \gamma_{3b}^\dagger \gamma_{5c}^\dagger \gamma_{6c}^\dagger \gamma_{7a} \rangle \end{aligned} \right\} \begin{matrix} I \\ II \\ III \end{matrix} \\ &+ (6 \leftrightarrow 7) + (3 \leftrightarrow 4) + (3 \leftrightarrow 4, 6 \leftrightarrow 7) \end{aligned} \quad (\text{D.12})$$

$$\begin{aligned} \langle \gamma_{1'a}^{(1)\dagger} \gamma_{1a}^{(1)} \rangle &= \frac{1}{4} \sum_{b,c} \int d_{234567} \delta_{34}^{1'2} \delta_{67}^{15} T_{1'234} \Delta_t(-\omega_{34}^{1'2}) \Delta_t(\omega_{34}^{12}) \\ &\times \left[T_{1567}^* \langle \gamma_{4a}^\dagger \gamma_{3b}^\dagger \gamma_{2b}^\dagger \gamma_{5c}^\dagger \gamma_{6c}^\dagger \gamma_{7a} \rangle + (6 \leftrightarrow 7) + (3 \leftrightarrow 4) + (3 \leftrightarrow 4, 6 \leftrightarrow 7) \right] \quad (\text{D.13}) \end{aligned}$$

APPENDIX D. PERTURBATIVE DERIVATION OF THE QUANTUM BOLTZMANN EQUATION

Using Wick's rule, we have

$$\langle \gamma_{1'a}^{(0)\dagger} \gamma_{1a}^{(1)} \rangle = it \delta_{1'}^1 \Omega_1 n_1 \quad (\text{D.14})$$

$$\langle \gamma_{1'a}^{(0)\dagger} \gamma_{1a}^{(2)} \rangle = \delta_{1'}^1 (\text{I} + \text{II} + \text{III}) \quad (\text{D.15})$$

$$\langle \gamma_{1'a}^{(1)\dagger} \gamma_{1a}^{(1)} \rangle = \delta_{1'}^1 (\text{IV}) \quad (\text{D.16})$$

where

$$\begin{aligned} \text{I} &= - \int d_{234} \delta_{34}^{12} E_t(0; \omega_{34}^{12}) R_{1234} n_1 n_3 n_4 + E_t(0; 0) \int d_2 \Omega_2 (NT_{1221} - T_{1212}) n_2 \\ \text{II} &= \int d_{234} \delta_{34}^{12} E_t(0; \omega_{34}^{12}) R_{1234} (n_1 n_2 n_4 + n_1 n_2 n_3) - E_t(0; 0) \int d_2 \frac{\Omega_1 + \Omega_2}{2} (NT_{1221} - T_{1212}) n_2 \\ \text{III} &= - \int d_{234} \delta_{34}^{12} E_t(0; \omega_{34}^{12}) R_{1234} (n_1 n_2 \tilde{n}_3 + n_1 n_2 \tilde{n}_4) - E_t(0; 0) \int d_2 \frac{\Omega_1 + \Omega_2}{2} (NT_{1221} - T_{1212}) n_2 \\ \text{IV} &= \int d_{234} \delta_{34}^{12} |\Delta_t(\omega_{34}^{12})|^2 R_{1234} \tilde{n}_2 n_3 n_4 + \frac{1}{2} |\Delta_t(0)|^2 \Omega_1^2 n_1 \end{aligned} \quad (\text{D.17})$$

with

$$R_{1234} = \frac{1}{2} T_{1234}^* (NT_{1234} - T_{1243}) + (3 \leftrightarrow 4) \quad (\text{D.18})$$

$$\Omega_1 = \int d_2 (NT_{1221} - T_{1212}) n_2. \quad (\text{D.19})$$

Now, recalling the standard relations (Benney and Newell, 1969)

$$E_t(0; 0) = \frac{t^2}{2}, \quad \Delta_t(0) = t, \quad (\text{D.20})$$

we see that the terms which involve these factors in the previous expressions are undesirable. Their growth is $O(t^2)$ at long times, by far the most secular behavior, but they do not correspond to terms in the expected kinetic equation. Fortunately, it is straightforward to check that the sum of all these undesirable terms arising from I-IV exactly cancel. Also, the $O(\alpha)$ term from (D.14) has vanishing

APPENDIX D. PERTURBATIVE DERIVATION OF THE QUANTUM BOLTZMANN EQUATION

real part and thus gives a zero contribution to the evolution of the occupation numbers. Then, using

$$2 \operatorname{Re} E_t(0; x) = |\Delta_t(x)|^2 = \frac{2(1 - \cos(xt))}{x^2}, \quad (\text{D.21})$$

and

$$n_1 n_3 n_4 - n_1 n_2 n_4 - n_1 n_2 n_3 + n_1 n_2 \tilde{n}_3 + n_1 n_2 \tilde{n}_4 - \tilde{n}_2 n_3 n_4 = n_1 n_2 \tilde{n}_3 \tilde{n}_4 - \tilde{n}_1 \tilde{n}_2 n_3 n_4, \quad (\text{D.22})$$

together with $\langle \gamma_{1'a}^\dagger \gamma_{1a} \rangle = n_1 \delta_{1'}^1$, we can combine (D.15)-(D.16) to get

$$n_1(t) = n_1(0) - \alpha^2 \int d_{234} \delta_{34}^{12} \frac{2(1 - \cos(\omega_{34}^{12} t))}{(\omega_{34}^{12})^2} R_{1234} (n_1 n_2 \tilde{n}_3 \tilde{n}_4 - \tilde{n}_1 \tilde{n}_2 n_3 n_4). \quad (\text{D.23})$$

This is equivalent to the expression (4.9) in the text.

There is another approach in the literature for dealing with the undesirable $O(t^2)$ terms which we should briefly mention. It is possible to exactly remove those terms by a *frequency renormalization* (Zakharov *et al.*, 1992; Nazarenko, 2011; Newell and Rumpf, 2011), introducing

$$\tilde{\omega}_1 = \omega_1 + \alpha \Omega_1$$

into the Heisenberg equations (D.3), which then becomes

$$i\dot{\gamma}_{1a} = \tilde{\omega}_1 \gamma_{1a} + \frac{\alpha}{2} \sum_b \int d_{234} \delta_{34}^{12} \left[T_{1234}^* \left(\gamma_{2b}^\dagger \gamma_{3b} \gamma_{4a} - \langle \gamma_{2b}^\dagger \gamma_{3b} \rangle \gamma_{4a} + \langle \gamma_{2b}^\dagger \gamma_{4a} \rangle \gamma_{3b} \right) + (3 \leftrightarrow 4) \right]. \quad (\text{D.24})$$

The rest of the derivation is as before, except that now one defines $\tilde{\gamma}_{1a} = e^{i\tilde{\omega}_1 t} \gamma_{1a}$ using the renormalized frequency. The counterterms which appear in the renormalized Heisenberg equations of motion can be readily checked to cancel all of the $O(t^2)$ terms in each of the individual expressions I-IV, without the necessity of adding them together. The final result is the same as (D.23) except that ω_{34}^{12} is replaced with $\tilde{\omega}_{34}^{12} = \tilde{\omega}_1 + \tilde{\omega}_2 - \tilde{\omega}_3 - \tilde{\omega}_4$.

APPENDIX D. PERTURBATIVE DERIVATION OF THE QUANTUM BOLTZMANN EQUATION

This alternate procedure yields the same kinetic equation as discussed in the text, but with bare frequencies replaced by renormalized frequencies. There might thus naively appear to be an inconsistency between the two approaches. In particular, the quantum Boltzmann equation for electrons in graphene obtained by the alternate procedure would disagree with that derived previously (Kashuba, 2008; Fritz *et al.*, 2008), with the bare frequency $\omega_s(\mathbf{k}) = sv_F k$ undergoing an additional renormalization or, equivalently, with an additional renormalization of the Fermi velocity v_F . However, this inconsistency is only apparent. As is well-known in the wave turbulence literature (e.g. (Zakharov *et al.*, 1992) p.71), the two approaches lead to equivalent kinetic equations to order $O(\alpha^2)$, since the frequency renormalization is $O(\alpha)$ and thus corrects the kinetic equation only to order $O(\alpha^3)$. The frequency renormalization is therefore entirely optional in the derivation of the kinetic equation at order $O(\alpha^2)$. The consistency of the two approaches is further evidenced by the fact that the undesirable $O(t^2)$ terms cancel completely at order $O(\alpha^2)$ without any use of a frequency renormalization.

Appendix E

Lattice Wigner Function in Finite Volume

In this appendix, we generalize the spectrum defined in section 2.3 by introducing the Wigner function. To our knowledge, not many works in the literature discussed Wigner functions for lattice systems. Mielke (2006) considered the lattice Wigner function as the standard continuum Wigner function supported on the lattice and applied results from Markowich *et al.* (1997). In contrast, Marcià (2004), Spohn (2006), and Lukkarinen and Spohn (2007) defined the lattice Wigner function as a distribution. These authors start in an infinite-volume lattice and then consider the zero-lattice-spacing limit. However to understand how the closure equations arise from a physical system, it is crucial to consider systems with finite volume. Mathematically, keeping the lattice spacing fixed has the benefit of avoiding the known hard problem of constructing limiting random field on $a\mathbb{Z}^d$ as $a \rightarrow 0$ (Glimm and Jaffe, 1987). For these reasons we shall define the lattice Wigner function in finite volume and also keep the lattice spacing a fixed as we did for the spectrum in Chap. 2.

APPENDIX E. LATTICE WIGNER FUNCTION IN FINITE VOLUME

First we define the empirical Wigner function on the finite-volume lattice

$$\widehat{W}_L(\mathbf{k}, \mathbf{x}) = \sum_{\boldsymbol{\eta} \in \Lambda_L^*} e^{2i\boldsymbol{\eta} \cdot \mathbf{x}} \widetilde{A}(\mathbf{k} + \boldsymbol{\eta}) \widetilde{A}^*(\mathbf{k} - \boldsymbol{\eta}), \quad (\mathbf{k}, \mathbf{x}) \in \Gamma_L = \Lambda_L^* \times \Lambda_L. \quad (\text{E.1})$$

Note there is no average involved in the definition and the empirical Wigner function is indeed a random variable with information on the fluctuations of the Fourier coefficients. We want the definition to guarantee both the scale and spatial locality of the Wigner function. We summarize the properties in the following Proposition.

Proposition E.1 *The empirical Wigner function defined in (E.1) satisfies the following properties:*

- (i) $\widehat{W}_L(\mathbf{k}, \mathbf{x})$ is real;
- (ii) $\left(\frac{2\pi}{L}\right)^d \sum_{\mathbf{k} \in \Lambda_L^*} \widehat{W}_L(\mathbf{k}, \mathbf{x}) = |u(\mathbf{x})|^2$;
- (iii) $\left(\frac{a}{L}\right)^d \sum_{\mathbf{x} \in \Lambda_L} \widehat{W}_L(\mathbf{k}, \mathbf{x}) = |\widetilde{A}(\mathbf{k})|^2$.

We require $M = L/a$ to be an odd integer.

The requirement that M is odd helps to establish the following useful lemma that is essential in the proof of Prop. E.1.

Lemma E.2 *For M an odd integer, there is a unique solution $x \in \mathbb{Z}_M$ of the equation $2x \equiv z \pmod{M}$ for any $z \in \mathbb{Z}_M$.*

Proof If z is an even integer, then $x = z/2$. If z is an odd integer, then $x = (z + M)/2$. If there is another integer y that also solves the equation, then $2(x - y)$ is an integer multiple of M . Since M is odd, $x - y$ is also an integer multiple of M . \square

We can now prove the properties of the empirical Wigner function.

Proof of Prop. E.1 (i) It is easy to check $W_L(\mathbf{k}, \mathbf{x}) = W_L^*(\mathbf{k}, \mathbf{x})$ by taking $\boldsymbol{\eta} \rightarrow -\boldsymbol{\eta}$.

APPENDIX E. LATTICE WIGNER FUNCTION IN FINITE VOLUME

(ii) We first define the Kronecker delta function on a discrete lattice Λ_L to be

$$\delta_{\Lambda_L}(\mathbf{x}) = \begin{cases} 1, & \text{if } \frac{x_i}{a} \text{ is an integer and } \frac{x_i}{a} \equiv 0 \pmod{M} \text{ for all } i = 1, \dots, d \\ 0, & \text{otherwise} \end{cases} \quad (\text{E.2})$$

Note then

$$\begin{aligned} \sum_{\mathbf{k} \in \Lambda_L^*} \tilde{A}(\mathbf{k} + \mathbf{p}) \tilde{A}^*(\mathbf{k} - \mathbf{q}) &= \left(\frac{L}{2\pi}\right)^d \frac{1}{N^2} \sum_{\mathbf{k} \in \Lambda_L^*} \sum_{\mathbf{x}, \mathbf{x}' \in \Lambda_L} u(\mathbf{x}) e^{-i(\mathbf{k} + \mathbf{p}) \cdot \mathbf{x}} u^*(\mathbf{x}') e^{i(\mathbf{k} - \mathbf{q}) \cdot \mathbf{x}'} \\ &= \left(\frac{a}{2\pi}\right)^d \sum_{\mathbf{x}, \mathbf{x}' \in \Lambda_L} u(\mathbf{x}) u^*(\mathbf{x}') e^{-i(\mathbf{p} \cdot \mathbf{x} + \mathbf{q} \cdot \mathbf{x}')} \frac{1}{N} \sum_{\mathbf{k} \in \Lambda_L^*} e^{-i\mathbf{k} \cdot (\mathbf{x} - \mathbf{x}')} \\ &= \left(\frac{a}{2\pi}\right)^d \sum_{\mathbf{x} \in \Lambda_L} |u(\mathbf{x})|^2 e^{-i(\mathbf{p} + \mathbf{q}) \cdot \mathbf{x}} \end{aligned} \quad (\text{E.3})$$

where in the last equality we use the fact that $\frac{1}{N} \sum_{\mathbf{k} \in \Lambda_L^*} e^{-i\mathbf{k} \cdot (\mathbf{x} - \mathbf{x}')} = \delta_{\Lambda_L}(\mathbf{x} - \mathbf{x}')$. Hence

$$\begin{aligned} \left(\frac{2\pi}{L}\right)^d \sum_{\mathbf{k} \in \Lambda_L^*} \widehat{W}_L(\mathbf{k}, \mathbf{x}) &= \left(\frac{2\pi}{L}\right)^d \sum_{\boldsymbol{\eta} \in \Lambda_L^*} e^{2i\boldsymbol{\eta} \cdot \mathbf{x}} \sum_{\mathbf{k} \in \Lambda_L^*} \tilde{A}(\mathbf{k} + \boldsymbol{\eta}) \tilde{A}^*(\mathbf{k} - \boldsymbol{\eta}) \\ &= \frac{1}{N} \sum_{\boldsymbol{\eta}} e^{2i\boldsymbol{\eta} \cdot \mathbf{x}} \sum_{\mathbf{x}'} |u(\mathbf{x}')|^2 e^{-2i\boldsymbol{\eta} \cdot \mathbf{x}'} \\ &= |u(\mathbf{x})|^2 \end{aligned} \quad (\text{E.4})$$

where in the last equality we use the fact that $\frac{1}{N} \sum_{\boldsymbol{\eta}} e^{2i\boldsymbol{\eta} \cdot (\mathbf{x} - \mathbf{x}')} = \delta_{\Lambda_L}(2(\mathbf{x} - \mathbf{x}')) = \delta_{\Lambda_L}(\mathbf{x} - \mathbf{x}')$. This follows directly from Lemma E.2 if we write $\delta_{\Lambda_L}(2\mathbf{x}) = \prod_{i=1}^d \delta_{\mathbb{Z}_M}(2x_i/a)$.

(iii) Define the Kronecker delta function on a discrete lattice Λ_L^* to be

$$\delta_{\Lambda_L^*}(\boldsymbol{\eta}) = \begin{cases} 1, & \text{if } \frac{L\eta_i}{2\pi} \text{ is an integer and } \frac{L\eta_i}{2\pi} \equiv 0 \pmod{M} \text{ for all } i = 1, \dots, d \\ 0, & \text{otherwise} \end{cases} \quad (\text{E.5})$$

By Lemma E.2, we have $\delta_{\Lambda_L^*}(2\boldsymbol{\eta}) = \prod_{i=1}^d \delta_{\mathbb{Z}_M}(\frac{L}{\pi}\eta_i) = \prod_{i=1}^d \delta_{\mathbb{Z}_M}(\frac{L}{2\pi}\eta_i) = \delta_{\Lambda_L^*}(\boldsymbol{\eta})$. Hence

APPENDIX E. LATTICE WIGNER FUNCTION IN FINITE VOLUME

$\frac{1}{N} \sum_{\mathbf{r} \in \Lambda_L^*} e^{2i\boldsymbol{\eta} \cdot \mathbf{r}} = \delta_{\Lambda_L^*}(2\boldsymbol{\eta}) = \delta_{\Lambda_L^*}(\boldsymbol{\eta})$. Therefore

$$\frac{1}{N} \sum_{\mathbf{x} \in \Lambda_L} \sum_{\boldsymbol{\eta} \in \Lambda_L^*} e^{2i\boldsymbol{\eta} \cdot \mathbf{x}} \tilde{A}(\mathbf{k} + \boldsymbol{\eta}) \tilde{A}^*(\mathbf{k} - \boldsymbol{\eta}) = |\tilde{A}(\mathbf{k})|^2. \quad (\text{E.6})$$

□

We now extend the definition of the empirical Wigner function \widehat{W}_L to the continuum

$$\widehat{W}_L^c(\mathbf{k}, \boldsymbol{\xi}) = \widehat{W}_L(\mathbf{k}_L, \mathbf{x}_L), \quad (\mathbf{k}, \boldsymbol{\xi}) \in \Gamma = \frac{2\pi}{a} \mathbb{T}^d \times \mathbb{T}^d. \quad (\text{E.7})$$

Recall the notation introduced in section 2.2 the d -torus $\mathbb{T}^d = [-\frac{1}{2}, \frac{1}{2}]^d$. Here the wavevector $\mathbf{k}_L = \lfloor \frac{\mathbf{k}L}{2\pi} \rfloor \cdot \frac{2\pi}{L} \in \Lambda_L^*$ converges to \mathbf{k} . Note that $\boldsymbol{\xi}$ is a dimensionless position (rescaled by L), in contrast to $\mathbf{x} \in \Lambda_L$ in the earlier discussions. The lattice location $\mathbf{x}_L = \lfloor \frac{L\boldsymbol{\xi}}{a} \rfloor \cdot a \in \Lambda_L$ and $\frac{1}{L}\mathbf{x}_L$ converges to $\boldsymbol{\xi}$ in the infinite-volume limit. We denote $\lfloor \cdot \rfloor$ the integer part. We now define the finite-volume mean Wigner function on the continuum as (c.f. Spohn (2006, eq.(3.23)))

$$W_L(\mathbf{k}, \boldsymbol{\xi}) = \left\langle \widehat{W}_L^c(\mathbf{k}, \boldsymbol{\xi}) \right\rangle, \quad (\mathbf{k}, \boldsymbol{\xi}) \in \Gamma. \quad (\text{E.8})$$

and assume its infinite-volume limit

$$W(\mathbf{k}, \boldsymbol{\xi}) = \lim_{L \rightarrow \infty} W_L(\mathbf{k}, \boldsymbol{\xi}) \quad (\text{E.9})$$

is well-defined and finite almost everywhere. Similarly, we define the finite-volume multiple-point Wigner function on Γ^n (c.f. Spohn (2006, eq.(3.24)))

$$W_L(\mathbf{k}_1, \boldsymbol{\xi}_1, \dots, \mathbf{k}_n, \boldsymbol{\xi}_n) = \left\langle \prod_{i=1}^n \widehat{W}_L^c(\mathbf{k}_i, \boldsymbol{\xi}_i) \right\rangle \quad (\text{E.10})$$

APPENDIX E. LATTICE WIGNER FUNCTION IN FINITE VOLUME

and assume

$$W(\mathbf{k}_1, \boldsymbol{\xi}_1, \dots, \mathbf{k}_n, \boldsymbol{\xi}_n) = \lim_{L \rightarrow \infty} W_L(\mathbf{k}_1, \boldsymbol{\xi}_1, \dots, \mathbf{k}_n, \boldsymbol{\xi}_n) \quad (\text{E.11})$$

is well-defined and finite almost everywhere. The Prop. E.1 then implies the following corollary for the Wigner function $W(\mathbf{k}, \mathbf{x})$.

Corollary E.3 *Assume $\|W_L\|_{L^\infty(\Gamma)}$ is bounded uniformly in L and the limit (E.9) exists almost everywhere. Then the Wigner function $W(\mathbf{k}, \boldsymbol{\xi})$ satisfies*

(i) $W(\mathbf{k}, \boldsymbol{\xi})$ is real;

(ii) $\int_{\frac{2\pi}{a}\mathbb{T}^d} d^d k W(\mathbf{k}, \boldsymbol{\xi}) = \lim_{L \rightarrow \infty} \langle |u_L(\mathbf{x}_L)|^2 \rangle$ a.e. where $\mathbf{x}_L = \lfloor \frac{L\boldsymbol{\xi}}{a} \rfloor \cdot a$;

(iii) $\int_{\mathbb{T}^d} d^d \xi W(\mathbf{k}, \boldsymbol{\xi}) = n(\mathbf{k})$ a.e..

Proof (i) This follows from the reality of $\widehat{W}_L(\mathbf{k}_L, \mathbf{x}_L)$.

(ii) Note

$$\int_{\frac{2\pi}{a}\mathbb{T}^d} d^d k \widehat{W}_L^c(\mathbf{k}, \boldsymbol{\xi}) = \left(\frac{2\pi}{L}\right)^d \sum_{\mathbf{k} \in \Lambda_L^*} \widehat{W}_L(\mathbf{k}, \mathbf{x}_L) = |u_L(\mathbf{x}_L)|^2 \quad (\text{E.12})$$

Hence

$$\int_{\frac{2\pi}{a}\mathbb{T}^d} d^d k W(\mathbf{k}, \boldsymbol{\xi}) = \int_{\frac{2\pi}{a}\mathbb{T}^d} d^d k \lim_{L \rightarrow \infty} \langle \widehat{W}_L^c(\mathbf{k}, \boldsymbol{\xi}) \rangle = \lim_{L \rightarrow \infty} \langle |u_L(\mathbf{x}_L)|^2 \rangle. \quad (\text{E.13})$$

The second equality follows from dominated convergence theorem.

(iii) Note

$$\int_{\mathbb{T}^d} d^d \xi \widehat{W}_L^c(\mathbf{k}, \boldsymbol{\xi}) = \left(\frac{a}{L}\right)^d \sum_{\mathbf{x} \in \Lambda_L^*} \widehat{W}_L(\mathbf{k}, \mathbf{x}) = |\tilde{A}_L(\mathbf{k})|^2. \quad (\text{E.14})$$

Hence

$$\int_{\mathbb{T}^d} d^d \xi W(\mathbf{k}, \boldsymbol{\xi}) = \int_{\mathbb{T}^d} d^d \xi \lim_{L \rightarrow \infty} \langle \widehat{W}_L^c(\mathbf{k}, \boldsymbol{\xi}) \rangle = \lim_{L \rightarrow \infty} \langle |\tilde{A}_L(\mathbf{k})|^2 \rangle = n(\mathbf{k}). \quad (\text{E.15})$$

APPENDIX E. LATTICE WIGNER FUNCTION IN FINITE VOLUME

The second equality follows from dominated convergence theorem and the last equality follows from definition (2.25). \square

From property (iii), we see that the Wigner function $W(\mathbf{k}, \boldsymbol{\xi})$ reduces to the spectrum $n(\mathbf{k})$ defined in (2.25) when the ensemble is spatially homogeneous. One can define the condition of statistical independence of far apart regions (c.f. Spohn (2006, eq.(3.26)))

$$\lim_{L \rightarrow \infty} \left[W_L(\mathbf{k}_1, \boldsymbol{\xi}_1, \mathbf{k}_2, \boldsymbol{\xi}_2) - W_L(\mathbf{k}_1, \boldsymbol{\xi}_1) W_L(\mathbf{k}_2, \boldsymbol{\xi}_2) \right] = 0 \quad (\text{E.16})$$

for $\boldsymbol{\xi}_1 \neq \boldsymbol{\xi}_2$. When this condition holds, the empirical Wigner function $\widehat{W}_L^c(\mathbf{k}, \boldsymbol{\xi})$ as $L \rightarrow \infty$ converges in probability to the Wigner function $W(\mathbf{k}, \boldsymbol{\xi})$ in weak- \star topology on Radon measures on Γ . The proof is similar to the law of large numbers given in section 2.3. By definition,

$$\lim_{L \rightarrow \infty} \left\langle \widehat{W}_L^c(\mathbf{k}, \boldsymbol{\xi}) \right\rangle = W(\mathbf{k}, \boldsymbol{\xi})$$

Therefore, it is enough to show that

$$\lim_{L \rightarrow \infty} \left\langle \left| \int_{\Gamma} d^d k d^d \xi \lambda(\mathbf{k}, \boldsymbol{\xi}) \widehat{W}_L^c(\mathbf{k}, \boldsymbol{\xi}) - \int_{\Gamma} d^d k d^d \xi \lambda(\mathbf{k}, \boldsymbol{\xi}) W_L(\mathbf{k}, \boldsymbol{\xi}) \right|^2 \right\rangle = 0$$

for any continuous function $\lambda(\mathbf{k}, \boldsymbol{\xi})$ on Γ . Now a direct calculation of the above average shows that it equals

$$\int_{\Gamma^2} d^d k_1 d^d k_2 d^d \xi_1 d^d \xi_2 \lambda(\mathbf{k}_1, \boldsymbol{\xi}_1) \lambda(\mathbf{k}_2, \boldsymbol{\xi}_2) \left[W_L(\mathbf{k}_1, \boldsymbol{\xi}_1; \mathbf{k}_2, \boldsymbol{\xi}_2) - W_L(\mathbf{k}_1, \boldsymbol{\xi}_1) W_L(\mathbf{k}_2, \boldsymbol{\xi}_2) \right]$$

Assuming condition (E.16) and that the integrand is bounded almost everywhere uniformly in L , we have the result by dominated convergence theorem.

Appendix F

Derivation of the Linear Transport Equation for the Wigner Function

Our starting point for deriving the linear transport equation is the following equation of motion defined by a discrete pseudo-differential operator

$$\frac{dA_{\mathbf{k}}^{\sigma}}{dt} = \frac{i\sigma}{N} \sum_{\mathbf{p} \in \Lambda_L^*} \sum_{\mathbf{r} \in \Lambda_L} \omega\left(\frac{\mathbf{k} + \mathbf{p}}{2}, \mathbf{r}\right) A_{\mathbf{p}}^{\sigma} e^{-i\sigma(\mathbf{k} - \mathbf{p}) \cdot \mathbf{r}}. \quad (\text{F.1})$$

Such equations with a spatially-dependent frequency may arise from the boundary condition of a spatially-varying topography (Long, 1973), or from the frequency renormalization of an n -wave ($n > 3$) weakly interacting system (Zakharov *et al.*, 1992; Nazarenko, 2011). To illustrate the latter, we consider the Hamiltonian density with 4-wave resonance

$$H = H_0 + \delta H = \sum_{\mathbf{k}} \omega(\mathbf{k}) |A_{\mathbf{k}}|^2 + \frac{\epsilon^2}{2} \sum_{\mathbf{k}_1, \mathbf{k}_2, \mathbf{k}_3, \mathbf{k}_4} A_{\mathbf{k}_1}^* A_{\mathbf{k}_2}^* A_{\mathbf{k}_3} A_{\mathbf{k}_4} \delta_{\mathbf{k}_1 + \mathbf{k}_2, \mathbf{k}_3 + \mathbf{k}_4}. \quad (\text{F.2})$$

APPENDIX F. THE FORMAL DERIVATION OF THE LINEAR TRANSPORT EQUATION FOR THE WIGNER FUNCTION

This is the example of frequency renormalization considered by Newell *et al.* (2012). The Hamiltonian equations of motion for the Fourier coefficients are

$$\frac{dA_{\mathbf{k}}}{dt} = i \frac{\partial H}{\partial A_{\mathbf{k}}^*} = i\omega(\mathbf{k})A_{\mathbf{k}} + i\epsilon^2 \sum_{\mathbf{k}_2, \mathbf{k}_3, \mathbf{k}_4} A_{\mathbf{k}_2}^* A_{\mathbf{k}_3} A_{\mathbf{k}_4} \delta_{\mathbf{k}+\mathbf{k}_2, \mathbf{k}_3+\mathbf{k}_4}. \quad (\text{F.3})$$

We define $\widehat{W}_L^<(\mathbf{k}, \boldsymbol{\eta}) = \widetilde{A}(\mathbf{k} + \boldsymbol{\eta}) \widetilde{A}^*(\mathbf{k} - \boldsymbol{\eta})$. Note that this is the Fourier transform of the empirical Wigner function \widehat{W}_L defined in (E.1), if we define the Fourier transform by ¹

$$\widehat{W}_L^<(\mathbf{k}, \boldsymbol{\eta}) = \frac{1}{N} \sum_{\mathbf{r} \in \Lambda_L} \widehat{W}_L(\mathbf{k}, \mathbf{r}) e^{-2i\boldsymbol{\eta} \cdot \mathbf{r}}, \quad \boldsymbol{\eta} \in \Lambda_L^*. \quad (\text{F.4})$$

Then the equation of motion for normalized $\widetilde{A}_{\mathbf{k}}$ is given by

$$\frac{d\widetilde{A}_{\mathbf{k}}}{dt} = i\omega(\mathbf{k})\widetilde{A}_{\mathbf{k}} + i\epsilon^2 \left(\frac{2\pi}{L} \right)^d \sum_{\mathbf{k}_2, \mathbf{k}_4 \in \Lambda_L^*} \widehat{W}_L^< \left(\mathbf{k}_2 + \frac{\mathbf{k} - \mathbf{k}_4}{2}, \frac{\mathbf{k} - \mathbf{k}_4}{2} \right) \widetilde{A}_{\mathbf{k}_4}. \quad (\text{F.5})$$

We can then write (F.5) as

$$\frac{d\widetilde{A}_{\mathbf{k}}}{dt} = \frac{i}{N} \sum_{\mathbf{p} \in \Lambda_L^*} \sum_{\mathbf{r} \in \Lambda_L} \left(\omega \left(\frac{\mathbf{k} + \mathbf{p}}{2} \right) + \epsilon^2 \left(\frac{2\pi}{L} \right)^d \sum_{\mathbf{k}_2 \in \Lambda_L^*} \widehat{W}_L \left(\mathbf{k}_2 + \frac{\mathbf{k} - \mathbf{p}}{2}, \mathbf{r} \right) \right) e^{-i(\mathbf{k} - \mathbf{p}) \cdot \mathbf{r}} \widetilde{A}_{\mathbf{p}}. \quad (\text{F.6})$$

Here $\frac{\mathbf{k} - \mathbf{p}}{2}$ is a lattice vector if we assume $M = L/a$ is an odd integer as we did in Appendix E, In that case, it can be shifted away in the above equation. Averaging over inhomogeneous ensembles and employing Wick's rule to decouple the average, we have

$$\frac{d\widetilde{A}_{\mathbf{k}}}{dt} = \frac{i}{N} \sum_{\mathbf{p} \in \Lambda_L^*} \sum_{\mathbf{r} \in \Lambda_L} \left(\omega \left(\frac{\mathbf{k} + \mathbf{p}}{2} \right) + 2\epsilon^2 \left(\frac{2\pi}{L} \right)^d \sum_{\mathbf{k}_2 \in \Lambda_L^*} W_L \left(\mathbf{k}_2, \frac{\mathbf{r}}{L} \right) \right) e^{-i(\mathbf{k} - \mathbf{p}) \cdot \mathbf{r}} \widetilde{A}_{\mathbf{p}}. \quad (\text{F.7})$$

¹Recall the definition (E.1) $\widehat{W}_L(\mathbf{k}, \mathbf{x}) = \sum_{\boldsymbol{\eta} \in \Lambda_L^*} e^{2i\boldsymbol{\eta} \cdot \mathbf{x}} \widehat{W}_L^<(\mathbf{k}, \boldsymbol{\eta})$. Multiply both sides by $e^{-2i\boldsymbol{\eta}' \cdot \mathbf{x}}$ and sum over $\mathbf{x} \in \Lambda_L$, we have

$$\sum_{\mathbf{x}} \widehat{W}_L(\mathbf{k}, \mathbf{x}) e^{-2i\boldsymbol{\eta}' \cdot \mathbf{x}} = N \sum_{\boldsymbol{\eta}} \widehat{W}_L^<(\mathbf{k}, \boldsymbol{\eta}) \delta_{\Lambda_L^*}(2\boldsymbol{\eta} - 2\boldsymbol{\eta}') = \widehat{W}_L^<(\mathbf{k}, \boldsymbol{\eta}'),$$

where we have used Kronecker delta function $\delta_{\Lambda_L^*}$ defined in (E.5) and the relation $\delta_{\Lambda_L^*}(2\boldsymbol{\eta} - 2\boldsymbol{\eta}') = \delta_{\Lambda_L^*}(\boldsymbol{\eta} - \boldsymbol{\eta}')$ that follows from Lemma E.2 when $M = L/a$ is an odd integer.

APPENDIX F. THE FORMAL DERIVATION OF THE LINEAR TRANSPORT EQUATION FOR THE WIGNER FUNCTION

Note that the factor of 2 arises because (F.3) is symmetrical in $\mathbf{k}_3, \mathbf{k}_4$ and \mathbf{k}_2 can be contracted with both in applying Wick's rule.

We now begin our formal derivation of the linear transport equation. The equation of motion for the empirical Wigner function $\widehat{W}_L(\mathbf{k}, \mathbf{x})$ is

$$\frac{\partial \widehat{W}_L(\mathbf{k}, \mathbf{x}, t)}{\partial t} = \sum_{\boldsymbol{\eta} \in \Lambda_L^*} e^{2i\boldsymbol{\eta} \cdot \mathbf{x}} \frac{i}{N} \left\{ \sum_{(\mathbf{p}, \mathbf{r}) \in \Lambda_L^* \times \Lambda_L} \omega\left(\frac{\mathbf{k} + \boldsymbol{\eta} + \mathbf{p}}{2}, \mathbf{r}\right) e^{-i(\mathbf{k} + \boldsymbol{\eta} - \mathbf{p}) \cdot \mathbf{r}} \tilde{A}(\mathbf{p}, t) \tilde{A}^*(\mathbf{k} - \boldsymbol{\eta}, t) \right. \quad (\text{F.8})$$

$$\left. - \sum_{(\mathbf{p}, \mathbf{r}) \in \Lambda_L^* \times \Lambda_L} \omega\left(\frac{\mathbf{k} - \boldsymbol{\eta} + \mathbf{p}}{2}, \mathbf{r}\right) e^{i(\mathbf{k} - \boldsymbol{\eta} - \mathbf{p}) \cdot \mathbf{r}} \tilde{A}(\mathbf{k} + \boldsymbol{\eta}, t) \tilde{A}^*(\mathbf{p}, t) \right\} \quad (\text{F.9})$$

Introducing the change of variable through $2\boldsymbol{\eta}' = \boldsymbol{\eta} + \mathbf{p} - \mathbf{k}$ in (F.8) and $2\boldsymbol{\eta}' = \mathbf{k} - \mathbf{p} + \boldsymbol{\eta}$ in (F.9), we have

$$\partial_t \widehat{W}_L(\mathbf{k}, \mathbf{x}, t) = \frac{i}{N} \sum_{\boldsymbol{\eta}, \boldsymbol{\eta}' \in \Lambda_L^*} \sum_{\mathbf{r} \in \Lambda_L} e^{2i(\boldsymbol{\eta} \cdot \mathbf{x} - \boldsymbol{\eta}' \cdot \mathbf{r})} \left\{ \omega(\mathbf{k} + \boldsymbol{\eta}', \mathbf{r}) \widehat{W}_L^<(\mathbf{k} - \boldsymbol{\eta}'', \boldsymbol{\eta}') \right. \quad (\text{F.10})$$

$$\left. - \omega(\mathbf{k} - \boldsymbol{\eta}', \mathbf{r}) \widehat{W}_L^<(\mathbf{k} + \boldsymbol{\eta}'', \boldsymbol{\eta}') \right\}$$

where $\boldsymbol{\eta}'' = \boldsymbol{\eta} - \boldsymbol{\eta}'$. Now rescale by $\mathbf{x} = L\boldsymbol{\xi}$, then we have the equation of motion for \widehat{W}_L^c defined in (E.7)

$$\partial_t \widehat{W}_L^c(\mathbf{k}, \boldsymbol{\xi}, t) = \frac{i}{N} \sum_{\boldsymbol{\eta}, \boldsymbol{\eta}' \in \Lambda_L^*} \sum_{\boldsymbol{\rho} \in \frac{1}{L}\Lambda_L} e^{2iL(\boldsymbol{\eta} \cdot \boldsymbol{\xi} - \boldsymbol{\eta}' \cdot \boldsymbol{\rho})} \left\{ \tilde{\omega}(\mathbf{k} + \boldsymbol{\eta}', \boldsymbol{\rho}) \widehat{W}_L^<(\mathbf{k} - \boldsymbol{\eta}'', \boldsymbol{\eta}') \right. \quad (\text{F.11})$$

$$\left. - \tilde{\omega}(\mathbf{k} - \boldsymbol{\eta}', \boldsymbol{\rho}) \widehat{W}_L^<(\mathbf{k} + \boldsymbol{\eta}'', \boldsymbol{\eta}') \right\}$$

Here $\tilde{\omega}(\mathbf{k}, \boldsymbol{\rho}) = \omega(\mathbf{k}, L\boldsymbol{\rho})$ is the rescaled dispersion relation. This equation can be rewritten entirely in terms of \widehat{W}_L^c by introducing the discrete gradient operator

$$\nabla_L f(\boldsymbol{\xi}) = \sum_{\boldsymbol{\eta} \in \Lambda_L^*} (2iL\boldsymbol{\eta}) e^{2iL\boldsymbol{\eta} \cdot \boldsymbol{\xi}} \widehat{f}(\boldsymbol{\eta}). \quad (\text{F.12})$$

APPENDIX F. THE FORMAL DERIVATION OF THE LINEAR TRANSPORT EQUATION FOR THE WIGNER FUNCTION

The result is expressed in terms of discrete analogues of pseudodifferential operators, as:

$$\partial_t \widehat{W}_L^c(\mathbf{k}, \boldsymbol{\xi}, t) = i \left\{ \widetilde{\omega}(\mathbf{k} + \frac{\vec{\nabla}_L}{2iL}, \boldsymbol{\xi}) \widehat{W}_L^c(\mathbf{k} - \frac{\overleftarrow{\nabla}_L}{2iL}, \boldsymbol{\xi}) - \widetilde{\omega}(\mathbf{k} - \frac{\overleftarrow{\nabla}_L}{2iL}, \boldsymbol{\xi}) \widehat{W}_L^c(\mathbf{k} + \frac{\vec{\nabla}_L}{2iL}, \boldsymbol{\xi}) \right\} \quad (\text{F.13})$$

The arrows above the discrete gradient operators indicate whether they act on the $\boldsymbol{\xi}$ -dependence either to the right or the left of the operator. In the limit as $L \rightarrow \infty$, the discrete gradient operator becomes the usual spatial gradient operator $\nabla_{\boldsymbol{\xi}}$ for functions on the torus. The limiting function $W(\mathbf{k}, \boldsymbol{\xi}, t) = \lim_{L \rightarrow \infty} \langle \widehat{W}_L^c(\mathbf{k}, \boldsymbol{\xi}, t) \rangle$ and $\widetilde{\omega}(\mathbf{k}, \boldsymbol{\xi})$ are both assumed to be smooth in $\boldsymbol{\xi}$, corresponding to quantities slowly varying in space on length-scale L . We can then formally Taylor-expand to obtain:

$$\partial_t W(\mathbf{k}, \boldsymbol{\xi}, t) \simeq \frac{1}{L} \nabla_{\mathbf{k}} \widetilde{\omega}(\mathbf{k}, \boldsymbol{\xi}) \cdot \nabla_{\boldsymbol{\xi}} W(\mathbf{k}, \boldsymbol{\xi}, t) - \frac{1}{L} \nabla_{\boldsymbol{\xi}} \widetilde{\omega}(\mathbf{k}, \boldsymbol{\xi}) \cdot \nabla_{\mathbf{k}} W(\mathbf{k}, \boldsymbol{\xi}, t) + O\left(\frac{1}{L^2}\right). \quad (\text{F.14})$$

Now let us briefly discuss the derivation of eq.(5.1) in the thesis. We expect similar procedures as discussed in Chap. 2 would yield the generalized wave-kinetic equation, which contains both linear advection and collisions of waves

$$\begin{aligned} & \partial_t W(\mathbf{k}, \boldsymbol{\xi}, t) - \frac{1}{L} \nabla_{\mathbf{k}} \omega(\mathbf{k}, \boldsymbol{\xi}) \cdot \nabla_{\boldsymbol{\xi}} W(\mathbf{k}, \boldsymbol{\xi}, t) + \frac{1}{L} \nabla_{\boldsymbol{\xi}} \omega(\mathbf{k}, \boldsymbol{\xi}) \cdot \nabla_{\mathbf{k}} W(\mathbf{k}, \boldsymbol{\xi}, t) \\ = & 36\pi\epsilon^2 \sum_{\boldsymbol{\sigma} = (-1, \sigma_2, \sigma_3)} \int_{(\Lambda^*)^2} d^d \bar{\mathbf{k}}_2 d^d \bar{\mathbf{k}}_3 |H_{\underline{\mathbf{k}}}^{\boldsymbol{\sigma}}|^2 \delta(\boldsymbol{\sigma} \cdot \omega(\underline{\mathbf{k}})) \delta_{\Lambda^*}(\boldsymbol{\sigma} \cdot \underline{\mathbf{k}}) \\ & \times \left\{ W(\bar{\mathbf{k}}_2, \boldsymbol{\xi}, t) W(\bar{\mathbf{k}}_3, \boldsymbol{\xi}, t) - \sigma_2 W(\mathbf{k}, \boldsymbol{\xi}, t) W(\bar{\mathbf{k}}_3, \boldsymbol{\xi}, t) - \sigma_3 W(\mathbf{k}, \boldsymbol{\xi}, t) W(\bar{\mathbf{k}}_2, \boldsymbol{\xi}, t) \right\}. \end{aligned} \quad (\text{F.15})$$

Recall the conditions for validity of the wave-kinetic equations given at the end of section 2.5.1, namely, for validity at a given wavenumber k one must have

- 1) one has to be able to find an intermediate time T between the linear time $t_L \sim 1/k|\nabla_{\mathbf{k}} \omega|$ and the nonlinear time $t_{NL} \sim W/C[W]$, where $C[W]$ is the collision integral in (F.15). That is, $t_L \ll T \ll t_{NL}$.

APPENDIX F. THE FORMAL DERIVATION OF THE LINEAR TRANSPORT EQUATION FOR THE WIGNER FUNCTION

- 2) this intermediate time must also satisfy $T \ll L/|\nabla\omega(\mathbf{k})|$ so that the wavevector space can be treated as a continuum.

For the generalized wave-kinetic equation F.15, there is another linear time scale t_{AD} corresponding to the advection terms

$$t_{AD} \sim \frac{LW}{|\nabla_{\mathbf{k}}\omega||\nabla_{\boldsymbol{\xi}}W|} \sim \frac{L}{\kappa|\nabla_{\mathbf{k}}W|} \sim \frac{Lk}{\kappa}t_L \gg t_L \quad (\text{F.16})$$

where κ is the dimensionless characteristic wavenumber for $W(\mathbf{k}, \boldsymbol{\xi})$ as a function of $\boldsymbol{\xi}$. The condition to derive the generalized wave-kinetic equation becomes that one must find an intermediate time T such that

$$t_L \ll T \ll t_{AD} \ll t_{NL}. \quad (\text{F.17})$$

The first condition is necessary so that the approximate delta function δ_T becomes a Dirac delta function. The second condition is necessary so that the finite difference $(W(\mathbf{k}, \boldsymbol{\xi}, T) - W(\mathbf{k}, \boldsymbol{\xi}, 0))/T$ can be well approximated by the derivative $\partial_t W(\mathbf{k}, \boldsymbol{\xi})$. The last condition is necessary so that the collision integral is much smaller than the advection terms

$$\frac{1}{L}|\nabla_{\mathbf{k}}\omega \cdot \nabla_{\boldsymbol{\xi}}W| \gg \epsilon^2 C[W]. \quad (\text{F.18})$$

This implies that L cannot be too large

$$L \ll \frac{\kappa}{k} \frac{t_{NL}}{t_L}. \quad (\text{F.19})$$

One might find it alarming that there is an upper bound for L . Indeed there is also a lower bound for L that comes from the condition $L/|\nabla_{\mathbf{k}}\omega| \gg T$ for the continuum approximation and $t_{AD} \gg T$,

APPENDIX F. THE FORMAL DERIVATION OF THE LINEAR TRANSPORT EQUATION FOR THE WIGNER FUNCTION

which can be written as

$$L \gg \max \left\{ T |\nabla_{\mathbf{k}} \omega|, \frac{\kappa}{k} \frac{T}{t_L} \right\} = \max \left\{ \frac{1}{k}, \frac{\kappa}{k} \right\} \frac{T}{t_L} = \frac{\kappa}{k} \frac{T}{t_L} \quad (\text{F.20})$$

since $\kappa \geq 2\pi$. We can clearly choose L to satisfy both constraints

$$\frac{\kappa}{k} \frac{T}{t_L} \ll L \ll \frac{\kappa}{k} \frac{t_{NL}}{t_L}. \quad (\text{F.21})$$

As a matter of fact, the upper bound (F.19) for L arises because in our definition of the Wigner function eqs.(E.7) and (E.8) we rescale by a factor of L and implicitly assume $|\nabla_{\boldsymbol{\xi}} \omega|$ and $|\nabla_{\boldsymbol{\xi}} W|$ are $O(1)$ in the derivation of eq.(F.14). We may replace L by a different length-scale $\ell \gg a$. Then the factor in front of the advection terms in (F.14) becomes $1/\ell$. As a result, the bound (F.19) will be imposed on the length-scale ℓ instead of L .

Bibliography

- Arnold, V. I., Varchenko, A., and Gusein-Zade, S. M. (2012). *Singularities of differentiable maps: Volume I: The classification of critical points, caustics, and wave fronts*. Monographs in Mathematics. Birkhäuser Boston. ISBN 9781461251545.
- Balk, A. M. and Zakharov, V. E. (1988a). Stability of slightly turbulent Kolmogorov spectra. *Sov. Phys. Dokl.*, **33**, 270–272.
- Balk, A. M. and Zakharov, V. E. (1988b). Stability of weak turbulence Kolmogorov spectra. In *Plasma theory and nonlinear and turbulent processes in physics, Proc. Int. Workshop, Kiev/USSR 1987*, volume 1, pages 359–376. World Scientific Publishing Co., Singapore.
- Balk, A. M. and Zakharov, V. E. (1998). Stability of weak-turbulence Kolmogorov spectra. *Amer. Math. Soc. Transl. Ser. 2*, **182**, 31–82.
- Balk, A. M., Nazarenko, S. V., and Zakharov, V. (1990). Nonlocal turbulence of drift waves. *Sov. Phys. JETP*, **71**, 249–260.
- Benney, D. J. and Newell, A. C. (1967). Sequential time closures of interacting random waves. *Stud. Appl. Math.*, **46**, 363–393.
- Benney, D. J. and Newell, A. C. (1969). Random wave closures. *Stud. Appl. Math.*, **48**(1), 29–53.
- Biferale, L. (2003). Shell models of energy cascade in turbulence. *Annu. Rev. Fluid. Mech.*, **35**, 441–468.

BIBLIOGRAPHY

- Biferale, L., Lambert, A., Lima, R., and Paladin, G. (1995). Transition to chaos in a shell model of turbulence. *Physica D*, **80**(1), 105 – 119.
- Biven, L., Nazarenko, S., and Newell, A. (2001). Breakdown of wave turbulence and the onset of intermittency. *Phys. Lett. A*, **280**(1), 28–32.
- Bogolyubov, N. N. (1946). *Problemi Dinamicheskoi Teorii v Statisticheskoi Fizike*. Izdatel'stvo O.G.I.Z. Gostekhizdat, Moscow. English translation: “Problems of a dynamical theory in statistical physics,” Studies in Statistical Mechanics, Vol. 1, eds. J. de Boer and G. E. Uhlenbeck, North-Holland, Amsterdam, 1962.
- Boltzmann, L. (1872). Weitere Studien über das Wärmegleichgewicht unter Gasmolekülen. *Sitzungsberichte Akad. Wiss.*, **66**, 275–370.
- Brout, R. and Prigogine, I. (1956). Statistical mechanics of irreversible processes Part VIII: general theory of weakly coupled systems. *Physica*, **22**(6), 621–636.
- Caillol, P. and Zeitlin, V. (2000). Kinetic equations and stationary energy spectra of weakly nonlinear internal gravity waves. *Dynam. Atmos. Oceans*, **32**, 81–112.
- Choi, Y., Lvov, Y. V., and Nazarenko, S. (2005a). Joint statistics of amplitudes and phases in wave turbulence. *Physica D*, **201**(1-2), 121–149.
- Choi, Y., Lvov, Y. V., Nazarenko, S., and Pokorni, B. (2005b). Anomalous probability of large amplitudes in wave turbulence. *Phys. Lett. A*, **339**(3-5), 361–369.
- Choi, Y., Jo, S. G., Kim, H. I., and Nazarenko, S. V. (2009). Aspects of two-mode probability density function in weak wave turbulence. *J. Phys. Soc. Jap.*, **78**(8), 084403.
- Cohen, E. G. D. (1993). Fifty years of kinetic theory. *Physica A*, **194**, 229–257.
- Connaughton, C., Nazarenko, S., and Newell, A. C. (2003). Dimensional analysis and weak turbulence. *Physica D*, **184**, 86–97.

BIBLIOGRAPHY

- Cover, T. M. and Thomas, J. A. (1991). *Elements of Information Theory*. Wiley Series in Telecommunications and Signal Processing. John Wiley & Sons. ISBN 0471241954.
- de Verdiere, Y. C. and Vey, J. (1979). Le lemme de Morse isochore. *Topology*, **18**(4), 283 – 293.
- Dubrulle, B. and Zahn, J.-P. (1991). Nonlinear instability of viscous plane Couette flow Part 1. Analytical approach to a necessary condition. *J. Fluid Mech.*, **231**, 561–573.
- Dyachenko, A. I. and Zakharov, V. E. (1994). Is free-surface hydrodynamics an integrable system? *Phys. Lett. A*, **190**, 144–148.
- Erofeev, V. I. and Malkin, V. M. (1989). Kinetics of weakly turbulent wave fields. *Sov. Phys. JETP*, **69**, 943–958.
- Esposito, R., Marra, R., and Lebowitz, J. L. (1998). Solutions to the Boltzmann equation in the Boussinesq regime. *J. Stat. Phys.*, **90**, 1129–1178.
- Eyink, G. L. and Xin, J. (2000). Self-similar decay in the Kraichnan model of a passive scalar. *J. Stat. Phys.*, **100**, 679–741.
- Falcon, E., Fauve, S., and Laroche, C. (2007). Observation of intermittency in wave turbulence. *Phys. Rev. Lett.*, **98**(15), 154501.
- Falcon, E., Aumaître, S., Falcón, C., Laroche, C., and Fauve, S. (2008). Fluctuations of energy flux in wave turbulence. *Phys. Rev. Lett.*, **100**, 064503.
- Falkovich, G. E. and Shafarenko, A. V. (1987). On the stability of Kolmogorov spectra of a weak turbulence. *Physica D*, **27**(3), 399–411.
- Federer, H. (1959). Curvature measure. *Trans. Amer. Math. Soc.*, **93**, 418–491.
- Federer, H. (1969). *Geometric measure theory*. Grundlehren der mathematischen Wissenschaften. Springer.

BIBLIOGRAPHY

- Fedoryuk, M. V. (1971). The stationary phase method and pseudodifferential operators. *Russ. Math. Surv.*, **26**(1), 65–115.
- Fritz, L., Schmalian, J., Müller, M., and Sachdev, S. (2008). Quantum critical transport in clean graphene. *Phys. Rev. B*, **78**(8), 085416.
- Gallagher, I., Saint-Raymond, L., and Texier, B. (2013). *From Newton to Boltzmann: Hard Spheres and Short-range Potentials*. European Mathematical Society. ISBN 3037191295.
- Galtier, S. (2003). Weak inertial-wave turbulence theory. *Phys. Rev. E*, **68**, 015301.
- Glimm, J. and Jaffe, A. (1987). *Quantum Physics - A Functional Integral Point of View*. Springer, New York.
- Goldenfeld, N. (1992). *Lectures on Phase Transitions and the Renormalization Group*, volume 85 of *Frontiers in Physics*. Addison-Wesley, Advanced Book Program. ISBN 0201554089.
- González, J., Guinea, F., and Vozmediano, M. (1999). Marginal-fermi-liquid behavior from two-dimensional Coulomb interaction. *Phys. Rev. B*, **59**(4), R2474.
- Griffith, W. C. (1981). Shock waves. *J. Fluid Mech.*, **106**, 81–101.
- Guillemin, V. and Pollack, A. (1974). *Differential topology*. Prentice-Hall, Inc., Englewood Cliffs, New Jersey. ISBN 0-13-212605-2.
- Hasselmann, K. (1962). On the non-linear energy transfer in a gravity-wave spectrum. Part 1. General theory. *J. Fluid Mech.*, **12**, 481–500.
- Hasselmann, K. (1963a). On the non-linear energy transfer in a gravity-wave spectrum. Part 2. Conservation theorems; wave-particle analogy; irreversibility. *J. Fluid Mech.*, **15**, 273–281.
- Hasselmann, K. (1963b). On the non-linear energy transfer in a gravity-wave spectrum. Part 3. Evaluation of the energy flux and swell-sea interaction for a neumann spectrum. *J. Fluid Mech.*, **15**, 385–398.

BIBLIOGRAPHY

- Hofmann, J., Barnes, E., and Sarma, S. D. (2014). Why does graphene behave as a weakly interacting system? *Phys. Rev. Lett.*, **113**(10), 105502.
- Hörmander, L. (1983). *The analysis of linear partial differential operators I: Distribution theory and Fourier analysis*, volume 256 of *Grundlehren der mathematischen Wissenschaften*. Springer-Verlag Berlin Heidelberg New York.
- Jakobsen, P. and Newell, A. C. (2004). Invariant measures and entropy production in wave turbulence. *J. Stat. Mech.-Theory E.*, **2004**(10), L10002.
- Kadanoff, L., Lohse, D., and Schörghofer, N. (1997). Scaling and linear response in the GOY turbulence model. *Physica D*, **100**(1), 165–186.
- Kashuba, A. B. (2008). Conductivity of defectless graphene. *Phys. Rev. B*, **78**, 085415.
- Keldysh, L. V. (1965). Diagram technique for nonequilibrium processes. *Sov. Phys. JETP*, **20**(4), 1018–1026.
- Klimontovich, Y. L. (1967). *The Statistical Theory of Non-Equilibrium Processes in a Plasma*. International series of monographs in natural philosophy. Pergamon Press.
- Kotov, V. N., Uchoa, B., Pereira, V. M., Guinea, F., and Neto, A. C. (2012). Electron-electron interactions in graphene: Current status and perspectives. *Rev. Mod. Phys.*, **84**(3), 1067.
- Kraichnan, R. H. (1970). Convergents to turbulence functions. *J. Fluid Mech.*, **41**, 189–217.
- Kurbanmuradov, O. (1995). Convergence of numerical models for the Gaussian fields. *Russ. J. Numer. Anal. M.*, **10**(4), 311–323.
- Lanford, O. E. (1975). Time evolution of large classical systems. In J. Moser, editor, *Dynamical Systems, Theory and Applications*, volume 38 of *Lecture Notes in Physics*, pages 1–111. Springer Berlin / Heidelberg.
- Lanford, O. E. (1976). On the derivation of the Boltzmann equation. *Asterisque*, **40**, 117–137.

BIBLIOGRAPHY

- Lang, S. (2012). *Differential manifolds*. Springer-Verlag New York, second edition. ISBN 9781468402650.
- Leith, C. E. (1971). Atmospheric predictability and two-dimensional turbulence. *J. Atmos. Sci.*, **28**, 145–161.
- Lewin, L. (1981). *Polylogarithms and associated functions*. North Holland. ISBN 9780444005502.
- Long, R. B. (1973). Scattering of surface waves by an irregular bottom. *J. Geophys. Res.-Oc. Atm.*, **78**.
- Lukkarinen, J. and Spohn, H. (2007). Kinetic limit for wave propagation in a random medium. *Arch. Ration. Mech. Anal.*, **183**, 93–162.
- Lukkarinen, J. and Spohn, H. (2011). Weakly nonlinear Schrödinger equation with random initial data. *Invent. Math.*, **183**, 79–188.
- L’vov, V. S., L’vov, Y., Newell, A. C., and Zakharov, V. (1997). Statistical description of acoustic turbulence. *Phys. Rev. E*, **56**, 390–405.
- Majda, A. J., McLaughlin, D. W., and Tabak, E. G. (1997). One-dimensional model for dispersive wave turbulence. *J. Nonlinear Sci.*, **7**, 9–44.
- Malý, J., Swanson, D., and Ziemer, W. (2003). The coarea formula for Sobolev mappings. *Trans. Amer. Math. Soc.*, **355**, 477–492.
- Marcia, F. (2004). Wigner measures in the discrete setting: high-frequency analysis of sampling & reconstruction operators. *SIAM J. Math. Anal.*, **36**, 347–383.
- Markowich, G. P., Mauser, P. A., and Poupaud, N. J. (1997). Homogenization limits and Wigner transforms. *Comm. Pure Appl. Math.*, **50**, 323–379.
- McKean, H. P. (1966). A class of Markov processes associated with nonlinear parabolic equations. *P. Natl. Acad. Sci. USA*, **56**, 1907–1911.

BIBLIOGRAPHY

- Michel, C., Garnier, J., Surret, P., Randoux, S., and Picozzi, A. (2011). Kinetic description of random optical waves and anomalous thermalization of a nearly integrable wave system. *Lett. Math. Phys.*, **96**, 415–447.
- Mielke, A. (2006). Macroscopic behavior of microscopic oscillations in harmonic lattices via Wigner-Husimi Transforms. *Arch. Rational Mech. Anal.*, **181**, 401–448.
- Milnor, J. M. (1963). *Morse theory*, volume 51 of *Annals of mathematics studies*. Princeton University Press.
- Müller, M., Schmalian, J., and Fritz, L. (2009). Graphene: a nearly perfect fluid. *Phys. Rev. Lett.*, **301**, 025301.
- Nazarenko, S. (2011). *Wave turbulence*, volume 825 of *Lecture Notes in Physics*, Berlin Springer Verlag.
- Nazarenko, S., Lukaschuk, S., McLelland, S., and Denissenko, P. (2010). Statistics of surface gravity wave turbulence in the space and time domains. *J. Fluid Mech.*, **642**, 395–420.
- Newell, A. C. and Aucoin, P. J. (1971). Semidispersive wave systems. *J. Fluid Mech.*, **49**, 593–609.
- Newell, A. C. and Rumpf, B. (2011). Wave turbulence. *Annu. Rev. Fluid Mech.*, **43**, 59–78.
- Newell, A. C. and Zakharov, V. E. (2008). The role of the generalized Phillips’ spectrum in wave turbulence. *Phys. Lett. A*, **372**(23), 4230–4233.
- Newell, A. C., Nazarenko, S., and Biven, L. (2001). Wave turbulence and intermittency. *Physica D*, **152-153**, 520–550.
- Newell, A. C., Rumpf, B., and Zakharov, V. E. (2012). Spontaneous breaking of homogeneity symmetry in wave turbulence. *Phys. Rev. Lett.*, **108**, 19.
- Peierls, R. (1929). Zur kinetischen Theorie der Wärmeleitung in Kristallen. *Annalen der Physik*, **395**, 1055–1101.

BIBLIOGRAPHY

- Rumpf, B., Newell, A. C., and Zakharov, V. E. (2009). Turbulent transfer of energy by radiating pulses. *Phys. Rev. Lett.*, **103**, 074502.
- Sachdev, S. (1998). Nonzero-temperature transport near fractional quantum Hall critical points. *Phys. Rev. B*, **57**(12), 7157.
- Schmid, P. J. and Henningson, D. S. (2001). *Stability and Transition in Shear Flows*, volume 142 of *Applied Mathematical Sciences*. Springer. ISBN 0387989854.
- Son, D. T. (2007). Quantum critical point in graphene approached in the limit of infinitely strong Coulomb interaction. *Phys. Rev. B*, **75**(23), 235423.
- Spohn, H. (1984). Boltzmann hierarchy and Boltzmann equation. In C. Cercignani, editor, *Kinetic Theories and the Boltzmann Equation*, volume 1048 of *Lecture Notes in Mathematics*, pages 207–220. Springer Berlin / Heidelberg. ISBN 978-3-540-12899-1.
- Spohn, H. (2006). The phonon Boltzmann equation, properties and link to weakly anharmonic lattice dynamics. *J. Stat. Phys.*, **124**, 1041–1104.
- Suret, P., Randoux, S., Jauslin, H., and Picozzi, A. (2010). Anomalous thermalization of nonlinear wave systems. *Phys. Rev. Lett.*, **104**.
- Van Hove, L. (1953). The occurrence of singularities in the elastic frequency distribution of a crystal. *Phys. Rev.*, **89**, 1189–1193.
- Yamasaki, Y. (1985). *Measures on infinite dimensional spaces*, volume 5 of *Pure Mathematics*. Singapore Philadelphia: World Scientific. ISBN 9971978520.
- Yokoyama, N. (2004). Statistics of gravity waves obtained by direct numerical simulation. *J. Fluid Mech.*, **501**, 169–178.
- Zakharov, V. E. and Filonenko, N. N. (1967a). Energy spectrum for stochastic oscillations of a fluid surface. *Sov. Phys. Dok.*, **11**, 881–884.

BIBLIOGRAPHY

- Zakharov, V. E. and Filonenko, N. N. (1967b). Weak turbulence of capillary waves. *J. Appl. Mech. Tech. Phys.*, **4**, 506.
- Zakharov, V. E. and L'vov, V. S. (1975). Statistical description of nonlinear wave fields. *Radiophys. Quantum El.*, **18**, 1084–1097.
- Zakharov, V. E. and Sagdeev, R. Z. (1970). Spectrum of acoustic turbulence. *Sov. Phys. Dok.*, **15**, 439.
- Zakharov, V. E., L'vov, V. S., and Falkovich, G. (1992). *Kolmogorov spectra of turbulence I. Wave turbulence*. Springer series in nonlinear dynamics. Springer Berlin.
- Zakharov, V. E., Korotkevich, A. O., Pushkarev, A. N., and Dyachenko, A. I. (2005). Mesoscopic wave turbulence. *Sov. Phys. JETP*, **82**, 487–491.
- Zaslavskii, G. M. and Sagdeev, R. Z. (1967). Limits of statistical description of a nonlinear wave field. *Sov. Phys. JETP*, **25**, 718–724.

Vita

Yi-Kang Shi was born in 1987 in Shanghai, China. He attended Nanyang Model High School from 2003-2006 and Fudan university from 2006-2010. He received the Bachelor of Science degree in Mathematics and Applied Mathematics from Fudan University in 2010. He then enrolled in the Applied Mathematics and Statistics Ph.D. program at the Johns Hopkins University.